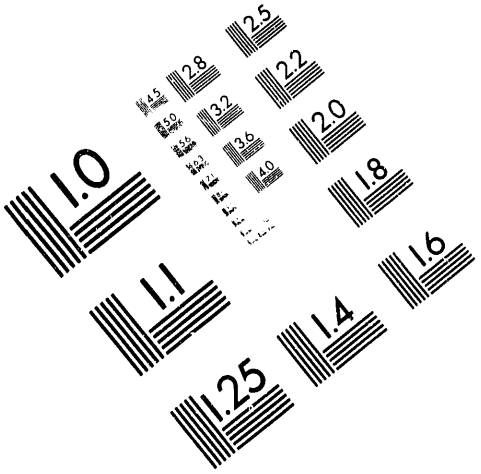

Association for Information and Image Management

1100 Wayne Avenue, Suite 1100
Silver Spring, Maryland 20910

301/587-8202

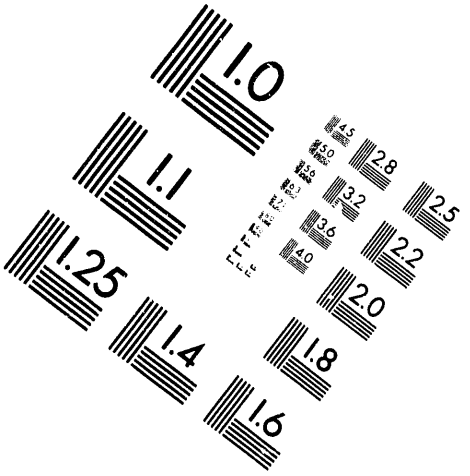

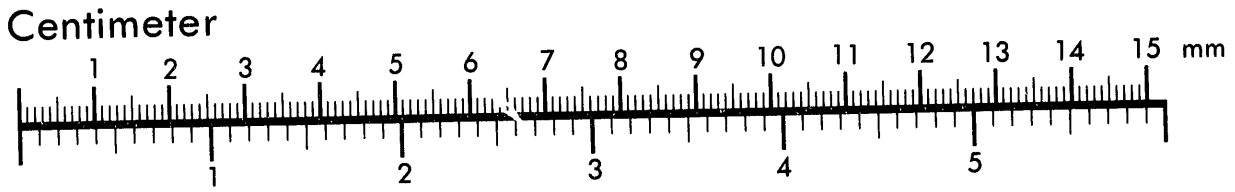

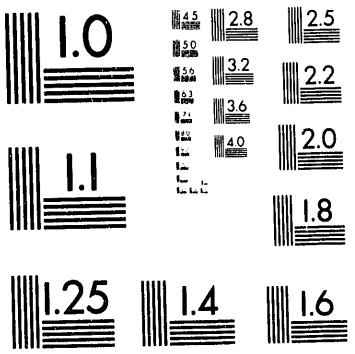

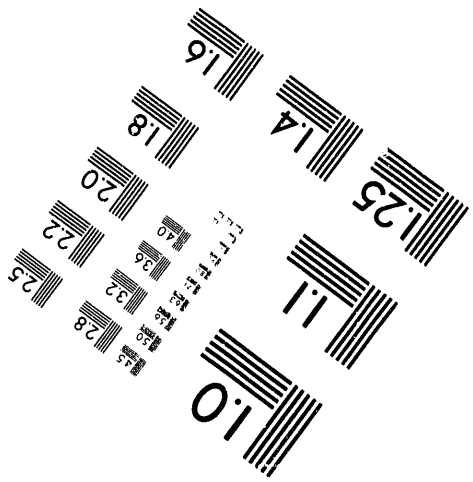

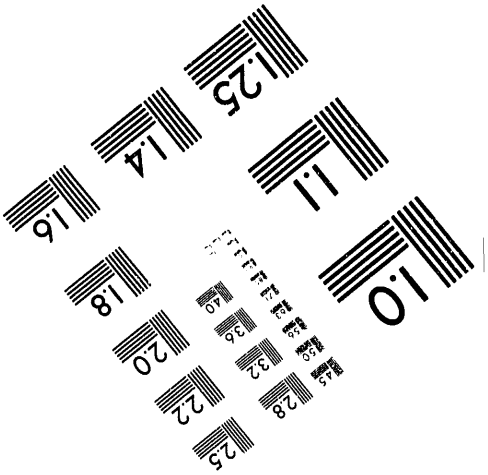

1 of 4

DOE/PC/89876-T18
(DE93014938)
Distribution Category UC-108

BIOLOGICAL PRODUCTION OF ETHANOL FROM COAL

FINAL REPORT

Published: December 1992

Prepared by

University of Arkansas
Department of Chemical Engineering
Fayetteville, Arkansas 72701

Prepared for

The United States Department of Energy
Pittsburgh Energy Technology Center
Contract No. DE-AC22-89PC89876

TABLE OF CONTENTS

TABLE OF CONTENTS (continued)

TABLE OF CONTENTS (continued)

LIST OF TABLES

LIST OF FIGURES

LIST OF FIGURES (continued)

LIST OF FIGURES (continued)

LIST OF FIGURES (continued)

LIST OF FIGURES (continued)

LIST OF FIGURES (continued)

LIST OF FIGURES (continued)

ACKNOWLEDGEMENT

Financial support for this work was provided by the United States Department of Energy, Pittsburgh Energy Technology Center, on Contract No. DE-AC22-89PC89876.

1.0 INTRODUCTION

Due to the abundant supply of coal in the United States, significant research efforts have occurred over the past 15 years concerning the conversion of coal to liquid fuels. Researchers at the University of Arkansas have concentrated on a biological approach to coal liquefaction, starting with coal-derived synthesis gas as the raw material. Synthesis gas, a mixture of CO, H_2, CO_2, CH_4 and sulfur gases, is first produced using traditional gasification techniques. The CO, CO_2 and H_2 are then converted to ethanol using a bacterial culture of *Clostridium ljungdahlii*.

C. ljungdahlii was initially isolated from animal waste at the University of Arkansas. The bacterium converts CO, CO_2 and H_2 to ethanol and acetate by the equations:

$$6\ CO + 3\ H_2O \rightarrow C_2H_5OH + 4\ CO_2 \quad (1.1)$$

$$2\ CO_2 + 6\ H_2 \rightarrow C_2H_5OH + 3\ H_2O \quad (1.2)$$

$$4\ CO + 2\ H_2O \rightarrow CH_3COOH + 2\ CO_2 \quad (1.3)$$

$$2\ CO_2 + 4\ H_2 \rightarrow CH_3COOH + 2\ H_2O \quad (1.4)$$

In these equations, ethanol is the desired product if the resultant product stream is to be used as a liquid fuel. However, under normal operating conditions, the "wild strain" produces acetate in favor of ethanol in conjunction with growth in a 20:1 molar ratio. Thus, research is necessary to determine the conditions necessary to maximize not only the ratio of ethanol to acetate, but also to maximize the concentration of ethanol resulting in the product stream.

Significant progress has been made toward reaching this goal.[1] Several factors have been identified that cause the culture to produce ethanol in favor of acetate. These factors include manipulation of the nutrients

composition and concentration, the addition of reducing agents or sporulating agents to liquid medium and reduction of the medium pH. Many of these techniques have been demonstrated in batch and continuous culture, both individually and together as multiple parameter experiments. Manipulation of these parameters has led to the realization that acetate is produced in conjunction with growth and energy production, whereas ethanol is produced when growth is minimized and when energy is used instead of produced. The parameters that enhance ethanol production suppress growth and/or produce energy for ultimate use by the cell during ethanol production.

The purpose of this report is to present the results of studies aimed at demonstrating the feasibility of ethanol production from *C. ljungdahlii* in batch and continuous culture. Areas of study include optimization of culturing conditions to maximize ethanol production studies aimed at improving the ethanol to acetate product ratio and ethanol product concentration, continuous reactor studies and an economic evaluation. It has been shown that it is both technically and economically feasible to produce ethanol from syngas biologically.

2.0 BACKGROUND ON *CLOSTRIDIUM LJUNGDAHLII*

In 1987, researchers at the University of Arkansas reported the isolation of a strictly anaerobic mesophilic bacterium from animal waste that was capable of converting CO, H_2 and CO_2 to a mixture of acetate and ethanol.[2] This discovery was the result of extensive screening studies utilizing natural inocula, such as sewage sludge, animal waste, coal pile runoff and soils. The method of successive transfer was applied, while simultaneously blocking methanogenesis.

Early batch fermentation experiments with the newly isolated microorganism, tentatively identified as a member of the *Clostridium* genera, did not show a high degree of reproducibility. Although product ratios of 1 mole ethanol to 10 moles of acetate (1:10) were sometimes obtained, the standard product ratio in these early studies was 1:20. Ethanol concentrations were also quite low, although the concentration could be increased in batch culture through multiple gas additions. Clearly, an experimental program was needed to increase the product ratio and concentration of ethanol while, at the same time, carrying out parallel studies on culture identification and process stoichiometry.

An earlier experimental program was thus developed to identify and characterize the bacterium, evaluate overall culture stoichiometry, improve the ethanol/acetate ratio and optimize culture operating conditions. Highlights of this work include improving the product ratio from 1:20 (ethanol to acetate) to 3:1, and improving the specific ethanol productivity of the culture by 800 percent. These and other results are summarized in the paragraphs below.

2.1 Culture Isolation and Characterization

Bacterial isolation and characterization studies showed that the culture was a new clostridial species, named *Clostridium ljungdahlii*, Strain PETC, in honor of Dr. Lars G. Ljungdahl. *C. ljundahlii* is a gram-positive, motile, rod-shaped anaerobic bacterium which sporulates infrequently. The bacterium only produces ethanol at pH levels below 6.0. At higher pH levels, acetate is the only liquid phase product.

A list of substrates tested for growth as the sole carbon and energy source is shown in Table 2.1. In these studies, 1 g/L of yeast extract was

added to the medium along with the substrate, and all fermentations were carried out at an initial pH of 6.0. As noted in Table 2.1, growth was obtained when H_2/CO_2, ethanol, pyruvate, xylose, arabinose and fructose were used as substrates. *C. ljungdahlii* grew weakly in the presence of fumarate, ribose, glucose and casamino acids.

Table 2.1

Growth of C. ljungdahlii on Substrates as the Sole Carbon/Energy Source

$H_2:CO_2$	+	ribose	w
CO	+	xylose	+
formate	-	arabinose	+
methanol	-	fructose	+
ethanol	+	glucose	w
pyruvate	+	galactose	-
lactate	-	mannose	-
glycerol	-	sorbitol	-
succinate	-	sucrose	-
fumarate	w	maltose	-
citrate	-	lactose	-
		starch	-
		casamino acids	w

+ positive growth
- no growth
w weak growth

C. ljungdahlii is distinguishable from related organisms by its substrate use, pH requirements, end-products of fermentation and physical characteristics. It can be distinguished from *Clostridium aceticum* by its pH optimum, and the utilization of glucose, formate, ribose and xylose as substrates. The bacterium can be distinguished from *Clostridium barkeri* by the end-products of fermentation, motility, and the utilization of glucose, lactate and xylose as substrates. *C. ljungdahlii* is distinguishable from *Clostridium formicoaceticum* by the utilization of glucose, lactate, ribose and H_2/CO_2 as substrates, and is distinguished from *Clostridium thermoaceticum* and

Clostridium thermoautotrophicum by thermophilicity and the utilization of glucose as a substrate.

The bacterium can also be differentiated from other acetate forming species. It is distinguished from *Acetobacterium* sp. by spore formation and the utilization of formate, lactate and pentoses as substrates. It is distinguished from *Eubacterium limosum* by motility, spore formation, and the utilization of glucose, lactate, methanol, ethanol and arabinose as substrates.

Figure 2.1 shows an electron micrograph of *C. ljungdahlii*, Strain PETC. As is seen in the micrograph, the cells are petrichously flagellated. Also, there is good evidence for an internal membrane structure, which is visible both in fixed and unfixed preparations and in fixed and unfixed cells stained with uranyl acetate or phosphotungstic acid. The membranes are also seen in different culture preparations. These internal structures, which have not been observed in clostridial species before and which usually require thin sectioning to visualize in any eubacteria, may explain how the organism can metabolize in the presence of acetic acid at pH 4.

DNA composition studies have shown that *C. ljungdahlii* contains 22 mole percent guanine plus cytosine. This composition is at the lowest end of bacteria, with only one other clostridia having a composition this low. This result further substantiates the fact that *C. ljundahlii*, Strain PETC is a new clostridial species.

Figure 2.1. Electron micrograph of *Clostridium ljungdahlii*, strain PETC.

2.2 Evaluation of Reaction Stoichiometry

The stoichiometry for the formation of acetate from carbon monoxide, as well as hydrogen and carbon dioxide, has been well-established for many acetogenic bacteria.[3] These reactions are:

$$4\ CO + 2\ H_2O \rightarrow CH_3COOH + 2\ CO_2 \qquad (1.1)$$

$$\Delta G^\circ = -37.8\ \text{kcal/gmole}\ CH_3COOH$$

and

$$2\ CO_2 + 4\ H_2 \rightarrow CH_3COOH + 2\ H_2O \qquad (1.2)$$

$$\Delta G^\circ = -18.6\ \text{kcal/gmole}\ CH_3COOH$$

Similar equations may be written for the formation of ethanol from CO, CO_2 and H_2:

$$6\ CO + 3\ H_2O \rightarrow C_2H_5OH + 4\ CO_2 \qquad (1.3)$$

$$\Delta G^\circ = -59.9\ \text{kcal/gmole}\ C_2H_5OH$$

and

$$2\ CO_2 + 6\ H_2 \rightarrow C_2H_5OH + 3\ H_2O \qquad (1.4)$$

$$\Delta G^\circ = -23.2\ \text{kcal/gmole}\ C_2H_5OH$$

Experiments were carried out in the University of Arkansas laboratories to verify the stoichiometries of Equations (1.1-1.4) for *C. ljungdahlii*.[4] Both single substrate (CO or CO_2/H_2) studies and mixed substrate (CO, CO_2 and H_2) studies were conducted. The results of these studies indicated that stoichiometric quantities of acetate and ethanol were produced from CO, CO_2 and H_2 as indicated in Equations (1.1-1.4), thus verifying the stoichiometric relationships.

3.0 ENHANCING FUEL PRODUCTION IN CLOSTRIDIAL FERMENTATIONS

3.1 Biochemistry and Energetics of Clostridia

As mentioned previously, the production of ethanol by *C. ljungdahlii* is accompanied by the production of acetate, an undesirable by-product if a fuel

is sought. Although *C. ljungdahlii* is the first organism to show the production of ethanol from CO, H_2 and CO_2, several other clostridial species are known to manufacture ethanol from sugars.[5] *C. thermocellum*, *C. thermohydrosulfuricum* and *C. saccharolyticum* have been shown to produce ethanol from complex carbohydrates such as cellulose and starch, and from simple sugars such as glucose. In all three cases, however, acetic acid and sometimes lactic acid are always produced as by-products of the fermentation. It is very likely that similar biochemical pathways exist for these bacteria and *C. ljungdahlii*, thus providing information on the methanisms that lead to the production of ethanol and acetate.

The ethanologenic clostridia convert sugars to pyruvate via the fructose-biphosphate pathway producing two moles of ATP and two moles of NADH per mole of hexose, as shown in Figure 3.1. The majority of the pyruvate is converted to acetyl-CoA with small amounts going to lactate or CO_2 and H_2. Acetyl-CoA can then be reduced to acetaldehyde and then to ethanol, or it can be converted into acetate with stoichiometric production of ATP.

The pathway utilized by clostridial species and other acetogenic bacteria to autotrophically grow on H_2/CO_2 and CO has been recently established by Wood *et al.*[6] in studies conducted with *C. thermoaceticum*, and has been termed "the acetyl-CoA pathway". Evidence is accumulating that this pathway is utilized by other bacteria that grow with CO_2 and H_2 as the sources of carbon and energy. This group includes all of the acetogenic bacteria, the methane producing bacteria and the sulfate-reducing bacteria. The mechanism involves the reduction of one molecule of CO_2 to a methyl group and then its combination with a second molecule of CO_2 (or a molecule of CO) and CoA to

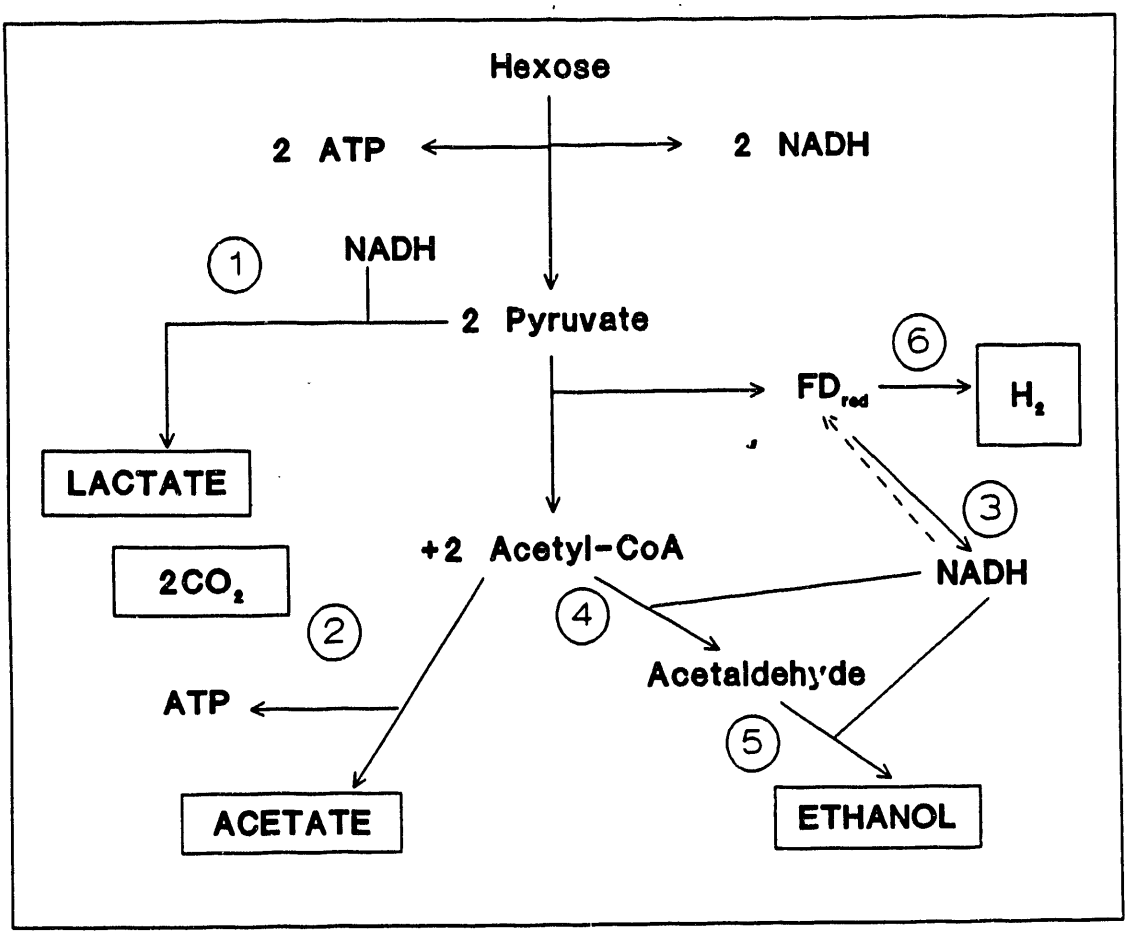

Figure 3.1. Clostridial ethanolic fermentations. Numbers indicate enzymes: (1) Lactate dehydrogenase; (2) Phosphotransacetylase + acetate kinase; (3) NADH ferredosin oxidoreductase; (4) Acetaldehyde dehydrogenase; (5) Ethanol dehydrogenase; (6) Hydrogenase.

form acetyl-CoA. The reduction of CO_2 to a methyl group in the tetrahydrofolate pathway requires one molecule of ATP and one molecule of NADH per molecule of CO_2 reduced. Also, it is important to note that the conversion of acetyl-CoA to acetate is the only source of substrate level phosphorylation in the acetogenic clostridia during unicarbonotrophic growth.[7] When terminating in acetate, the pathway is balanced in ATP and the production of ethanol or other end-products would result in a net consumption of ATP which would not support growth of the bacteria.

The high growth yields of homoacetogenic bacteria on sugars and the discovery of a large variety of electron transport proteins have provided the first clues to indicate that in clostridial species, ATP may be generated by a proton gradient mechanism and electron coupled phosphorylation. It has been suggested that the generation of the proton gradient may be caused by the free flow of H_2 through the cyloplasmic membrane and the presence of membrane bound hydrogenase.[7] In view of these findings, it is possible to expect that end products other than acetate (such as ethanol) may be manufactured in microcarbonotrophic growth of clostridial species. The understanding of the basic energetics supporting growth and metabolism is fundamental to the development of products other than acetate in clostridial fermentations.

3.2 Elimination of Acetate as a Product

Clostridial fermentations yield a wide variety of end-products which include two to five major acids and/or solvents as well as gaseous products such as H_2 and CO_2. The amount of reduced versus neutral and oxidized products is always balanced with the amount of H_2 and also ATP produced and has the potential of a great deal of natural variation. Several strategies have been employed in other clostridial fermentations, particularly the

acetone-butanol fermentation by *C. acetobutylicum*, which have led to increases in the selectivity of solvents versus acids. Some of these strategies have been investigated with *C. ljungdahlii* and the results are summarized below.

3.2.1 Control of Growth Rate Parameters

Studies in the acetone-butanol fermentation have shown that high solvent yields depend upon adjusting growth-limiting factors such as phosphate, nitrogen, etc. in a range which allows some growth but not under optimum conditions.[8,9,10] Solventogenesis, then, is apparently a metabolic response to a condition of unbalanced growth where the utilizable energy source remains in excess but growth is restricted by other limiting factors or growth inhibitors. Still, the molecular changes that trigger the formation of solvents due to growth restriction are unknown.

Early in the studies conducted with *C. ljungdahlii*, the importance of the yeast extract concentration employed in the medium on the ratio of ethanol to acetate obtained during a fermentation was recognized. In a typical batch fermentation, the production of ethanol occurs simultaneously and a rather constant ratio of products is maintained along the fermentation. The ratio of ethanol to acetate, however, is highly dependent upon the yeast extract concentration as is shown in Figure 3.2 for higher levels of yeast extract. Unfortunately, the bacteria have adapted to lower levels of yeast extract and the effect observed in batch culture has not proven useful in continuous experiments.

While growth control in continuous culture has not been successful through nutrient limitation strategies, the rate of growth of bacteria in chemostats can be easily controlled by adjusting the dilution rate. At

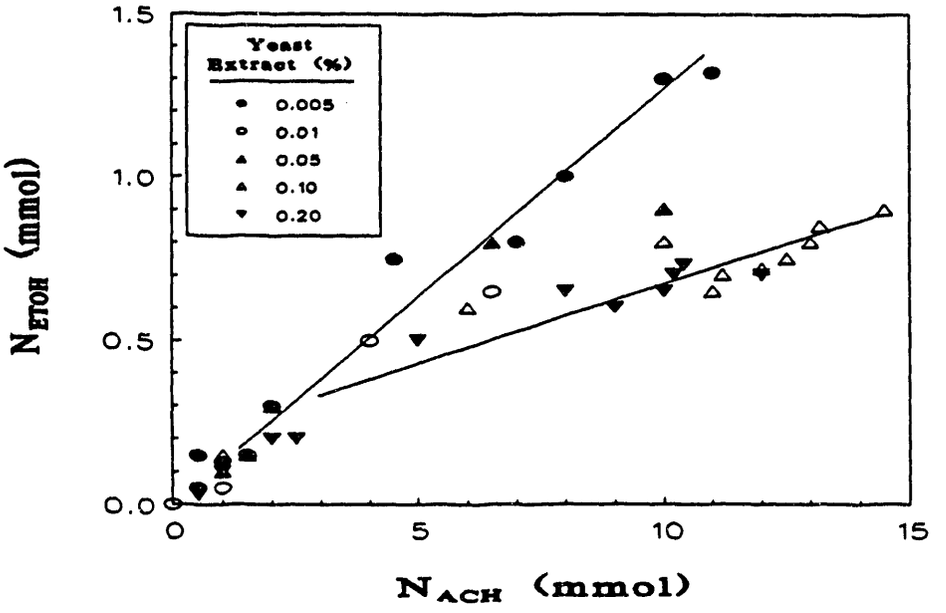

Figure 3.2. Effect of yeast extract concentration on the product ratio for *C. ljungdahlii*.

steady-state, in a continuous stirred-tank reactor that is fed a cell-free solution, it is necessary that the specific growth rate equals the dilution rate.[11] Therefore, low growth rates can be achieved by using low dilution rates. The molar product ratio of ethanol to acetate achieved at various liquid flow rates in a New Brunswick Bioflo C.30 chemostat specially adapted for anaerobic operation is shown in Figure 3.3. As is observed, when all other variables are held constant, the lower dilution rates yielded the higher ratios. Values of 0.6-0.7 mol of ethanol/mol of acetate were maintained for over 20 days.

Better product ratios have been obtained in other continuous experimental studies where a combination of factors that are known to improve solventogenesis in other clostridial fermentations are applied. The product ratios obtained in two other runs are shown in Figures 3.4 and 3.5. A combination of sudden decreases in yeast extract concentration with decreases in dilution rates led to oscillatory behavior with ratios as high as 1.2 mol ethanol/mol acetate. Even higher ratios (as much as 2.8 mol ethanol/mol acetate) were achieved by employing a sudden decrease in the operating pH from 5.0 to 4.0, followed by a decrease in the dilution rate. The sudden change in operating pH, however, may have brought about an induction of sporogenesis in the culture and is discussed below.

This same pH shift technique was repeated while using a lower yeast extract concentration in the liquid medium (0.02%). These experiments were carried out after a long period of culture acclimation, so that liquid flow rates over 600 mL/day were possible as opposed to flow rates of 200-400 mL/day in previous studies. The major significance of the latter results is in the increase in specific productivity of the culture with acclimation. The

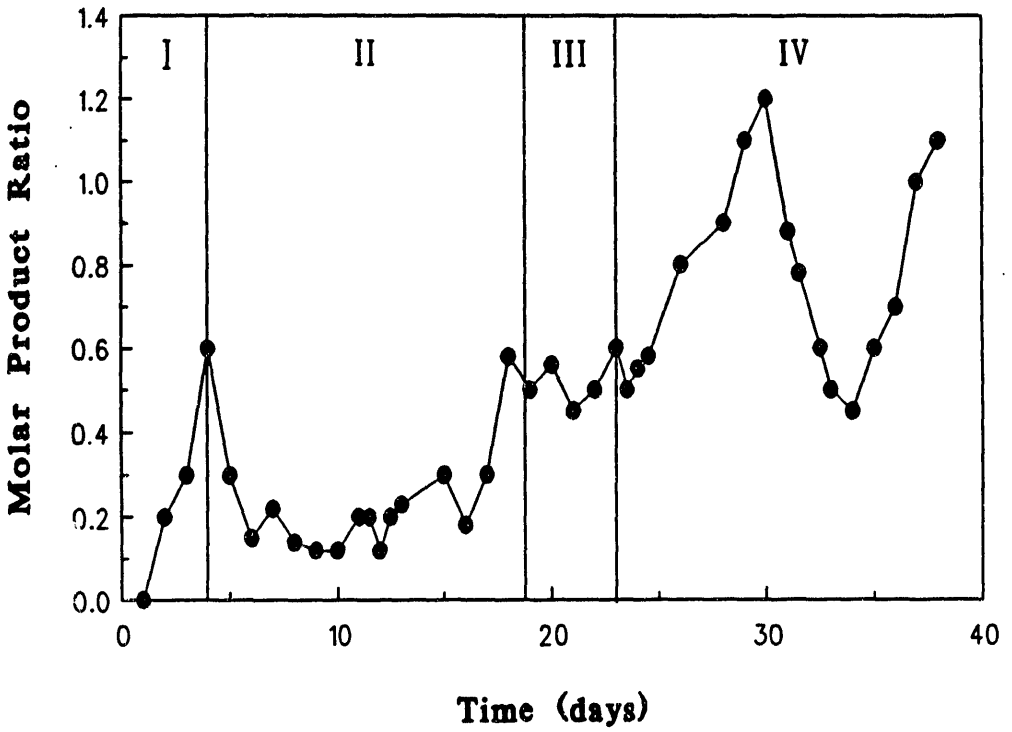

Figure 3.3. Molar product ratio for *C. ljungdahlii* in a CSTR.

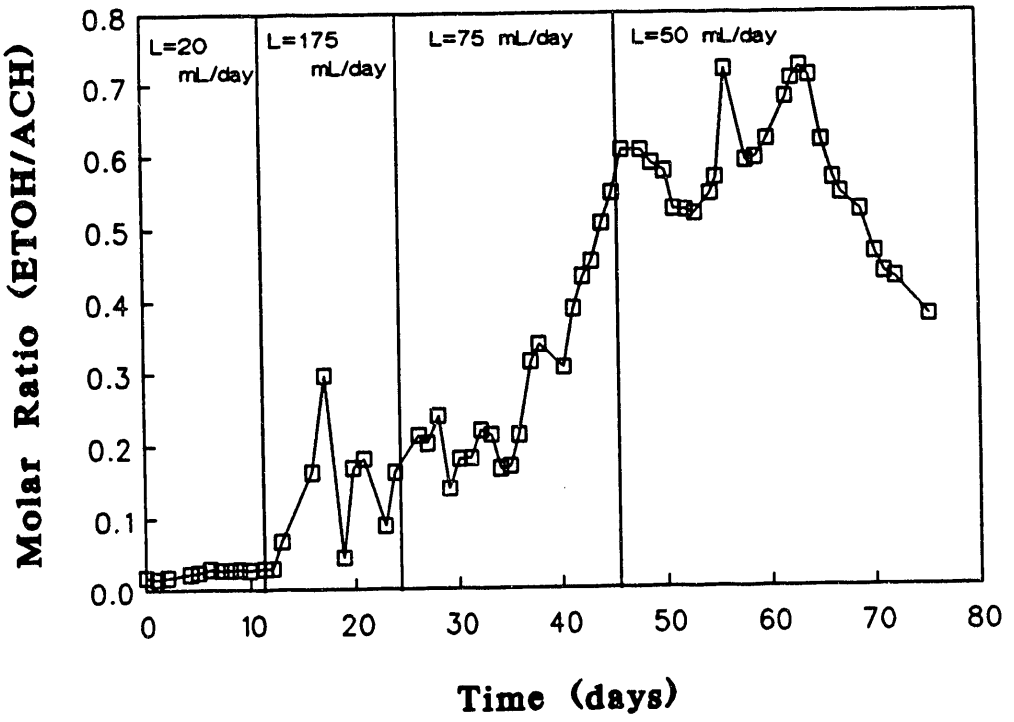

Figure 3.4. Molar product ratio versus liquid flow rate in a CSTR.

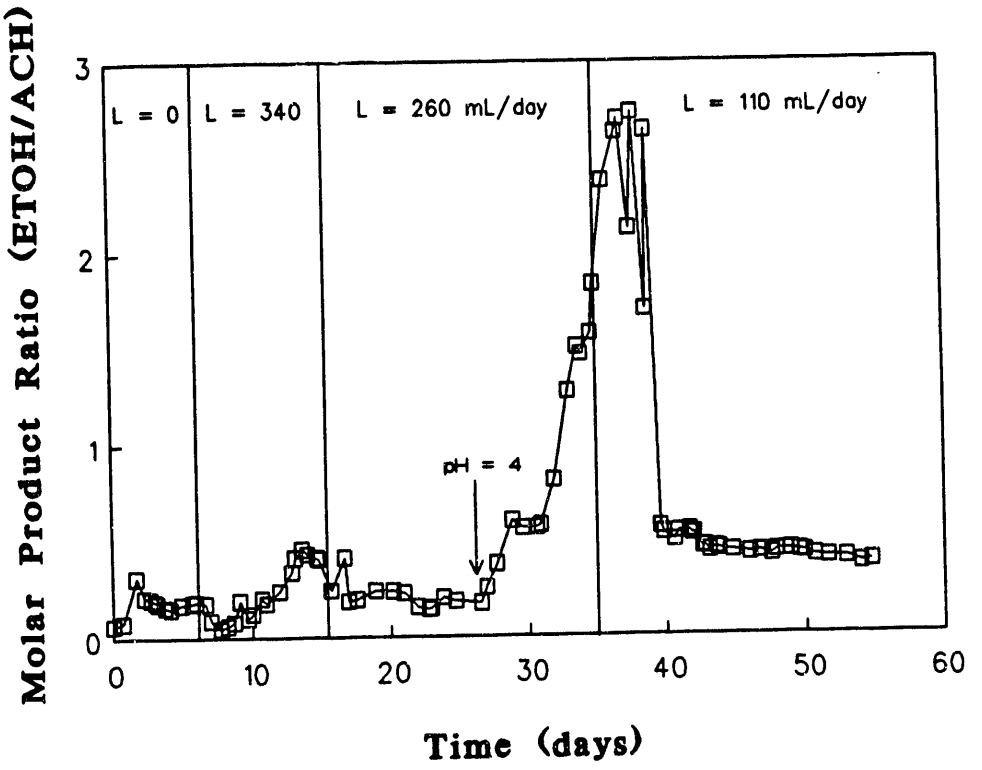

Figure 3.5. Molar product ratio in a CSTR with yeast extract depletion.

specific productivity may be defined as the quantity of ethanol produced per unit of cells per unit time, typically in units of mmol ethanol/gcell•day. This parameter sets the quantity of ethanol that can be produced from a culture (per cell) in a given reactor volume. Previously a peak ethanol concentration of 1.6 g/L was achieved at a liquid flow rate of 60 mL/day. In the latter work, a peak ethanol concentration of 0.7 g/L was reached at a liquid flow rate of 530 mL/day. The productivity in the latter work was 178 mmol EtOH/gcell•day, which is an 800 percent improvement in the quantity of ethanol produced per cell. Improvements such as this will significantly enhance process economics in a commercial production scheme.

3.2.2 The Use of Reducing Agents as a Method to Improve the Ethanol/Acetate Product Ratio

Several researchers have shown that the presence of reducing agents in the liquid media of clostridial fermentations has brought about an increase in solvent formation in the product stream at the expense of acid formation. Rao and Mutharasan,[12] for example, showed a five-fold increase in acetone yields from glucose at pH 5 when adding methyl viologen to a culture of *C. acetobutylicum*. In a similar study, the addition of benzyl viologen to the media in a *C. acetobutylicum* fermentation was responsible for increasing the quantity of butanol in the product stream to over 90% of the total solvents formed. Acid formation decreased significantly in favor of butanol formation. Other reducing agents produced similar results on *Clostridium* strains, including sodium sulfide, cysteine hydrochloride, sodium thioglycolate and electrochemical energy.[13-16] Reducing agents apparently cause altered electron flow, which direct carbon flow and acid to alcohol production. Reducing equivalents are directed to the formation of NADH which, in turn, resulted in increased alcohol production.

Since the bacteria isolated at the University of Arkansas for the conversion of CO, H_2 and CO_2 to ethanol and acetate is also a *Clostridium*, it was felt that the addition of reducing agents to the medium might also result in increased solvent (ethanol) production at the expense of acid formation. Batch experiments were thus carried out with small quantities of reducing agents (30, 50 and 100 ppm) added to the feed in order to assess the feasibility of increasing the ethanol to acetate ratio through reducing agent addition. The experiment carried out with 100 ppm of reducing agents resulted in very limited growth in all cases. On the other hand, 50 ppm and 30 ppm concentrations were successful in improving the ethanol to acetate ratio in some cases, as is shown in Table 3.1. The flask containing benzyl viologen at a concentration of 30 ppm produced 3.7 mmol of ethanol with a product ratio of 1.1, the highest ratio observed in batch experiments so far. It is interesting to mention that those reducing agents that improved the product ratio always resulted in slower growth rates of the bacteria, as could be expected from decreased ATP formation.

Table 3.1

Peak Levels for Ethanol Production and the Molar Ratio (ETOH/ACH) at 30 and 50 ppm Reducing Agent Concentrations

	(50 ppm)		(30 ppm)	
Reducing agent	ETOH(mmol)	ETOH/ACH	ETOH(mmol)	ETOH/ACH
Control	0.60	0.12	1.40	0.24
Sodium thioglycolate	1.30	0.20	1.30	0.25
Ascorbic acid	1.50	0.24	1.50	0.25
Methyl Viologen	1.90	0.20	2.50	0.40
Benzyl Viologen	1.25	0.21	3.70	1.10

3.2.3 Induction of Sporulation

Recently, the connection between sporulation and solventogenesis has been the subject of extensive studies, both in batch cultures[17-19] and chemostat cultures.[10,20] Under certain conditions, which are strain-dependent, a shift of the bacteria into a sporulation phase occurs which is accompanied by morphological changes (elongation of the cells) and the production of solvents rather than acids. In some cases, such as *C. thermosaccharolyticum*, an uptake of previously produced acetate takes place during sporulation.[21] The selection of two classes of mutants, the *cls* and the *spo* mutants of *C. acetobutylicum*, has confirmed the relationship between sporulation and solventogenesis. The *cls* mutants are unable to form a clostridial stage and cannot switch to solventogenesis. The *spo* mutants, however, blocked at a later stage in sporogenesis, can all produce solvents.[17]

The conditions that cause the onset of sporulation and solventogenesis vary among the clostridial strains. In the case of *C. thermosaccharolyticum*, significant ethanol production and elongated cell formation both require a combined signal of a specific carbon source (L-arabinose or L-xylose), lower pH and a restricted supply rate of the energy source.[22] In the case of *C. acetobutylicum*, switching to the solventogenic phase and differentiation to the clostridial stage requires the presence of glucose and nitrogen, low pH and a minimum acetate and butyrate concentration. It has also been observed that, in general, good sporulation can be induced in batch culture using carbon sources that tend to reduce the bacterial growth rate.[23]

Experiments have been conducted with *C. ljungdahlii* grown in basal media at pH 5.0 with a 0.01% concentration of various carbohydrates (starch, galactose, rhamnose and cellobiose) in the presence of synthesis gas. Table 3.2 summarizes the results obtained for each of the nutrient studies, along with the maximum values obtained for cell concentration, ethanol concentration and molar product ratios. As noted, the highest product ratios were obtained for cellobiose with product ratios over 3 times the ratio obtained in the presence of yeast extract. Ethanol and cell concentrations were highest in the presence of cellobiose and galactose, where the ethanol concentrations were over 4 times the value obtained in the presence of yeast extract.

Table 3.2

Summary of Results with Nutrient Sources
Bringing About Sporulation

Nutrient	Cell Conc (mg/L)	ETOH (mmol)	ETOH/ACH molar ratio
Yeast Extract	140	0.13	0.13
Cellobiose	170	0.56	0.45
Rhamnose	135	0.31	0.31
Galactose	168	0.53	0.36
Starch	130	0.27	0.36

4.0 MATERIALS AND METHODS

4.1 Organism and Medium

Clostridium ljungdahlii, Strain PETC, was originally isolated from chicken waste in the University of Arkansas laboratories, and later identified and characterized by Dr. R. S. Tanner, University of Oklahoma, Department of Botany and Microbiology. The culture was stored in a non-shaking incubator (Precision Scientific, Chicago, IL) at pH 5 and 37°C on basal medium (see

Table 4.1) and synthesis gas (65% CO, 24% H_2, and 11% CO_2), and transferred every two weeks. The medium of Table 4.1 was also used in most of the early experimental studies. However, in several studies the yeast extract concentration was varied or eliminated. In other studies, a minimal medium modified from the undefined medium of Savage and Drake[26] without amino acids was utilized.

Table 4.1

Basal Medium for C. ljungdahlii

	per 100 mL
Pfennig's mineral solution[24]	5.0 mL
B-vitamins[25]	0.5 mL
Yeast extract	0.1 g
Pfennig's trace metal solution[25]	0.1 mL
Cysteine-HCl, 2.5% solution	2.0 mL
Resazurin, 0.1% solution	0.1 mL

The specific components of the basal medium (without yeast extract) are shown in Table 4.2. As noted, the medium contained a wide variety of salts, vitamins and trace metals. The medium composition employed in later studies where the effects of medium composition are studied will be presented in the results and discussion.

4.2 General Laboratory Procedures

Detailed procedures for inoculation, gas addition and gas and liquid sampling are shown in Appendices A2-A4. These procedures were developed after several months of refinement and modification. The anaerobic techniques employed are essentially those of Hungate,[27] as modified by Bryant[28] and Balch and Wolfe.[29]

Table 4.2

Basal Medium Composition*

Constituent		Concentration (mg/L)
Pfennig Minerals		
	KH_2PO_4	500
	$MgCl_2 \cdot 6H_2O$	330
	NaCl	400
	NH_4Cl	400
	$CaCl_2 \cdot 2H_2O$	50
Pfennig Trace Metals		
	$ZnSO_4 \cdot 7H_2O$	0.100
	$MnCl_2 \cdot 4H_2O$	0.030
	H_3BO_3	0.300
	$CoCl_2 \cdot 6H_2O$	0.200
	$CuCl_2 \cdot H_2O$	0.010
	$NiCl_2 \cdot 6H_2O$	0.020
	$Na_2MoO_4 \cdot 2H_2O$	0.030
	$FeCl_2 \cdot 4H_2O$	1.500
	Na_2SeO_3	0.010
B Vitamins		
	Biotin	0.100
	Folic Acid	0.100
	Pyridoxal HCl	0.050
	Lipoic a.(Thiotic a.)	0.300
	Riboflavin	0.250
	Thiamine HCl	0.250
	Ca-D-Pantothenate	0.250
	Cyanocobalamin	0.250
	P-aminobenzoic acid	0.250
	Nicotinic acid	0.250
Cysteine HCl		490

*resazurin also added as indicator of anaerobicity

The development of procedures for quantitatively using gas substrates (CO, CO_2/H_2) with *Clostridium* sp. was necessary. An outline of the procedures for quantitative gas utilization is shown in Appendix B.

4.2.1 Batch Equipment and Procedures

After preparation, the medium (200 mL per bottle) was then transferred to bottles 1216 ± 2 mL in total volume. In some cases, smaller bottles (150 mL nominal volume) were substituted for the 1200 mL bottles. The bottles were sealed with butyl rubber stoppers and aluminum seals. The bottles were then autoclaved at 121°C for 20 minutes.

A seed culture was started in a smaller bottle, approximately 157.5 mL in volume. The composition of the seed culture medium was the same as described above. The culture was typically grown for 13 days in the presence of 1 atm of synthesis gas with one replacement of the gas phase in this period.

Once the seed culture was prepared, a reducing solution was added to each bottle and left in the shaker incubator for about 15 minutes to allow for complete oxygen removal and temperature acclimation. A 10 mL aliquot of the seed culture was then aseptically added to each bottle. The bottles with desired operating pressures below atmospheric pressure gauge were first flushed with helium, followed by synthesis gas addition with a syringe. The bottles with desired pressures at or above atmospheric pressure were flushed directly with the synthesis gas mixture (24% H_2, 65% CO, and 11% CO_2) and then adjusted to the final desired pressure with the help of a manometer in the inlet gas line. Argon (200 mL) at atmospheric conditions were then introduced into each bottle to serve as the inert gas for the component analysis. The inert gas allowed the determination with high accuracy the changes in total pressure inside the bottles and thus the total amount of each component in the

gas phase. The bottles were left in the shaker incubator (100 rpm) at 37°C during the experiment. Sampling for gas composition, optical density, pH, acetate, and ethanol was carried out at adequate intervals.

In later batch experiments, approximate pH control was achieved in the bottles by base or acid addition following sampling. A BASIC program, CORRPH, written by Dr. T. Klasson was used to estimate the volume of sodium hydroxide solution required to correct to the desired pH. CORRPH assumes an acetate/acetic acid buffer and calculates the required volume of several base solutions for neutralization of the fermentation broth to a target pH. Required inputs to the program are the acetate concentration, pH, liquid volume and target pH. It is therefore necessary to determine liquid product concentrations at the time of sampling so that the pH can be successfully controlled.

4.2.2 Chemostat Equipment and Procedures

A New Brunswick Bioflo C.30 chemostat was adapted for use under anaerobic conditions with continuous flow of gas. The chemostat was actually a semibatch reactor with continuous pH control. Figure 4.1 shows a schematic diagram of the experimental system. The reactor vessel was made of Pyrex glass, 750 mL nominal volume. Agitation was provided by magnetic coupling in the range of 200-1000 rpm. Verification of the agitation level indicator against a tachometer has shown no significant deviation. The system was equipped with temperature and pH control, and had gas flow meters.

The gas flowed from the pressurized tank through a fine metering valve and rotameter into the reactor. A large capacity oxygen trap, an oxygen indicator column and a filter were installed in the gas line to eliminate all traces of oxygen from the synthetic gas feed, and to avoid contamination. A 1

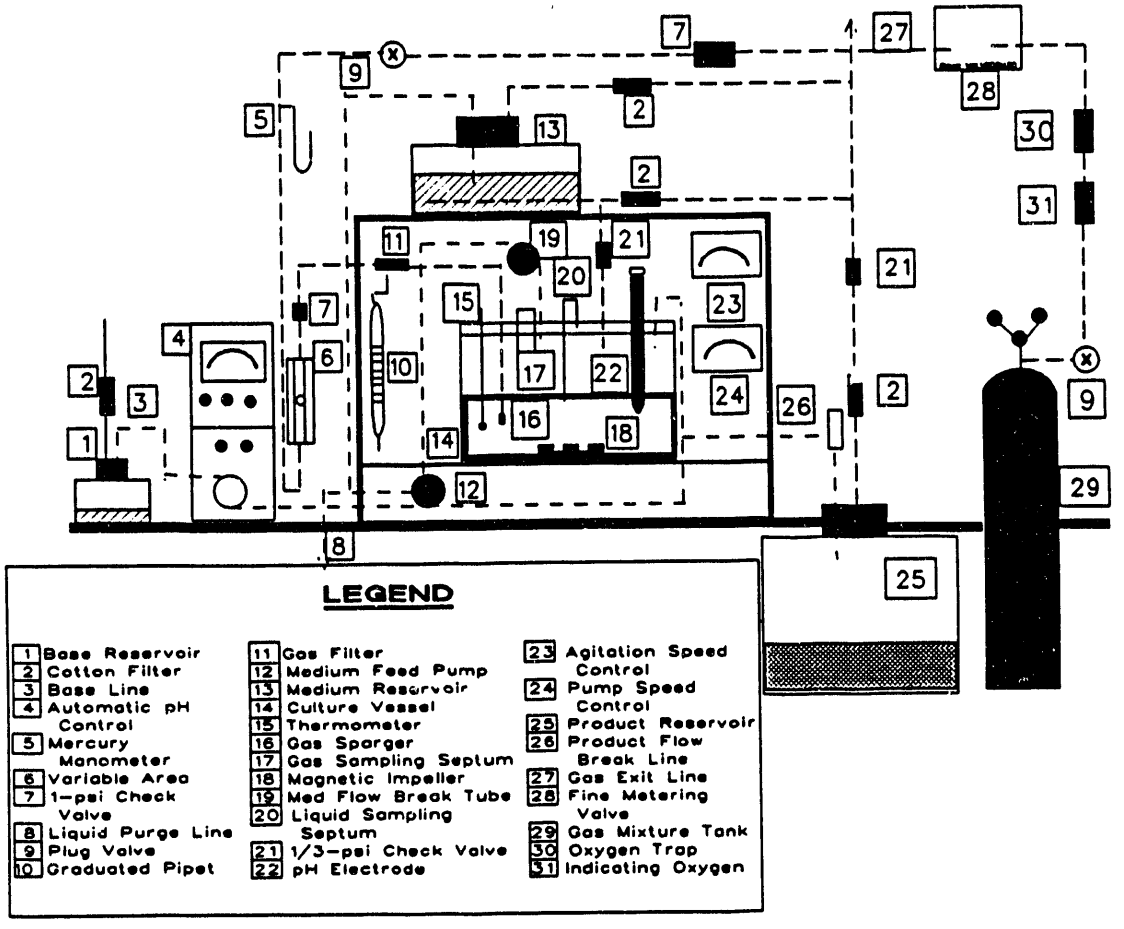

Figure 4.1. Schematic of the chemostat fermentation system.

psig check valve was placed before the gas sparger to help stabilize the flow at the very low flow rates employed. The gas exited the system either through the liquid overflow and finally from the product reservoir or directly from the reactor. In both cases, 1/3 psig check valves were located in the exit gas line to help maintain the system slightly above atmospheric pressure. This arrangement prevented any air leaks into the reactor system. All tubing connections were made of butyl rubber or stainless steel.

The anaerobic techniques for the start-up of the chemostat system and the preparation of media used in the studies were slightly different from those used in traditional batch culture. The feed reservoir and reactor vessel, filled with medium, as well as the product reservoir, empty, were autoclaved separately. The medium contained all of the required components except the reducing agent. A large cotton filter attached by a screw cap to the vessels allowed for pressure equilibrium inside the autoclave. After autoclaving, an oxygen free mixture of nitrogen and carbon dioxide was introduced into each vessel until they cooled. Enough carbon dioxide was bubbled into the media solutions to make up for that lost during autoclaving by disproportioning of biocarbonate into carbonate and carbon dioxide. When cool, the media solutions were clear; any color was due to the added resazurin, which is blue when organic reducing matter such as yeast extract is not present or light red otherwise. The cotton filter was then replaced by previously sterilized screw cap with a septum and all lines in and out of the vessel were clamped.

The reactor vessel was then connected to the gas lines of the system and allowed to flow for about 8 hours prior to inoculation. The gas composition used in the continuous studies consisted of 19.28 percent H_2, 15.29 percent Ar, 55.59 percent CO and 9.89 percent CO_2. Other compositions may be used if

desired. The argon was used as an inert in determining conversion, as described previously. The medium in the reactor was then reduced by the addition of cysteine hydrochloride. Cysteine hydrochloride was chosen due to its adequacy in previous experiments. The standard redox potential achieved with cysteine (-210mV) is less negative than that of sodium sulfide (-571mV). In our system, cysteine hydrochloride has allowed growth and gas uptake to occur. Still, a careful study to determine the optimum reducing agent to use and its effects on the ratios of alcohol/acetate obtained will be required in the future. Five milliliters of stock culture was used as the inoculum. the reactor was then operated batchwise for the liquid and continuously for the gas (about 4.2 mL/min of gas flow rate) for 138 hours. The agitation rate was 400 rpm during this experiment.

The externally controlled variables in the system were the agitation level, the pH level, and gas flow rate. These parameters can be controlled in all experiments. Other variables expected to affect the performance of the system are nutrient level and addition of antifoam. Antifoam is required to avoid excessive foaming, and is added directly into the reactor at regular intervals or when considered necessary. Three to five drops from a needle was usually enough to provide a foam free liquid culture.

Sampling of the reactor gas composition was routinely carried out with gas-tight syringe through a setpum placed on top of the reactor vessel. Liquid samples were withdrawn directly from the reactor through an immersed tube ending in a septum on top of the reactor vessel and analyzed for cell and acetate concentrations. To avoid the emergence of a pink color in the sample which interferes with optical density measurements, a sterile syringe and a spectronic tube sealed with parafilm were flushed with an oxygen free gas

mixture prior to sampling. When dilutions are needed, a solution of approximately 0.05 weight percent $Na_2 \cdot 9H_2O$ was employed.

4.2.3 Cell Recycle System

In order to boost product concentrations in the existing CSTR, a cell recycle system has been constructed. This system should be able to maintain a higher cell concentration inside the reactor than in a comparable CSTR without cell recycle since part of the exiting broth is filtered with the cells and returned to the reactor. This corresponds to a CSTR system with different residence times for the cells and the liquid medium. Since filter clogging is one of the main obstacles in using cell recycle, a novel self-cleaning filtration system has been constructed (See Figure 4.2) which consists of two cycles, a "feed cycle" and a "filtration cycle." During the feed cycle, fresh feed is used to clear the filter as it enters the reactor. During the filtration cycle, the exiting liquid stream is filtered. The cells deposited on the filter are then returned to the reactor during the next feed cycle. Each cycle is approximately 1-2 min long. In order to further extend the life of the filter, the feed cycle is slightly longer than the filtration cycle, allowing a longer cleaning time. To maintain a constant volume in the CSTR, an overflow control is also used to adjust for the slightly higher feed rate. Thus, the total effluent will consist of a filtered and an unfiltered part, the filtered part being larger. This will assure cell renewal and removal of old or deal cells, a problem with immobilized cell systems.

4.3 Analytical Techniques

Standard analytical techniques used on a routine basis included cell density measurements using optical density, gas analysis using gas-solid chromatography, liquid analysis using gas-solid chromatography, and reaction pH. Each of these techniques is briefly discussed in Appendix C. Other

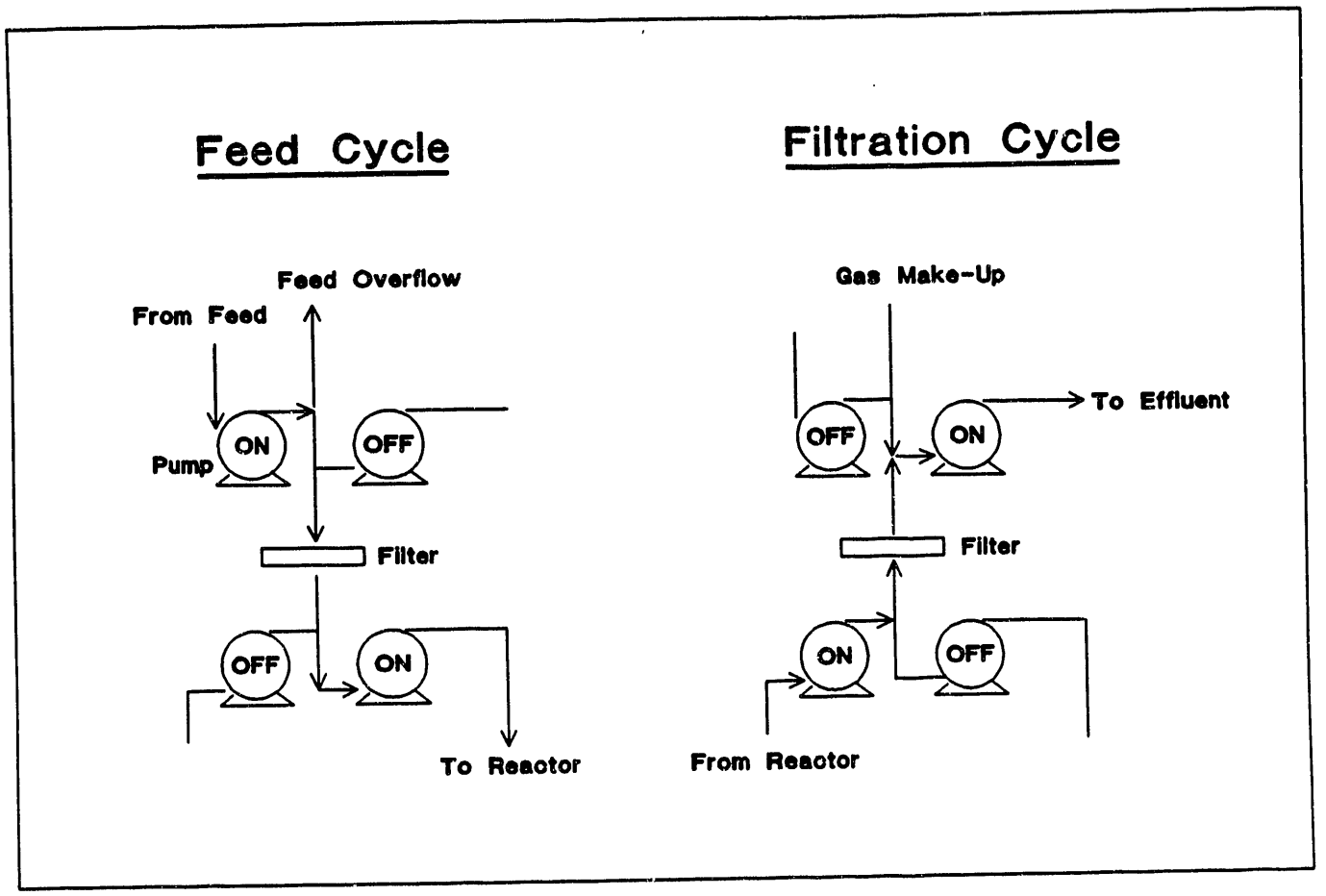

Figure 4.2. Pump and Filter Set-Up for Cell Recycle System.

analytical techniques used in culture identification are standard microbiological techniques and are not discussed.

5.0 PARAMETERS AFFECTING ETHANOL CONCENTRATION AND PRODUCT RATIO

5.1 The Effects of H_2 Partial Pressure on the Performance of *C. ljungdahlii*.

Batch experiments were carried out to measure the effects of increased H_2 partial pressure on growth, substrate uptake and product formation by *C. ljungdahlii*. The batch experiments were carried out in serum bottles inoculated with *C. ljungdahlii* into basal medium supplemented with 0.01 percent yeast extract. The experiments were carried out at an initial pH of 5.0 using cysteine hydrochloride as the reducing agent. The gas phase consisted of CO and CO_2 at 1 atm into which various partial pressures of H_2 were added. The partial pressures of H_2 utilized were 0.15, 0.2, 0.25, 0.29, and 0.40 atm, which correspond to 6, 8, 9.6, 11.4, and 15.4 mmole H_2. The quantity of CO was held constant in the experiments at 44 mol present.

The effects of increased H_2 partial pressure on the growth of *C. ljungdahlii* on CO, CO_2, H_2 is shown in Figure 5.1. As is noted in the figure, the H_2 partial pressure had essentially no effect on the rate of growth of *C. ljungdahlii* nor the maximum attained cell concentration at H_2 partial pressures up to 0.40 atm. However, the lag phases were different for the various partial pressures, although lag phase did not increase with H_2 partial pressure. It should be noted that the maximum cell concentration and the rate of growth after the lag phases were essentially identical. It is also noteworthy to mention the slight declines in cell concentration seen after the maximum was reached during the experiment. This result is probably due to the low level of yeast extract used in the experiment which limits growth but helps promote ethanol formation.

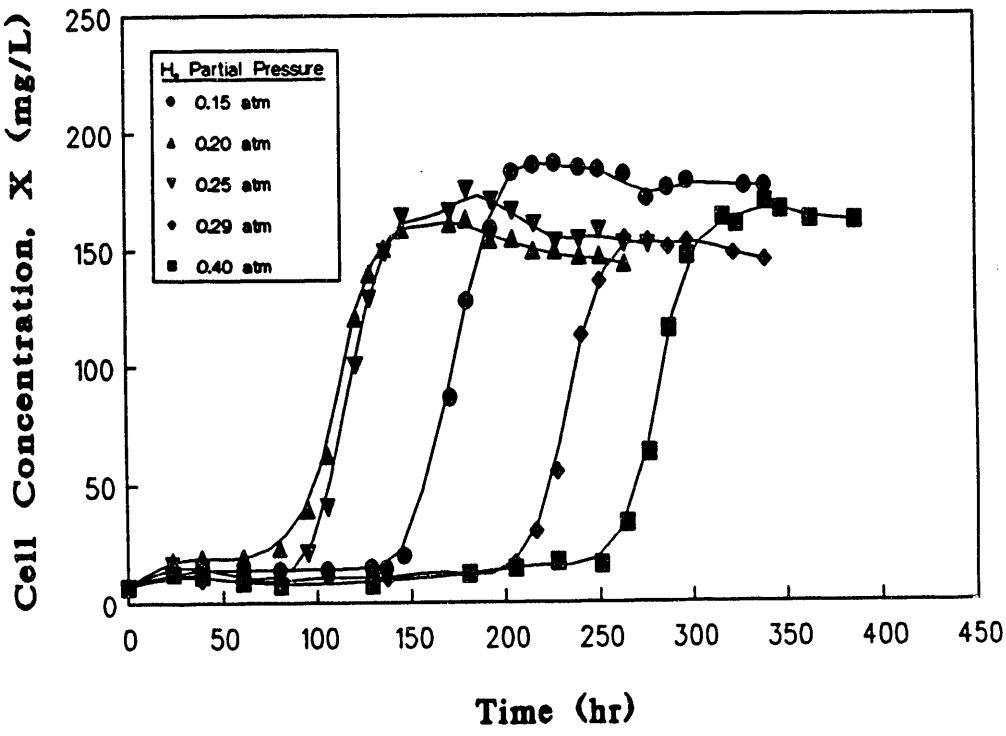

Figure 5.1. Effect of H_2 partial pressure on cell growth by *C. ljungdahlii* grown on CO and H_2.

The effect of increased H_2 partial pressure on CO uptake by the bacterium is shown in Figure 5.2. As was seen in Figure 5.1, all bottles showed the same rate of CO uptake after the lag phase, and reached complete CO utilization except at the highest H_2 partial pressure. The time required for the onset of CO utilization was about 145 hrs for a partial pressure of 0.15 atm, 80 hrs for partial pressures of 0.2 and 0.25 atm, 215 hrs for a partial pressure of 0.29 atm and 260 hrs for a partial pressure of 0.4 atm.

H_2 uptake in Figure 5.3 paralleled CO uptake in Figure 5.2. As is seen by the slopes of the curves in Figure 5.3, the rate of H_2 uptake increased with increasing H_2 partial pressure. The exception to this rule again occurs at a 0.15 atm partial pressure. This result agrees well with results presented previously for varying CO partial pressure. All bottles but one again yielded complete H_2 conversion. However, the onset of H_2 uptake occurred between 25 and 50 hrs after the onset of CO conversion. This result is contrary to the results obtained at lower H_2 partial pressures, but agrees with results obtained in continuous culture where H_2 utilization is often seen to stop when adequate utilization (90 percent conversion) of CO is not obtained. Thus, CO is the preferred substrate at higher H_2 partial pressures and in continuous culture.

The effects of increased H_2 partial pressure on ethanol and acetate formation by the bacterium are shown in Figures 5.4 and 5.5. As noted in comparing Figures 5.4 and 5.5, ethanol and acetate formation occurred at essentially the same time as the onset of growth and substrate uptake. The maximum ethanol concentrations increased with increasing partial pressure, except at a H_2 partial pressure of 0.15 atm (see Figure 5.4). The ethanol concentration decreased with time after reaching a maximum. If the results

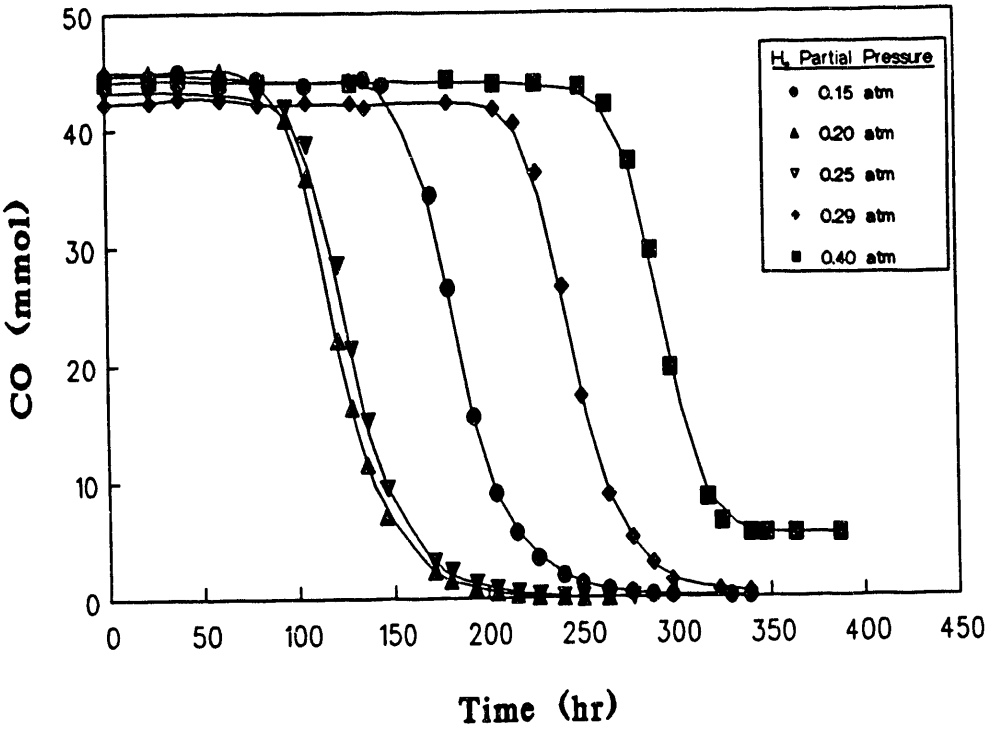

Figure 5.2. Effect of H_2 partial pressure on CO uptake by *C. ljungdahlii* grown on CO and H_2.

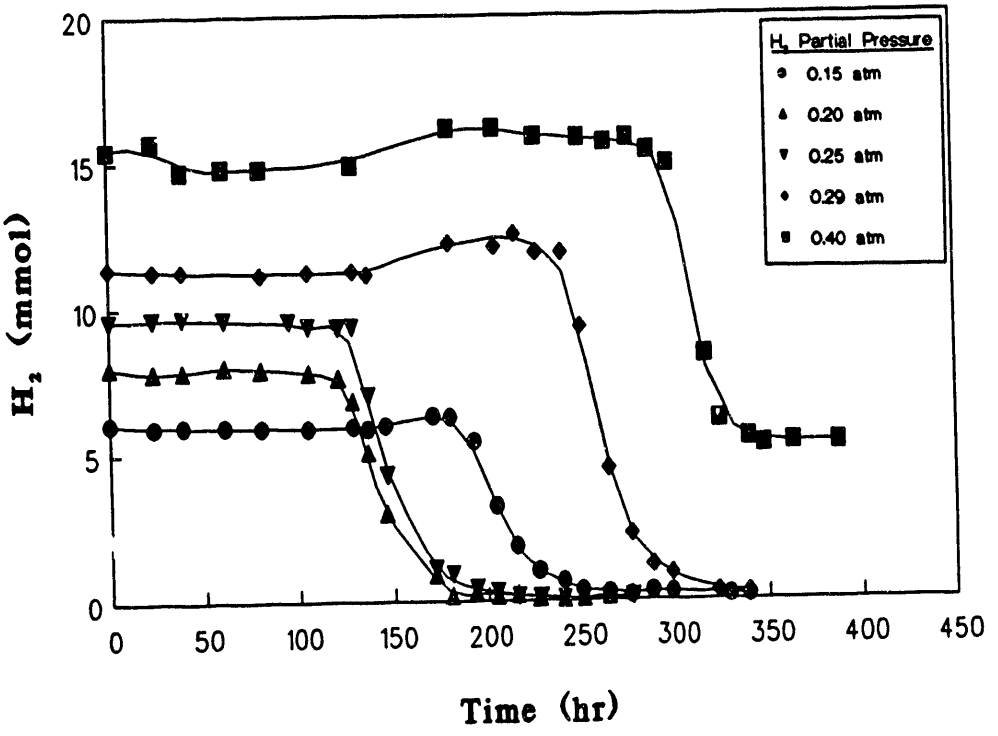

Figure 5.3.. Effect of H_2 partial pressure on H_2 uptake by *C. ljungdahlii* grown on CO and H_2.

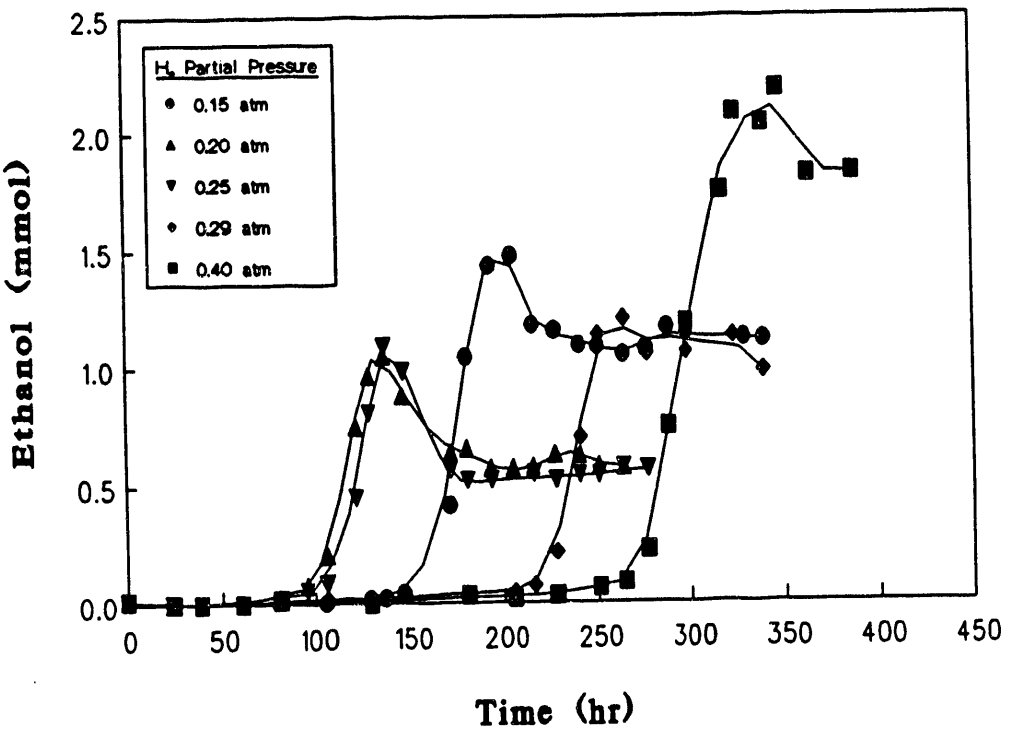

Figure 5.4. Effect of H_2 partial pressure on ethanol production by *C. ljungdahlii* grown on CO and H_2.

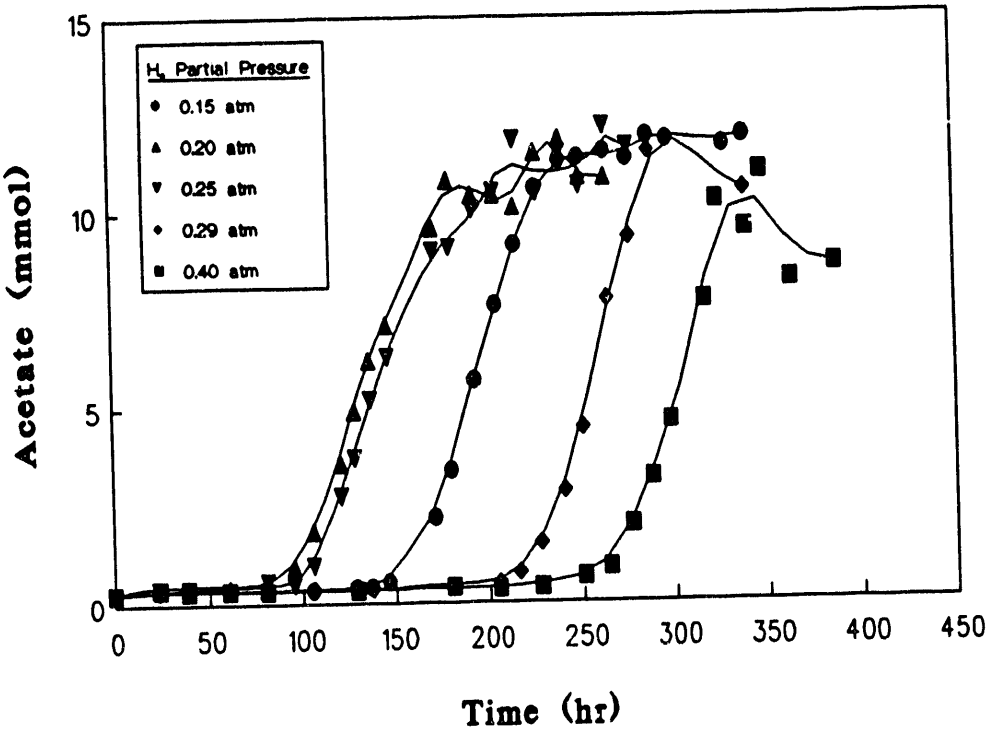

Figure 5.5. Effect of partial pressure on acetate production by *C. ljungdahlii* grown on CO and H_2.

obtained at H_2 partial pressure of 0.15 atm are excluded, it appears that increasing H_2 partial pressure resulted in increased ethanol formation. However, this increase in ethanol production could be attributed to additional substrate conversion from H_2 rather than a shift in reaction pathway from ethanol to acetate. A look at acetate formation should be useful in answering this question.

As is noted in Figure 5.5, a single maximum acetate concentration of about 11 mmol was obtained. The acetate concentration decreased after reaching a maximum at the highest partial pressure. Thus, by increasing the ethanol concentration in Figure 5.4 while the acetate concentration was constant (Figure 5.5), the ratio of ethanol to acetate increases with increasing H_2 partial pressure.

5.2 Effects of pH on Culture Performance in a Fed Batch Chemostat

Cell concentration, ethanol concentration and acetate concentration profiles for the fed batch (chemostat with continuous gas introduction only) runs at three pH levels are shown in Figure 5.6-5.8, respectively. As was mentioned previously, gas phase conversion profiles are not shown due to the scatter of the data obtained in this type of reaction system. Figure 5.6 clearly shows that high pH levels favor cell production over lower pH levels, although the profiles were nearly identical at pH 4.5 and pH 5.0. The maximum cell concentration at pH 5.0 was about 490 mg/L after 650 hr and the maximum at pH 4.0 was only 330 mg/L after 470 hr.

Figure 5.7 shows nearly identical ethanol concentration profiles at pH 4.0 and pH 4.5 (if the two data points at 220 and 260 hr for pH 4.5 are excluded). Furthermore, the profile run at pH 5.0 yielded a much lower maximum ethanol concentration than at pH 4.0 and pH 4.5. The maximum ethanol

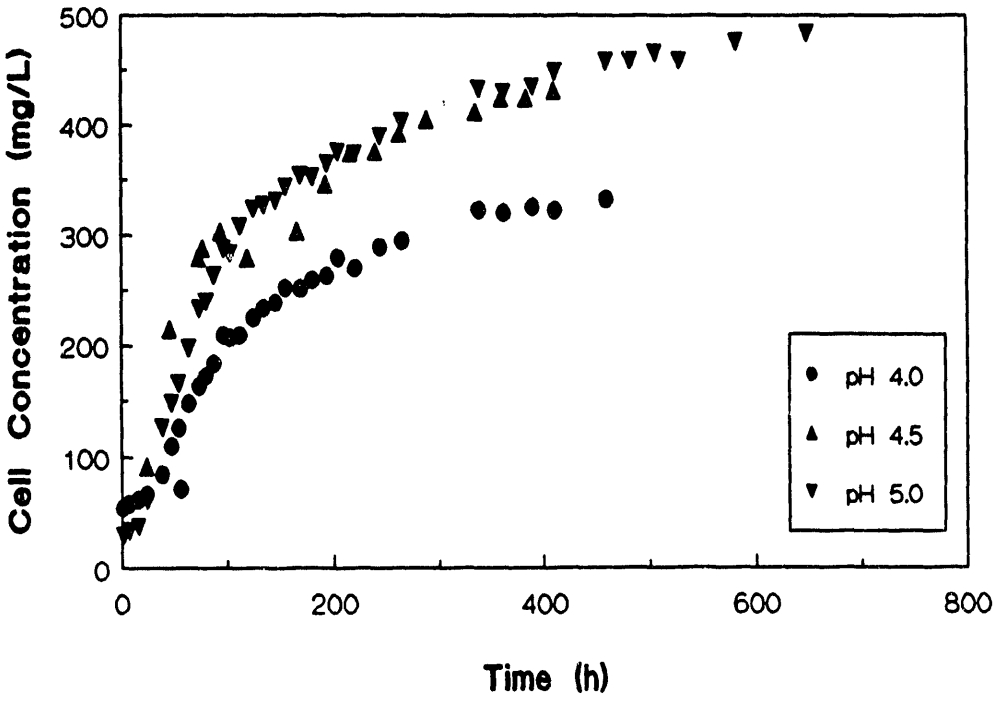

Figure 5.6. Cell concentration profiles for *C. ljungdahlii* on CO, CO_2, and H_2 at various controlled pH levels in a fed batch reactor.

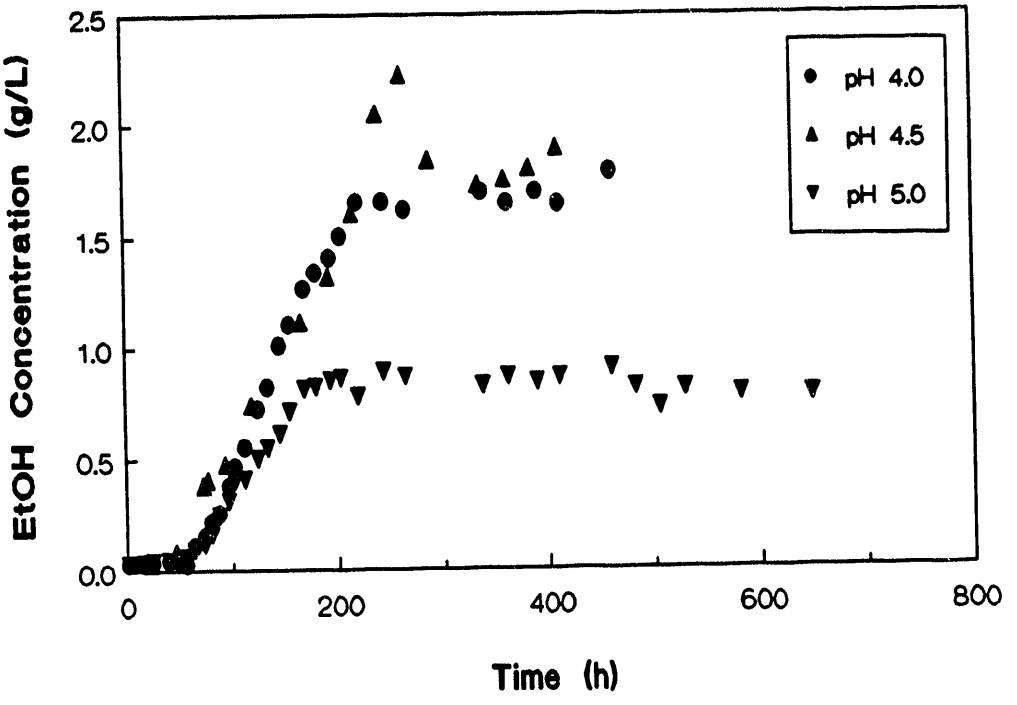

Figure 5.7. Ethanol concentration profiles for *C. ljungdahlii* on CO, CO_2, and H_2 at various controlled pH levels in a fed batch reactor.

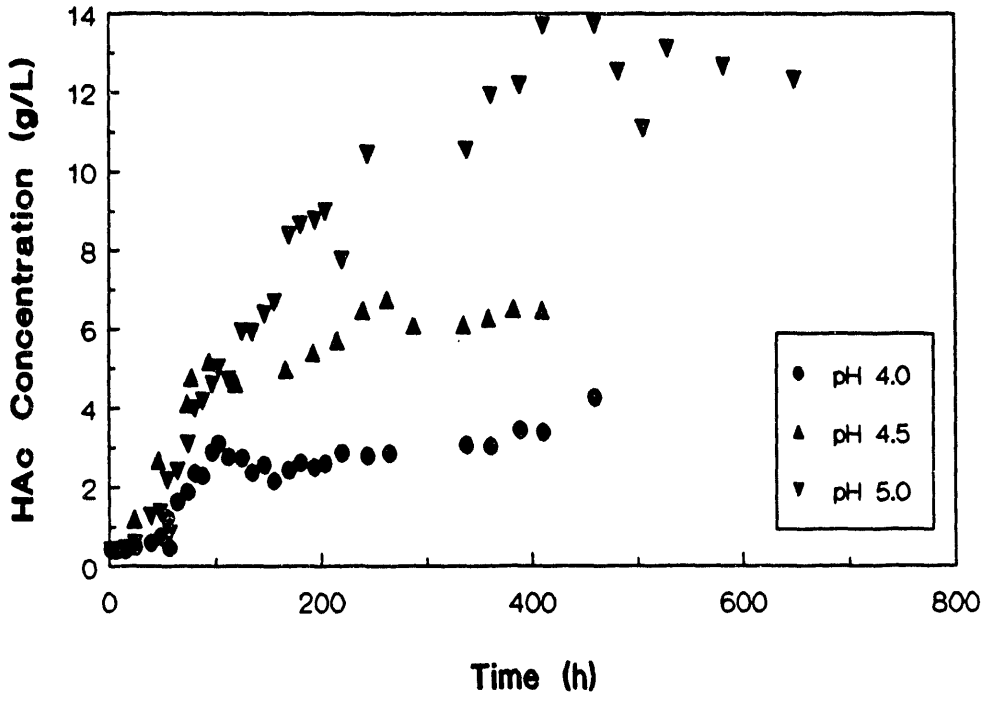

Figure 5.8. Acetate concentration profiles for *C. ljungdahlii* on CO, CO_2, and H_2 at various controlled pH levels in a fed batch reactor.

concentration at pH 5.0 was 0.8 g/L after only 180 hr and the maximum at pH 4.5 was about 1.8 g/L after 300 hr. The ethanol concentration was quite steady after reaching a maximum at a given pH level.

Figure 5.8 shows that the acetate concentration increased significantly with pH, reaching a maximum of 4.0 g/L after 470 hr at pH 4.0, a maximum of 6.0 g/L after 230 hr at pH 4.5 and a maximum of about 13 g/L after 400 hr at pH 5.0.

In comparing Figures 5.6-5.8, it is seen that the acetate concentration continued to increase after the maximum ethanol concentration was reached, indicating that, late in the fermentation, substrate was converted mainly to acetate. Also, it appears that acetate production was more closely related to growth and ethanol production was not growth related. This latter observation is consistent with results reported with other clostridia, where acid production was shown to be growth associated and ethanol production was shown to be non-growth associated.

The ethanol to acetate molar product ratio at the maximum ethanol concentration was 0.74 at pH 4.0, 0.39 at pH 4.5 and 0.12 at pH 5.0. The addition of other controlled parameters such as nutrients concentration, agitation rate, H_2 addition, etc. should increase this ratio significantly.

5.3 Effects of Yeast Extract on *C. ljungdahlii* Previously Grown in the Presence of H_2S

Experiments were performed on *C. ljungdahlii* previously grown in the presence of H_2S using various yeast extract concentrations ranging from 0 to 0.1% at pH 4.5. Previous experiments using varying yeast extract concentrations showed that high yeast extract concentrations promoted growth and acetate formation, while low yeast extract concentrations suppressed

growth while yielding increased ethanol concentrations. However, no experiments were carried out without the presence of yeast extract (except for the very small quantity transferred with the inoculum) or without careful pH control. Furthermore, it was felt that a culture that was stressed by first growing it in the presence of H_2S might aid in promoting ethanol production. Growth in the presence of H_2S was slowed significantly, although growth did not stop.

Figures 5.9-5.11 show cell concentration, ethanol concentration and acetate concentration profiles for varying yeast extract concentrations for the H_2S grown culture at pH 4.5. Although the cell concentration profiles were a bit scattered (see Figure 5.9), the cell concentration was seen to generally increase with increasing yeast extract concentration. The cell concentration leveled off at about 250 g/L when yeast extract was not present in the medium, while the leveled off cell concentration was about 400 g/L at a 0.1% yeast extract concentration. These cell concentration results are qualitatively the same as seen previously with other *C. ljungdahlii* cultures under less controlled pH conditions.

Figure 5.10 shows significantly increased ethanol concentrations with decreasing yeast extract concentration. All experiments showed a lag phase of nearly 300 hrs prior to the onset of a significant ethanol concentration that was not growth associated (refer to Figure 5.9 to see no similar lag phase with growth). The leveled off ethanol concentration was approximately 1 g/L at a yeast extract concentration of 0.1%, 1.5 g/L at a yeast extract concentration of 0.01%; 4.5 g/L at a 0.001% yeast extract concentration and about 8 g/L without yeast extract present in the medium. The ethanol concentration without the presence of yeast extract was the most variable

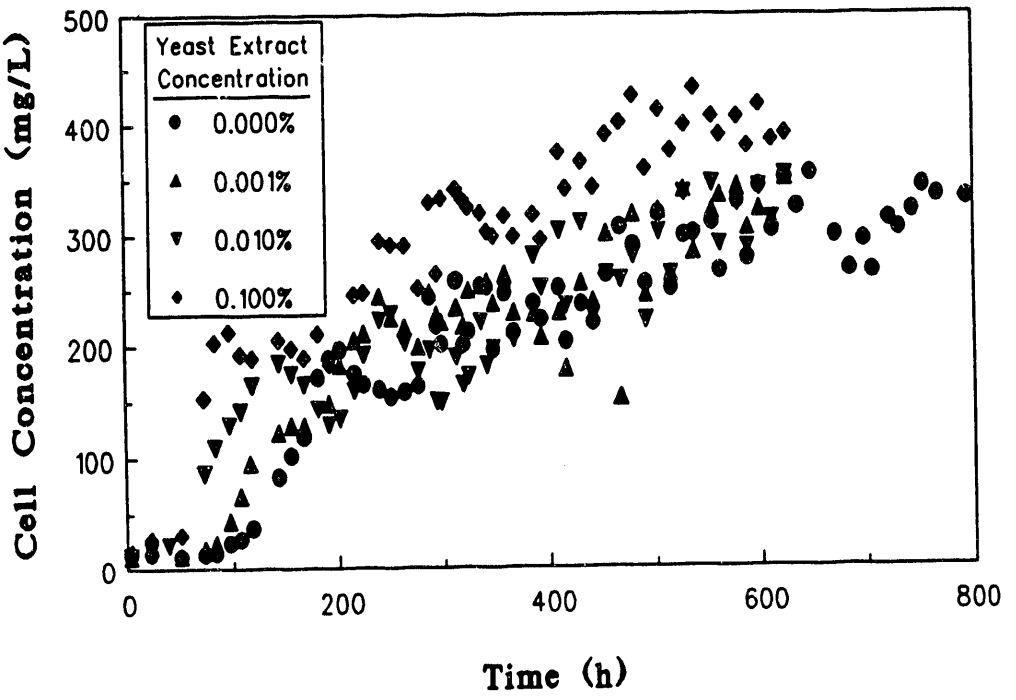

Figure 5.9. Effect of yeast extract on the growth of *C. ljungdahlii* previously grown in the presence of H_2S at pH 4.5.

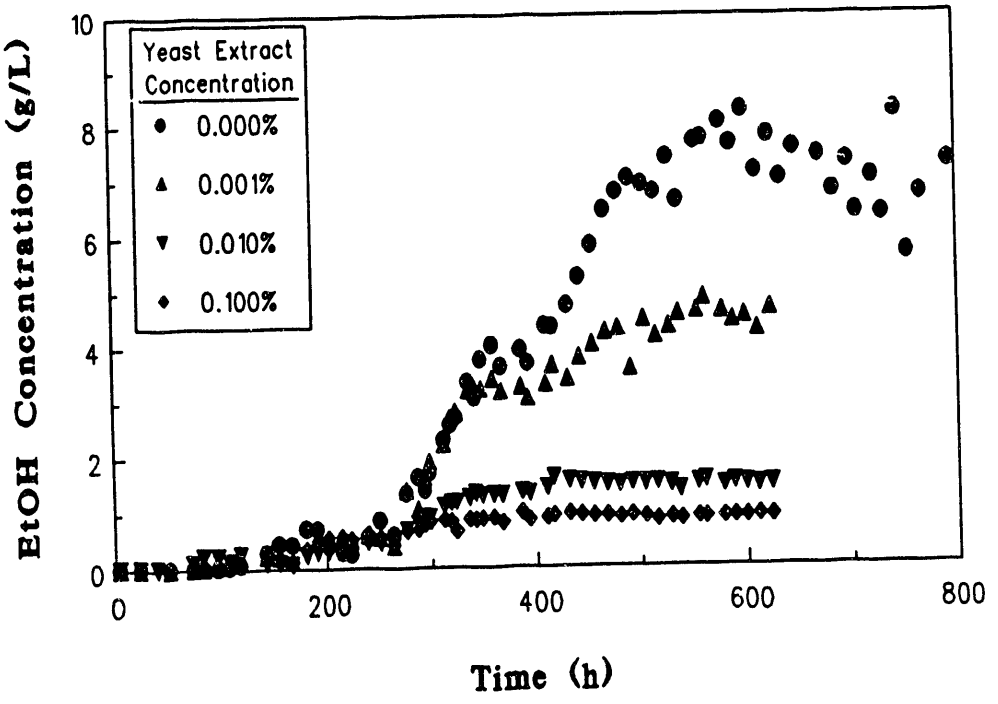

Figure 5.10. Effect of yeast extract on ethanol production by *C. ljungdahlii* previously grown in the presence of H_2S at pH 4.5.

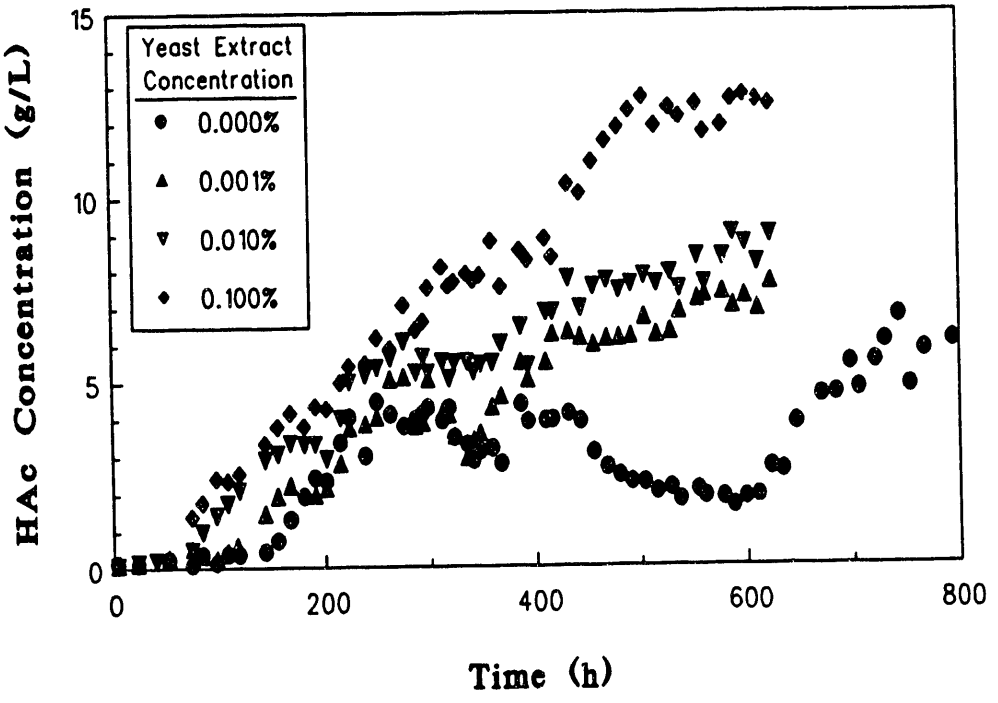

Figure 5.11. Effect of yeast extract on acetate production by *C. ljungdahlii* previously grown in the presence of H_2S at pH 4.5.

after "leveling off," possibly due to nutrient limitation or, at least, near limitation. Figure 5.11 shows essentially the opposite behavior for the acetate concentration profiles as was noted in Figure 5.10. Only a brief lag phase was seen, quite similar to the lag phase noted in Figure 5.9 with growth. The leveled off acetate concentration was approximately 13 g/L when using a 0.1% yeast extract concentration, was about 8 g/L with 0.01% yeast extract, was about 7 g/L with 0.001% yeast extract and was only 2 g/L when the ethanol concentration was 8 g/L without yeast extract in the medium. The "leveled off" acetate concentration without yeast extract was quite variable as was seen with the ethanol concentration.

The ethanol to acetate product ratio without yeast extract present reached a maximum of about 4.0, although the ratio dropped with time. This ratio is far in excess of any ratio previously presented in batch culture. The effects of previous culture conditions (grown in the presence of yeast extract) are uncertain, although it is intuitively felt that the elimination of yeast extract had a larger effect on product ratio than the previous culture conditions. A lower medium pH might have an even larger effect on the ethanol to acetate ratio.

5.4 The Performance of Various *C. ljungdahlii* Cultures with Varying Cysteine Hydrochloride Concentrations

Four different *C. ljungdahlii* cultures were used in experiments also evaluating the effects of the concentration of the reducing agent, cysteine hydrochloride, on culture performance. The cultures and their designations are as follows:

1. BIOB - a culture previously used in the second reactor of a two-stage CSTR system at pH 4
2. BIOB-10* - a culture previously exposed to NaCl

3. BH_2S - a culture previously exposed to H_2S

4. BIT - the original culture

The normal volume of the 2.5 percent cysteine hydrochloride used in the typical medium shown in Table 4.1 was 2.0 mL. In these studies, both 2.0 mL and 5.0 mL of 2.5 percent cysteine-HCl were utilized. Also, due to the success of previous studies without yeast extract in the medium, no yeast extract was employed in these studies.

Cell and product concentration profiles for the various *C. ljungdahlii* cultures in the presence of 2.0 mL of cysteine-HCl (and no yeast extract) are shown in Figures 5.12-5.14. The cell concentration profiles (see Figure 5.12) showed that the BIOB and BIOB-10* cultures grew the best, reaching a cell concentration of more than 250 mg/L. It should be remembered, however, that the maximum attainable cell concentrations (and, to a lesser extent, product concentrations) depend upon the inoculum levels and the condition of the cells in the inoculum. The maximum ethanol concentration reached (see Figure 5.13) was by the BIOB culture, reaching a concentration of more than 3 g/L (but far less than the 8 g/L level previously obtained). The acetate concentration profiles were all quite similar except for the BIT culture, (see Figure 5.14), which showed a maximum acetate concentration of slightly less than 1.5 g/L. The results of each of these experiments are summarized in Table 5.1.

Cell and product profiles for the cultures in the presence of 5.0 mL of cysteine-HCl (and no yeast extract) are shown in Figures 5.15-5.17. Higher cell concentrations were reached in these experiments (see Figure 5.15), reaching a level of nearly 400 mg/L for all three cultures. The maximum

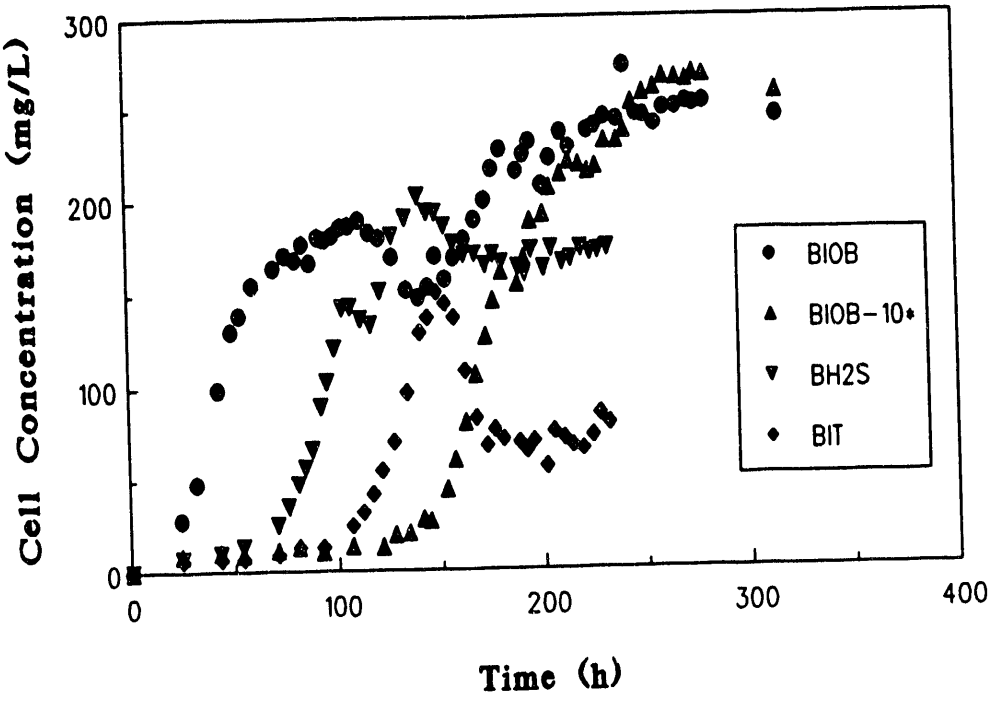

Figure 5.12. Cell concentration profiles for various *C. ljungdahlii* cultures (2.0 mL cysteine-HCl, no yeast extract).

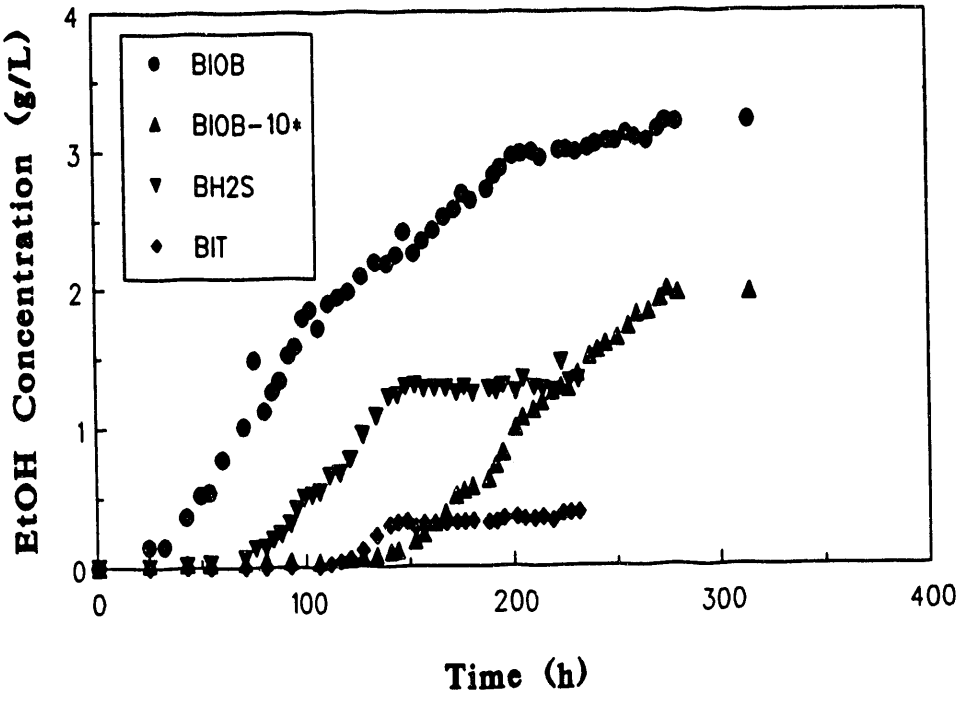

Figure 5.13. Ethanol concentration profiles for various *C. ljungdahlii* cultures (2.0 mL cysteine-HCl, no yeast extract).

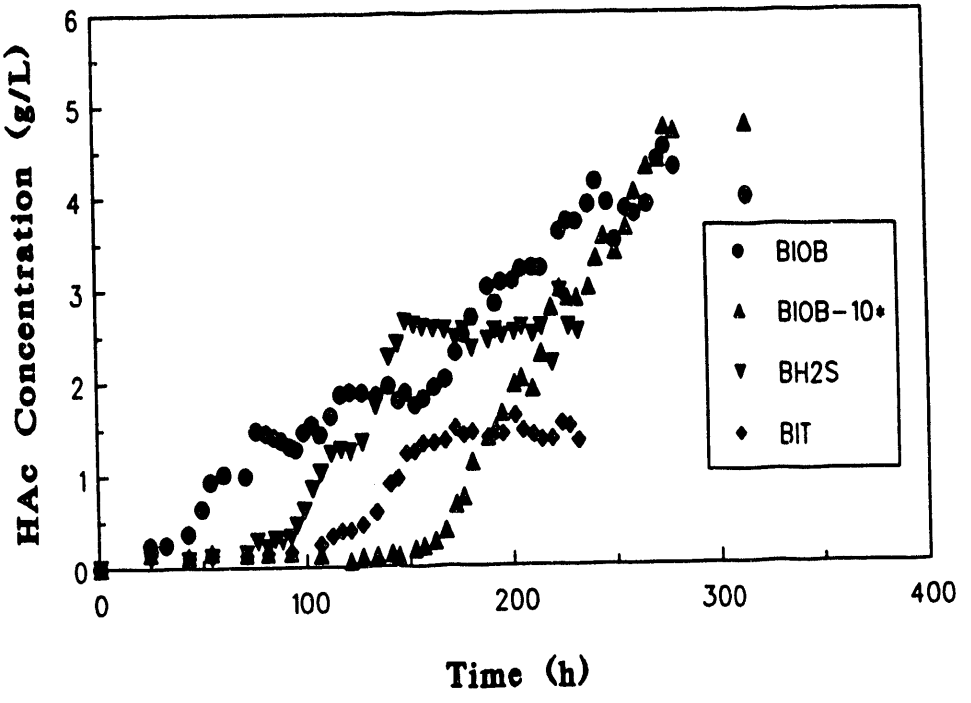

Figure 5.14. Acetate concentration profiles for various *C. ljungdahlii* cultures (2.0 mL cysteine-HCl, no yeast extract).

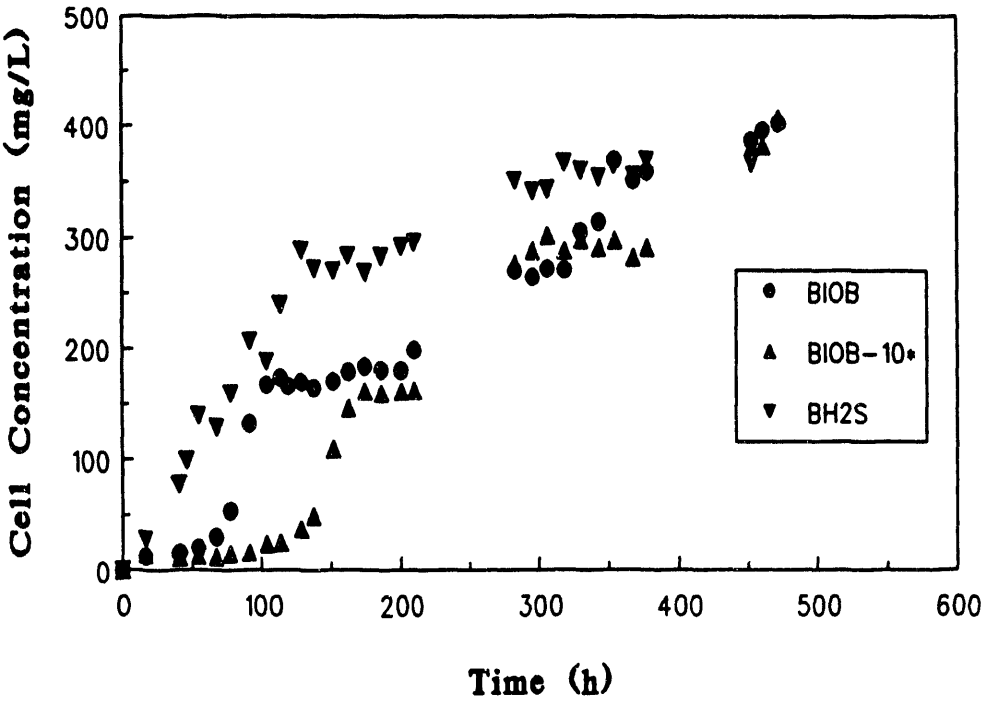

Figure 5.15. Cell concentration profiles for various *C. ljungdahlii* cultures (5.0 mL cysteine-HCl, no yeast extract).

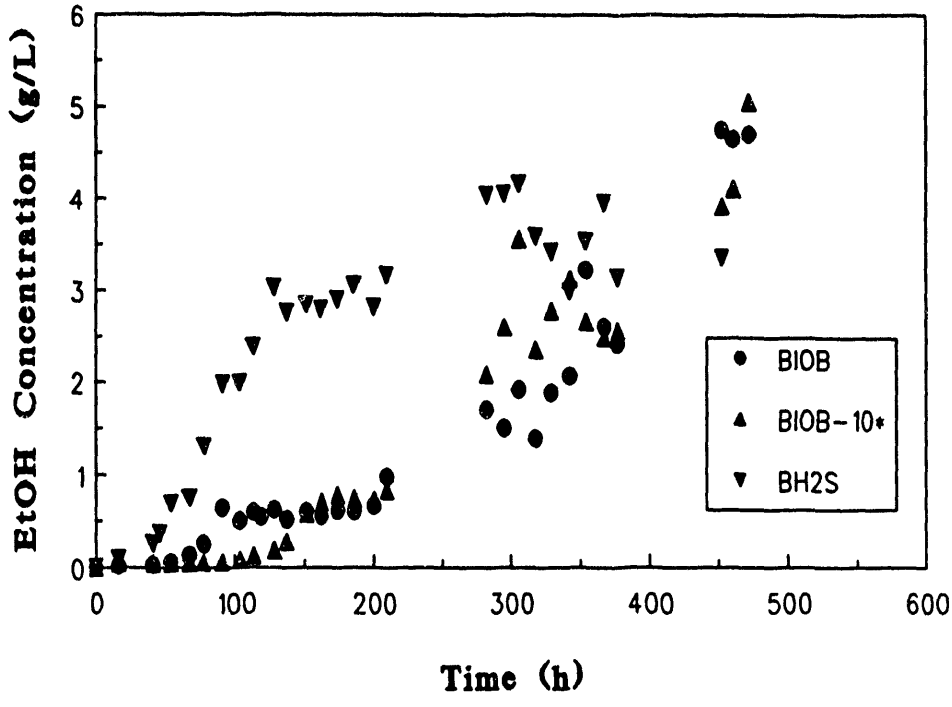

Figure 5.16. Ethanol concentration profiles for various *C. ljungdahlii* cultures (5.0 mL cysteine-HCl, no yeast extract).

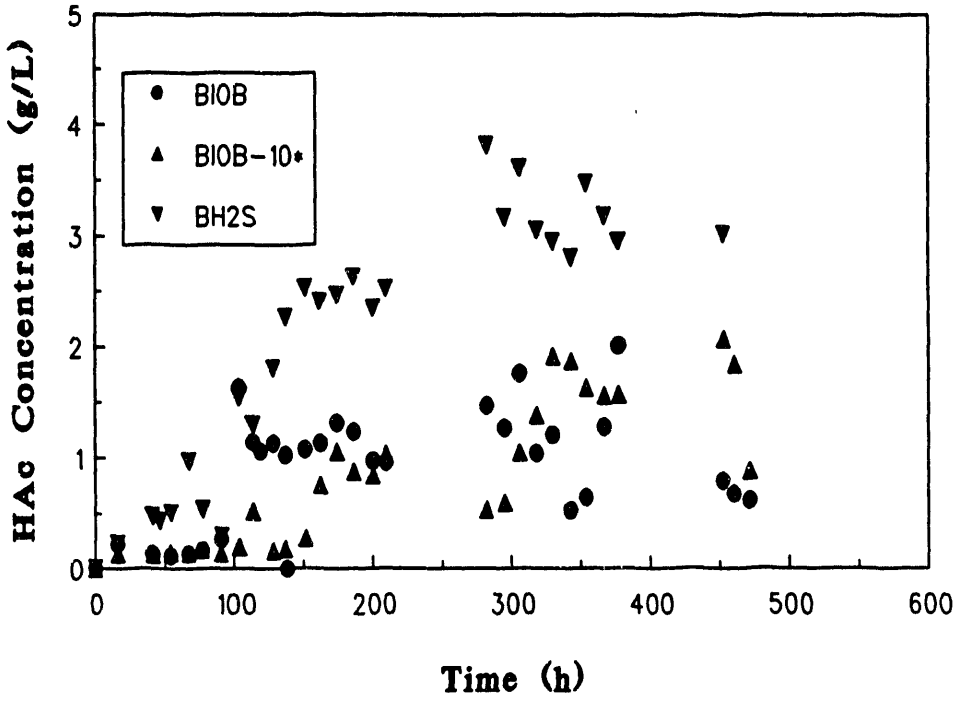

Figure 5.17. Acetate concentration profiles for various *C. ljungdahlii* cultures (5.0 mL cysteine-HCl, no yeast extract).

ethanol and acetate concentrations were also higher (see Figures 5.16 and 5.17, respectively), reaching levels of 5 g/L ethanol and over 3 g/L acetate. The results of these experiments are also summarized in Table 5.1.

In analyzing the results presented in Table 5.1, it is seen that the performance of the cultures varied considerably, perhaps due to the presence of differing quantities of cysteine-HCl, but also possibly due to variances in inocula and other culturing conditions. The BIOB-10* culture performed poorly in one experiment, while performing quite well in the other study. The results of the experiments in this study are thus not clear, and thus judged to be inconclusive. All cultures produce ethanol and acetate, with the previous history of the culture and culturing conditions affecting the ratio of ethanol to acetate.

Table 5.1

The Performance of Various C. ljungdahlii Cultures

Culture	"Leveled off" Concentration Cells (mg/L)	Ethanol (g/L)	Acetate (g/L)	"Leveled off" EtOH/HAc Ratio (mol/mol)
With 2.0 mL Cysteine-HCl				
BIOB	260	3.2	4.2	0.76
BIOB-10*	270	1.9	4.6	0.41
BH_2S	170	1.3	2.6	0.50
BIT	80	0.3	1.3	0.23
With 5.0 mL Cysteine-HCl				
BIOB	400	4.7	0.7[a]	6.71
BIOB-10*	380	5.0	0.8[a]	6.25
BH_2S	370	4.1	3.1[a]	1.32

[a] final value used due to high degree of variability
[b] difficult to estimate due to variance in acetate concentrations

5.5 Effects of pH Without Yeast Extract

Experiments were also performed on *C. ljungdahlii* using three pH levels between 4.0 and 5.0 without yeast extract present in the medium. This culture was the standard culture not subjected to any external stress such as H_2S.

Figures 5.18-5.20 show cell concentration, ethanol concentration and acetate concentration profiles for pH 4.0, 4.5 and 5.0 without yeast extract present in the medium. The cell concentration profiles were essentially the same as pH 4.0 and 4.5, reaching a leveled off cell concentration of 200-250 mg/L. The cell concentration was higher at pH 5.0, reaching a leveled off concentration of about 300 mg/L. The leveled off cell concentration without yeast extract at pH 4.5 in Figure 5.9 with the H_2S-exposed culture was about 400 mg/L. The difference in these observed cell concentrations could be due to differences in inocula or differences in culture behavior.

The effect of pH on the culture without yeast extract is shown in Figure 5.19. A lag phase of 200 hrs, which is not growth associated, was seen before the onset of significant ethanol production. This result was also observed in Figure 5.10, although the lag phase in Figure 5.10 was 300 hrs. The leveled off ethanol concentration was about 2.8 g/L at pH 5.0, 4.5 g/L at pH 4.5 and 6 g/L at pH 4.0. The ethanol concentration was higher in Figure 5.10, but the scatter in ethanol concentrations without yeast extract (observed in Figure 5.10) was not seen in Figure 5.19. Acetate concentration profiles as a function of pH are shown in Figure 5.20. Again, a similar lag phase as was seen with growth was shown with acetate production. the leveled off acetate concentration was about 12 g/L at pH 5.0, 6 g/L at pH 4.5 and 3.0 g/L at pH 4.0. The leveled off ethanol to acetate ratio was thus 0.23 at pH 5.0, 0.75 at pH 4.5 and 2.0 at pH 4.0.

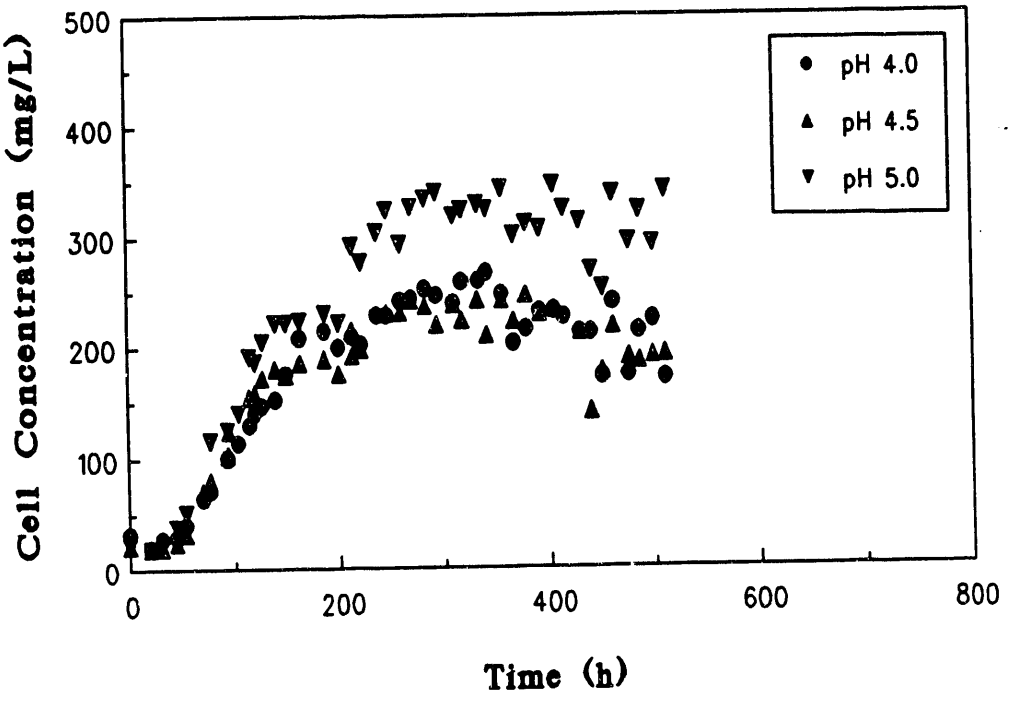

Figure 5.18. Effect of pH on cell growth (no yeast extract present).

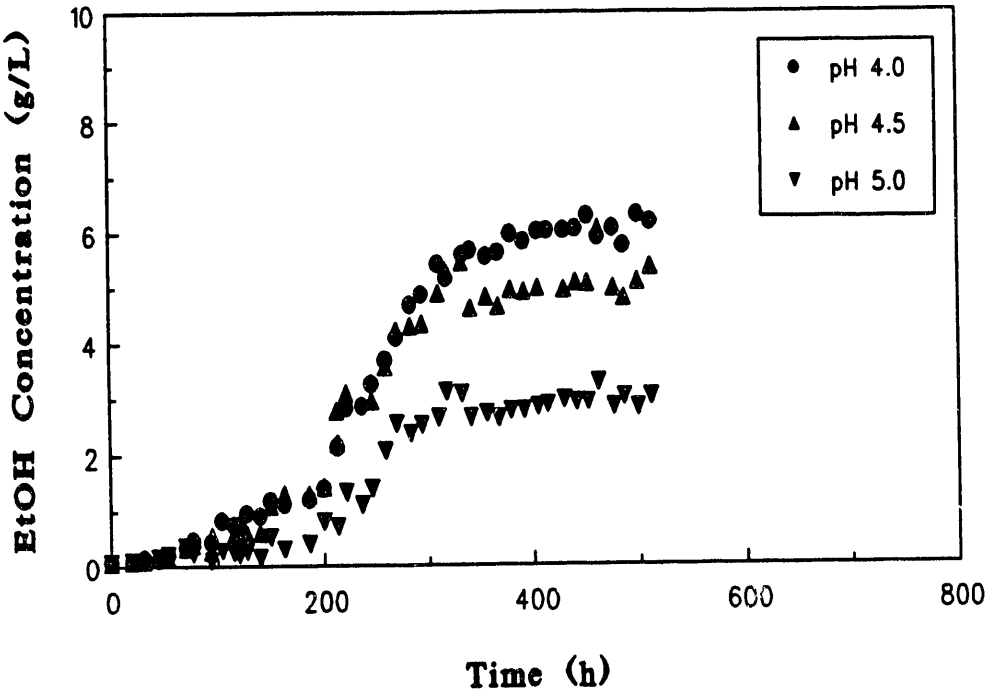

Figure 5.19. Effect of pH on ethanol production (no yeast extract present).

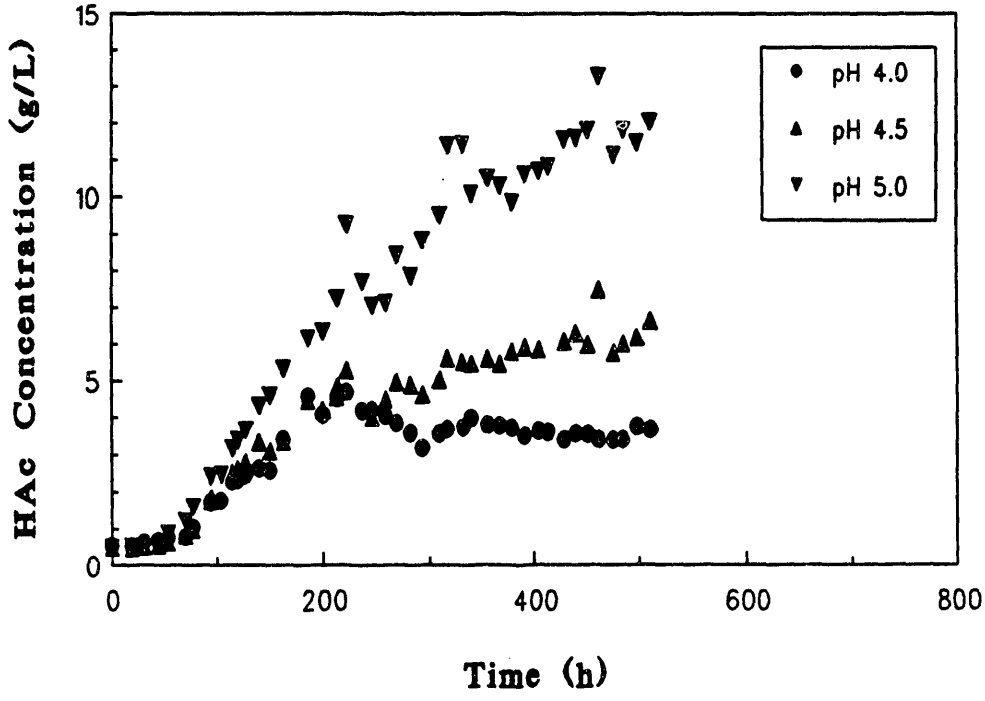

Figure 5.20. Effect of pH on acetate production (no yeast extract present).

The behavior of the H_2S-exposed culture was superior with regard to ethanol production than the unexposed (normal) culture. Again, this difference in behavior may be due to inoculum size or inoculum conditions, culturing conditions at the time of the experiment which caused variation or actual differences in the cultures due to H_2S exposure. Because of these results, it is expected that a higher ethanol to acetate ratio would have been obtained at pH 4.0 for the H_2S-exposed culture.

5.6 Performance Studies with Increased Concentrations of Medium Constituents

Because of the success in improving ethanol concentrations and product ratios in previous studies without yeast extract present in the medium, a series of experiments were run without yeast extract, but with increased concentrations of basal medium constituents in the medium. It was postulated that the cultures might require some other essential nutrient present in yeast extract now that yeast extract was removed from the medium. This additional nutrient may allow higher ethanol concentrations with increased cell growth.

Four batch bottles were inoculated with *C. ljungdahlii* in basal medium (containing no yeast extract) supplemented with additional basal medium constituents. Bottle 1 contained the medium of Table 4.2 the standard basal medium containing B-vitamins, Pfennig minerals, Pfennig trace metals, cysteine-HCl as the reducing agent and resazurin as an indicator of anaerobicity. Bottle 2 contained the standard basal medium of Table 4.2 with double Pfennig minerals, Bottle 3 contained basal medium with double B-vitamins and Bottle 4 contained basal medium with double Pfennig trace metals. No yeast extract was added to any of the bottles except for insignificant amounts transferred with the inoculum.

Figures 5.21-5.24 show cell and product (ethanol and acetate) concentration profiles for the medium studies at pH 4.0. As is noted in the figures, the cell concentration profiles for the four experiments were quite similar, each producing a maximum cell concentration of 500-520 mg/L. The sharp decreases in cell concentration seen in Figures 5.21-5.23 occurred primarily as a result of regassing the bottles. Thus, additional nutrients did not result in increased cell concentrations.

Product concentration profiles in the four bottles were, however, affected by the additional nutrients. A maximum ethanol concentration of 7.4 g/L and a maximum acetate concentration of 3.0 g/L were obtained without additional nutrients (see Figure 5.21). The maximum ethanol concentration occurred at an acetate concentration of 0.7 g/L, yielding a very favorable ethanol:acetate product ratio of 10.6 g/g. When the Pfennig minerals concentration was doubled (see Figure 5.22), the maximum ethanol concentration was 2.4 g/L, the maximum acetate concentration was 3.1 g/L and the highest product ratio was only 0.8 g/g. When the B-vitamins concentration was doubled (see Figure 5.23), the maximum ethanol concentration was 3.8 g/L, the maximum acetate concentration was 6.3 g/L and the highest product ratio was 0.9 g/g. Finally, when the Pfennig trace metals concentration was doubled (see Figure 5.24), the maximum ethanol concentration was 5.1 g/L, the maximum acetate concentration was 4.4 g/L and the highest product ratio was 1.2 g/g. Clearly, it is not advantageous, necessary or desirable to add additional nutrients to the basal medium upon elimination of yeast extract. It may, in fact, be preferential to lower the concentration of particular medium constituents.

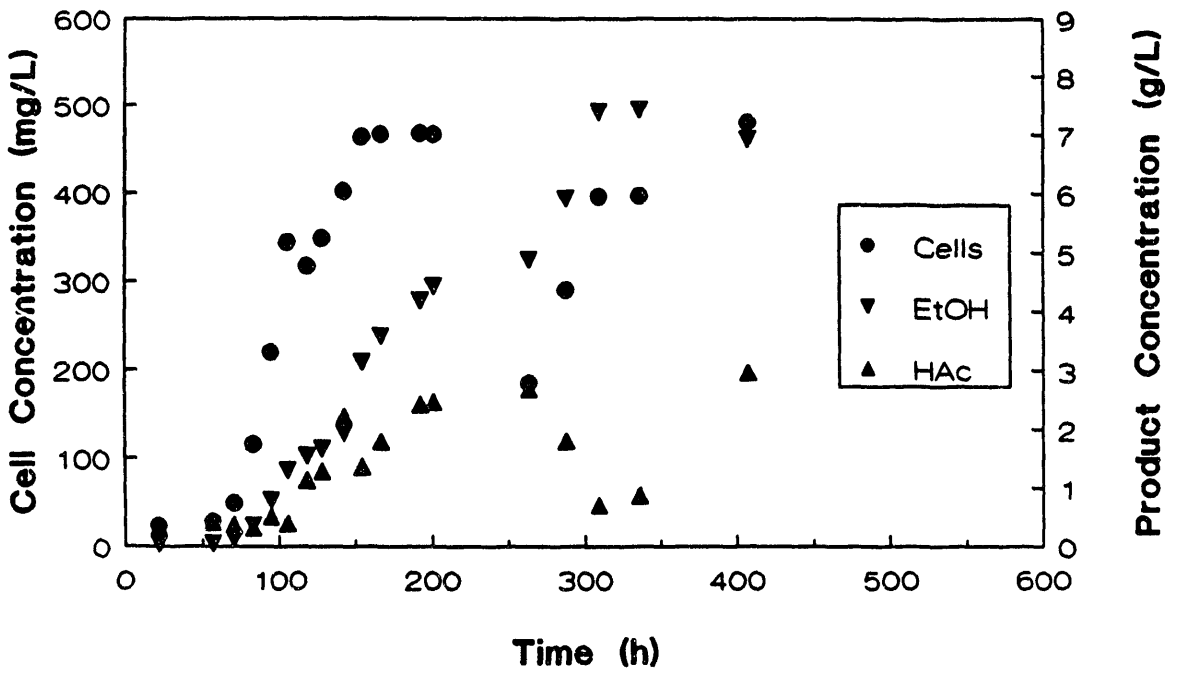

Figure 5.21. Cell and product concentration profiles for *C. ljungdahlii* using basal medium (pH 4.0, 0.0009 percent yeast extract).

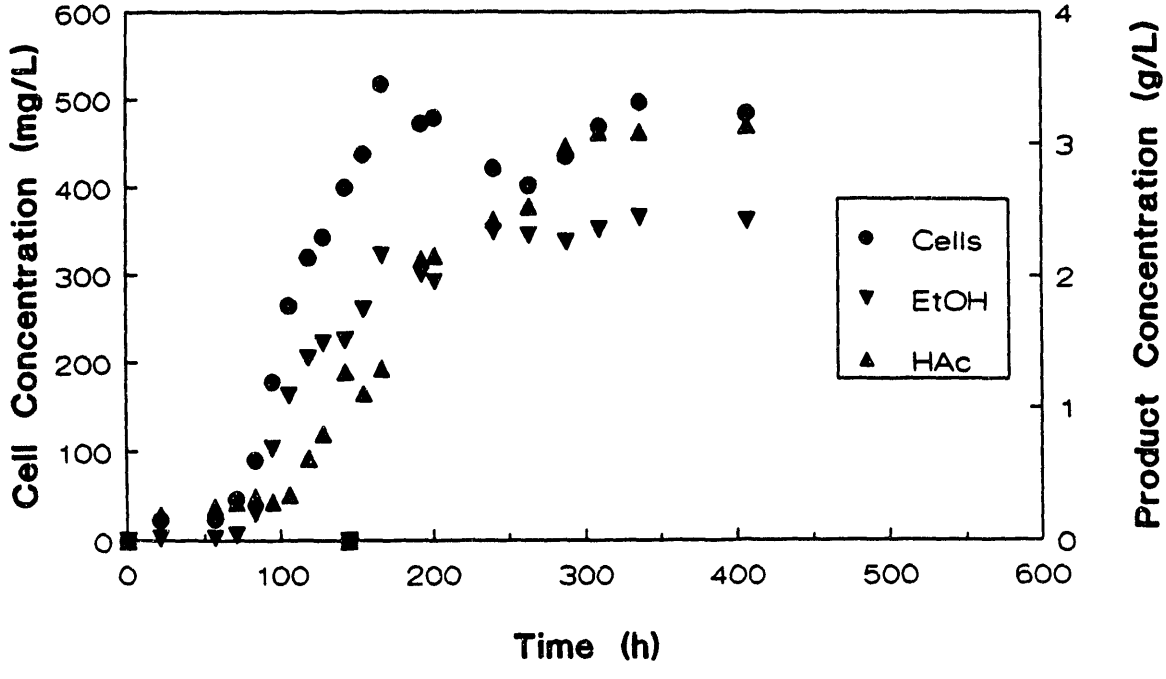

Figure 5.22. Cell and product concentration profiles for *C. ljungdahlii* using basal medium (pH 4.0, 0.0009 percent yeast extract) containing 200 percent of the Standard Pfennig's minerals.

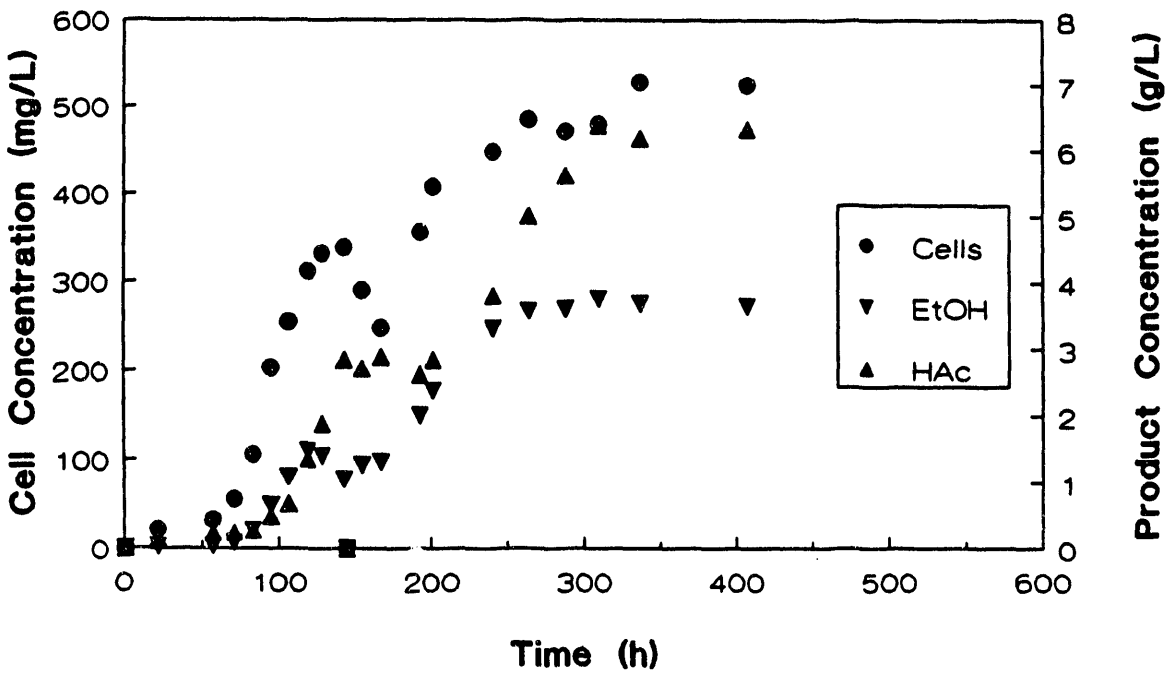

Figure 5.23. Cell and product concentration profiles for *C. ljungdahlii* using basal medium (pH 4.0, 0.0009 percent yeast extract) containing 200 percent of the Standard B vitamins.

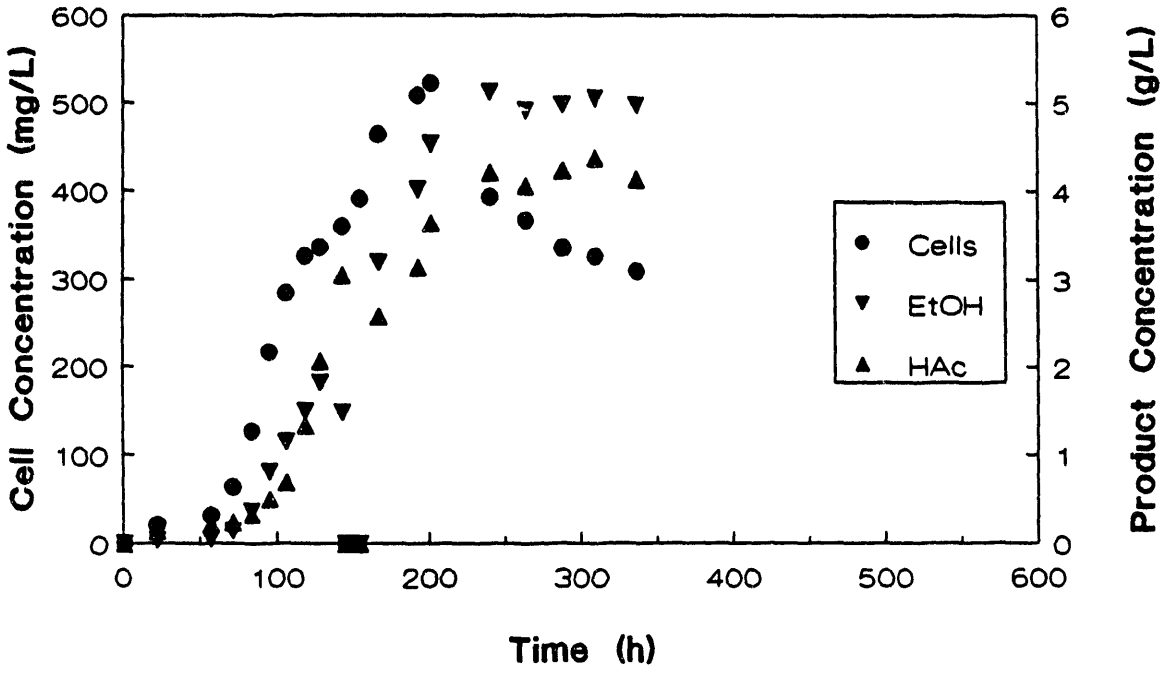

Figure 5.24. Cell and product concentration profiles for *C. ljungdahlii* using basal medium (pH 4.0, 0.0009 percent yeast extract) containing 200 percent of the Standard Pfennig's trace metals.

5.7 Performance Studies with Decreased Concentrations of Medium Constituents

As a follow-up to the studies of Figures 5.21-5.24, experiments were run with basal medium using half strength selected medium constituents. Four batch bottles were inoculated with *C. ljungdahlii* in modified basal medium (again containing no yeast extract). The first bottle contained the medium of Table 4.2, but with the concentration of each of the major constituents (Pfennig minerals, B-vitamins and Pfennig trace metals) cut in half. The second bottle contained the standard basal medium of Table 4.2, but with the Pfennig minerals concentration cut in half. Bottle 3 contained basal medium with half the concentration of B-vitamins and Bottle 4 contained basal medium with half the concentration of Pfennig trace metals. Again, none of the bottles contained yeast extract except for the insignificant amounts transferred with the inoculum.

Figures 5.25-5.28 show cell and product (ethanol and acetate) concentration profiles for the studies at pH 4.0. In contrast to the cell concentration profiles of Figures 5.21-5.24 the maximum cell concentrations obtained in Figures 5.25-5.28 varied considerably. The bottle with half basal medium showed a maximum cell concentration of 210 mg/L (see Figure 5.25). The bottle with half Pfennig minerals showed a maximum cell concentration of 370 mg/L (Figure 5.26), the bottle with half B-vitamins showed a maximum cell concentration of 460 mg/L (Figure 5.27) and the bottle with half Pfennig trace metals showed a maximum cell concentration of 250 mg/L (Figure 5.28). Batch growth with half B-vitamins showed nearly the same maximum cell concentration as with full strength basal medium, while all other bottles showed decreased growth.

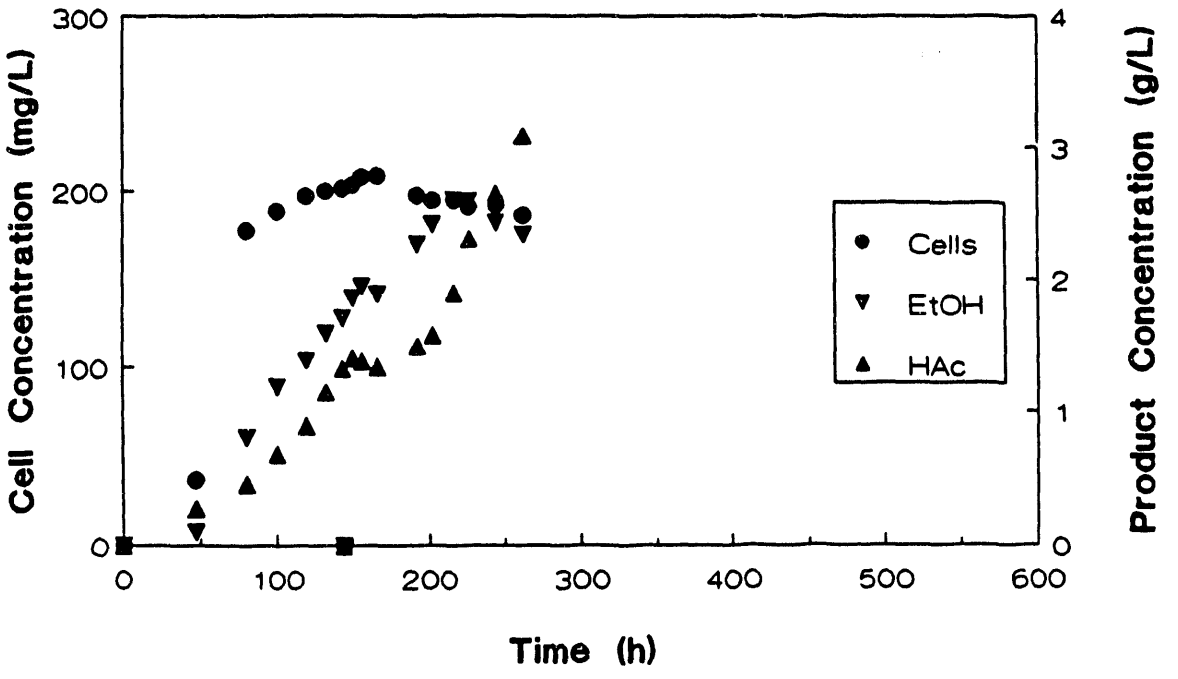

Figure 5.25. Cell and product concentration profiles for *C. ljungdahlii* half-strength basal medium (pH 4.0, 0.0009 percent yeast extract).

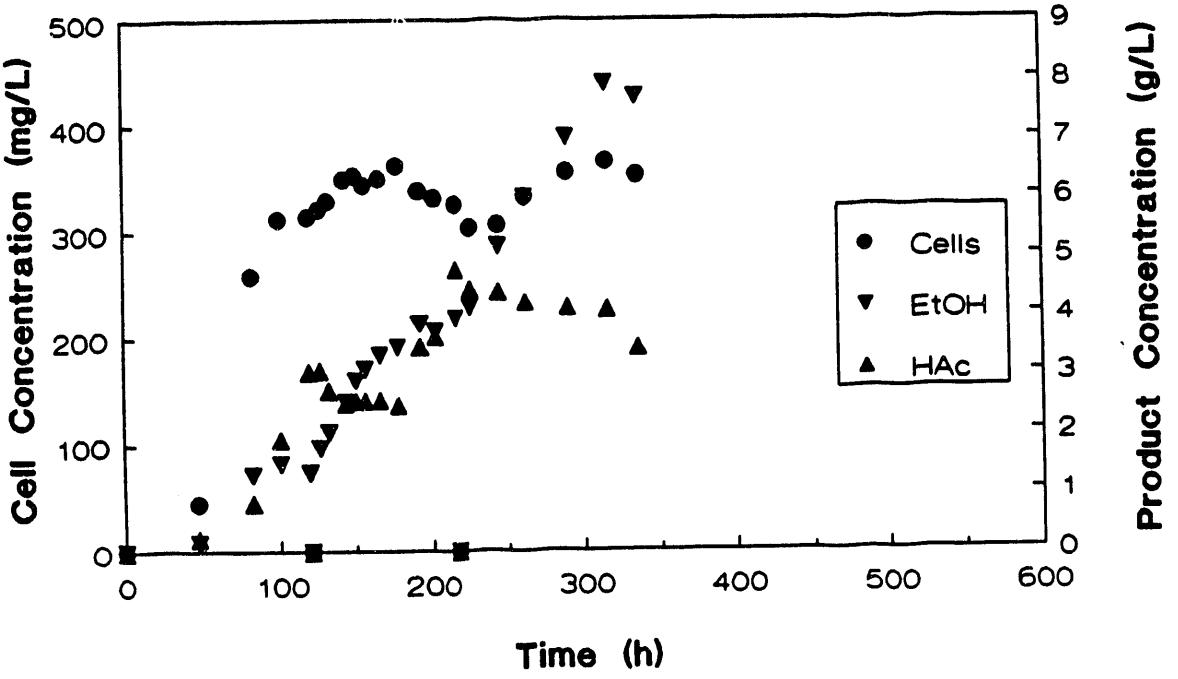

Figure 5.26. Cell and product concentration profiles for *C. ljungdahlii* using basal medium (pH 4.0, no yeast extract) containing 50 percent of the Standard Pfennig's minerals.

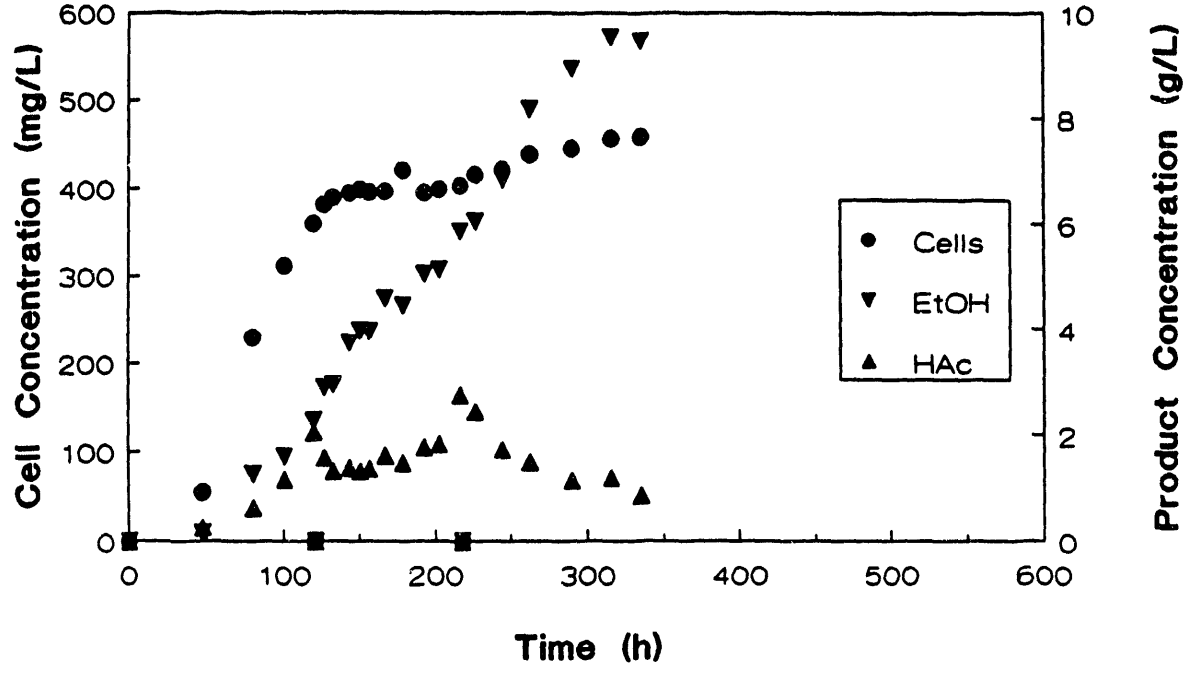

Figure 5.27. Cell and product concentration profiles for *C. ljungdahlii* using basal medium (pH 4.0, no yeast extract) containing 50 percent of the Standard B vitamins.

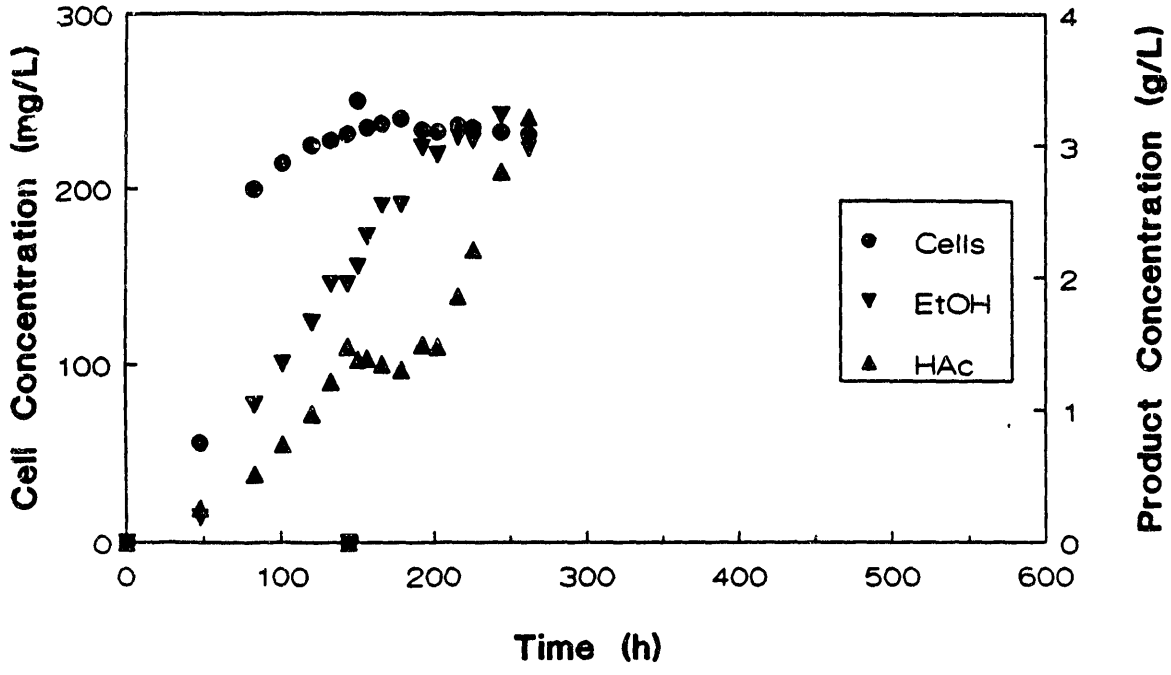

Figure 5.28. Cell and product concentration profiles for *C. ljungdahlii* using basal medium (pH 4.0, no yeast extract) containing 50 percent of the Standard Pfennig's trace metals.

The ethanol and acetate concentration profiles also varied with the decreased nutrients concentrations. The bottle with half strength basal medium showed a maximum ethanol concentration of 2.6 g/L, a maximum acetate concentration of 3.1 g/L and maximum product ratio of 1.5 g/L (see Figure 5.25). The bottle containing half strength Pfennig minerals (Figure 5.26) showed a maximum ethanol concentration of 7.9 g/L, a maximum acetate concentration of 4.8 g/L and a maximum product ratio of 2.2 g/g. The bottle containing half strength B-vitamins (Figure 5.27) showed a maximum ethanol concentration of 9.5 g/L, a maximum acetate concentration 2.8 g/L and a maximum product ratio of 11.0 g/g. Finally, the bottle containing strength Pfennig trace metals (Figure 5.28) showed a maximum ethanol concentration of 3.2 g/L, a maximum acetate concentration of 3.2 g/L and a maximum product ratio of 2.0 g/g.

Basal medium with half B-vitamins was shown to yield the highest cell concentration, the highest ethanol concentration and the best product ratio. This result is very encouraging since it was previously thought that increased growth meant acetate production instead of ethanol. Further studies should thus be carried out with varying B-vitamin concentrations in basal medium.

5.8 Performance Studies with Decreased Concentrations of B-vitamins

As a follow-up to the studies of Figures 5.25-5.28, experiments were run with basal medium using decreased concentrations of B-vitamins. Four batch bottles were inoculated with *C. ljungdahlii* in modified basal medium (containing no yeast extract), with B-vitamin concentrations ranging from 8 to 92 percent of the standard basal medium concentration. Bottle 1 contained the medium of Table 4.2, except that the B-vitamins concentration was only 8 percent of the value in Table 4.2. Bottle 2 contained basal medium with 21

percent of the standard B-vitamins, Bottle 3 contained basal medium with 29 percent of the standard B-vitamins and Bottle 4 contained basal medium with 92 percent of the standard B-vitamins.

Figures 5.29-5.32 show cell and product (ethanol and acetate) concentration profiles for the studies at pH 4.0. The bottle with 8 percent B-vitamins showed a maximum cell concentration of 300 mg/L, a maximum ethanol concentration of 1.9 g/L, a maximum acetate concentration of 0.4 g/L and a maximum product ratio of 8.4 g/g (see Figure 5.29). The bottle containing 21 percent B-vitamins showed a maximum cell concentration of 430 mg/L, a maximum ethanol concentration 2.1 g/L, a maximum acetate concentration of 3.6 g/L and a maximum product ratio of 1.0 g/g (see Figure 5.30). The bottle containing 29 percent B-vitamins (Figure 5.31) showed a maximum cell concentration of 420 mg/L, a maximum ethanol concentration of 1.8 g/L, a maximum acetate concentration of 4.3 g/L and a maximum product ratio of 0.8 g/g. Finally, the bottle containing 92 percent B-vitamins (Figure 5.32) showed a maximum cell concentration of 420 mg/L, a maximum ethanol concentration of 1.2 g/L, a maximum acetate concentration of 5.0 g/L and an early maximum product ratio of 1.1 g/g.

Thus, it was seen that a low maximum cell concentration was obtained for 8 percent B-vitamins, but that the maximum increased to essentially the same level as in Figures 5.25-5.28 at the higher B-vitamin concentrations. An essential vitamin is apparently limiting growth with 8 percent B-vitamins. The ethanol concentration decreased with increased B-vitamins concentration. Since production has been shown previously to be directly linked to growth, a higher cell concentration is needed with 8 percent B-vitamins to yield a higher ethanol concentration. Experiments should thus be run with 8 percent B-vitamins supplemented with one or more essential vitamins.

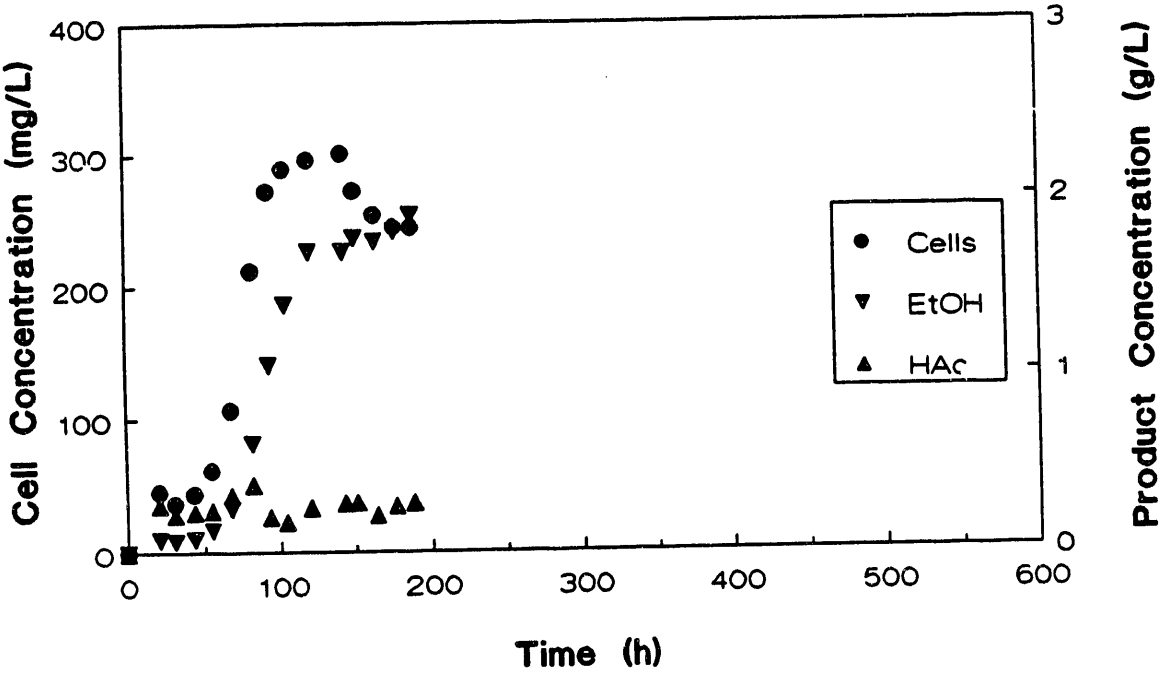

Figure 5.29. Cell and product concentration profiles for *C. ljungdahlii* using basal medium (pH 4.0, no yeast extract) containing 8 percent of the Standard B vitamins.

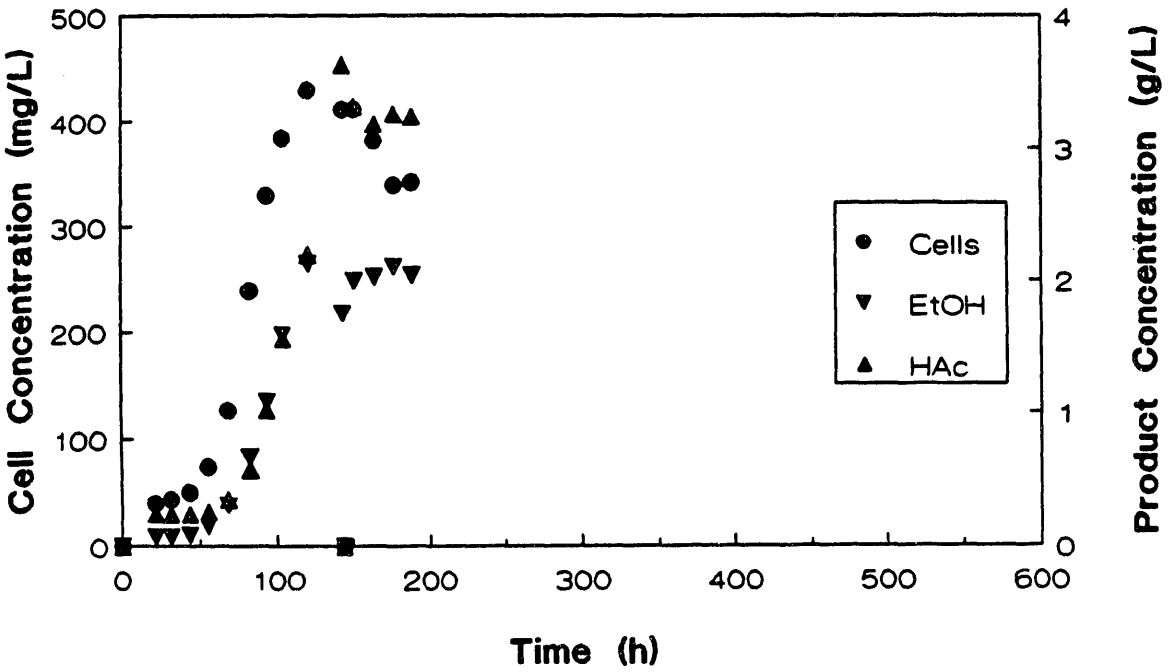

Figure 5.30. Cell and product concentration profiles for *C. ljungdahlii* using basal medium (pH 4.0, no yeast extract) containing 21 percent of the Standard B vitamins.

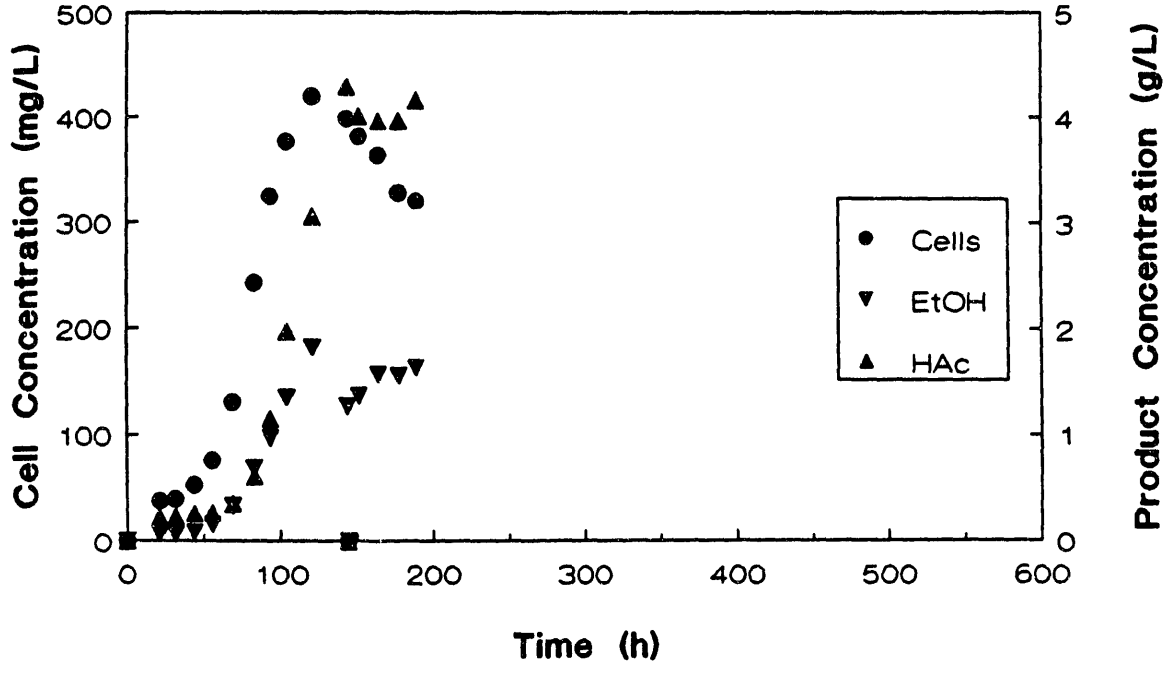

Figure 5.31. Cell and product concentration profiles for *C. ljungdahlii* using basal medium (pH 4.0, no yeast extract) containing 29 percent of the Standard B vitamins.

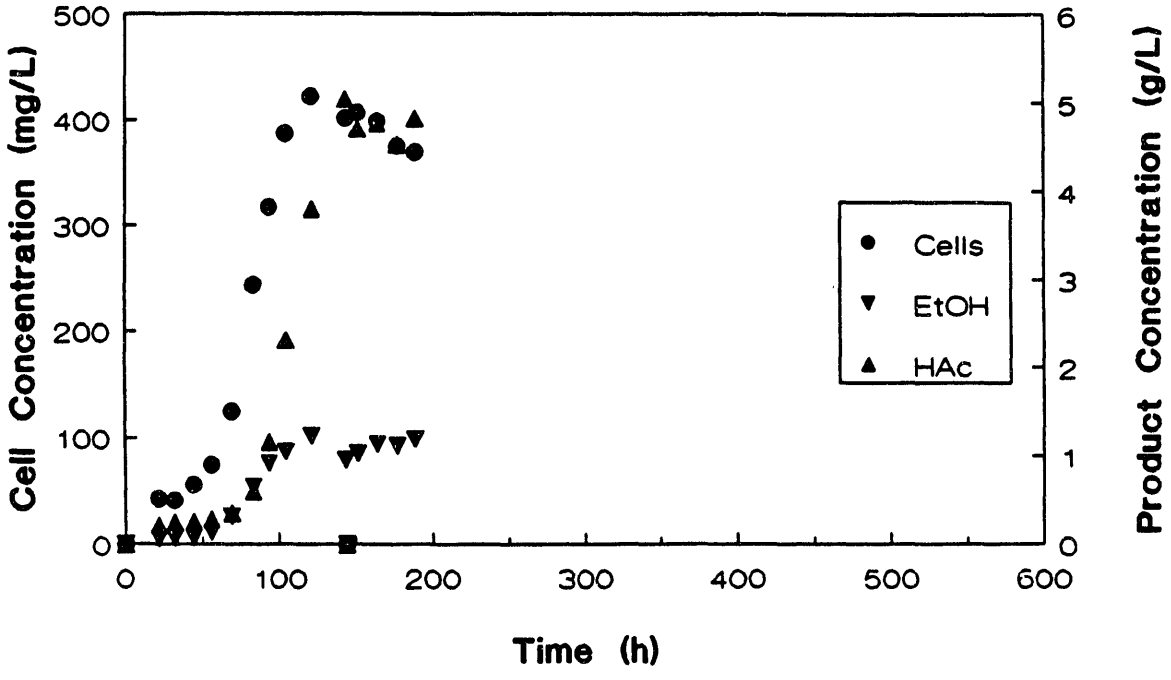

Figure 5.32. Cell and product concentration profiles for *C. ljungdahlii* using basal medium (pH 4.0, no yeast extract) containing 92 percent of the Standard B vitamins.

5.9 Performance Studies with 8 Percent B-vitamins Supplemented with Essential Vitamins

As a follow-up to the studies of Figures 5.29-5.32, experiments were run with basal medium using 8 percent B-vitamins supplemented with one or more vitamins normally thought to be essential for microbial growth. Five batch bottles were inoculated with *C. ljungdahlii* in modified basal medium (containing no yeast extract), with 8 percent B-vitamins along with biotin, thiamine or calcium pantothenate. Bottle 1 contained the medium of Table 4.2 except that the B-vitamins concentration was reduced to 8 percent of the normal value. This bottle was identical to Bottle 1 of the previous experiments. Bottle 2 contained basal medium with 8 percent B-vitamins supplemented with biotin, Bottle 3 contained basal medium with 8 percent B-vitamins supplemented with thiamine-HCl, Bottle 4 contained basal medium with 8 percent B-vitamins supplemented with Ca-pantothenate and Bottle 5 contained basal medium with 8 percent B-vitamins supplemented with biotin, thiamine-HCl and Ca-pantothenate.

Figures 5.33-5.37 show cell and product (ethanol and acetate) concentration profiles for the studies at pH 4.0. The bottle containing 8 percent B-vitamins only (Figure 5.33) showed a maximum cell concentration of 240 mg/L, a maximum ethanol concentration of 1.5 g/L, a maximum acetate concentration of 0.4 g/L and a maximum product ratio of ∞ (no acetate). These are not identical but compare well with the data of Figure 5.29. The bottle with biotin (Figure 5.34) showed a maximum cell concentration of 240 mg/L, a maximum ethanol concentration of 1.4 g/L, a maximum acetate concentration of 0.3 g/L and a maximum product ratio of ∞. The bottle with thiamine-HCl (Figure 5.35) showed a maximum cell concentration of 210 mg/L, a maximum

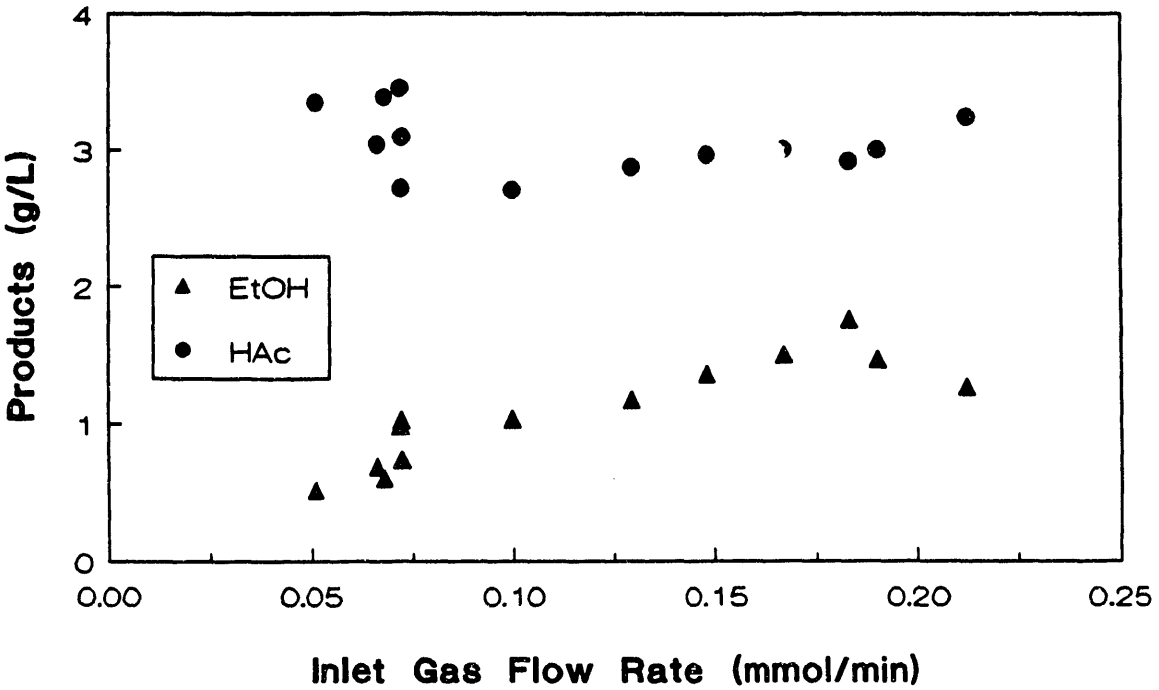

Figure 5.33. Product Concentrations from growth of *C. ljungdahlii* in Basal Medium in the CSTR.

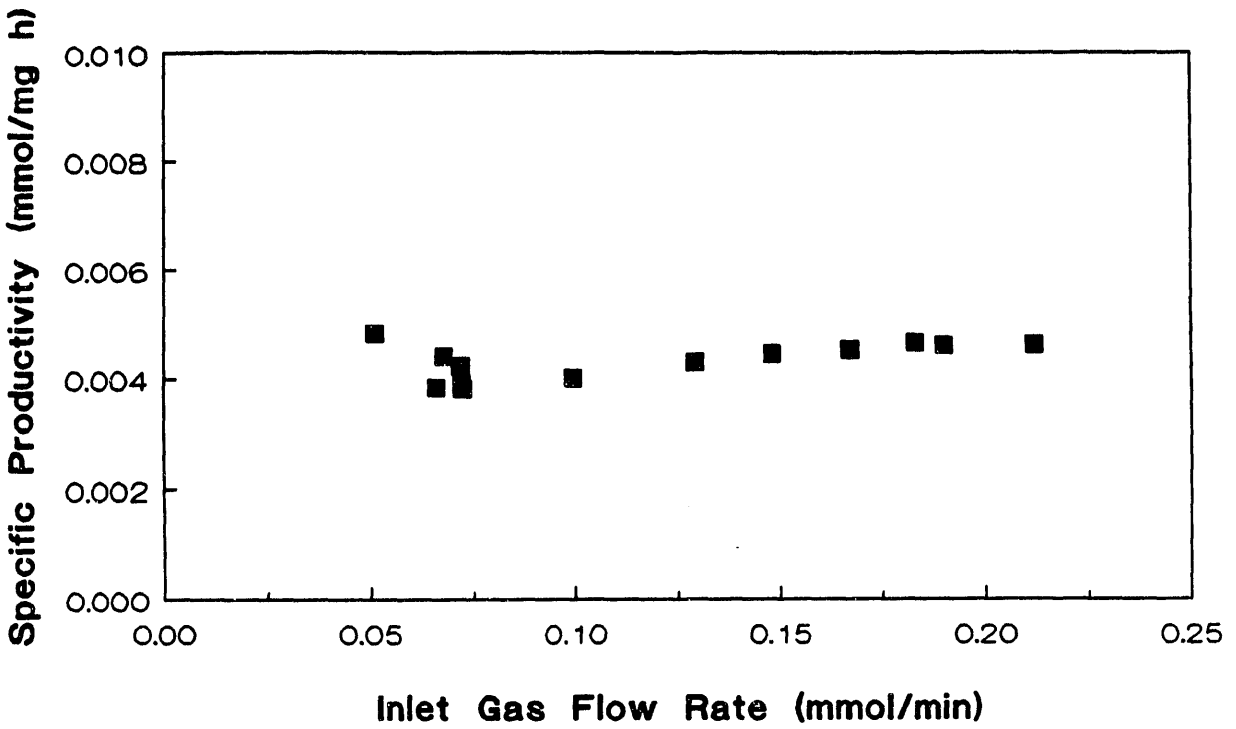

Figure 5.34. Specific Productivity of *C. ljungdahlii* Grown in Basal Medium in the CSTR.

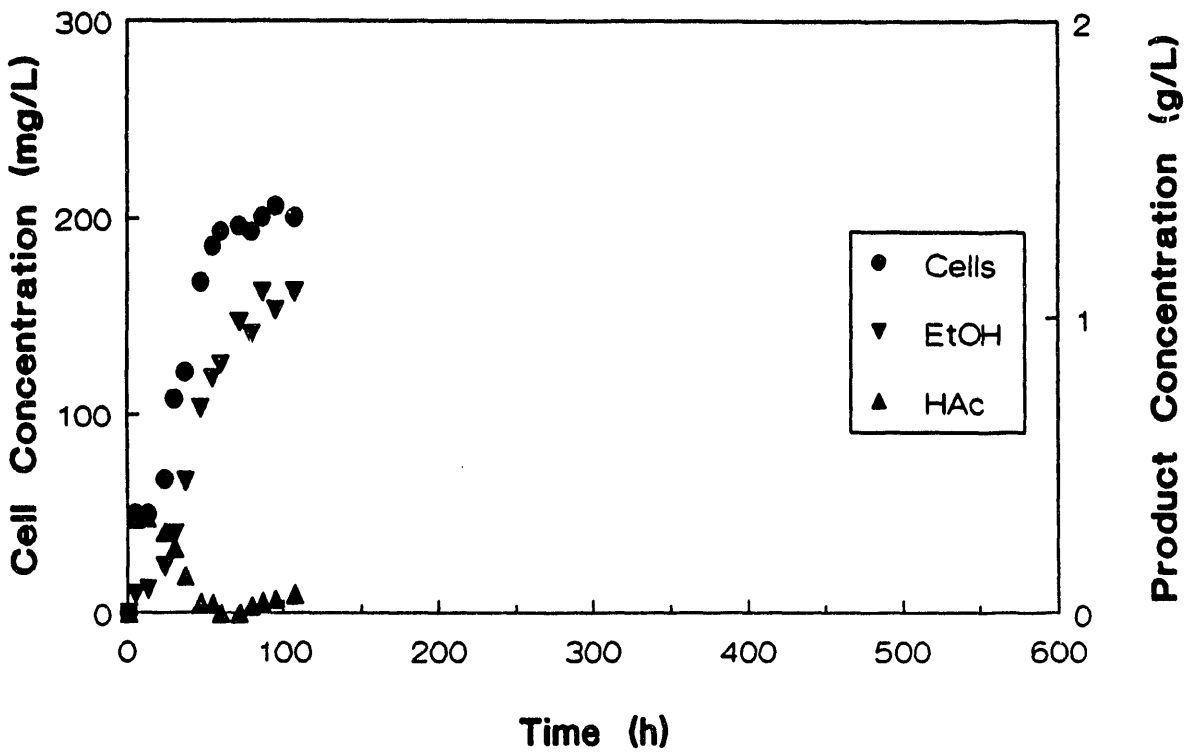

Figure 5.35. Cell and product concentration profiles for *C. ljungdahlii* using basal medium (ph 4.0, no yeast extract) containing 8 percent of the Standard B vitamins plus Thiamine HCl.

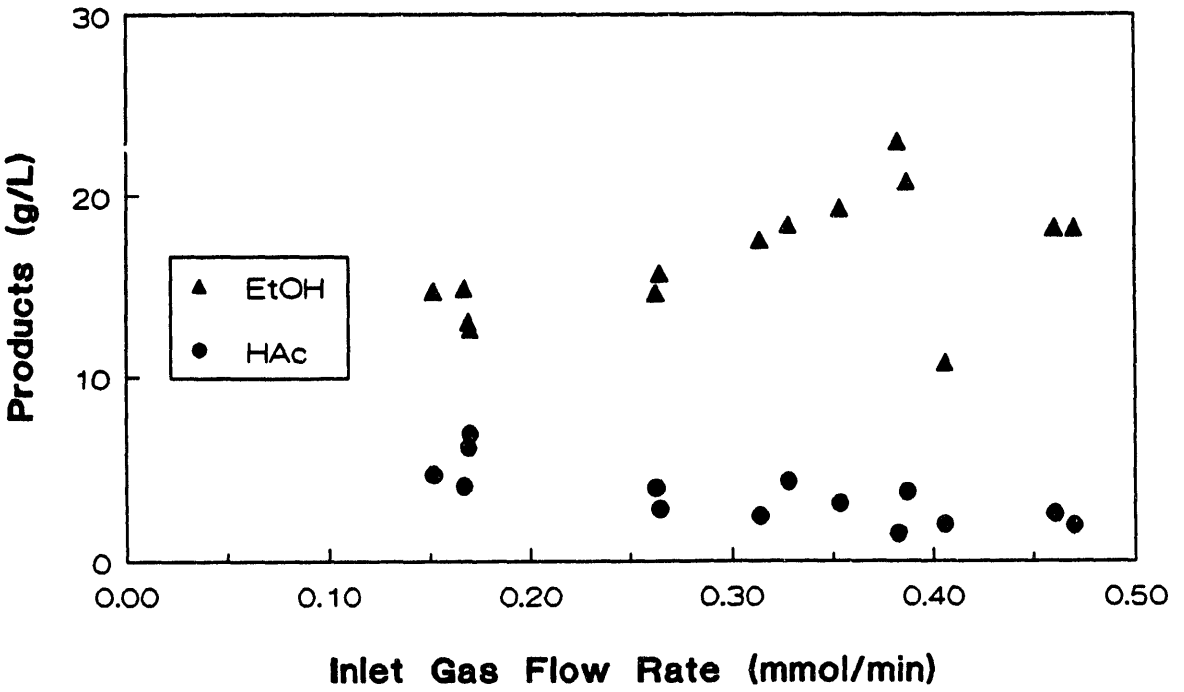

Figure 5.36. Product Concentrations from growth of *C. ljungdahlii* in Designed Medium in the CSTR.

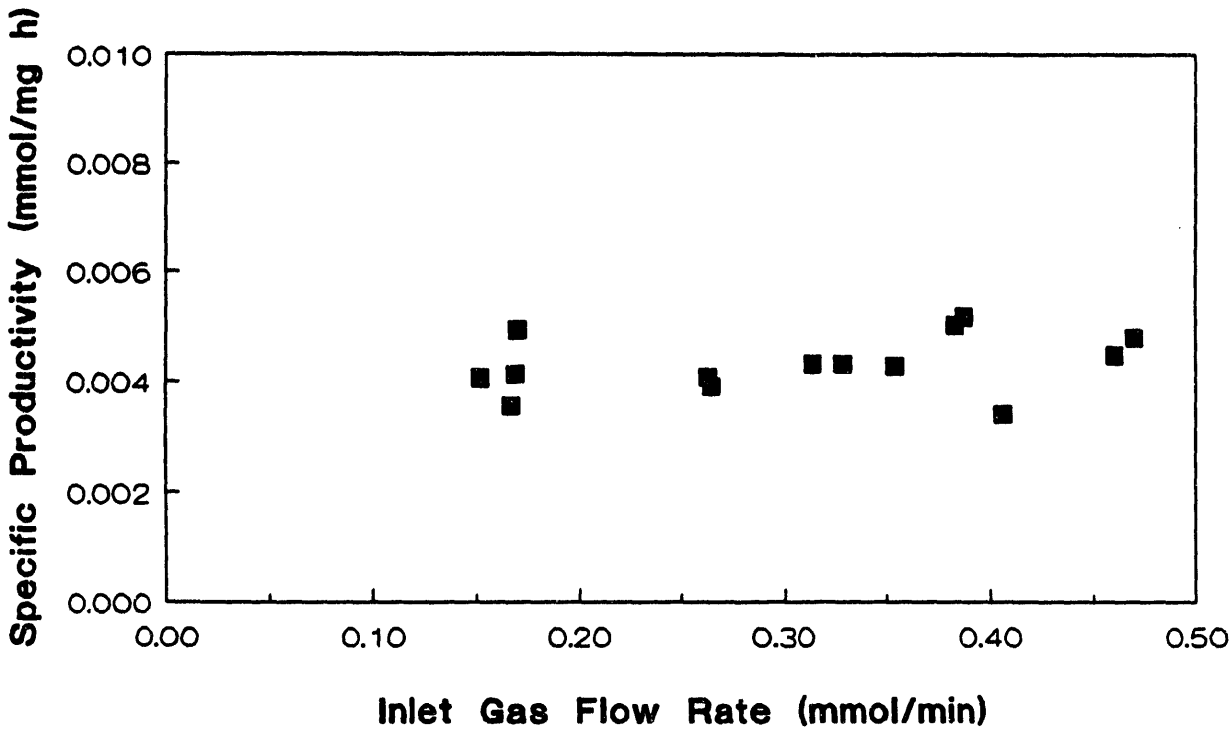

Figure 5.37. Specific Productivity of *C. ljungdahlii* Grown in Designed Medium in the CSTR.

ethanol concentration of 1.1 g/L, a maximum acetate concentration of 0.3 g/L and a maximum product ratio of ∞. The bottle with Ca-pantothenate (Figure 5.36) showed a maximum cell concentration of 370 mg/L, a maximum ethanol concentration of 2.0 g/L, a maximum acetate concentration of 2.9 g/L and a maximum product ratio of 7.6 g/g. Finally, the bottle with all three vitamins (Figure 5.37) showed a maximum cell concentration of 470 mg/L, a maximum ethanol concentration of 4.7 g/L, a maximum acetate concentration of 2.6 g/L and a maximum product ratio of 4.8 g/g.

These experiments indicate the Ca-pantothenate is required for growth, as evidenced by the much higher cell concentration when Ca-pantothenate is present. The experiment with Ca-pantothenate showed quite a bit of acetate being produced, however, indicating that the medium is too rich so that acetate is the favored product. More research needs to be carried out with medium manipulation since it is clear that growth and ethanol production can occur simultaneously if the medium is formulated correctly.

5.10 Agitation Rate Studies

Figures 5.38-5.42 show cell and product (ethanol and acetate) concentration profiles for *C. ljungdahlii* utilizing synthesis gas at various pH levels and agitation rates. In comparing the results shown in Figures 5.38 and 5.39 at a constant pH level of 4.0, it is seen that the experiment run at the higher agitation rate of 300 rpm (see Figure 5.39) gave higher cell concentrations and higher ethanol concentrations that at the lower agitation rate of 200 rpm (see Figure 5.38). The maximum cell concentration reached at 200 rpm was about 200 mg/L, while the maximum at 300 rpm was just over 300 mg/L. The maximum ethanol concentration at 200 rpm was about 0.5 g/L, while the maximum at 300 rpm was nearly 2.0 g/L. The acetate concentration at both

AIIM

Association for Information and Image Management

1100 Wayne Avenue, Suite 1100
Silver Spring, Maryland 20910
301/587-8202

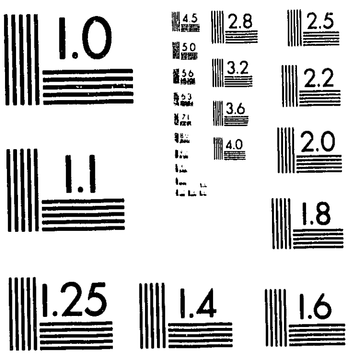

2 of 4

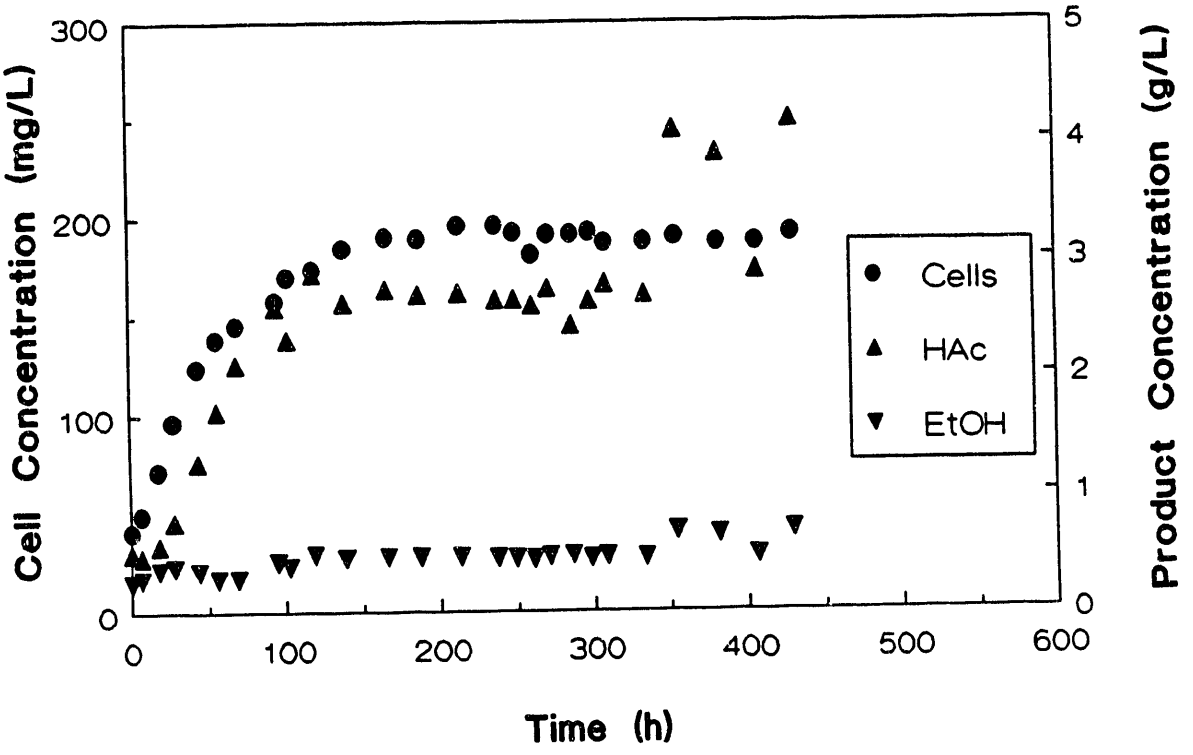

Figure 5.38. Cell and product concentration profiles for *C. ljungdahlii* at pH 4 and 200 rpm.

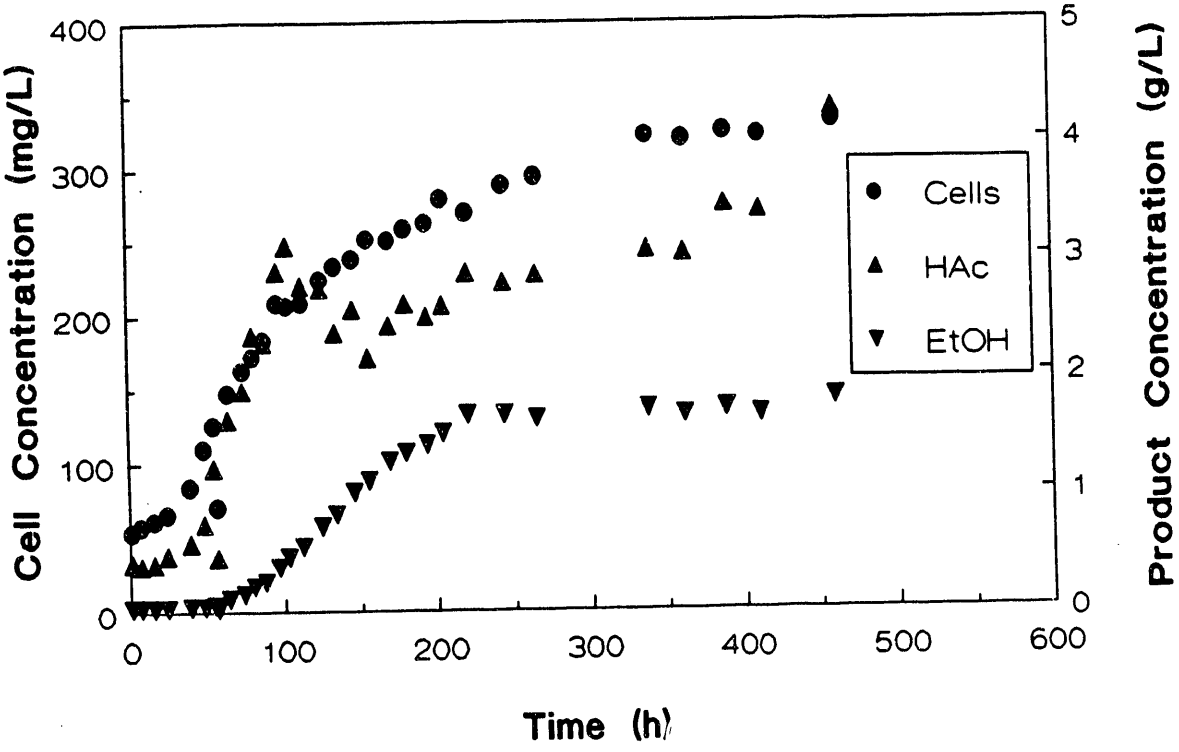

Figure 5.39. Cell and product concentration profiles for *C. ljungdahlii* at pH 4 and 300 rpm.

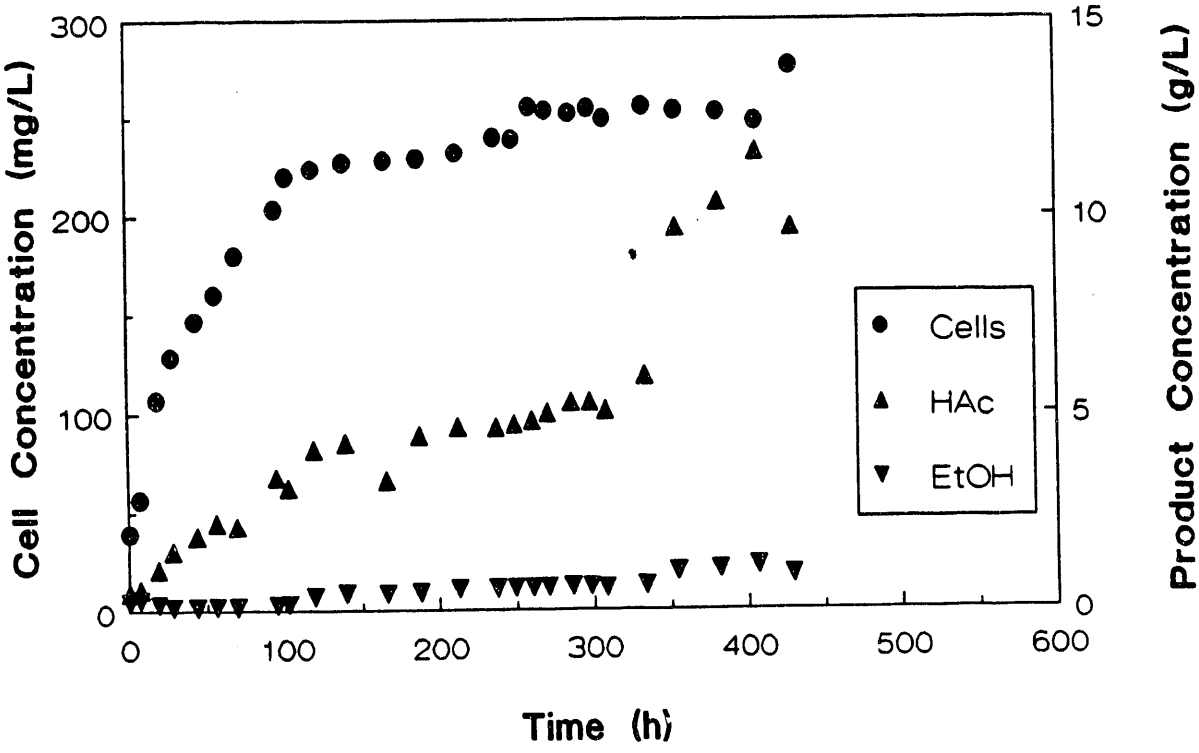

Figure 5.40. Cell and product concentration profiles for *C. ljungdahlii* at pH 5 and 200 rpm.

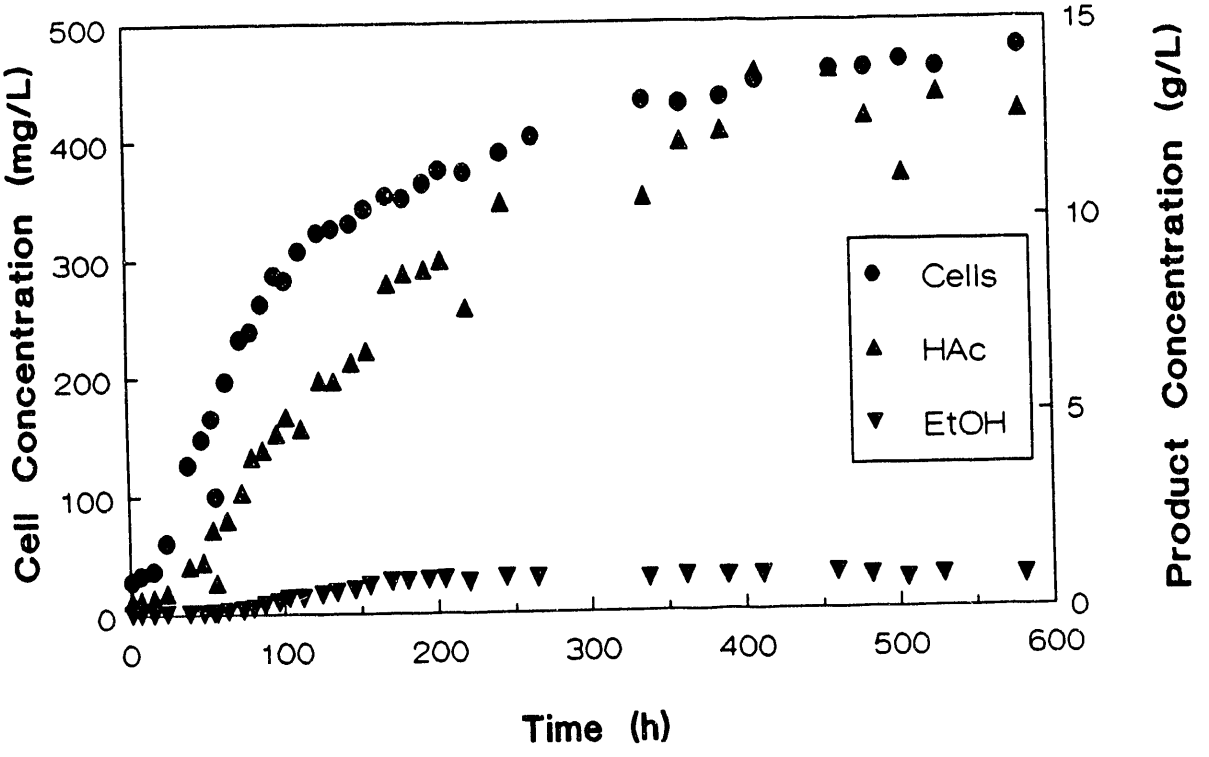

Figure 5.41. Cell and product concentration profiles for *C. ljungdahlii* at pH 5 and 300 rpm.

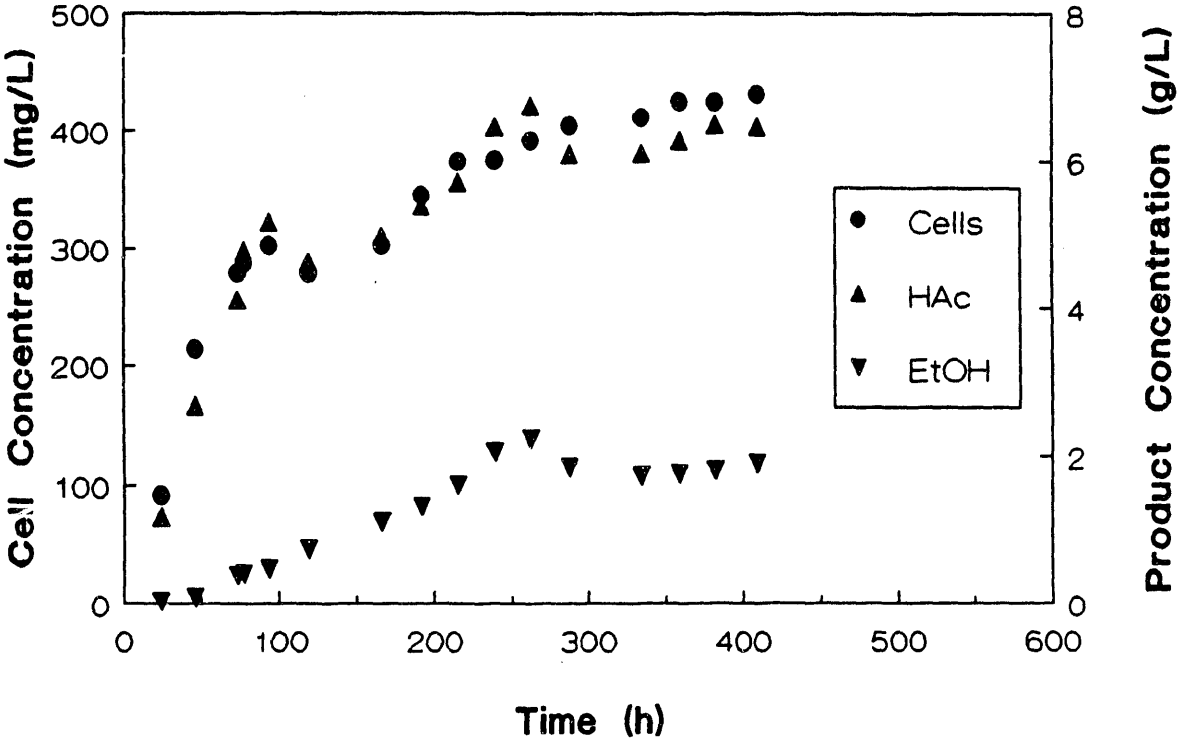

Figure 5.42. Cell and product concentration profiles for *C. ljungdahlii* at pH 4.5 and 350–400 rpm.

agitation rates was approximately 3.0 g/L. Thus, as hypothesized earlier, the increased dissolved CO concentration was apparently responsible for both increased cell concentrations and ethanol concentrations. The use of increased agitation rates either in batch or continuous culture might thus be instrumental in increasing both the product ratio and the overall ethanol concentration due to higher cell concentrations.

Similar, although not identical, behavior is shown in Figures 5.40 and 5.41 where the medium pH is raised to 5.0. Figure 5.40 shows the profiles for an agitation rate of 200 rpm and Figure 5.41 shows the profiles for an agitation rate of 300 rpm. As is noted in these figures, the maximum cell concentration at 200 rpm was nearly 250 mg/L and the maximum cell concentration was almost 500 mg/L at an agitation rate of 300 rpm. The maximum ethanol concentration at both agitation rates was about 1 g/L. Finally, the maximum acetate concentration was about 5 g/L at 200 rpm and about 13 g/L at 300 rpm. Thus, at this higher pH level, the increased agitation rate was responsible for increased cell growth but did not result in increased ethanol production. In fact, an increase in acetate production was seen.

In contrasting the results shown in Figures 5.38-5.41 at the two pH levels and two agitation rates, it is seen that an increase in agitation rate must be accompanied by low medium pH in order to yield both increased cell concentrations and product ratios. At higher pH levels, the increased agitation rates do not stress the culture and thus produce large numbers of cells and the resultant increase in acetate concentrations associated with good cell growth. Only at lower pH levels is the culture stressed enough to result in increased ethanol production.

As a test of this hypothesis, an additional batch experiment was carried out at pH 4.5 and even higher agitation rates (350-400 rpm). As is shown in Figure 5.42 a maximum cell concentration of about 420 mg/L was obtained. The maximum product concentrations were 6.5 g/L acetate and just over 2 g/L ethanol. The results shown in Figure 5.42 fit the pattern established in Figures 5.38-5.41. First, the increased agitation rate resulted in higher cell concentrations, although not nearly as high as would be expected at a higher medium pH. Secondly, intermediate pH (between 4 and 5) and higher agitation rates resulted in maximum ethanol concentrations that matched the levels at pH 4.0. Thirdly, the medium pH and increased agitation rate unfortunately resulted in increased acetate production in favor of ethanol.

The overall conclusion from this study is that conditions of low pH and high agitation rate result in higher ethanol and cell concentrations, while minimizing the acetate concentration. It should be realized, however, that extrapolation of this data to very high agitation rates may not be advisable. Very high agitation rates are quite expensive, although increased mass transfer in other types of reactors is possible without increased expense. It should also be realized that CO is inhibitory to the culture at some higher dissolved concentration which might be reached at increased pressure. High cell concentrations must be used under these conditions to prevent severe inhibition or cell death.

5.10.1 Analysis of Rate Date

In 1959, Luedeking and Piret[30] developed an equation which states that the rate of product formation, dP/dt, is a linear function of the cell growth rate, dX/dt, and the cell concentration, x:

$$\frac{dP}{dt} = Y_{P/X} \frac{dX}{dt} + a\,X \qquad (5.1)$$

In Equation (5.1), a and $Y_{P/X}$ are both constants, with $Y_{P/X}$ known as the yield of product from cells. The ratio of the constants, $Y_{P/X/a}$, indicates how growth associated product formation is for a given fermentation. If the ratio is quite high, there is a direct link between the growth of the organism and the formation of fermentation products. Such products are known as primary metabolites.

Equation (5.1) may be rearranged to yield:

$$\frac{1}{X}\frac{dP}{dt} = Y_{P/X}\frac{1}{X}\frac{dX}{dt} + a \qquad (5.2)$$

The quantity $\frac{1}{X}\frac{dP}{dt}$ is known as the specific production rate or the rate of production of product per cell. This term is given the symbol ν. The quantity $\frac{1}{X}\frac{dX}{dt}$ is known as the specific growth rate or the average rate of growth per cell, and is given the symbol μ. Equation (5.2) may thus be written as:

$$\nu = Y_{P/X}\,\mu + a \qquad (5.3)$$

In analyzing Equation (5.3), it is seen that a plot of the specific production rate, ν, as a fraction of the specific growth rate, μ, should yield a straight line for fermentations conforming to Luedeking-Piret kinetics. Such a plot is shown in Figure 5.43 for the data of Figures 5.38-5.42 presented earlier. Since little yeast extract was employed in these studies, growth on yeast extract does not have to be accounted for. The specific production rate in Figure 5.42 is defined as the total specific production rate, accounting for the production of both ethanol and acetate. The specific rates were calculated by computer regression analysis of the batch data.

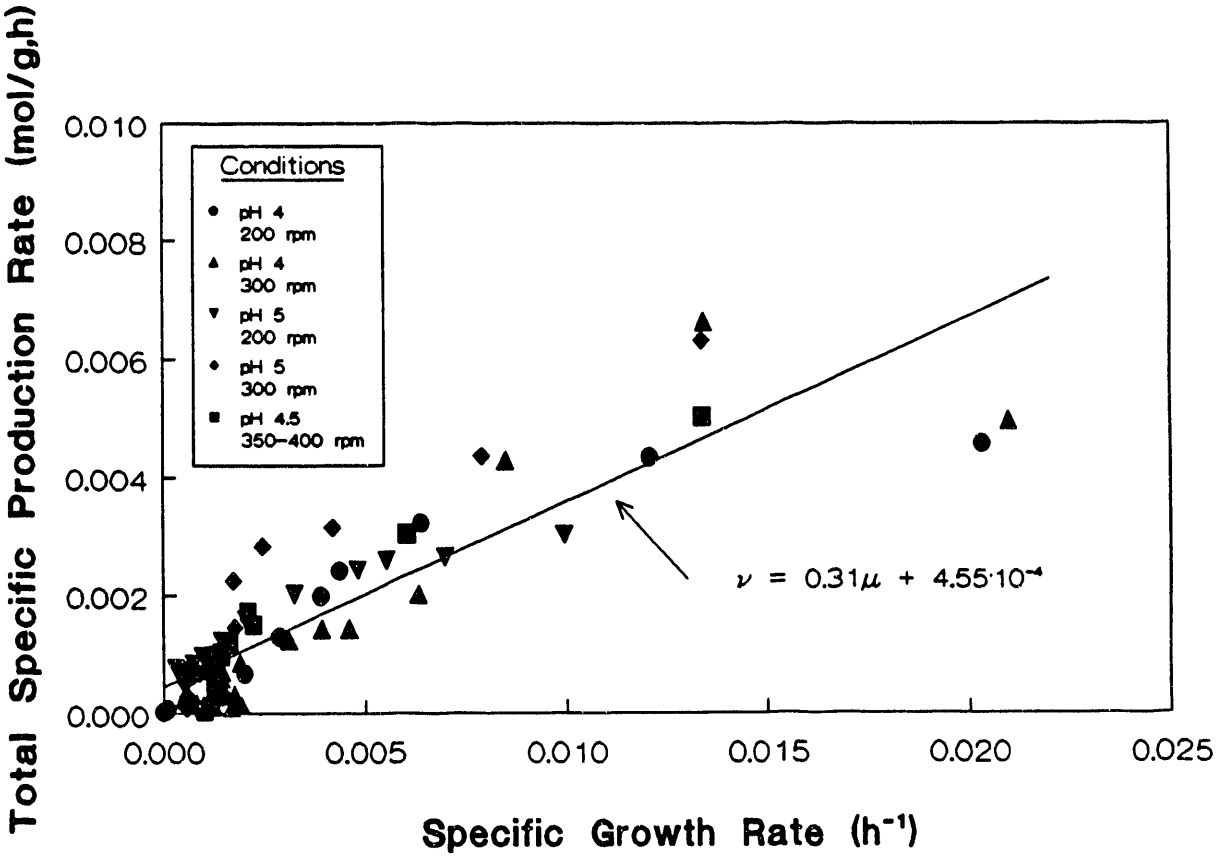

Figure 5.43. Determination of growth parameters for *C. ljungdahlii* grown on H_2, CO, and CO_2 in fed batch culture.

As is noted in Figure 5.43 a straight line was obtained when plotting the total specific production rate as a function of the specific growth rate. The constants in Equation (5.3) showed that $Y_{P/X}$ had a value of 0.31 mol product/g cells and "a" had a value of 4.55×10^{-4}. The ratio of the constants was very large, indicating that ethanol and acetate production from CO, CO_2 and H_2 in synthesis gas is growth dependent. For comparison purposes, Tyree *et al.*[31] found a ratio of the constants of 3.5 when fermenting glucose to lactate by *Lactobacillus xylosus*. Thus, the key to getting more product (either ethanol or acetate) from *C. ljungdahlii* is to have more cells.

5.11 Carbon Balance in Batch Culture and Stoichiometric Relationships

An attempt was made to close the carbon mass balance for the batch culture experiments presented earlier. In these batch fermentations, the medium composition was varied in a modified basal medium without yeast extract. These nutrient and carbon poor media make it ideal to trace the carbon transfer from substrate to products. Since CO is the preferred substrate over H_2 and CO_2 in the production of acetate and ethanol, the most predominant reactions taking place are those described in Equations (1.1) and (1.2). In addition, some of the carbon monoxide consumed is likely to be used for cell mass according to the reaction described by Equation (5.4).

$$CO + a\,H_2O \rightarrow b\,CH_cO_d + (1-b)\,CO_2 \qquad (5.4)$$

where a, b, c and d are stoichiometric coefficients and cell composition parameters. As is seen in Equations (1.1), (1.3) and (5.4), the carbon substrate is CO and the products containing carbon are ethanol (C_2H_5OH), acetate (CH_3COOH), CO_2 and cell mass. Based upon gas and liquid sample analyses, all carbon-containing substrate and products may be easily measured. The only unknown carbon-containing product is the carbon content of the cells.

A review of the experiments is summarized in Table 5.2. In Figure 5.44 the amount of carbon present in the products (ethanol, acetate and CO_2) has been plotted as a function of the amount of CO (the substrate) in the system for Experiment PBBAN 1 through PBBAN 4. As is noted in the figure, all of the experimental data fell on a single straight line with a slope of -0.885 mol/mol. The negative value of the slope indicates carbon consumption to produce products, and the slope represents the fraction of carbon consumed (as CO) which may be accounted for in the products. Thus, a carbon yield, $Y_{P/S}$, of 88.5% was obtained for the combined products. The remaining 11.5% of the carbon was likely incorporated into the cell mass.

Another way of displaying the experimental data is by calculating the carbon yield on combined liquid products, $Y_{HAC,EtOH/S}$, and ethanol alone, $Y_{EtOH/S}$. The graphical representations of these two yields are shown in Figures 5.45 and 5.46, respectively. In Figure 5.45 the amount of carbon present in the liquid products has been plotted as a function of amount of carbon in the substrate. The slope has a value of -0.330, which gives a $Y_{HAc,EtOH/S}$ value of 33%, indicating that 33% of the carbon consumed ends up in the two liquid products, the remainder going to CO_2 and cells. In Figure 5.46 the amount of carbon present in the produced ethanol has been plotted as a function of the CO carbon. As is noted, a value of 19.5% for $Y_{EtOH/S}$ was obtained. Thus, 19.5% of the consumed carbon was converted into ethanol. The remaining data from the other experiments were treated in the same manner and the results are listed in Table 5.3. As is seen in the table, all yields remained nearly constant for all of the conditions employed, with a calculated average of 92%, 36% and 21% for the carbon yields $Y_{P/S}$, $Y_{HAc,EtOH/S}$ and $Y_{EtOH/S}$, respectively.

Table 5.2

Operating Conditions for Experiments Used in the Carbon Balance Calculations

Experiment Name	Study	Conditions (No yeast extract, pH 4, 37°C)
PBBAN 1	Medium Comp.	Standard basal medium (Petc Report No. 2-2-91, March 1991)
2	Medium Comp.	Standard basal medium plus 2 x Pfennig minerals
3	Medium Comp.	Standard basal medium plus 2 x B-vitamins
4	Medium Comp.	Standard basal medium plus 2 x Pfennig trace metals
PBBAQ 1	Medium Comp.	Half strength standard basal medium
2	Medium Comp.	Standard basal medium minus 0.5 x Pfennig minerals
3	Medium Comp.	Standard basal medium minus 0.5 x B-vitamins
4	Medium Comp.	Standard basal medium minus 0.5 x Pfennig trace metals
PBBAS 1	B-vitamins	Standard basal medium but only 0.08 x B-vitamins
2	B-vitamins	Standard basal medium but only 0.21 x B-vitamins
3	B-vitamins	Standard basal medium but only 0.29 x B-vitamins
4	B-vitamins	Standard basal medium but only 0.92 x B-vitamins
PBBAT 1	Selected vitamins	Standard basal medium, only 0.08 x B-vitamins
2	Selected vitamins	Standard basal medium, only 0.08 x B-vitamins plus biotin
3	Selected vitamins	Standard basal medium, only 0.08 x B-vitamins plus thiamine
4	Selected vitamins	Standard basal medium, only 0.08 x B-vitamins plus Ca-pantothenate
5	Selected vitamins	Standard basal medium, only 0.08 x B-vitamins plus all of above

Table 5.2

Operating Conditions for Experiments Used in the Carbon Balance Calculations

Experiment Name	Study	Conditions (No yeast extract, pH 4, 37°C)
PBBAN 1	Medium Comp.	Standard basal medium (Petc Report No. 2-2-91, March 1991)
2	Medium Comp.	Standard basal medium plus 2 x Pfennig minerals
3	Medium Comp.	Standard basal medium plus 2 x B-vitamins
4	Medium Comp.	Standard basal medium plus 2 x Pfennig trace metals
PBBAQ 1	Medium Comp.	Half strength standard basal medium
2	Medium Comp.	Standard basal medium minus 0.5 x Pfennig minerals
3	Medium Comp.	Standard basal medium minus 0.5 x B-vitamins
4	Medium Comp.	Standard basal medium minus 0.5 x Pfennig trace metals
PBBAS 1	B-vitamins	Standard basal medium but only 0.08 x B-vitamins
2	B-vitamins	Standard basal medium but only 0.21 x B-vitamins
3	B-vitamins	Standard basal medium but only 0.29 x B-vitamins
4	B-vitamins	Standard basal medium but only 0.92 x B-vitamins
PBBAT 1	Selected vitamins	Standard basal medium, only 0.08 x B-vitamins
2	Selected vitamins	Standard basal medium, only 0.08 x B-vitamins plus biotin
3	Selected vitamins	Standard basal medium, only 0.08 x B-vitamins plus thiamine
4	Selected vitamins	Standard basal medium, only 0.08 x B-vitamins plus Ca-pantothenate
5	Selected vitamins	Standard basal medium, only 0.08 x B-vitamins plus all of above

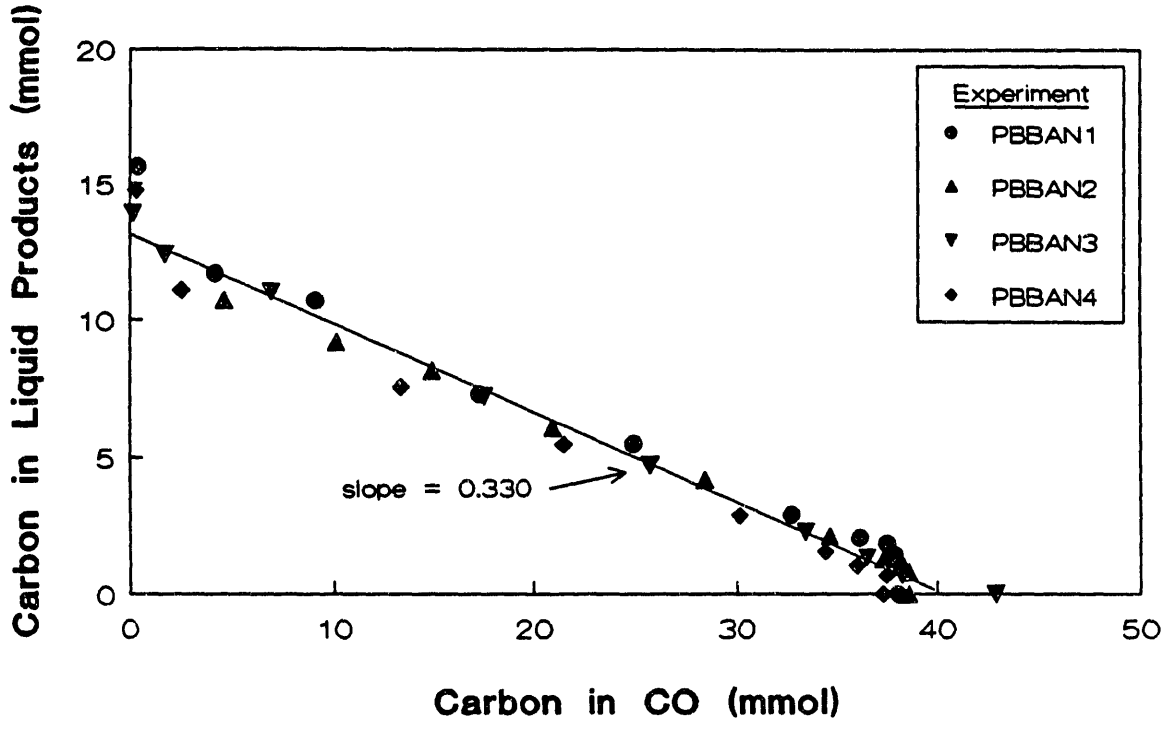

Figure 5.45 Amount of Carbon Present in Liquid Products as a Function of the Amount of Carbon in CO.

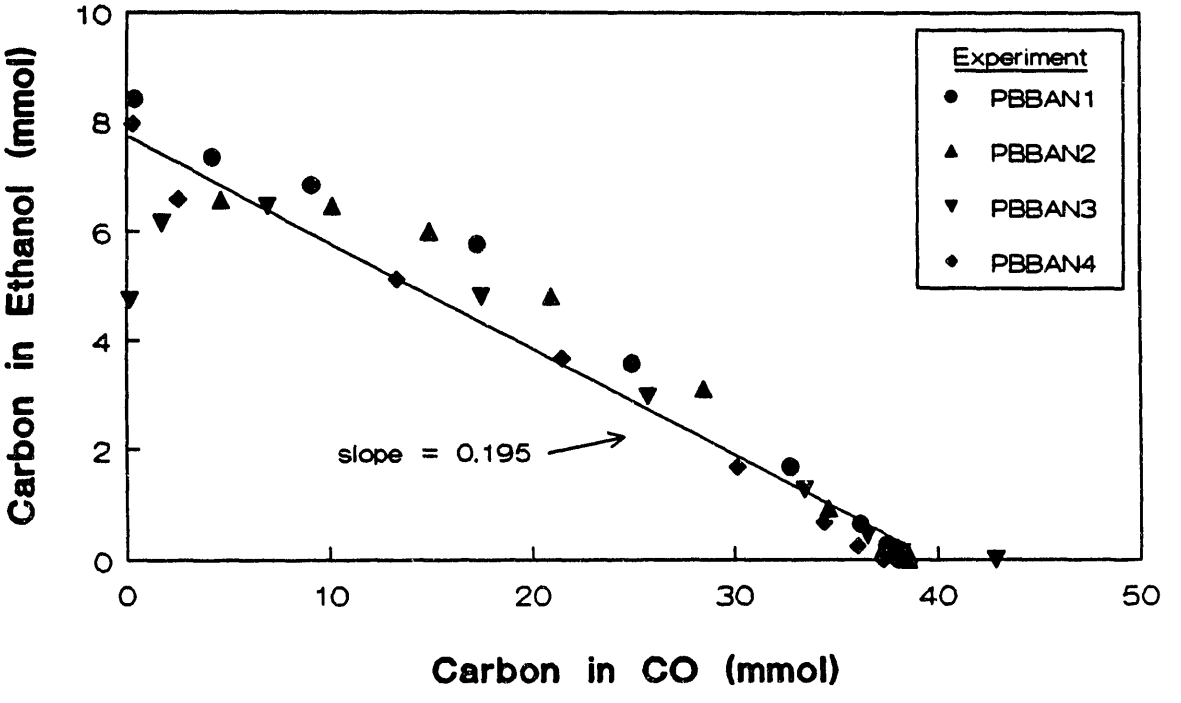

Figure 5.46 Amount of Carbon Present in Ethanol as a Function of the Amount of Carbon in CO.

Table 5.3

Carbon Yields and Stoichiometric Constants for Conducted Batch Experiments

Experiment Name	$Y_{P/S}$ (mol %)	$Y_{HAc,EtOH/S}$ (mol %)	$Y_{EtOH/S}$ (mol%)	1-b
PBBAN 1-4	88 (0.99)	33 (0.98)	19 (0.93)	0.43 (0.86)
PBBAQ 1-4	91 (1.0)	34 (0.97)	20 (0.95)	0.39 (0.70)
PBBAS 1-4	94 (0.99)	41 (0.94)	20 (0.82)	0.58 (0.78)
BBBAT 1-5	97 (0.99)	35 (0.97)	24 (0.87)	0.49 (0.78)
AVERAGE	92	36	21	0.47

(Values in parentheses indicate correlation coefficients of a linear fit)

An attempt to estimate the stoichiometric coefficients presented in Equation (5.4) has also been carried out. In this procedure, the amount of CO_2 produced in Equations (1.1) and (1.3) was subtracted from the total amount of CO_2 at any time and plotted as a function of the total amount of CO consumed in Equations (1.1) and (1.3) plus the CO present in the system. Such a plot is shown in Figure 5.47 for Experiments PBBAN 1-4. The negative slope corresponds to the constant "1-b" in Equation (5.4). As is noted in Figure 5.47, a value of 0.47 may be obtained from the slope of the curve. The additional data obtained in the other experiments were treated in the same fashion and, in Table 5.3, the values of "1-b" are listed for all of the experiments. The values obtained range from 0.39 to 0.58 mol/mol with an average of 0.47 mol/mol. Based upon an average value, Equation (5.4) may now be rewritten as:

$$CO + aH_2O \rightarrow 0.53\ CH_cO_d + 0.47\ CO_2 \qquad (5.5)$$

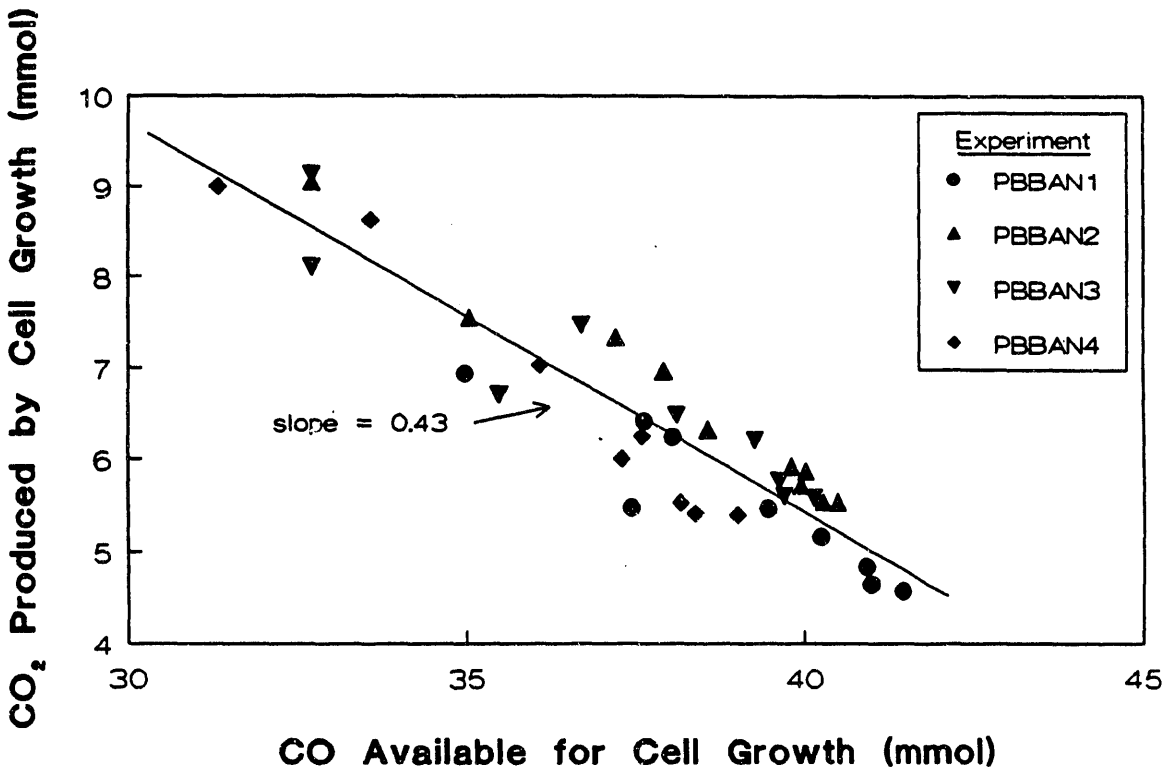

Figure 5.47 Amount of CO_2 Present as a Function of the Amount of CO. (Not Including the Reactions Involving Acetate and Ethanol.)

The constants a, c and d are still not determined without further information. One possible solution is to assume a rough, initial estimate of the cell formula, such as CH_2O. Based upon this formula, values of 0.53 or 0.47 may be obtained for the value of "a" from a hydrogen or oxygen balance over Equation (5.5). Even though there is a slight discrepancy, it is clear that the stoichiometric relationships and carbon balance equations proposed describe the CO uptake quite well in the batch system and that the rough estimate of the cell formula as CH_2O worked quite well in closing the final mass balance.

Finally, it should be added that the data used in the above treatment were obtained during the initial part of the fermentations. Typically, all of the initially added gas (CO, H_2, CO_2) was almost entirely consumed after which additional gas was added as required. Thus, the obtained data correspond to the first gas consumption cycle since the frequent addition of gas in the latter stages of the fermentation makes it hard to estimate overall CO consumption and CO_2 production. Qualitatively, it seems logical that the only carbon yield which may be significantly affected during the latter part of the fermentation is $Y_{EtOH/S}$ which is strongly linked to the composition of the medium.

5.12 Effect of Temperature on Growth and Product Formation by *C. ljundgahlii*

Temperature is known to affect both the growth and formation of products over a fairly narrow temperature range. Mesophilic organisms have an approximate operating temperature range of 10-47°C, with typical optimum temperatures of 30-45°C. Thermophilic organisms have a higher temperature operating range of 40-80°C, with an optimum of 55-75°C [32]. *C. ljungdahlii* is

a mesophile. Organisms usually continue to live at temperatures below their operating temperature range with significantly decreased metabolic activity, but usually die at temperatures only a few degrees above their operating range.

The growth and formation of ethanol and acetate by *C. ljungdahlii* were monitored over a temperature range of 35 to 40°C, with all other variables except pH held constant. Specific growth and production rates were then calculated for the exponential growth phases at each temperature. These rates were then compared at the various temperatures, along with the ratios of ethanol to acetate.

5.12.1 Equipment and Procedures

C. ljungdahlii was grown on basal medium without yeast extract and one-half the normal concentration of B-vitamins. The medium was reduced with 2.5% cysteine-HCl solution. All fermentations were carried out in 150 mL serum stoppered bottles, the medium occupying a volume of 50 mL.

The gas phase consisted of 65% CO, 24% H_2 and 11% CO_2 in each of the bottles. The bottles were pressurized to 10 psig with this synthetic synthesis gas initially and when replenishing the gas supply during the fermentation. All bottles were incubated in a horixontal position shaken in a New Brunswick shaker incubator at 100 rpm.

5.12.2 Results and Discussion

Typical cell concentration and total product (ethanol plus acetate) concentration profiles at a temperature of 34°C are shown in Figures 5.48 and 5.49. As is noted, two different pH levels were studied at this temperature, pH 4.5 and pH 5.0. The pH level reported is the time average pH value over the exponential growth period, defined as:

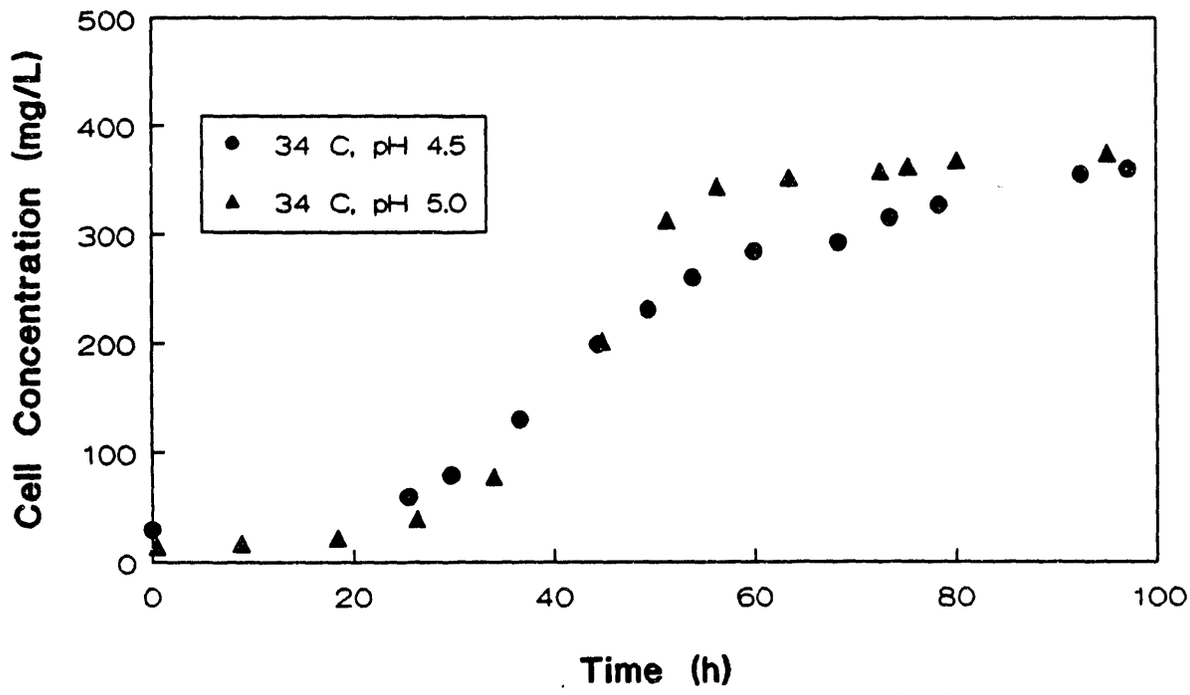

Figure 5.48 Batch Cell Concentration Profiles for *C. ljungdahlii* in Basal Medium (No Yeast Extract, 50 Percent of the Standard B Vitamins) at 34 Degrees C.

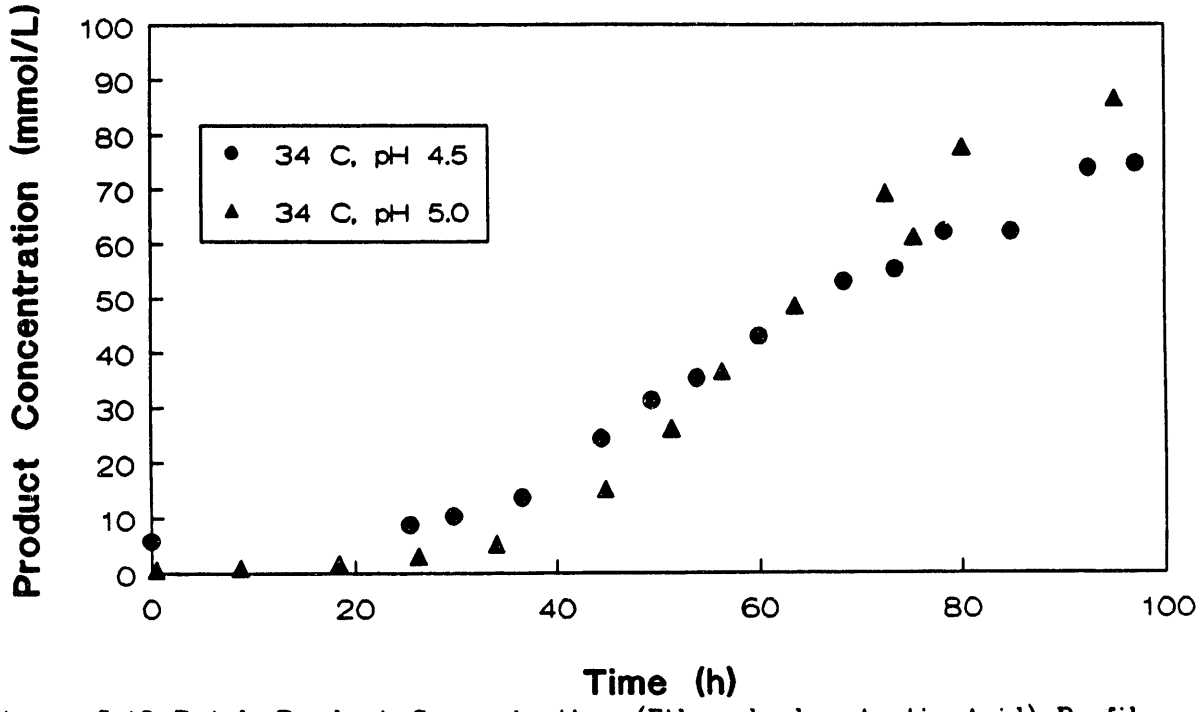

Figure 5.49 Batch Product Concentration (Ethanol plus Acetic Acid) Profiles for *C. ljungdahlii* in Basal Medium (No Yeast Extract, 50 Percent of the Standard B Vitamins) at 34 Degrees C.

$$\text{pH avg} = \frac{\int \text{pH } dt}{\Delta t} \tag{5.6}$$

where Δt is defined by the straight line data points used in obtaining the specific growth rate.

As is noted in Figures 5.48 and 5.49, pH had only a small effect on cell concentration and total product concentration. However, as was shown and discussed previously, the pH did affect the product ratio, with lower pH levels resulting in higher ethanol: acetate ratios (data not shown). The maximum call concentration reached at 34°C was approximately 350 mg/L, reached after 50-60 h of fermentation (see Figure 5.48) The maximum product concentration at 34°C was obtained at the end of the fermentation period, reaching a combined ethanol plus acetate concentration of nearly 90 mmol/L (see Figure 5.49).

Similar profiles to Figures 5.48 and 5.49 at all fermentation temperatures were then used to calculate the specific growth and production rates in the exponential growth phase. This procedure is demonstrated in Figures 5.50 and 5.51 for a temperature of 34°C and pH levels of 4.5 and 5.0. The specific growth rate, μ, is defined in the exponential growth phase as:

$$\mu = \frac{1}{X}\frac{dX}{dt} \tag{5.7}$$

Separating variables and integrating Equation (5.7) yields:

$$\int_{X_o}^{X} \frac{dX}{X} = \mu \int_{o}^{t} dt \tag{5.8}$$

and,

$$\ln \frac{X}{X_o} = \ln X - \ln X_o = \mu t \tag{5.9}$$

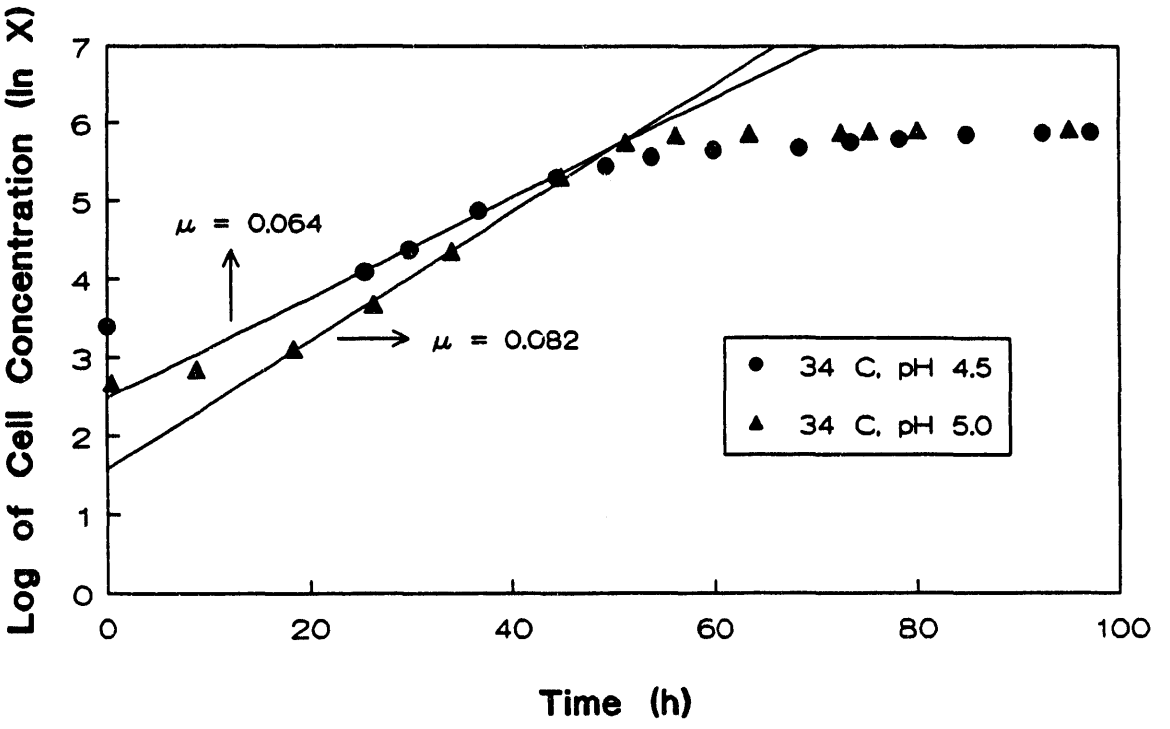

Figure 5.50 Determination of Specific Growth Rate (μ) During Exponential Growth of *C. ljungdahlii* in Batch Culture.

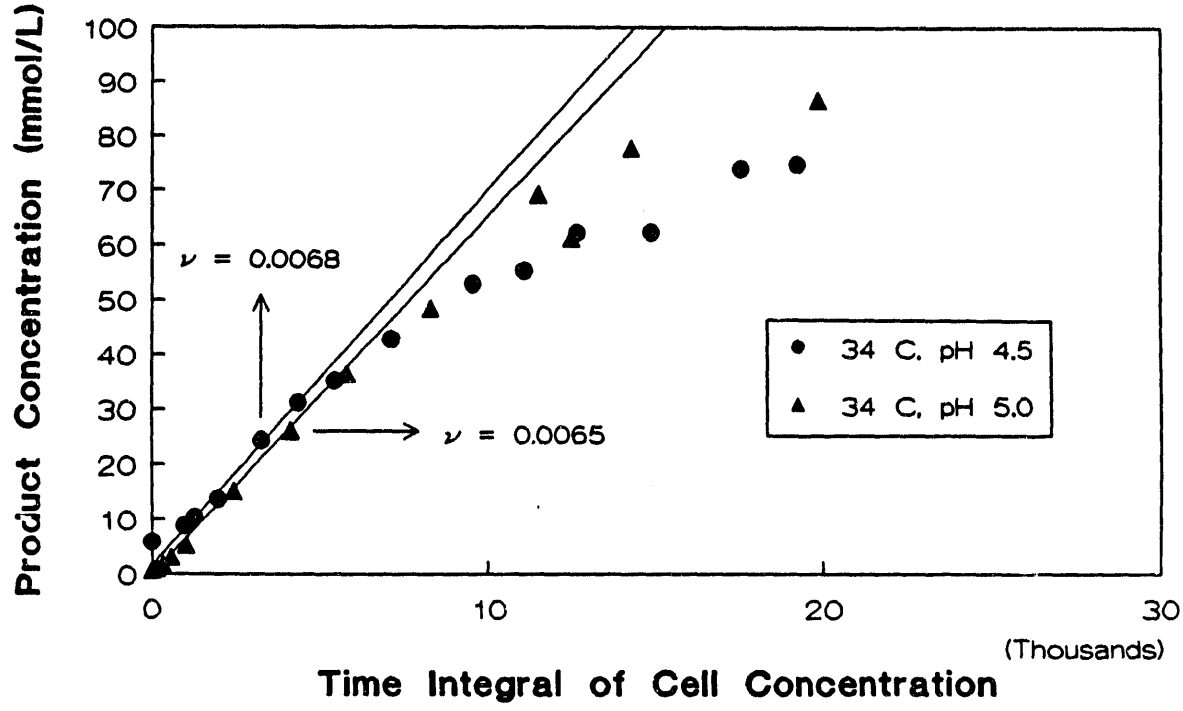

Figure 5.51 Determination of Specific Production Rate (ν) During Exponential Growth of *C. ljungdahlii* in Batch Culture.

Thus, a plot of ln X as a function of time should yield a straight line with a slope equal to μ in the exponential growth phase. As is shown in Figure 5.50, a straight line is obtained in the exponential growth phase at 34°C for both pH levels. The specific growth rate is 0.064 h^{-1} at pH 4.5 and 0.082 h^{-1} at pH 5.0.

The specific production rate, ν, is defined as:

$$\nu = \frac{1}{X} \frac{dP}{dt} \tag{5.10}$$

Rearranging Equation (5.10) yields:

$$dP = \nu X \, dt \tag{5.11}$$

Integration of Equation (10) yields:

$$P - P_o = \nu \int_o^t X \, dt \tag{5.12}$$

where P_o, the initial product concentration, equals zero. Thus, a plot of the total product concentration, P, as a function of the time integral of cell concentration, $\int_o^t X \, dt$, should yield a straight line over the exponential growth region with a slope equal to the specific production rate, ν. As is noted in Figure 5.51, the specific growth rate at 34°C and pH 4.5 is 0.0068 mmol/mg•h, and at pH 5.0 is 0.0065 mmol/mg•h.

A plot of specific growth rate and specific production rate as a function of temperature (regardless of pH) is shown in Figure 5.52. As is noted, both the average specific growth rate and the average specific production rate are seen to reach a maximum at a particular temperature. The maximum specific growth rate was 0.095 h^{-1} at about 37°C. The maximum specific production rate was 0.0095 mmol/mg•h at about 40°C. Thus, the best temperature for growth is at a typical optimum for mesophilic bacteria, while production is favored at a

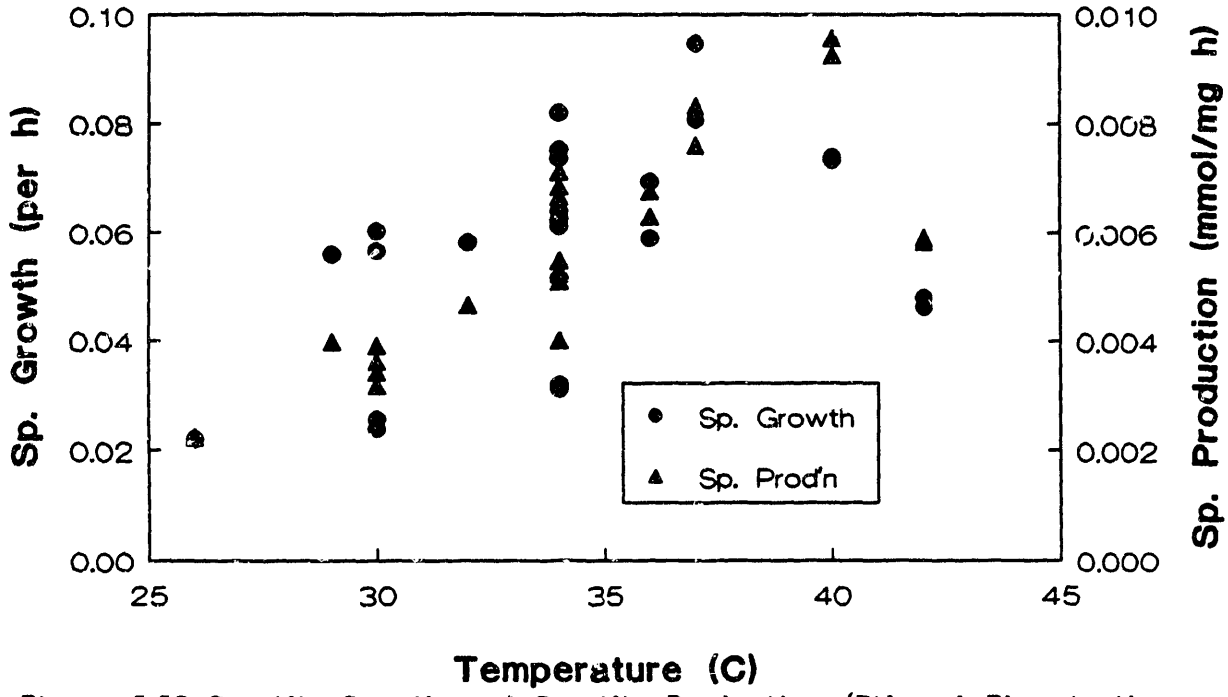

Figure 5.52 Specific Growth and Specific Production (Ethanol Plus Acetic Acid) Rates for *C. ljungdahlii* at Various Temperatures in Batch Culture.

slightly higher temperature. It should be noted that the product ratio (ethanol:acetate) was not significantly affected by temperature, but was affected by fermentation pH as expected.

The wide variation in the data presented in Figure 5.52 is due mainly to the variation of pH during fermentations. This variation is illustrated in Figure 5.53, where the specific growth and production rates at 34°C are plotted as a function of the time average pH (see Equation 5.6). As is noted, the specific growth rate was seen to increase with increasing pH. This result was expected since higher pH levels were shown earlier to be more suitable for both growth and acetate production. The specific production rate, on the other hand, was shown to be rather low at pH 3.75, but was essentially constant at the higher pH levels. The bacterium was shown earlier to function well at pH levels of 4.0 and above, and the total product formation (ethanol plus acetate) was shown to be essentially constant with pH. Ethanol production, of course, was favored at lower pH levels.

5.12.3 Data Analysis

The data presented on the effects of temperature on the performance of *C. ljungdahlii* indicate that the best temperature for the growth of bacterium was at 37°C, while product formation was favored at a slightly higher temperature of 40°C. However, the data from the temperature study were quite scattered, thereby making interpretation of the results difficult. This scattering was due to the fact that many different experimental runs were necessary to obtain the data, thereby leading to variances in inoculum history. Perhaps, a better way to interpret the data of many experimental runs is to normalize the data to the results obtained at an experimental condition common to all experiments.

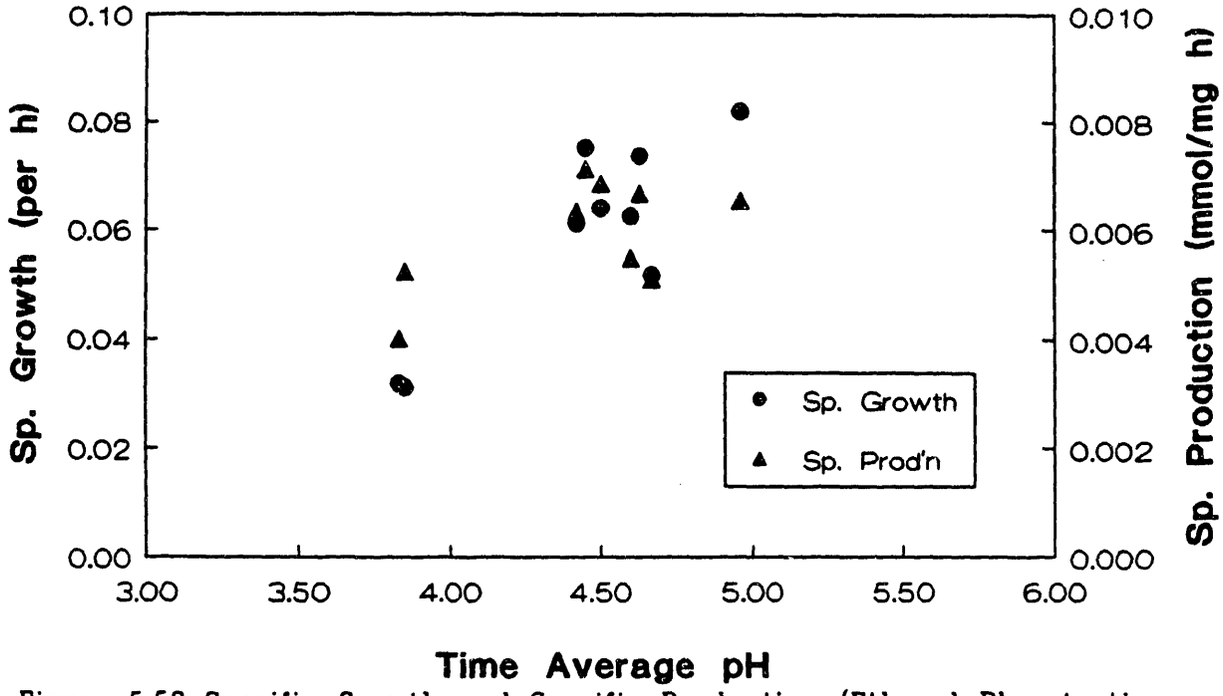

Figure 5.53 Specific Growth and Specific Production (Ethanol Plus Acetic Acid) Rates for *C. ljungdahlii* at Varying Average pH Levels in Batch Culture at 34 Degrees C.

Plots of normalized specific growth and production rates as a function of temperature using 34°C as a reference point use shown in Figures 5.54 and 5.55, respectively. Additional data carried out in larger batch bottles are included as open data points. In comparing these figures to the previous data, it is obvious that the experimental trends are easier to observe in the normalized figures. Figure 5.54, for example, shows that the specific growth rate increased with temperature up to a temperature of about 36°C, followed by a decrease as the temperature was further decreased. Figure 5.55 shows that the specific production rate increased with temperature up to 40°C, followed by a significant reduction at temperatures above 40°C. Thus, the growth was maximized at typical mesophilic operating tempertures (37°C), while production was favored at slightly higher temperature (40°C). As was mentioned previously, ethanol was favored at lower pH levels, but was unaffected by temperature over the range studied.

5.13 Sulfur Gas Tolerance of *C. ljungdahlii*

Many bacterial cultures capable of converting CO to products have been found to be quite tolerant of the sulfur gases H_2S and COS.[33,34] *Peptostreptococcus productus*, for example, which converts CO to acetate, was able to uptake CO in the presence of 19.7 percent H_2S or COS after culture acclimation. The methanogen, *Methanobacterium formicicum*, on the other hand, was only able to tolerate 6.6 percent H_2S or COS. This latter result is still encouraging, since typical coal-derived synthesis gas contains only 1-2 percent sulfur gases, mainly as H_2S.

C. ljungdahlii, grown with Na_2S in place of cysteine-HCl as the reducing agent for 14 weekly transfers, was evaluated for its tolerance to H_2S and COS in batch bottle experiments. The fermentation medium and techniques for

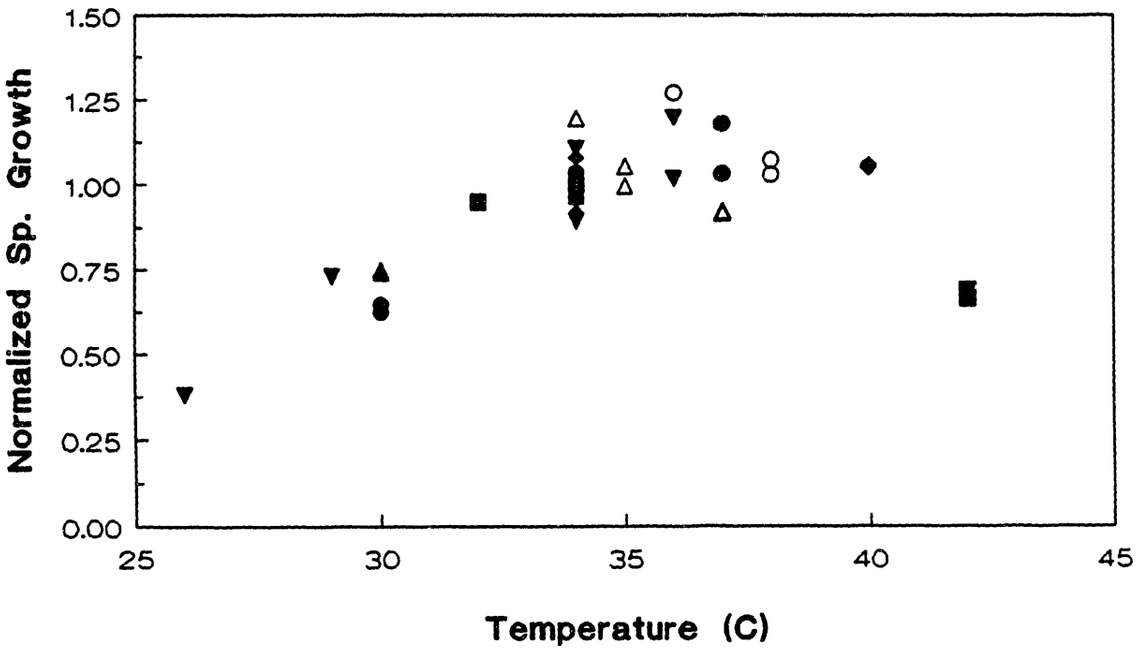

Figure 5.54 Normalized Specific Growth Rates for *C. ljungdahlii* at Various Temperatures in Batch Culture (Ref. Temp. 34°C).

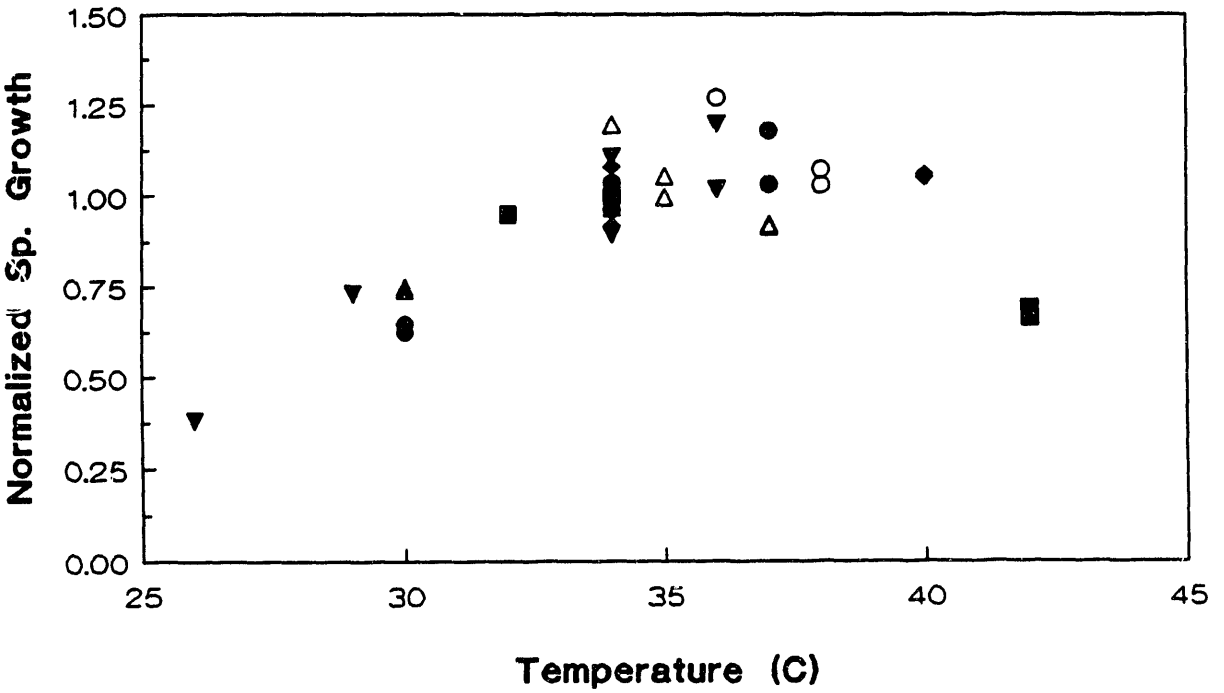

Figure 5.54 Normalized Specific Growth Rates for *C. ljungdahlii* at Various Temperatures in Batch Culture (Ref. Temp. 34°C).

culturing the bacterium were as outlined previously. The 157 mL bottles containing 50 mL of liquid medium adjusted to pH 4.3, were first gassed with synthesis gas to a pressure of 10.7 psig. The desired amount of H_2S or COS (2.5 mL-20 mL) at 1 atm was then added. Cysteine-HCl (0.2 mL) was added to some bottles, while others had no cysteine-HCl added. This batch system was then allowed to equilibrate overnight. As a final step, 10 mL of *C. ljungdahlii* were added prior to incubation at 34°C.

The effects of H_2S on growth, substrate uptake and produce formation by *C. ljungdahlii*, are shown in Figures 5.56-5.58, respectively. As is noted in Figure 5.56, growth was not significantly slowed in the presence of 10 mL of H_2S. This volume of H_2S corresponds to an initial gas phase concentration of 5.2 mole percent. Upon the addition of 20 mL of H_2S (9.9 percent H_2S), growth stopped. The presence of additional sulfur in the form of cysteine-HCl increased growth slightly. The results shown in Figure 5.56 are expected to improve with acclimation to H_2S. Similar results are noted with substrate uptake and product formation (see Figures 5.57 and 5.58). The presence of H_2S slowed the rates of substrate uptake and product formation only slightly up to an H_2S concentration of 5.2 mole percent.

The effects of COS on growth, substrate uptake and product formation are shown in Figures 5.59-5.61, respectively. As expected, COS was a more powerful inhibitor than H_2S. Growth and product formation were significantly inhibited by the presence of 10 mL of COS (5.2 mole percent), while uptake was inhibited significantly in the presence of 5 mL of COS (2.7 mole percent). Again, these results should improve dramatically with further acclimation to the sulfur gas.

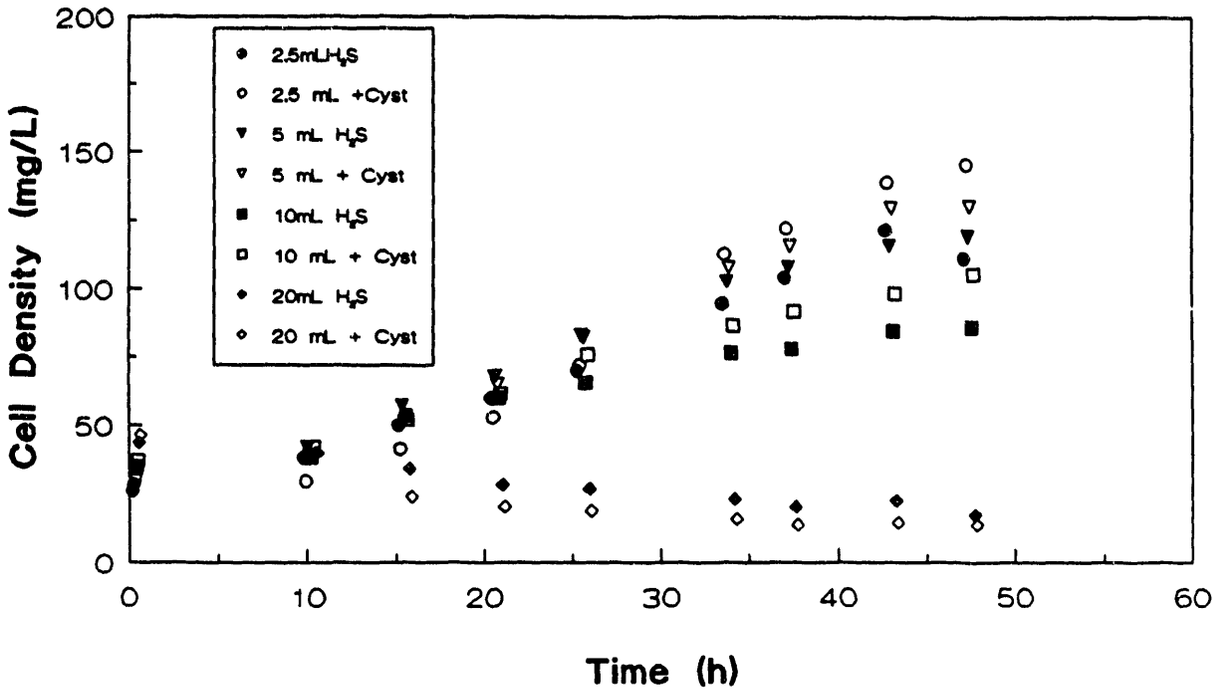

Figure 5.56 The Effect of H_2S on the Growth of *C. ljungdahlii* in Batch Culture.

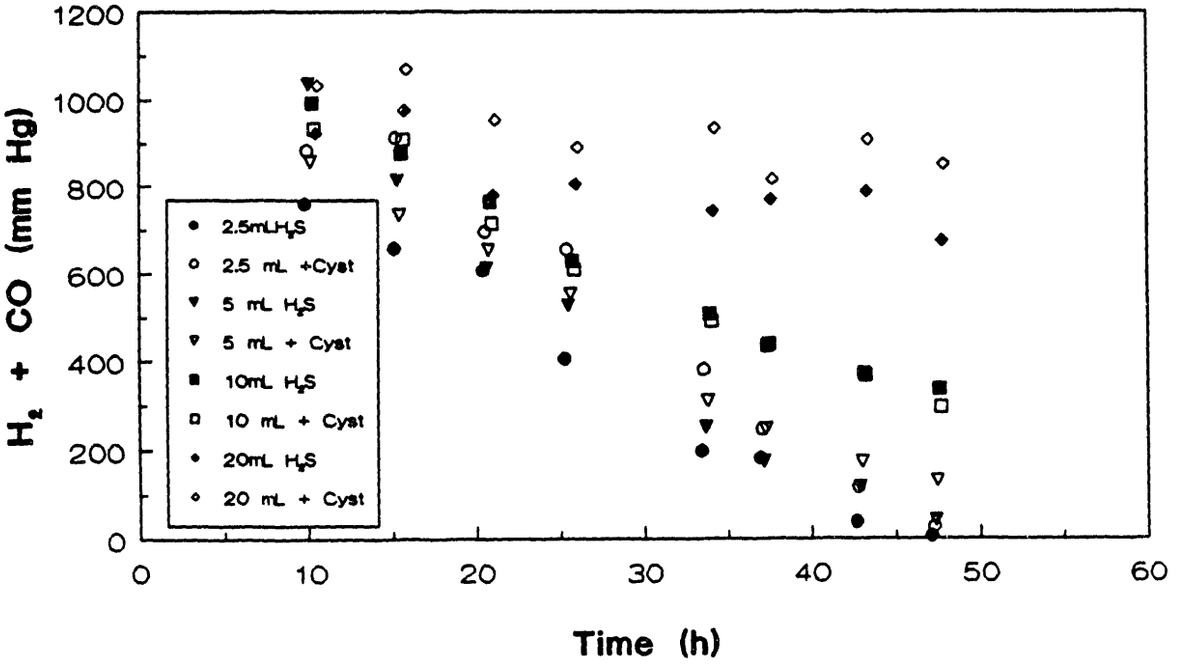

Figure 5.57 The Effect of H_2S on H_2 and CO Uptake by *C. ljungdahlii* in Batch Culture.

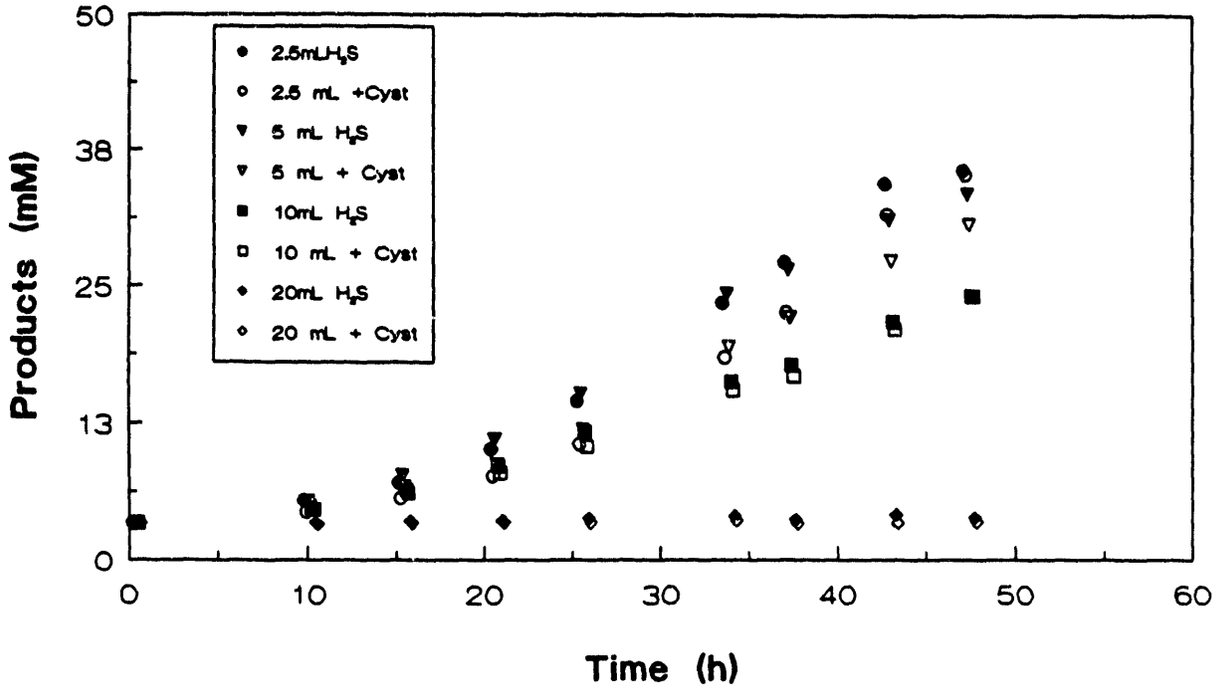

Figure 5.58 The Effect of H_2S on Total Product Formation by *C. ljungdahlii* in Batch Culture.

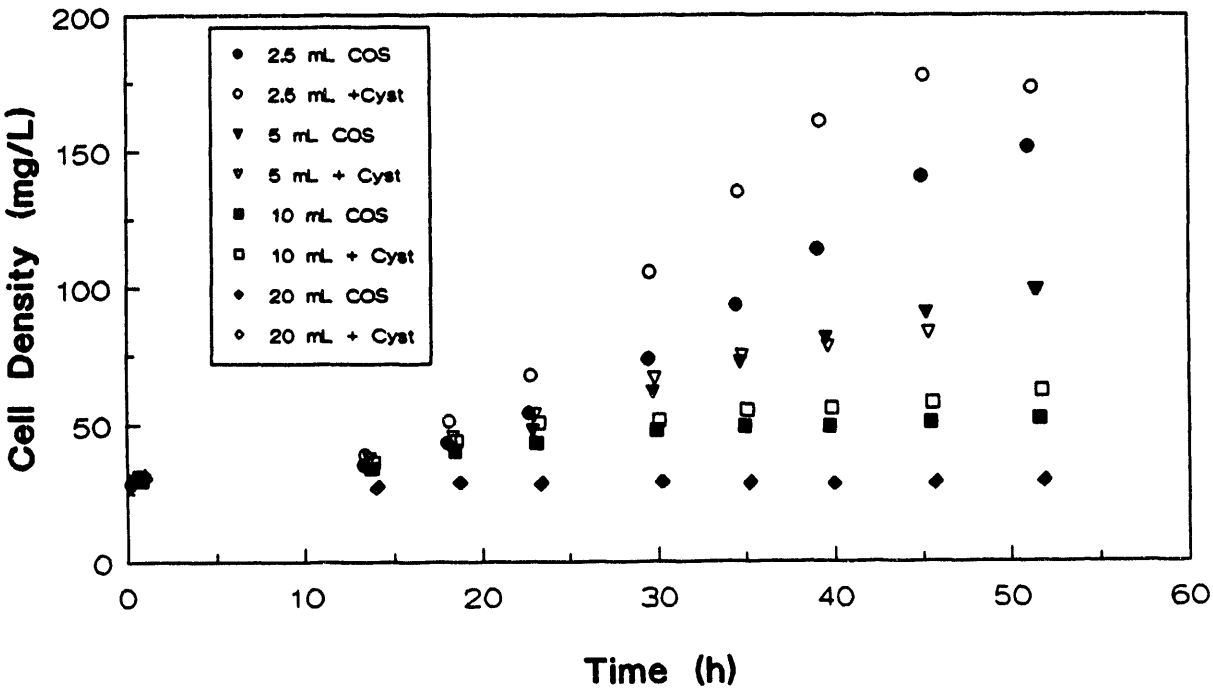

Figure 5.59 The Effect of COS on the Growth of *C. ljungdahlii* in Batch Culture.

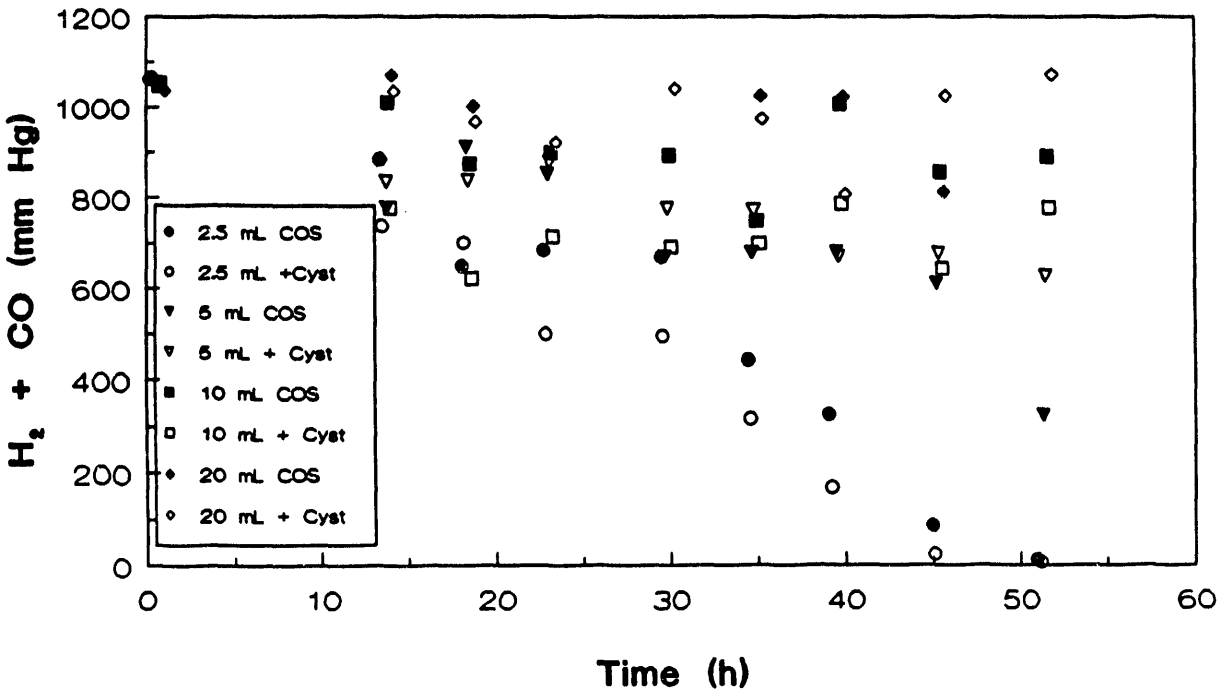

Figure 5.60 The Effect of COS on H_2 and CO Uptake by *C. ljungdahlii* in Batch Culture.

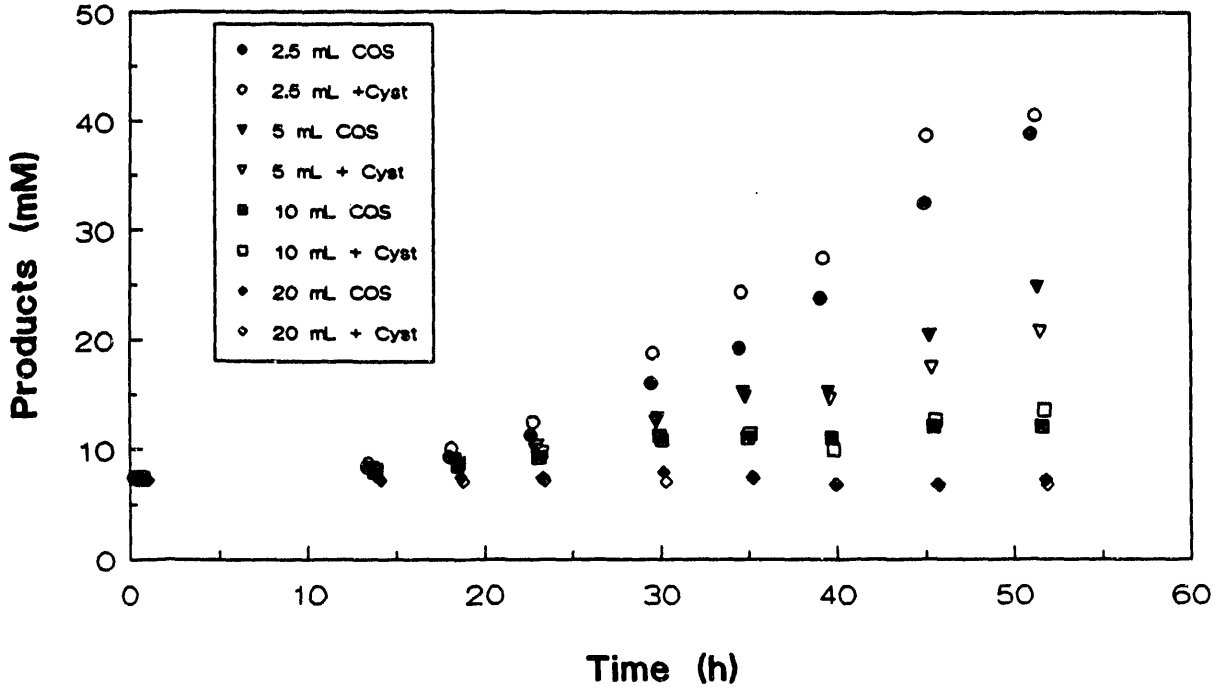

Figure 5.61 The Effect of COS on Total Product Formation by *C. ljungdahlii* in Batch Culture.

Perhaps a better view of the effect of sulfur gases on the performance of *C. ljungdahlii* can be obtained by observing the specific growth and production rates. As is noted in Figure 5.62, the specific production rate was highest in the presence of 2.5 mL of either sulfur gas and cysteine HCl. The addition of up to 10 mL of H_2S or COS gradually decreased the specific growth rate, while the specific growth rate fell to zero with 20 mL of sulfur gas. The specific production rate, shown as a function of the volume of sulfur gas in Figure 5.63, showed a similar trend. Again, the specific production rate was zero in the presence of 20 mL of sulfur gas.

Although these results may not seem encouraging at this point, it should be realized that dramatic effects can be obtained with further sulfur gas acclimation. *P. productus*, for example, was only marginally tolerant of H_2S and COS in initial studies. Very impressive results were obtained after a period of acclimation to the sulfur gases. Furthermore, these results are for an initially dilute batch culture incubated for only 48 hours. Sulfur gas inhibition might be manifested in such a culture and an extended lag time before growth begins. Inhibition may be lessened in the concentrated culture maintained in a continuous reactor.

5.14 Effect of Substrate on the Performance of *C. ljungdahlii*

The growth of *C. ljungdahlii* on synthesis gas containing CO, H_2, and CO_2 proceeds with preferential consumption of CO. A high availability of CO has also been shown to shift the product ratio, E/A (moles of ethanol per mole of acetate produced), toward ethanol.

The thermochemistry of Equations (1.1-1.4) has been reviewed and is summarized in Table 5.4. For each reaction the heat of reaction, ΔH_r, is the gain in enthalpy of the reaction products over the reactants. The negative

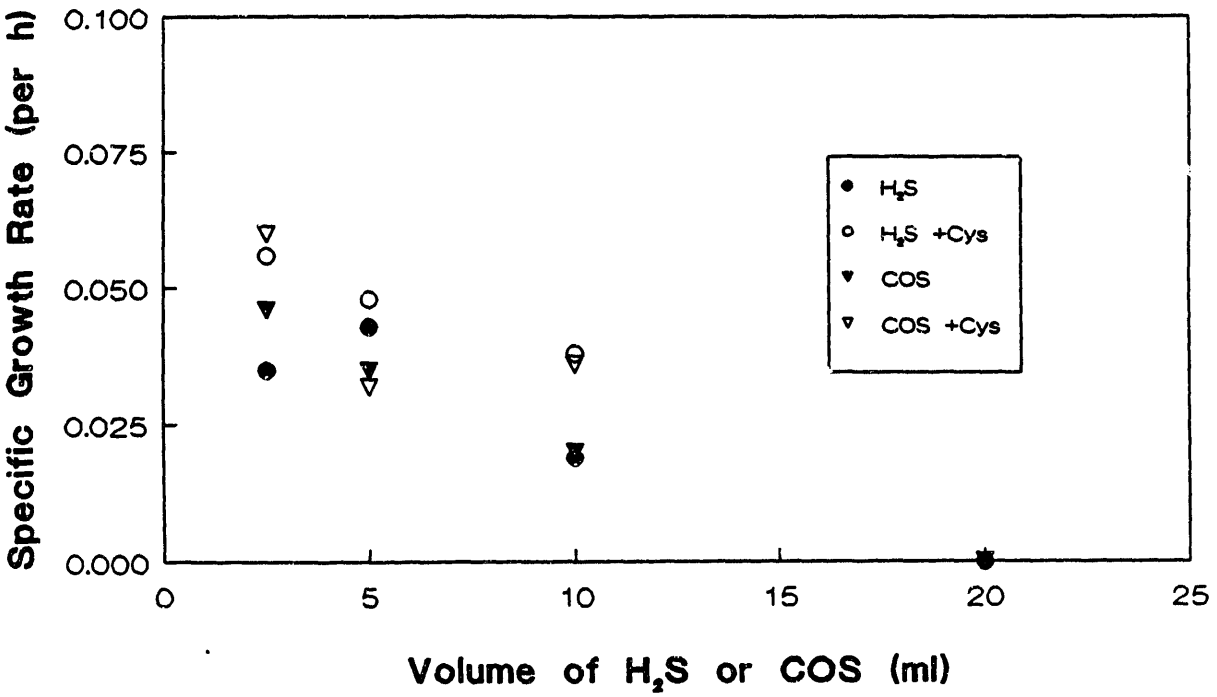

Figure 5.62 Specific Growth Rate of *C. ljungdahlii* in the Presence of Sulfur Gases.

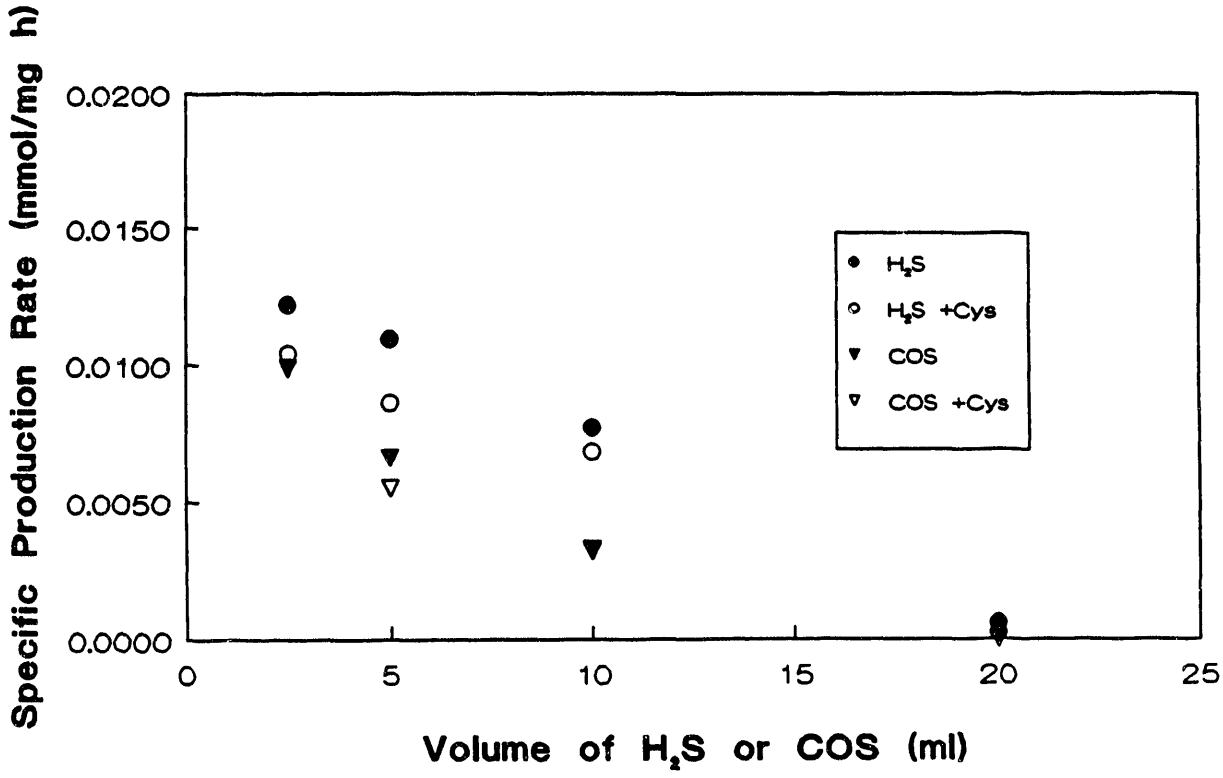

Figure 5.63 Specific Production Rate of *C. ljungdahlii* in the Presence of Sulfur Gases.

Table 5.4 Thermochemistry Summary for Ethanol and Acetate Production from CO, CO2 and H2.

	$\Delta H°r$ kJ/mol rxn	$\Delta G°'$ kJ/mol rxn	$T\Delta S°$ kJ/mol rxn	HHV Conserved %
Rxn 1	-260.27	-175.3	-85.0	77.0
Rxn 2	-271.67	-94.9	-176.8	76.2
Rxn 3	-331.03	-224.8	-106.2	80.5
Rxn 4	-348.13	-104.6	-243.8	79.7

values in Table 5.4 indicate exothermic reactions. The Gibbs free energy change, ΔG_r, of the reaction is indicative of the driving force for the reaction and determines the thermodynamically possible extent of the reaction. The heat of reaction and free energy change at a constant temperature are related by the equation:

$$\Delta G_r = \Delta H_r - T\Delta S_r \qquad (5.13)$$

The entropy term, $T\Delta S_r$, is the portion of the heat of reaction that is required to overcome system randomness and is thus not available to drive the reaction. The values given in Table 5.4 are for the reaction of reactants to products each at 1.0 M concentrations for liquid species, or 1.0 atm partial pressure for gases, at 25°C. The prime (') indicates reaction at pH 7.0. The data of Table 5.4 show that the heat of reaction of carbon monoxide going to acetate or ethanol (Equations (1.1) and (1.3)) is nearly identical to that for the reaction of hydrogen to the same product (Equations (1.2) and (1.4)). The useful energy from the reactions, indicated by the free energy change, is nearly double for CO in comparison to H_2. This results from the consumption of more gas phase reactants for which the initial entropy is higher in the H_2/CO_2 reactions.

The energy conservation of each reaction, defined as the heat of combustion of the products (higher heating value) divided by the heat of combustion of the reactants, is also given in Table 5.4. The production of ethanol retains about 80 percent of the energy value of the reactants, while the production of acetic acid retains about 77 percent, for reaction of either CO or H_2/CO_2. These values of energy conservation apply only to the fermentation and ignore the energy costs of production and recovery, but give an upper bound for estimation of the efficiency.

These differences in the useful energy from the reaction of CO and H_2/CO_2 must affect the performance of *C. ljungdahlii*. Additional substrate effects may arise from the effect of CO versus H_2 on the electrochemical potential of the fermentation. Effects of substrate may be seen in yields, rates and inhibition.

A series of batch experiments were run to compare growth and production on carbon monoxide, and hydrogen with carbon dioxide as sole sources of energy and carbon. The experiments were run in 157 mL serum bottles with 50 mL of basal medium without yeast extract and with one half of the standard B-vitamins. The bottles were filled to various pressures with either CO/CO_2 (80% CO, 20% CO_2), H_2/CO_2 (mixed in a gassing manifold to various compositions), or synthesis gas (25% H_2, 65% CO, 10% CO_2). The medium was reduced with 1.0 mL of 2.5% cysteine $HCl \cdot H_2O$, inoculated with 5 mL of seed culture, and shaken at 36°C. Growth, production, and substrate consumption were followed as previously reported. The culture pH was maintained near 4.5 by the addition of 0.5 M NaOH. Some of the bottles were allowed to consume all of the initial substrate (experiments DA and DB); others were recharged to sustain growth. Table 5.5 shows the initial composition of nine bottles.

The quantity of substrate (CO plus H_2) consumed and the amount of cells and products (ethanol plus acetate) formed are shown for the nine bottles in Table 5.6. Data for representative bottles are plotted in Figures 5.64-5.67. These data were from the initial charge of substrate gas for which the material balance is most accurate. The DE and DF experiments were recharged at 58 hours with H_2/CO_2 to allow growth to continue. Table 5.6 shows generally comparable reaction times and substrate consumption without regard to substrate. Cell growth, however, is clearly much stronger in cultures grown on CO.

Table 5.5 Composition of Bottles for Substrate Consumption Studies.

Expt	%H2	%Ar	%CO	%CO2	No(mmol)
DA-1	0.0	6.9	75.0	18.2	4.22
DA-3	0.0	5.3	76.7	18.0	6.20
DA-5	0.0	3.3	78.7	18.1	8.17
DB-5	48.4	4.5	0.0	45.6	10.03
DE-3	46.6	8.4	0.1	44.9	7.42
DF-1	36.1	9.6	0.0	54.3	8.21
DF-2	26.5	10.3	0.0	63.2	8.21
DF-3	23.1	9.0	58.4	9.5	8.21
DF-4	23.3	6.8	60.1	9.8	8.21

Table 5.6 Substrate Consumed, Products and Cells Produced by *C. ljungdahlii.*

Expt	Time (h)	Hydrogen (mmol)	CO (mmol)	Ethanol (mmol)	Acetate (mmol)	Cells (mg)
DA-1	31.48	0.00	3.17	0.28	0.47	8.05
DA-3	47.50	0.00	4.75	0.37	0.66	8.90
DA-5	47.70	0.00	6.42	0.57	0.83	11.05
DB-5	55.00	3.64	0.00	0.22	0.77	1.87
DE-3	45.00	3.25	0.01	0.20	0.49	1.41
DF-1	57.30	2.97	0.00	0.03	0.57	1.46
DF-2	51.80	2.18	0.00	0.01	0.47	0.90
DF-3	57.70	0.96	4.79	0.54	0.49	7.44
DF-4	57.80	1.86	4.94	0.42	0.64	7.33

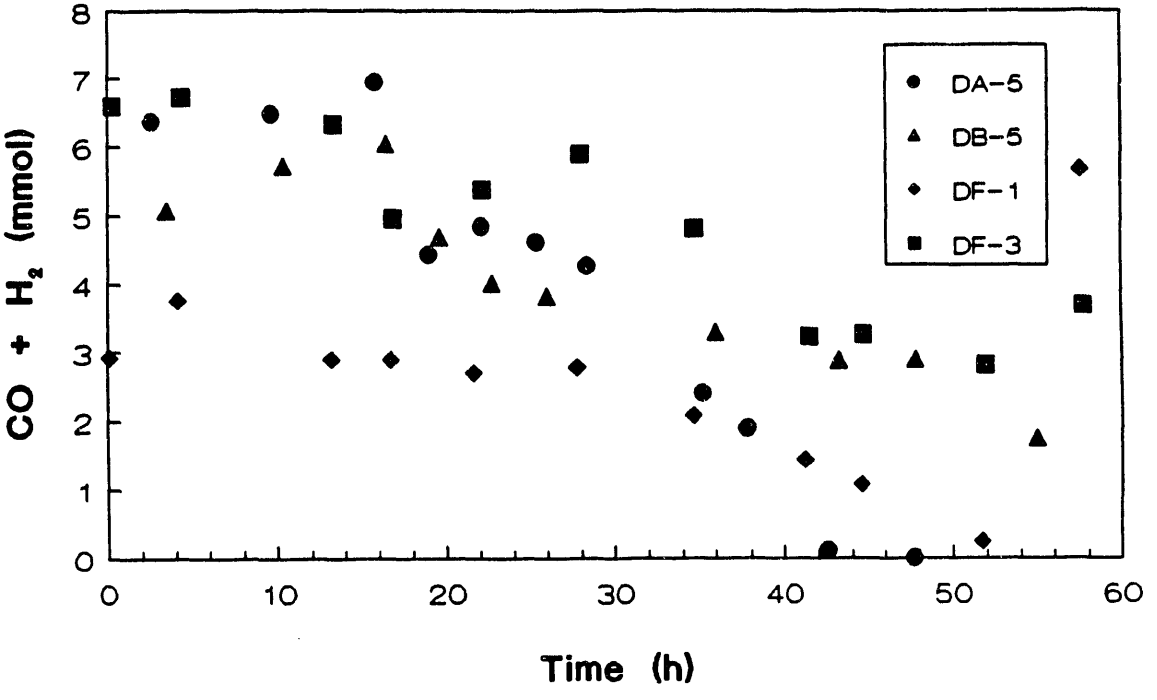

Figure 5.64 Combined CO and H_2 Consumption by *C. ljungdahlii* for Various Substrate Compositions.

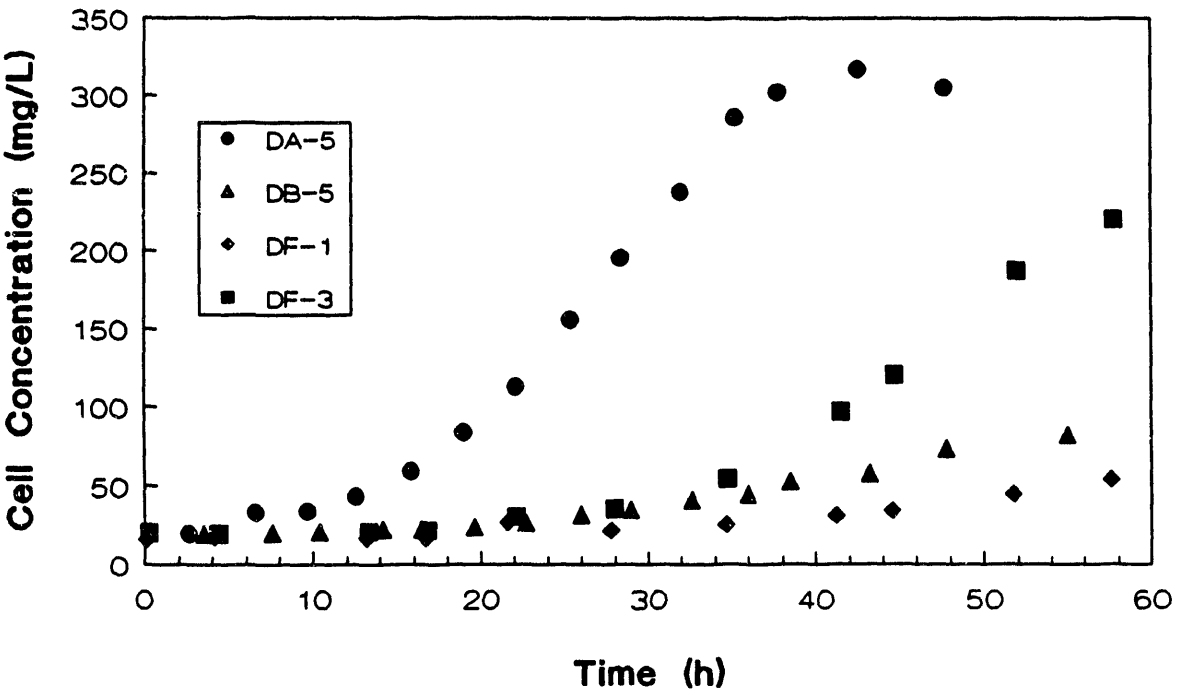

Figure 5.65 Cell Concentration Profiles for *C. ljungdahlii* for Various Substrate Compositions.

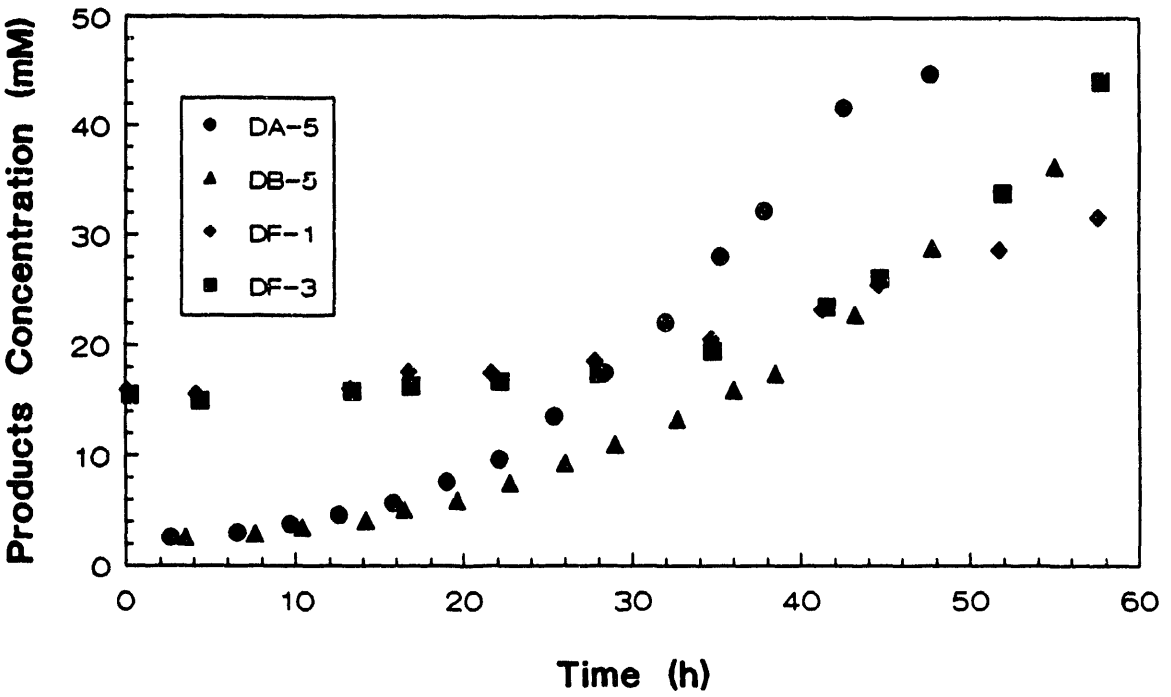

Figure 5.66 Combined Products Concentrations for *C. ljungdahlii* for Various Substrate Compositions.

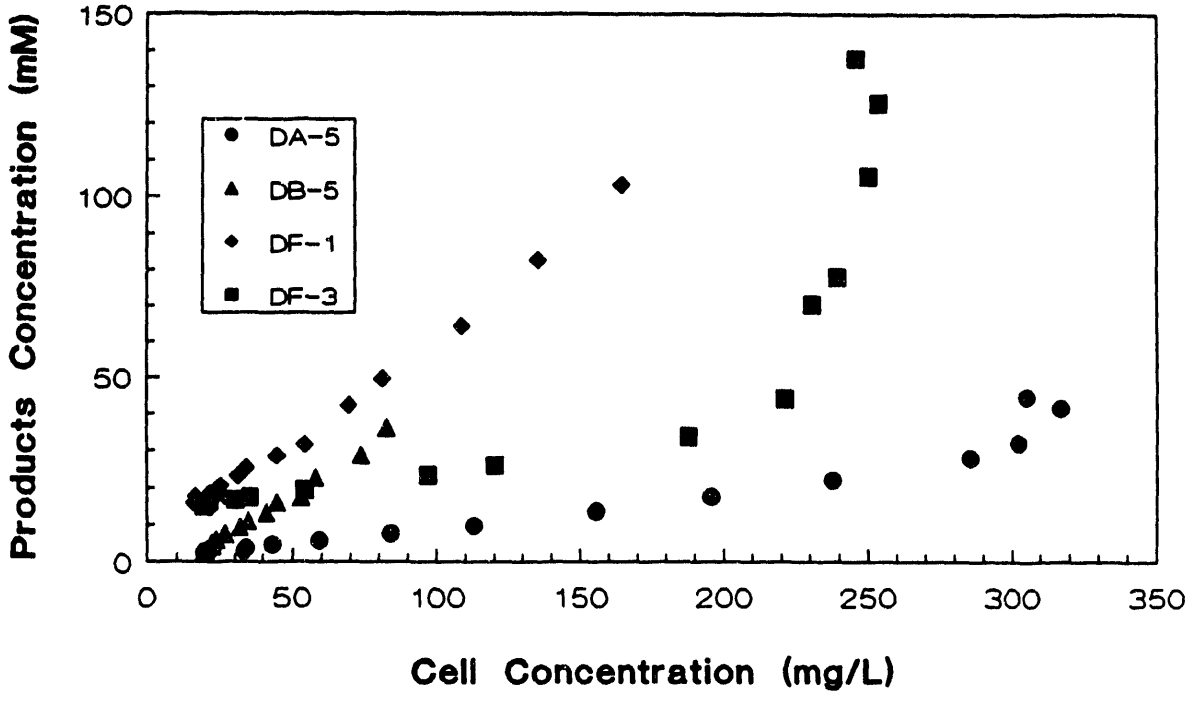

Figure 5.67 Combined Products Concentrations as a Function of the Cell Concentration for *C. ljungdahlii* for Various Substrate Compositions.

Figure 5.64 shows generally comparable rates of substrate consumption for all of the bottles. The scatter of the data in Figure 5.64 compared to the smooth curves of Figures 5.65-5.67 illustrates the difficulty in accurately determining gas concentrations, particularly when hydrogen is involved. The final points (at 58 hours) for DF-1 and 3 indicate the recharge of substrate.

Figure 5.65 shows differences in growth rate and cell concentration achieved on CO alone (DA-5), on mixed substrate (DF-3), and on H_2/CO_2 (DB-5 and DF-1). This is striking when it is noted that similar amounts of substrate on a molar basis were consumed to achieve this growth. Note that experiment DA-5 achieved the nutrient growth limit of about 350 mg of cells/L previously noted for this medium.

The product concentrations obtained from the initial substrate charge are shown in Figure 5.66. Similar product concentrations were reached without regard to substrate. The product concentration profiles for experiments DF-1 and 3 are significantly different as they were inoculated with seed culture grown on H_2/CO_2 and were sampled less frequently. The seed culture grown on H_2/CO_2 resulted in a higher initial product concentration (16 mM) at the same cell concentration (20 mg/L) used in the other bottles; this may have resulted in retarded growth rates from product inhibition. Less frequent sampling would result in a dilution of the concentrations since a higher volume of liquid relative to the gas was retained. The other differences in product concentration are the result of differences in the amount of available substrate, and by the exponential nature of the cell concentration with time.

The plot of product concentration versus cell concentration in Figure 5.67 illustrates the relationship of production to growth as a function of substrate. The relationship is linear for a given substrate with the slope,

equivalent to the yield of products on cells ($Y_{p/x}$), much steeper for H_2/CO_2 (DB-5 and DF-1) than for CO (DA-5 and DF-3). The recharge of experiments DF-1 and 3 with H_2/CO_2 is reflected in the extension of the plots; for DF-1 a smooth continuation, for DF-3 a sharp increase in slope with the change in substrate. The hooks at the end of the plots for DA-5 and DF-3 are indicative of retrenchment in the cell concentration as the nutrient limitation is reached. This is probably the result of substrate inhibition which is particularly pronounced for CO.

Fermentation parameters calculated for the nine bottles are summarized in Table 5.7. The specific growth rate on H_2/CO_2 averaged 70 percent less than that on CO (0.028 and 0.085 h^{-1} respectively), while the specific productivity was 73 percent higher (0.0141 versus 0.0074 mole/g h). Specific rates for mixed substrate were intermediate to the pure substrate rates but were near those for CO, the preferred substrate. The product ratio, defined as the moles of ethanol per mole of acetate, was higher for growth on CO, but ethanol production from H_2/CO_2 appears quite feasible. The closure of the mass balance is indicated using the stoichiometry of Equations (1.1)-(1.4) to compare the products formed to the substrate assumed. The sum of 6 times the moles of ethanol and 4 times the moles of acetate produced was divided by the sum of the moles of H_2 and CO consumed (6E + 4A/S). Values near 1.00 indicate good closure of the mass balance. Values over 1.0 may indicate growth on other substrates, such as cysteine, while low values may indicate loss of substrate gas. These values are very sensitive to the calculation of the substrate consumed, which depends on the accuracy of the initial and final analyses of the gas phase.

Table 5.7 Fermentation Parameter *C. ljungdahlii* Grown on Various Substrates.

Expt	Sp.Growth (per h)	Sp.Prod. (mol/g h)	E/A (mol/mol)	6E+4A/S (mol/mol)	Yx/s (g/mol)	Yp/s (mol/mol)	Yp/x (mol/g)	Yp/s(calc) (mol/mol)
DA-1	0.0922	0.0082	0.60	1.12	2.54	0.237	0.093	0.219
DA-3	0.0748	0.0066	0.56	1.02	1.87	0.217	0.116	0.220
DA-5	0.0865	0.0074	0.69	1.05	1.72	0.218	0.127	0.216
DB-5	0.0385	0.0179	0.29	1.21	0.51	0.272	0.529	0.231
DE-3	0.0253	0.0126	0.41	0.97	0.43	0.212	0.489	0.226
DF-1	0.0244	0.0127	0.05	0.83	0.49	0.202	0.411	0.246
DF-2	0.0238	0.0130	0.02	0.89	0.41	0.220	0.533	0.248
DF-3	0.0601	0.0074	1.10	0.90	1.29	0.179	0.138	0.206
DF-4	0.0627	0.0079	0.66	0.75	1.08	0.156	0.145	0.217
CO avg	0.0845	0.0074	0.61		2.04	0.224	0.112	0.218
H2 avg	0.0280	0.0141	0.19		0.46	0.227	0.491	0.238

Yields calculated from the nine bottles are also presented in Table 5.7. The yield of cells on substrate ($Y_{x/s}$) averaged 2.05 g of cells per mole of CO and 0.46 grams per mole of H_2. This translates to about 8.5 and 2.0 mole percent of the respective substrates fixed as cell carbon. The yield of products on substrate ($Y_{p/s}$) appears insensitive to substrate. $Y_{p/s}$ is sensitive to the product ratio (E/A) and a theoretical value of $Y_{p/s}$ has been calculated from E/A for comparison using the stoichiometry of Equations (1)-(4). The experimental values compare well with the expected values; however, $Y_{p/s}$ and $Y_{x/s}$ are subject to the accuracy of the calculation of substrate consumption. The yield of products on cells ($Y_{p/x}$) is the quotient of the first two yields ($Y_{p/s}/Y_{x/s}$) and is indicative of the efficiency of use of the nutrients required for growth. The production from H_2/CO_2, with an average $Y_{p/x}$ of 0.49 moles of product per gram of cells, is 4.5 times more nutrient efficient than for the production from CO with an average $Y_{p/x}$ of 0.11 moles per gram.

6.0 MEDIUM DEVELOPMENT STUDIES

C. ljungdahlii was initially isolated using a basal medium formulated by Pfennig[24] (Table 6.1A) and used extensively in the University of Arkansas, Chemical Engineering Biotechnology Laboratory for isolation and maintenance of anaerobic cultures. Growth of *C. ljungdahlii* on this basal medium gave less than 0.5 g/L of cells and the production of less than 10 g/L of ethanol and acetic acid even with long batch fermentation times. Product formation was strongly related to growth. Thus, the successful enhancement of product concentrations was clearly dependent upon increasing cell concentration. Attempts to increase cell concentration by simply doubling the medium component concentrations resulted in severe inhibition of growth, probably due

to a hypertonic solution. The nutritional requirements have subsequently been evaluated by reduction of medium component concentrations.

The reduction of the gross components of the basal medium (yeast extract, PFN minerals, . . .) resulted in the elimination of yeast extract as a required component, the identification of the PFN trace metals solution as the growth limiting component, and the reduction of the required B-vitamins concentration by a factor of six. The reduction of the B-vitamin concentration and elimination of yeast extract diminished growth potential slightly, but caused a significant increase in the ethanol to acetate product ratio. Furthermore, the basal medium without yeast extract is totally defined with chemical composition as given in Table 6.1A.

Definition of the medium composition allowed the application of elemental mass balances to the growth of *C. ljungdahlii* for analysis of the growth potential of the basal medium and design of the production medium. These mass balances assume that the chemicals fed to the fermentation are fixed in the cells in some "stoichiometry" which defines a limiting nutrient with all other nutrients being in excess. All excess nutrients remain in the liquid medium. The stoichiometry of growth is defined by the elemental composition of the organism, as yet undetermined for *C. ljungdahlii*. The elemental composition of *Eschericha coli* as given by Bailey and Ollis[35] was used to evaluate the growth potential of the basal medium (Table 6.1B). *E. coli* as an aerobic and unrelated species was expected to be a poor model but was chosen as it was conveniently available. Similar data were sought for other species of Clostridium but were not found. The predicted growth potential is about half of the growth observed in experiment, but the limiting element is predicted to

Basal Medium		Fresh Medium		Inoculum		Overall
Volume (ml)	100	50	100	5	56
Yeast Extract (g)	0	0	0	0	0
5xPFN Minerals(ml)	1	0.5	1	0.05	0.55
PFN Tr. Metals(ml)	0.1	0.05	0.1	0.005	0.055
B Vitamins (ml)	0.25	0.125	0.25	0.0125	0.1375
Resazurin (ml)	0.1	0.05	0.1	0.005	0.055
Cysteine HCl 2.5% (ml)	2	1	2	0.1	1.1
5xPFN Minerals	In Sol'n (g/l)	In Media (g/l)	In Sol'n (g/l)	In Media (g/l)	In Media (g/l)
KH2PO4	50	0.5	50	0.5	0.491
MgCl2.6H2O	33	0.33	33	0.33	0.324
NaCl	40	0.4	40	0.4	0.393
NH4CL	40	0.4	40	0.4	0.393
CaCl2.2H2O	5	0.05	5	0.05	0.049
PFN Trace Metals	In Sol'n (g/l)	In Media (mg/l)	In Sol'n (g/l)	In Media (mg/l)	In Media (mg/l)
ZnSO4.7H2O	0.1	0.1	0.1	0.1	0.098
MnCl2.4H2O	0.03	0.03	0.03	0.03	0.029
H3BO3	0.3	0.3	0.3	0.3	0.295
CoCl2.6H2O	0.2	0.2	0.2	0.2	0.196
CuCl2.H2O	0.01	0.01	0.01	0.01	0.010
NiCl2.6H2O	0.02	0.02	0.02	0.02	0.020
Na2MoO4.2H2O	0.03	0.03	0.03	0.03	0.029
FeCl2.4H2O	1.5	1.5	1.5	1.5	1.473
Na2SeO3	0.01	0.01	0.01	0.01	0.010
B Vitamins	In Sol'n (mg/l)	In Media (mg/l)	In Sol'n (mg/l)	In Media (mg/l)	In Media (mg/l)
Biotin	20	0.05	20	0.05	0.0491
Folic Acid	20	0.05	20	0.05	0.0491
Pyridoxal HCl	10	0.025	10	0.025	0.0246
Lipoic a. (Thiotic a.)	60	0.15	60	0.15	0.1473
Riboflavin	50	0.125	50	0.125	0.1228
Thiamine HCl	50	0.125	50	0.125	0.1228
Ca-D-Pantothenate	50	0.125	50	0.125	0.1228
Cyanocobalamin	50	0.125	50	0.125	0.1228
P-aminobenzoic acid	50	0.125	50	0.125	0.1228
Nicotinic acid	50	0.125	50	0.125	0.1228
	In Sol'n (g/l)	In Media (mg/l)	In Sol'n (g/l)	In Media (mg/l)	In Media (mg/l)
Cysteine HCl in 0.2 N NaOH	25	490	25	490	490
Total Ionic Strength (M)					0.048

Table 6.1A Basal Medium Composition

		E.coli	In Defined Media	Maximum Cell Wt.	
	A.W.	% dry wt.	(mmol/l)	(mg/l)	(*min)
Nitrogen	14.01	14	10.134	1014	4.90
Phosphorus	30.97	3	3.611	3728	18.01
Sulfur	32.06	1	2.791	8948	43.24
Potassium	39.1	1	3.611	14118	68.23
Sodium	22.99	1	10.649	24481	118.31
Calcium	40.08	0.5	0.381	3051	14.75
Magnesium	24.31	0.5	1.594	7751	37.46
Chlorine	35.45	0.5	20.811	147549	713.04
Iron	55.85	0.2	0.007	207	1.00
Biotin				2219	10.72
Thiamine HCl				2214	10.70
Ca-D-Pantothenate				1416	6.84
Predicted Maximum Cell Weight:			207	(mg/l)	

5xPFN Minis	Ions (M)	M.W.
KH2PO4	0.007	136
MgCl2.6H2O	0.005	203.3
NaCl	0.013	58.4
NH4CL	0.015	53.5
CaCl2.2H2O	0.001	129
Cys.HCl.H2O	0.007	175.64
FeCl2.4H2O	0.000	198.81
	0.048	

Analysis of E.coli from J.E. Bailey and D.F. Ollis, "Biochemical Engineering Fundamentals" 2nd ed., McGraw Hill 1986, Table 2.1 on p. 28

B Vitamin Requirements; J.R. Phillips, Univ. of Arkansas, 1991

Table 6.1B Basal Medium Mass Balance Analysis

be iron. Iron is added as part of the PFN trace metals which was found to be the limiting component of the basal medium. This initial success portends the utility of the model.

The analysis of the basal medium (Table 6.1B) reveals huge excesses of most elements (see "*min" column). The *E. coli* analysis was used to formulate a more balanced production medium in which cations containing required nutrients were matched with nutrient contributing anions. The resulting designed medium is defined in Table 6.2A and analyzed in Table 6.2B. The particular formulation given is for the feed to a continuously stirred tank reactor (CSTR) and has a predicted growth potential of 2.1 g/L cells, about 10 times the predicted potential of the basal medium. This medium is again predicted to be limited by the PFN trace metals, reported as iron. However, the growth potential predicted for iron is half of the growth observed. Thus, this medium should be limited by nitrogen (at 1.51 times the limit predicted for iron) and indeed appears to be limited by nitrogen in the CSTR. Performance studies using the designed medium are shown later.

7.0 PATHWAYS STUDIES FOR *C. LJUNGDAHLII*

7.1 Introduction

Many acetogenic bacteria are known to grow autotrophically on the components of synthesis gas, whereby carbon monoxide (CO) or carbon dioxide (CO_2) with hydrogen (H_2) serve as the sole source of carbon and energy. Acetic acid is formed by the equations:

$$4CO + 2H_2O \rightarrow CH_3COOH + 2CO_2 \quad \Delta G^{0\prime} = -175.3 \text{ kJ} \qquad (1.3)$$

$$2CO_2 + 4H_2 \rightarrow CH_3COOH + 2H_2O \quad \Delta G^{0\prime} = -94.9 \text{ kJ} \qquad (1.4)$$

Clostridium thermoaceticum has been studied extensively and is a typical example of such an acetogen.

JRP's Medium		Fresh Medium		Inoculum		Overall
Volume (ml)		100	2000	100	0	2020
JRP Minerals I (ml)		0.5	10	1	0	10
JRP Minerals II (ml)		5	100	1	0	100
JRP Salts (ml)		0.5	10	0.1	0	10
PFN Tr. Metals(ml)		1	20	0.1	0	20
JRP's Vitamins (ml)		0.1	2	0.02	0	2
Resazurin (ml)		0	0	0.1	0	0
Cysteine HCl 2.5% (ml)		1	20	2	0	20
JRP Minerals I		In Sol'n (g/l)	In Media (g/l)	In Sol'n (g/l)	In Media (g/l)	In Media (g/l)
	NH4Cl	0	0	20	0.2	0.000
	MgCl2.6H2O	100	0.5	5	0.05	0.495
	CaCl2.2H2O	40	0.2	2	0.02	0.198
JRP Minerals II		In Sol'n (g/l)	In Media (g/l)	In Sol'n (g/l)	In Media (g/l)	In Media (g/l)
	(NH4)2HPO4	40	2	20	0.2	1.980
JRP Salts		In Sol'n (g/l)	In Media (g/l)	In Sol'n (g/l)	In Media (g/l)	In Media (g/l)
	NaCl	40	0.2	40	0.04	0.198
	KCl	30	0.15	30	0.03	0.149
PFN Trace Metals		In Sol'n (g/l)	In Media (mg/l)	In Sol'n (g/l)	In Media (mg/l)	In Media (mg/l)
	ZnSO4.7H2O	0.1	1	0.1	0.1	0.990
	MnCl2.4H2O	0.03	0.3	0.03	0.03	0.297
	H3BO3	0.3	3	0.3	0.3	2.970
	CoCl2.6H2O	0.2	2	0.2	0.2	1.980
	CuCl2.H2O	0.01	0.1	0.01	0.01	0.099
	NiCl2.6H2O	0.02	0.2	0.02	0.02	0.198
	Na2MoO4.2H2O	0.03	0.3	0.03	0.03	0.297
	FeCl2.4H2O	1.5	15	1.5	1.5	14.851
	Na2SeO3	0.01	0.1	0.01	0.01	0.099
B Vitamins		In Sol'n (mg/l)	In Media (mg/l)	In Sol'n (mg/l)	In Media (mg/l)	In Media (mg/l)
	Biotin	101	0.101	101	0.020	0.1000
	Thiamine HCl	254	0.254	254	0.051	0.2515
	Ca-D-Pantothenate	401	0.401	401	0.080	0.3970
		In Sol'n (g/l)	In Media (mg/l)	In Sol'n (g/l)	In Media (mg/l)	In Media (mg/l)
Cysteine HCl in 0.2 N NaOH		25	248	25	490	248
			Total Ion Concentration (M)			0.070
Supplements		In Sol'n (mg/l)	Vol. Added (ml)			In Media (mg/l)
	Biotin	20	0.50			0.0050
	Folic Acid	20	0.50			0.0050
	Pyridoxal HCl	10	0.50			0.0025
	Lipoic a. (Thiotic a.)	60	0.50			0.0149
	Riboflavin	50	0.50			0.0124
	Thiamine HCl	50	0.50			0.0124
	Ca-D-Pantothenate	50	0.50			0.0124
	Cyanocobalamin	50	0.50			0.0124
	P-aminobenzoic acid	50	0.50			0.0124
	Nicotinic acid	50	0.50			0.0124
	H3PO4	1453500	2.00			1439.1

Table 6.2A Designed Medium Composition

		E.coli	In Defined Media	Maximum Cell Wt.	
	A.W.	% dry wt.	(mmol/l)	(mg/l)	(*min)
Nitrogen	14.01	14	31.401	3142	1.51
Phosphorus	30.97	3	29.682	30641	14.69
Sulfur	32.06	1	1.409	4518	2.17
Potassium	39.1	1	1.991	7784	3.73
Sodium	22.99	1	5.365	12334	5.91
Calcium	40.08	0.5	1.347	10797	5.18
Magnesium	24.31	0.5	2.435	11839	5.68
Chlorine	35.45	0.5	14.349	101732	48.77
Iron	55.85	0.2	0.075	2086	1.00
Biotin				4518	2.17
Thiamine HCl				4534	2.17
Ca-D-Pantothenate				4578	2.19
Predicted Maximum Cell Weight:			2086	(mg/l)	

	Ions		mM Media	Mini Soln	
JRP Minis	(M)	M.W.	(Fe @ .075	(M)	(g/l)
NH4Cl	0.000	53.49	1.71	0.750	40.1
(NH4)2HPO4	0.045	132.05	0.171	0.075	9.9
MgCl2.6H2O	0.007	203.31	0.035	0.015	3.1
CaCl2.2H2O	0.004	147.02	0.023	0.010	1.5
FeCl2.4H2O	0.000	198.81			
JRP Salts					
NaCl	0.007	58.5	0.07275	1.0	58.5
KCl	0.004	74.6	0.045	0.6	46.1
	0.070		0.044	M ions remain after predicted growth	

Cys.HCl.H2O	175.64
FeCl2.4H2O	198.81
H3PO4	97.99

Analysis of E.coli from J.E. Bailey and D.F. Ollis, "Biochemical Engineering Fundamentals" 2nd ed., McGraw Hill 1986, Table 2.1 on p.28

B Vitamin Requirements, J.R. Phillips, Univ. of Arkansas, 1991

Table 6.2B Designed Medium Mass Balance Analysis

Clostridium ljungdahlii also grows autotrophically by the acetogenic pathway on synthesis gas[36], but produces ethanol with, or instead of, acetic acid.

$$6CO + 3H_2O \rightarrow CH_3CH_2OH + 4CO_2 \qquad \Delta G^{0'} = -224.8 \frac{kJ}{mole} \qquad (1.1)$$

$$2CO_2 + 6H_2 \rightarrow CH_3CH_2OH + 3H_2O \qquad \Delta G^{0'} = -104.6 \frac{kJ}{mole} \qquad (1.2)$$

The overall stoichiometry as given in Equations (1.1-1.4) must represent the sum of the chemical reactions that comprise the biochemical pathway. The pathway can be a powerful tool in studies of fermentation mass and energy flows, and in developing control strategies. The acetogenic pathway of autotrophic growth has been defined and demonstrated over the past 25 years.[3,37] This work has typically focused on *C. thermoaceticum*, for which all of the pathway enzymes have been isolated and demonstrated *in vitro*. This work often employed artificial mediators and controlled conditions. Questions of enzyme structure and mechanism, *in vivo*, remain unanswered.

The pathway as it is presented in the literature will be reviewed, along with an attempt to reconcile the pathway summation with the overall stoichiometry. This review will be strict in the accounting of chemical species including water, protons, and electrons. And, although most acetogens can utilize a variety of substitutes, such as sugars, amino acids, and alcohols, this consideration will be restricted to the synthesis gas components CO, CO_2, and H_2.

7.2 Pathway

The overall biochemical pathway is given in Figure 7.1. CO is oxidized to CO_2 or H_2 to H^+ to provide electrons and protons for the reducing reactions. Some of the protons are expelled from the cell and re-enter via an ATPase forming adensonine triphosphate (ATP) which provides energy for cell growth.

The electrons obtained from the oxidation of CO or H_2 are used to reduce CO_2 through formate and three tetrahydrofolate (THF) bound intermediates to methyltetrahydrofolate. This methyl group is transferred via a corrinoid enzyme (CoE) to carbon monoxide dehydrogenase (CODH) where it is condensed with CO and coenzyme A (CoASH) to form acetyl-coenzymeA.

Some of the acetyl-CoA is diverted to anabolic production of cell material for growth and reproduction. Excess acetyl-CoA is cleaved to form acetic acid, and excess reducing equivalents can be stored in the reduction of acetic acid through acetaldehyde to ethanol.

7.3 Physiological Environments

The pathway reactions can be grouped by the environments in which they occur. The cell membrane separates the aqueous environments of the external medium and the cytoplasm. The membrane comprises a thin nonpolar layer in which the transport ions, electrons and substrate occurs. Other reactions occur at the interfaces of this membrane with the aqueous environments.

The optimum growth conditions of the extra-cellular medium are pH 6.8 and 60°C for *C. thermoaceticum*, and pH 6.0 and 37°C for *C. ljungdahlii*.[36] Both organisms are obligate anaerobes and use the substrate to reduce the electrochemical potential of the medium. The internal pH of the growing cells of *C. thermoaceticum* has been shown to remain about 0.6 pH units higher than

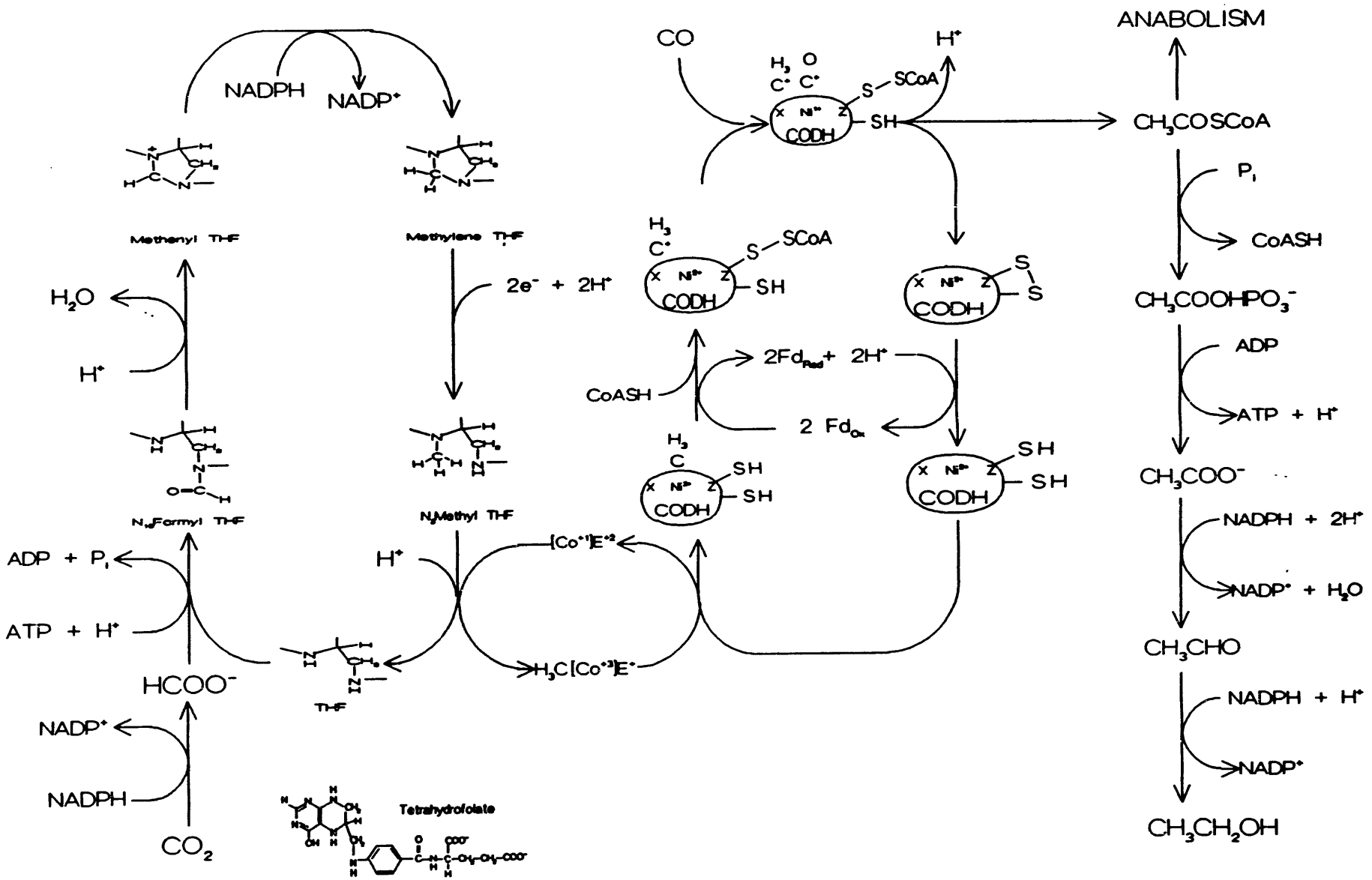

Figure 7.1 Overall Pathway for Ethanol Formation

the pH of the external medium, down to pH 5.0,[38] while the electrochemical potential drop across the membrane changes from 140 mV at pH 7.0 to 80 mV at pH 5.0 (lower potential inside the cell).

Acidic species involved in the reactions can exist in various forms in the aqueous environments. Formic acid (pKa 3.68) will appear primarily as formate ($HCOO^-$). Acetic acid (pKa 4.74) will be primarily acetate (CH_3COO^-) in the *C. thermoaceticum* fermentation but will also be found in the acid form (CH_3COOH) at the lower pH used with *C. ljungdahlii*. Assumed phosphate forms will be ATP^{4-} (pKa_4 6.95), ADP^{3-} (pKa_3 6.88), and P_i^{1-} ($H_2PO_4^{1-}$, pKa_2 7.21). Significant concentrations of ATP^{3-}, ADP^{2-}, and P_i^{2-} will exist at the physiological pH (5.0 to 7.5), but this should not affect the physiological function. CO_2 should exist as carbonic acid (H_2CO_3, pKa 6.38) but will be treated as CO_2 with the associated water ignored.

The cell membrane is a nonpolar organic barrier to diffusion of ionic species. Unchanged species, such as the organic products, acetic acid and ethanol, and the substrate gases will rapidly diffuse through this thin lipid layer and, unless there is a transport mechanism specific for that species, will be in nearly equal concentrations on either side of the membrane. Ionic species such as metals, phosphate, H^+, or acetate will be excluded or retained by the membrane, forming a concentration gradient which might be exploited in cell function.

Carbon monoxide dehydrogenase (CODH) forms a complex with several other enzymes and reaction mediators on the cytoplastic face of the cell membrane.[39-42] Included in this complex are CODH, ferredoxin, CODH disulfide reductase, the carrinoid enzyme, and methylene-tetrahydrofolate reductase. The environment may be isolated and intermediate between the aqueous cytoplasm

and the nonpolar membrane. It may differ significantly in pH and electrochemical potential from the nearby cytoplasm.

The ATPase is a protein structure that spans the membrane, joining the cytoplasm and the external medium. Protons from the exterior of the cell are conducted through a protein channel to drive the production of ATP, and then released into the cytoplasm.

7.4 Oxidation of Substrates

The pathway is a series of oxidation-reduction reactions. Energy and low potential electrons are supplied by the gaseous substrates CO and H_2. The electrons enter a respiratory electron transport chain as they are stripped from the oxidized substrate.

Carbon monoxide is the preferred substrate of the synthesis gas components. Oxidation of CO

$$CO + H_2O \rightarrow CO_2 + 2H^+ + 2e^- \quad \Delta G^{0'} = -99.8 \text{ kJ/mol} \qquad (7.1)$$

is catalyzed by carbon monoxide dehydrogenase (CODH) and occurs in an enzyme complex on the internal cell membrane. CO binds to a nickel-iron-sulfur center on CODH.[43,44] The nickel is reduced from Ni^{2+} to Ni^{1+} on binding of CO [45,46], while CO is attacked by water. The precise mechanism has not been determined, but we may postulate that two protons are released from water as the electrons reduce the Ni center on CODH as is shown in Figure 7.2. CO_2 is released by CODH and the electrons are transferred by ferredoxin to reduce NADP for cytoplasmic reaction or a membrane associated flavoprotein for entry into the electron transport chain for ATP production.[40,47]

The CODH associated ferredoxin[39] reduces a membrane bound flavoprotein which carries electrons and protons from the CO oxidation across the cell membrane. The flavoprotein reduces a b-type cytochrome (Cyt b_{559}) and

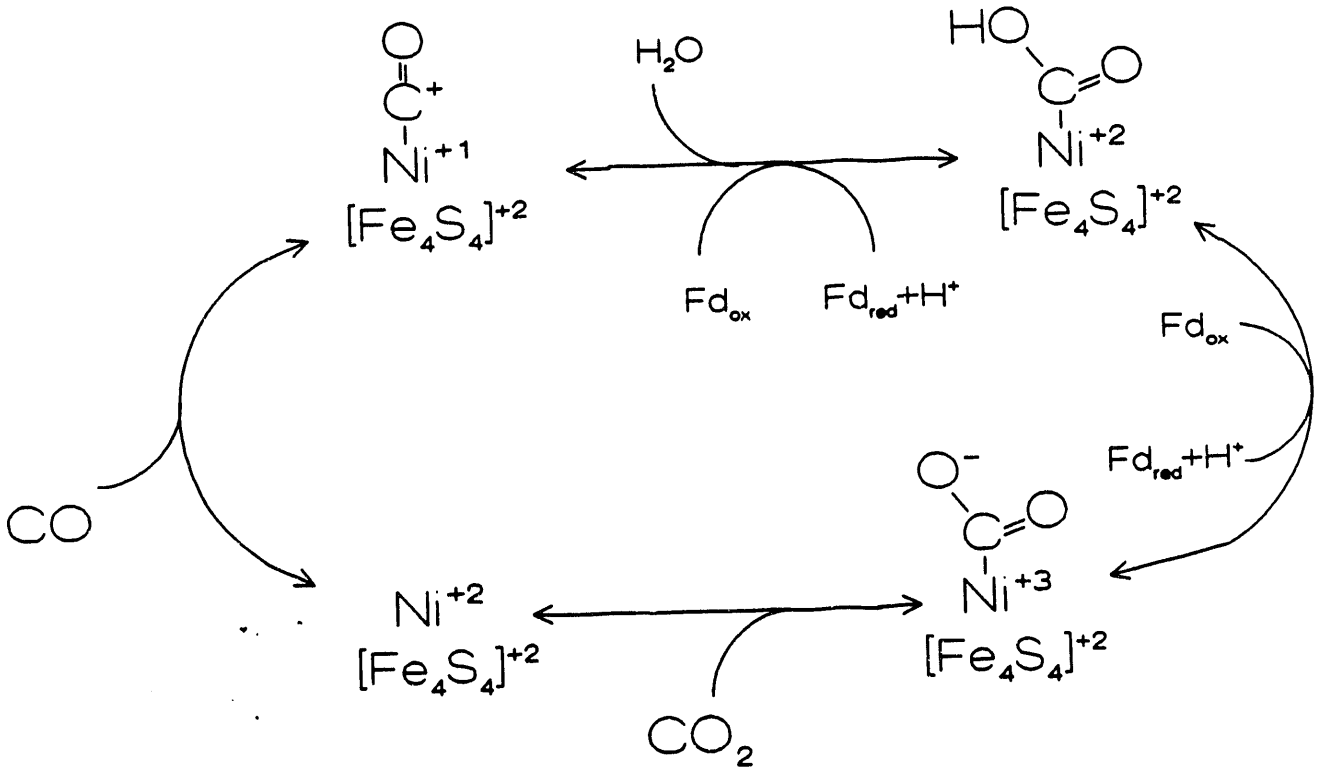

Figure 7.2 Proposed Mechanism of CO Oxidation

releases the protons to the extracellular medium generating a pH gradient.[40] Cyt b_{559} reduces an undetermined electron carrier, perhaps a ferredoxin, which transports electrons against the electrochemical potential to the cytoplasm where they reduce $NADP^+$ or other electron carriers, or are consumed in the reduction of methylenetetrahydrofolate to methyltetrahydrofolate.[48] The transport of electrons back to the cytoplasm may be assisted by exploiting a cation (Na^+) gradient.[49-51]

$$Fd_{ox} + e^- \rightarrow Fd_{red} \quad E^{0'} = -350 \text{ mV} \tag{7.2}$$

$$NADP^+ + 2e^- + H^+ \rightarrow NADPH \quad E^{0'} = -320 \text{ mV} \tag{7.3}$$

$$FP + 2e^- + 2H^+ \rightarrow FPH_2 \quad E^{0'} = -220 \text{ mV} \tag{7.4}$$

$$\text{Cyt } b_{559,ox} + e^- \rightarrow \text{Cyt } b_{559,red} \quad E^{0'} = -200 \text{ mV} \tag{7.5}$$

$$CH_2THF + 2e^- + 2H^+ \rightarrow CH_3THF \quad E^{0'} = -117\text{mv} \tag{7.6}$$

Some electrons may be diverted from Cyt b_{559} to high potential electrochemical couples via a menaquinone ($E^{0'}$ -70mV) and another cytochrome (Cyt b_{554}, $E^{0'}$ - 48 mV), but these are unlikely to be significant at the low potential of the fermentation.

H_2 is oxidized by hydrogenase (H_{2ase}), an iron-sulfur enzyme, located on the external cell membrane.[7,40,52,53]

$$H_2 \rightarrow 2H^+ + 2e^- \quad \Delta E^{0'} = -420 \text{ mV} \tag{7.7}$$

Protons are released to the external medium and the electrons enter the membrane electron transport chain of Cyt b_{559}. H_2 does not reduce the flavoprotein that induces electrons from CO oxidation into the electron transport chain. Instead, electrons from H_2 are used, at a higher potential than CO oxidation, to reduce CO_2 to bound CO on CODH (the reverse of Equation (7.1)) to form the carbonyl of acetate. CO is preferred as substrate over H_2/CO_2 and H_2 uptake is inhibited by CO. Concomitant uptake of CO and H_2 is seen in CO mass transfer limited cultures.

7.5 ATP Production

Adenosine triphosphate (ATP) is the primary source of intracellular energy for anabolic or self building processes. The conversion of synthesis gas to acetate via the acetogenic pathway yields no net ATP. Acetyl-CoA diverted to anabolism is formed with the expenditure of one mole of ATP per mole of acetyl-CoA. Acetogens capable of autotrophic growth must generate ATP by electron transport phosphorylation.

C. thermoaceticum has a complex F_1F_o•ATP_{ase} similar to ATP_{ases} of mitochondria and chlorophasts.[54,55] This ATP_{ase} exploits the proton motive force (Δp) imposed by the combination of the electrochemical potential and pH difference across the cell membrane.

$$\Delta p = E_m - (2.3\ RT/F)\ \Delta pH \qquad (7.8)$$

The term (2.3 RT/F) is 60 at 30°C and 65 at 57°C when Δp and E_m, the membrane potential drop, are in mV.[38]

$$\Delta p\ (kJ/mol\ H^+) = 0.0965\ \Delta_p\ (mV) \qquad (7.9)$$

This proton motive force has been measured for *C. thermoaceticum* to be 140 mV(13.5 kJ/mol H^+) at pH 7.0 decreasing to 80 mV (7.7 kJ/mol H^+) at pH 5.0.[38] The ATP_{ase} binds adenosine diphosphate (ADP), inorganic phosphate (P_i), and Mg^{2+} and then transfers the energy of protons driven by the proton motive force to the formation of ATP.

$$ADP^{3-} + P_i^- + Mg^{2+} \rightarrow MgATP^{2-} + H_2O \quad \Delta G^{0'} = 31.8\ kJ/mol \qquad (7.10)$$

The reaction is driven by forced changers in the conformation of the enzyme. Mg^{2+} binds to the phosphoryl groups of ATP and is required for activity of the acetogenic ATP_{ase}. However, an excess (Mg^{2+}:ATP > 1:2) is inhibitory.[56]

From Equations (1.3) and (1.4), at most 6 moles of extracellular H^+ can be obtained from the formation of 1 mole of acetic acid from CO (1 mole of CO

condenses to Acetyl-CoA without oxidation) or 8 moles H^+ from H_2. This would give a maximum of 3 moles of ATP from CO or 4 moles from H_2 per mole of acetic acid produced. Anaerobic bacteria typically produce 10 grams of cells per mol of ATP, or 30 and 40 grams of cells per mole of acetic acid from CO and H_2, respectively. We are currently growing *C. ljungdahlii* in a CSTR at pH 5.0 with the production of 0.17 M acetic acid and about 4 grams of cells per mole of acetic acid.

7.6 Reduction of CO2 to Methyl

The methyl group of acetic acid is formed from CO_2 via a series of reductions of a carbon bound to tetrahydrofolate. These reactions occur in the aqueous cytoplasm with the exception of the final reduction to methyl tetrahydrofolate. The enzyme that catalyzes this final step is part of a membrane bound complex.

CO_2 is reduced to formate by NADPH on formate dehydrogenase (FDH).

$$CO_2 + NADPH \rightarrow HCOO^- + NADP^+ \quad \Delta G^{0'} = +21.5 \text{ kJ/mol} \qquad (7.11)$$

The high free energy increase indicates that this reaction is thermodynamically unfavorable. This is underscored by the potential of the $CO_2/HCOO^-$ couple relative to that of $NADP^+$/NADPH (Equation (7.3)).

$$CO_2 + H^+ + 2e^- \rightarrow HCOO^- \quad E^{0'} = -420 \text{ mV} \qquad (7.12)$$

The equilibrium in these equations is very much toward CO_2, Keq = 2.35×10^{-2} for Equation (7.11) at pH 7.5 and 57°C.[56] The formate dehydrogenase of *C. thermoaceticum* is NADPH specific but other acetogens use lower potential electron carriers.[7,56] The activity of FDH is dependent on the trace metals concentrations increasing up to 250 times.[43] FDH of *C. thermoaceticum* contains 2 tungsten, 2 selenium, 36 iron and 50 inorganic sulfur per enzyme.[7] FDH in other acetogens contains molybdenum as well as or instead of tungsten or selenium.

Formate is bound to tetrahydrofolate with the consumption of one ATP in a reaction mediated by formyl tetrahydrofolate synthetase.

$$HCOO^- + H^+ + ATP^{4-} + H_2\text{"THF"} \rightarrow HCOH\text{"THF"} + ADP^{3-} + P_i^- \qquad \Delta G^{0'} = -9.0 \text{ kJ/mol} \qquad (7.13)$$

H_2"THF" is tetrahydrofolate with the reactive hydrogen shown for reaction accounting. Mg^{2+} is required for ATP binding[57] and the activity is stimulated by NH_4^+ and K^+ in *C. thermoaceticum*.[7] Formyl tetrahydrofolate synthetase may interact with formate dehydrogenase to enhance the conversion of CO_2.[57]

$$HCOH\text{"THF"} + H^+ \rightarrow HC^+\text{"THF"} + H_2O \qquad \Delta G^{0'} = -4.0 \text{ kJ/mol} \qquad (7.14)$$

$$HC^+\text{"THF"} + NADPH \rightarrow H_2C\text{"THF"} + NAD^+ \qquad \Delta G^{0'} = -4.9 \text{ kJ/mol} \qquad (7.15)$$

The dehydrogenase is NADPH specific.[58] In *C. formicoaceticum* the activities are separate and the dehydrogenase uses NADH.[58]

Methylenetetrahydrofolate is reduced by the methylenetetrahydrofolate reductase in the enzyme complex of the cell membrane.

$$H_2C\text{"THF"} + 2H^+ + 2e^- \rightarrow H_3CH\text{"THF"} \qquad \Delta G^{0'} = -16.0 \text{ kJ/mol} \qquad (7.16)$$

This reaction is the end of the electron transport chain that drives the ATPase.[40] The reductase is an iron-sulfur flavoprotein that contains zinc and FAD similar to the flavoprotein that begins the electron transport chain.[59] The reductase is reduced by an electron carrier that transports electrons from Cyt b_{559}. This unidentified electron carrier may also be involved with transport of Na^+ or other electrolytes across the membrane.[50,51] The potential to drive the reduction is the difference between the Cyt b_{559} redox couple ($E^{0'}$ -200 mV) and the CH_2THF/CH_3THF couple ($E^{0'}$ -117mV) in Equations (7.5) and (7.6).[7,59]

CO_2 originally reduced to formate is further reduced on tetrahydrofolate to methyl. This methyl group becomes the C_2 of acetate or ethanol. It is transferred to a corrinoid enzyme by methyltransferase,[48] regenerating tetrahydrofolate.

7.7 Condensation of CH_3, CO, and HSCoA

Methyltetrahydrofolate, carbon monoxide, and Coenzyme A are condensed to form acetyl-CoA in a complex of enzymes containing carbon monoxide dehydrogenase (CODH).

$$H_3CH"THF" + CO + HSCoA \rightarrow CH_3COSCoA + H_2"THF"$$
$$\Delta G^{0'} = -21.8 \text{ kJ/mol} \qquad (7.17)$$

This reaction occurs in distinct steps and depends on a methyltransferase, a corrinoid protein, CODH, ferredoxin and a disulfide reductase.[55]

The methyl group of methyltetrahydrofolate is transferred to a protein, containing a corrinoid similar to vitamin B_{12}, which acts as a methyl carrier. The protein also contains an iron-sulfur center, $[Fe_4S_4]$, which interacts with the cobalt of the carrinoid. The transfer is catalyzed by a methyltransferase.[45]

$$H_3CH"THF" + H^+ + Co^{1+}E^{2+} \rightarrow H_2"THF" + H_3CCo^{3+}E^{1+} \qquad (7.18)$$

The corrinoid protein is redox active and the transfer involves a nucleophilic attack by Co^{1+} on the methyl carbon.[60,61] The transferred species is a methyl carbonium ion (H_3C^+), but distribution of the change between Co and the $[Fe_4S_4]$ center stabilizes oxidation of Cox^+ to Co^{3+}, reducing the change on the methyl carbon.[47,62] The retention of stereochemistry, which is expected to result from nucleophilic methyl transfers to and from the corrinoid protein, supports this mechanism.[63] Methylation of the carrinoid protein is not reversible. The corrinoid protein is specific for methylation of CODH.

Carbon monoxide dehydrogenase, in addition to providing electrons from CO as noted above, mediates the entry of CO and CO_2 into acetate synthesis, and condenses the components (CH_3, CO, and HSCoA) into acetyl-CoA. Carbon enters the methyl synthesis as CO_2 while the carbonyl is formed directly from CO.[37,41] CODH catalyzes the conversion of one to the other by the reversible reaction of Equation (7.1). Ferredoxin bound to CODH mediates electron transfer within the complex of enzymes.[39,64] CODH is redox active and contains 6 Ni, 3 to 9 Zn, 36 Fe and 42 inorganic sulfur molecules in each active enzyme.[7,44] All of the iron is in iron-sulfur centers and a $[Fe_4S_4]$ center is associated with each of the active Ni sites.[45,46,65]

The corrinoid protein, a redox active iron-sulfur-cobalt protein, is required for methylation of CODH.[60] The corrinoid protein and ferredoxin bind CH_3 rapidly and specifically to the three active sites of CODH.[66]

$$H_3CCo^{+}E^{1+} + (N_i^{2+})CODH \rightarrow Co^{1+}E^{2+} + H_3C(N_i^{3+})CODH \qquad (7.19)$$

The methylation does not proceed at electrochemical potentials above -300 mV, but has its maximum partition of methyl to CODH (65% of CH_3 on CoE, 35% on CODH) at -315 mV.[60] The methyl group binds to the nickel site of CODH in a nucleophilic attack on the methyl cobamide of the corrinoid.[67] The methyl is then possibly transferred to a nearby cysteine residue in another nucleophilic transfer restoring the active N_i^{2+} site.

CODH catalyzes exchange reactions of CO, HSCoA, and CH_3 groups with acetyl-CoA.[47,64,67] This requires two sites for binding of methyl (N_i and cysteine), a site for binding CO (N_i), and two sites to final SCoA (a sulfide and arginine are suspected).[67] Chirality of the methyl group is retained in formation of acetyl-CoA from methyltetrahydrofolate, CO, and HSCoA,[63] and in the exchange of CO with with acetyl-CoA.[68] This supports the assumption of an

even number of nucleophilic methyl transfers in formation of acetyl-CoA and in the exchange reaction.

Binding of Coenzyme A (HSCoA) requires the reduction of a disulfide bond on CODH. CODH disulfide reductase contains 8 calcium and 4 zinc, and complexes with CODH and ferredoxin. Disulfide reductase is required for binding of HSCoA, reducing disulfide bonds at the three active sites to give maximum CODH activity.[7,47] CODH without the disulfide reductase will not mediate exchange of HSCoA with acetyl-CoA, but exchange of the carbonyl with CO is not impaired.[47] Arginine modifiers inhibit the carbonyl exchange with no effect on the oxidation of CO.[64] Destruction of the $[Fe_4S_4]$ centers inactivates CODH.[64] HSCoA apparently binds to a sulfur, possibly linked in a disulfide bond to the cysteine that accepts the methyl group from Ni, and is then transferred to arginine. Acetyl-CoA, however, can bind directly to the arginine residue for the carbonyl exchange reaction.

Carbon monoxide is bound to nickel in CODH as described in Figure 7.2 for CO oxidation.[46] Bound methyl, CO, and SCoA are condensed with the formation and release of acetyl-CoA and regeneration of the disulfide bond.

7.8 Anabolic Consumption of Acetyl-CoA

Acetyl-CoA is the precursor of the materials that make up the cell. It is converted by a reversal of the catabolic pathways for sugars, into sugar phosphates, amino acids, lipids, and all other compounds required for cell growth and function.[7]

7.9 Cleavage of Acetyl-CoA to Acetic Acid

Acetyl phosphate is formed in a reaction of acetyl-CoA and inorganic phosphate medicated by phosphotransacetylase.[45]

$$CH_3COSCoA + P_i^- \rightarrow CH_3COOHPO_3^- + HSCoA$$

$$\Delta G^{0\prime} = +15.5 \text{ kJ/mol} \qquad (7.20)$$

The reaction is stimulated by Mn^{2+}.

The formation of acetylphosphate is thermodynamically favorable only when coupled with the further consumption of acetylphosphate in phosphorylation of ADP to form ATP and acetate.

$$CH_3COOHPO_3^- \rightarrow CH_3COO^- + ATP^{4-} + H^+$$

$$\Delta G^{0'} = -16.3 \text{ kJ/mol} \qquad (7.21)$$

This reaction is catalyzed by acetate kinase.[45]

7.10 Reduction of Acetate to Ethanol

C. ljungdahlii converts acetate to ethanol in reactions requiring an aldehyde dehydrogenase and an alcohol dehydrogenase.

$$CH_3COO^- + 2H^+ + NADPH \rightarrow CH_3CHO + H_2O + NADP^+$$

$$\Delta G^{0'} = +50.4 \text{ kJ/mol} \qquad (7.22)$$

$$CH_3COOH + 2e^- + 2H^+ \rightarrow CH_3CHO + H_2O$$

$$E^{0'} = -581 \text{ mV} \qquad (7.23)$$

$$CH_3CHO + NADPH + H^+ \rightarrow CH_3CH_2OH + NADP^+$$

$$\Delta G^{0'} = -23.2 \text{ kJ/mol} \qquad (7.24)$$

$$CH_3CHO + 2e^- + 2H^+ \rightarrow CH_3CH_2OH \quad E^{0'} = -100 \text{ mV} \qquad (7.25)$$

Recently similar enzymes have been found in *C. formicoaceticum*.[69,70] The aldehyde dehydrogenase of *C. thermoaceticum* is tungsten dependent and is stimulated by selenium and low concentrations (10μM) of molybdenum. Molybdenum became inhibitory at 1 mM. The highest formation of ethanol, with CO as the reductant at a medium potential of -220 mV, was 200 times that obtained with formate as the reductant.[70]

7.11 Summary

The reactions of the pathway are summarized in Table 7.1. The reactions sum stoichiometrically to give the overall reactions for product synthesis, Equations (1.1-1.4).

Table 7.1 Acetogenic Pathway of Autotrophic Growth

Reactions of acetate and ethanol synthesis from CO or H_2/CO_2

$CO + H_2O \longrightarrow CO_2 + 2H^+ + 2e^-$
$H_2 \longrightarrow 2H^+ + 2e^-$

$Fd_{ox} + 2e^- \rightarrow Fd_{red}$
$NADP^+ + 2H^+ + 2e^- \rightarrow NADPH$

$CO_2 + NADPH \rightarrow HCOO^- + NADP^+$
$HCOO^- + H^+ + ATP^{4-} + H_2\text{"THF"} \rightarrow HCOH\text{"THF"} + ADP^{3-} + P_i^-$
$HCOH\text{"THF"} + H^+ \rightarrow HC^+\text{"THF"} + H_2O$
$HC^+\text{"THF"} + NADPH \rightarrow H_2C\text{"THF"} + NADP^+$
$H_2C\text{"THF"} + 2H^+ + 2e^- \rightarrow H_3CH\text{"THF"}$

$H_3CH\text{"THF"} + H^+ + Co^{1+}E^{2+} \rightarrow H_2\text{"THF"} + H_3CCo^{3+}E^{1+}$
$H_3CCo^{3+}E^{1+} + (Ni^{2+})CODH \rightarrow Co^{1+}E^{2+} + H_3C(Ni^{3+})CODH$
$H_3C(Ni^{3+})CODH + HSCoA \rightarrow H_3C(Ni^{3+})CODH\text{-}SCoA^- + H^+$
$H_3C(Ni^{3+})CODH\text{-}SCoA^- + CO \rightarrow H_3CCOSCoA + (Ni^{2+})CODH$

$CH_3COSCoA + P_i^- \rightarrow CH_3COOHPO_3^- + HSCoA$
$CH_3COOHPO_3^- + ADP^{3-} \rightarrow CH_3COO^- + H^+ + ATP^{4-}$

$CH_3COO^- + 2H^+ + NADPH \rightarrow CH_3CHO + H_2O + NADP^+$
$CH_3CHO + H^+ + NADPH \rightarrow CH_3CH_2OH + NADP^+$

The stoichiometry and mechanisms advanced in Figures 7.1 and 7.2 and in Table 7.1 reconcile the literature for the individual reactions with the overall reaction stoichiometry. The result is unproven and in places speculative. However, the overview of acetate and ethanol synthesis should be useful in indentifying limiting reactions, understanding culture behavior, and formulating strategies for fermentation improvement.

The reactions are largely electrochemically controlled. The importance of redox active enzymes highlights the need for balance of the culture medium, particularly with respect to iron, sulfur, and trace metals composition. This set of reactions can be used as a model for energy conservation by acetegens grown on synthesis gas. With assumed physiological conditions the model can be used to predict fermentation performance and guide experiment design.

8.0 MASS TRANSFER/KINETICS CONSIDERATIONS

8.1 Determination of Mass Transfer and Kinetic Parameters

Figures 8.1 and 8.2 show results from a batch synthesis gas fermentation using *C. ljungdahlii*. Initial CO partial pressures ranging from 1.44 atm to 4.27 atm were utilized in smaller batch reaction vessels in order to determine the effects of increased CO pressure on cell growth and substrate uptake. Basal medium containing 0.01% yeast extract was used in all experimental runs.

Figure 8.1 shows cell concentration profiles for the various CO partial pressures. As is noted, cell growth followed the same patterns for all CO partial pressures. As expected, the lag phase increased with CO partial pressure. The maximum cell concentration increased with increasing CO partial pressure. Figure 8.2 shows CO utilization with time as a function of initial CO partial pressure. As is noted, because of the lag phases the time for

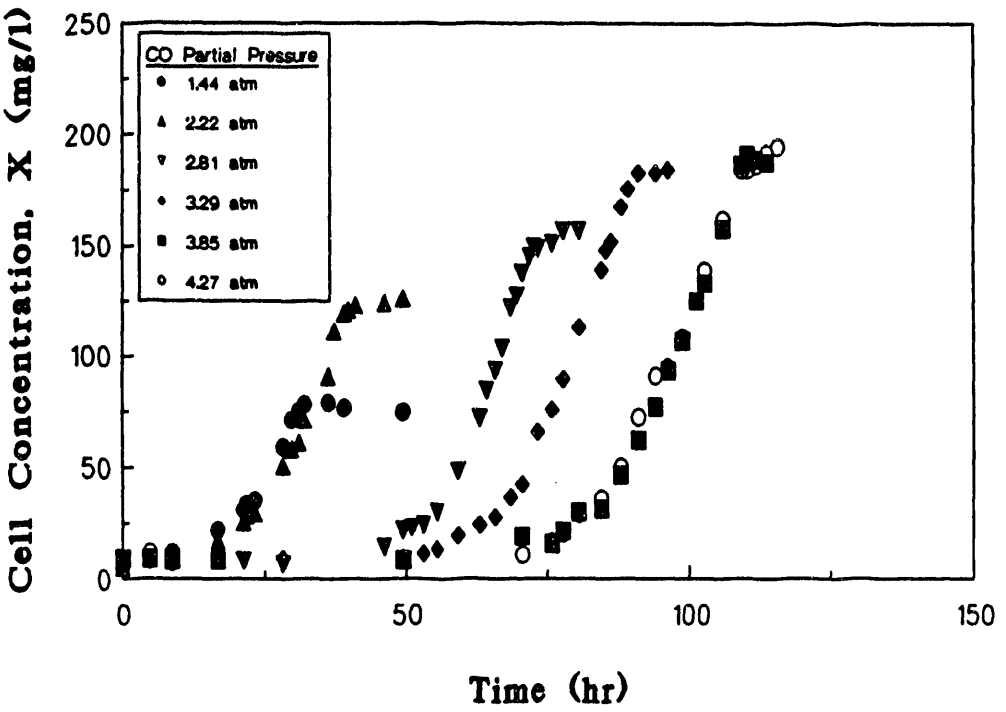

Figure 8.1. Effect of CO partial pressure on cell growth by *C. ljungdahlii* grown on CO.

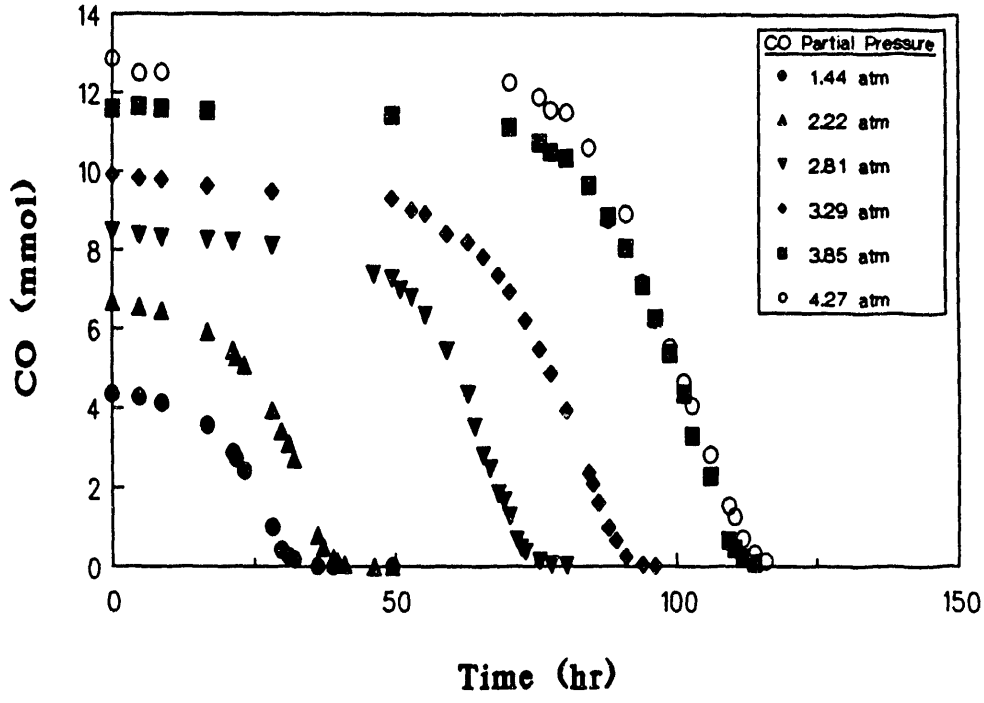

Figure 8.2. Effect of CO partial pressure on CO uptake by *C. ljungdahlii* grown on CO.

complete CO utilization increased with CO partial pressure. The rate of CO utilization, as obtained from the slopes of the plots, was essentially constant with initial CO partial pressure.

8.1.1 Mass Transfer Considerations

The conversion of CO, CO_2 and H_2 in synthesis gas to ethanol and acetate by *C. ljungdahlii* is a multi-phase process. First, the gas phase substrate must be transferred from the bulk gas phase to the liquid phase. Dissolved gas is then taken up by the solid organisms and converted to a liquid phase product. A small amount of the dissolved substrate is utilized for the growth of the bacteria, with the majority converted to ethanol or acetate.

The overall conversion scheme may be visualized using the following expression:

$$CO_{(g)} \xrightarrow{r} CO_{(l)} \xrightarrow{r} \begin{matrix}\text{Ethanol}\\ \text{Acetate}\\ \text{Cells}\end{matrix} \qquad (8.1)$$

In Equation (8.1), the gaseous substrate, in this case carbon monoxide ($CO_{(g)}$), is transported to the liquid phase ($CO_{(l)}$) through mass transport (t) after which it undergoes biocatalytic reaction (r) to ethanol, acetate and cells. In batch culture, the rate of transport (t) may be described by the following equation:

$$t = \frac{K_L a}{H} \left[P_{CO}^{G} - P_{CO}^{L}\right] \qquad (8.2)$$

where $K_L a$ is the overall mass transfer coefficient times the interfacial surface area (a necessary factor due to the virtual impossibility of of separately measuring the gas/liquid interfacial area), H is the Henry's law constant for carbon monoxide in the liquid culture, and $\left[P_{CO}^{G} - P_{CO}^{L}\right]$ is the

driving force, a function of the carbon monoxide partial pressure in the gas (g) and liquid (l) phases.

Equation (8.2) may be incorporated into a carbon monoxide mass balance for the gas phase which states that the rate of change in the number of moles of CO in the gas phase equals the rate of transport from the gas phase to the liquid phase, expressed as:

$$\frac{dN_{CO}^{G}}{dt} = - \frac{K_L a}{H} \left[P_{CO}^{G} - P_{CO}^{L}\right] V_L \qquad (8.3)$$

In Equation (8.3) the negative sign indicates the disappearance of CO from the gas phase. The liquid volume (V_L) is included in the equation for units agreement, since the mass transfer coefficient, K_La/H, is expressed in mmol CO/atm•L•hr.

As the fermentation proceeds in batch culture, the cell population grows to a point at which it consumes CO as quickly as it enters the liquid phase. At this point the overall reaction becomes mass transfer limited and the CO partial pressure in the liquid phase is reduced to zero. Under these limiting conditions, Equation (5.3) reduces to:

$$\frac{dN_{CO}^{G}}{dt} = - \frac{K_L a}{H} (P_{CO}^{G}) V_L \qquad (8.4)$$

Upon rearrangement, Equation (8.4) allows the graphical determination of $\frac{K_La}{H}$ the slope of a plot of P_{CO}^{G} as a function of $- \frac{1}{V_L} \frac{dN_{CO}^{G}}{dt}$ (shown in Figure 8.3). As is noted, for the mass transfer limited region of Figure 8.3, K_La/H equal 23.88 mol CO/atm•L•hr. Once K_La/H is determined, it can be used to calculate values for P_{CO}^{L} for the time during which the fermentation is not mass transfer limited. It should be noted that the value of K_La/H

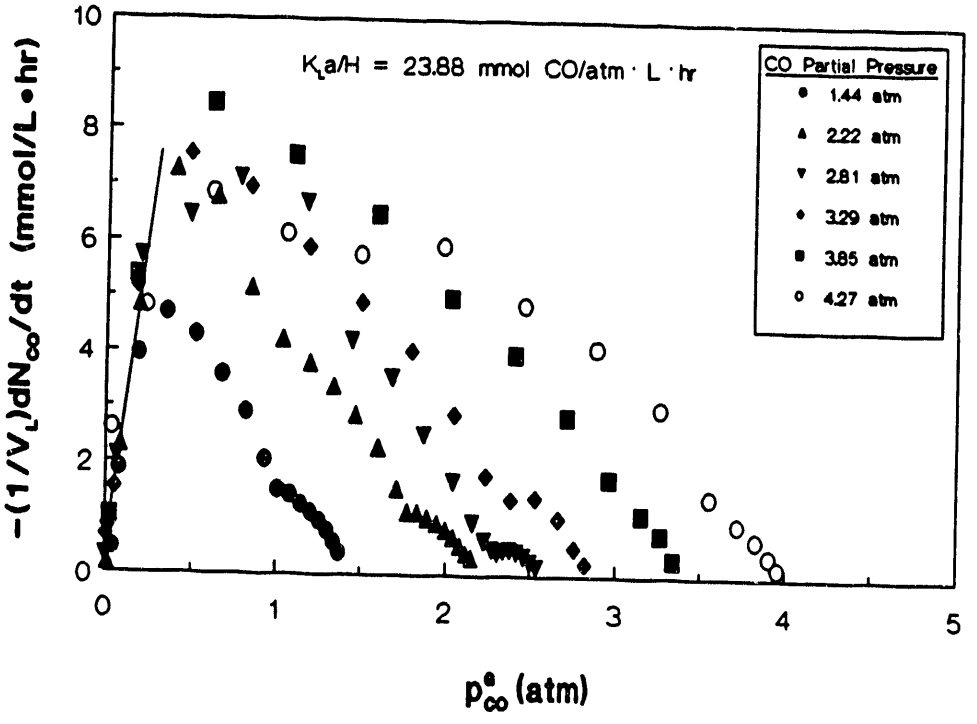

Figure 8.3.. Volumetric mass transfer coefficient for the fermentation of CO by *C. ljungdahlii*.

differs significantly from the result found earlier in different reaction vessels. This is expected since the mass transfer characteristics of the two reactors are different.

8.1.2 Reaction Kinetics

The second segment of Equation (8.1), representing the rate of biocatalytic reaction of carbon monoxide to products, may be expressed as:

$$r = q_{CO} X \tag{8.5}$$

where q_{CO} is the specific CO uptake rate and X is the cell concentration in the liquid medium. When incorporated into a CO balance for the liquid phase, the following relation results:

$$\frac{K_L a}{H} (P_{CO}^{G} - P_{CO}^{L}) V_L - q_{CO} X V_L = \frac{dN_{CO}^{L}}{dt} = \frac{dP_{CO}^{L}}{dt} \frac{V_L}{H} \tag{8.6}$$

Equation (8.6) states that the rate of change of CO in the liquid phase (expressed as $\frac{dN_{CO}^{L}}{dt}$ or in terms of the CO partial pressure in the liquid, $\frac{dP_{CO}^{L}}{dt} \frac{V_L}{H}$) is equal to the rate of transport into the liquid phase minus the rate of disappearance from the liquid phase resulting from biocatalytic conversion.

From this relation, the specific uptake rate of CO, q_{CO}, may be determined for use in a descriptive kinetic model. Additionally, the specific growth rate (μ) may be analogously defined as the time rate of change of cells per unit of cells present in the culture:

$$\mu = \frac{1}{X} \frac{dX}{dt} \tag{8.7}$$

When placed in kinetic models and accounting for substrate inhibition, the following equations are obtained as a function of the CO partial pressure in the liquid:

$$\mu = \frac{\mu_{max} P_{CO}^{L}}{K_p + P_{CO}^{L} + (P_{CO}^{L})^2/W} \tag{8.8}$$

and

$$q_{CO} = \frac{q_{max} P_{CO}^{L}}{K_p' + P_{CO}^{L} + (P_{CO}^{L})^2/W'} \tag{8.9}$$

where μ_{max} and q_{max} are the maximum specific growth and carbon monoxide uptake rates, respectively, K_p and K_p' are the liquid carbon monoxide partial pressures at which μ and q_{CO} are at one-half their maximum values, and W and W' are substrate inhibition parameters the magnitude of which is inversely proportional to the level of substrate inhibition.

Upon inversion and rearrangement of Equations (8.8) and (8.9) relations conducive to graphical representation are obtained:

$$\frac{P_{CO}^{L}}{\mu} = \frac{(P_{CO}^{L})^2}{\mu_{max} W} + \frac{P_{CO}^{L}}{\mu_{max}} + \frac{K_p}{\mu_{max}} \tag{8.10}$$

and

$$\frac{P_{CO}^{L}}{q_{CO}} = \frac{(P_{CO}^{L})}{q_{max} W'} + \frac{P_{CO}^{L}}{q_{max}} + \frac{K_p'}{q_{max}} \tag{8.11}$$

Figures 8.4 and 8.5 show how the calculated specific rates and the calculated partial pressures in the liquid phase fit Equations (8.10) and (8.11). Also shown are the results from the previous kinetic studies, shown as the short straight lines in the plots. For initial CO gas phase partial pressures at the current experimental levels (4.27 atm and below) no substrate inhibition was detectable and graphically, the intercepts were essentially zero giving a zero order reaction with respect to the partial pressure of CO in the liquid phase. The resulting values for μ_{max} and q_{max} were 0.079 hr^{-1}

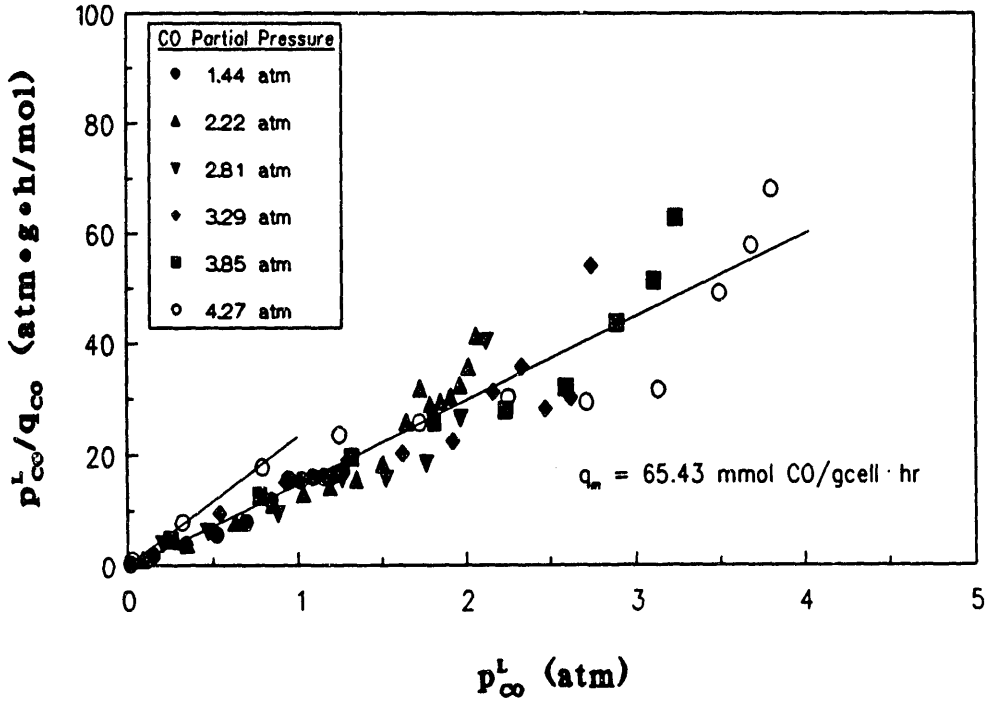

Figure 8.4. Monod model for the rate of CO uptake by *C. ljungdahlii* in batch fermentation.

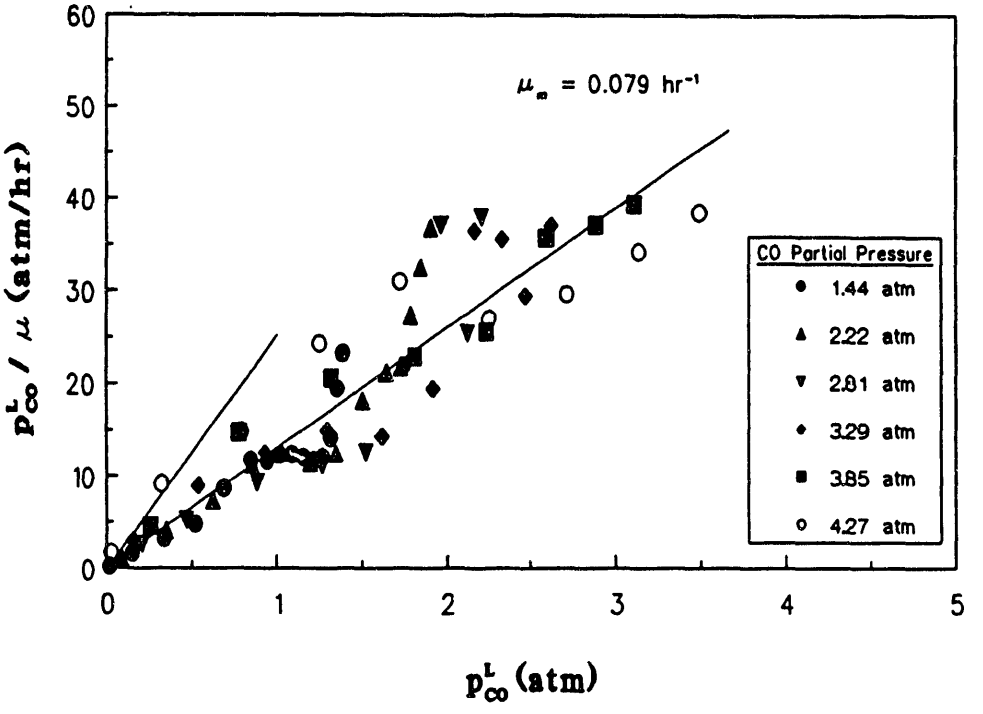

Figure 8.5.. Monod model for the rate of cell growth by *C. ljungdahlii* in batch fermentation.

and 65.43 $\frac{\text{mmol CO}}{\text{gcell}\cdot\text{hr}}$, respectively. Thus, $q = q_{max} = 65.43$ mmol CO/g•cell hr and $\mu = \mu_{max} = 0.079\ hr^{-1}$. The resulting zero order Monod model provides a a simple model for reactor design.

8.2 The Effect of Minimal Medium on Process Kinetics

A minimal medium containing salts, vitamins, minerals and essential amino acids was developed to replace the complex medium contains a large array of nutritional compounds. Phosphate limitation, for example, may be studied by utilizing the minimal medium by first removing all phosphate from the medium and then replacing a portion of the phosphate. In this manner, incremental amounts of phosphate can be investigated for their effect on the product ratio and process kinetics.

The effects of the minimal medium on process kinetics were studied utilizing the methods of kinetic analysis previously developed in the University of Arkansas laboratoaries. Five bottles (nominal volume of 1200 mL) were each filled with 200 mL of defined medium at pH 5.0 and with synthesis gas at approximately 7 psig. The culture medium was reduced with 0.5 g/L cysteine-HCl and inoculated with 10% by volume inoculum of *C. ljungdahlii* seed culture previously grown in defined medium. Figures 8.6-8.8 show experimental results for cell concentration, CO consumed and ethanol produced, respectively.

As is seen in Figure 8.6, the lag phase for cell growth ranged from approximately 100 to 150 hrs. This compares closely with lag phase times observed with fermentations in basal medium at similar synthesis gas pressures. Carbon monoxide consumption (Figure 8.7), though initiated at different times (e.g. lag phases), progressed at similar rates and fell to

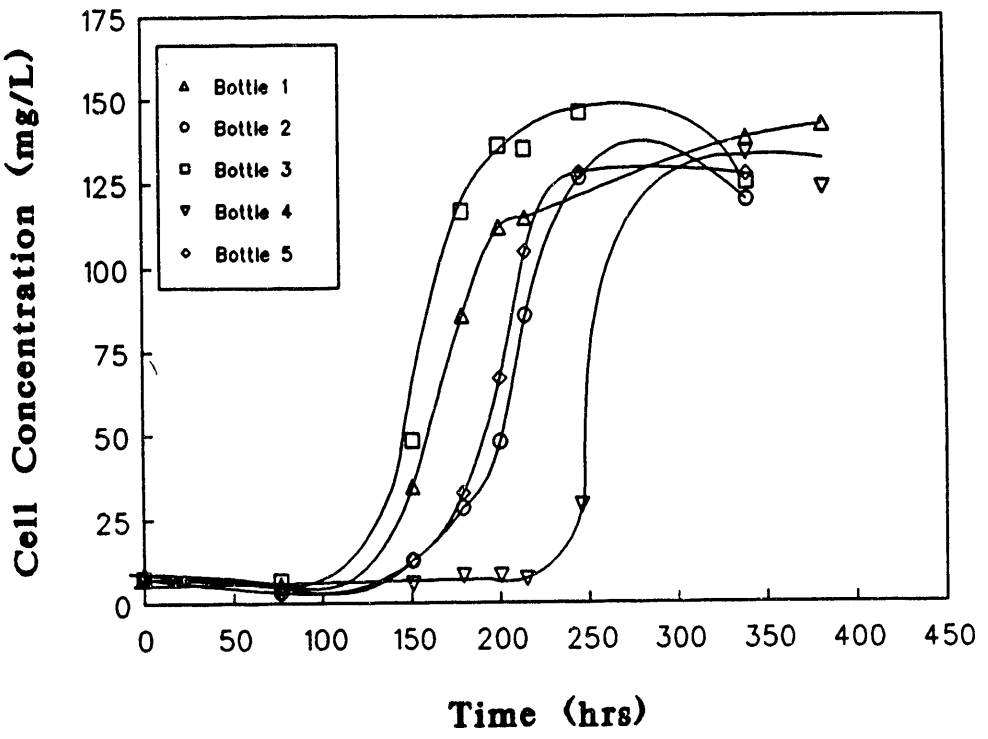

Figure 8.6. Cell concentration profile for *C. ljungdahlii* in batch culture with a defined medium.

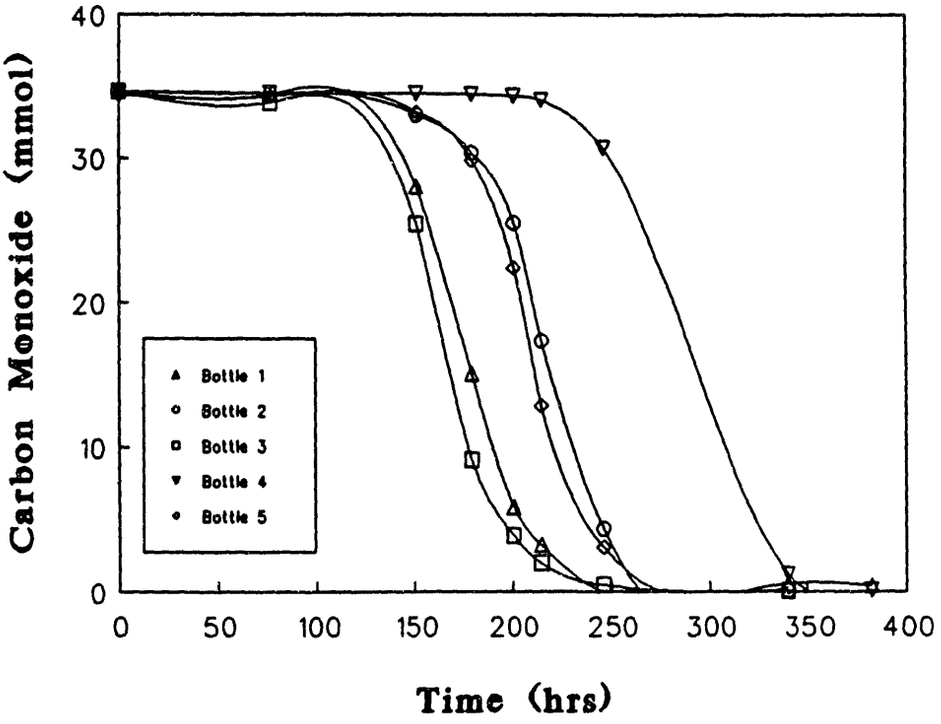

Figure 8.7. Cell consumption profile for *C. ljungdahlii* in batch culture with a defined medium.

zero concentration. When adjusted for the different lag phases, the time for complete conversion in each bottle was approximately 150 hrs; again, comparing closely with cultures grown in basal medium under similar operating conditions. Ethanol concentrations during the fermentation are given in nnomes in Figure 8.8. Peak levels of production for the five batch bottles ranged from 111 to 1.9 mmoles ethanol. As with the comparison made for the lag phase between this experiment and those using basal medium, these ethanol levels here are slightly higher than those obtained with *C. ljungdahlii* in basal medium. For cultures grown in basal medium at equivalent initial substrate levels, the peak ethanol levels varied from 0.6 to 1.1 mmol. However, these results are insufficient to attribute the slightly higher ethanol production solely to the change in medium composition.

The volumetric mass transfer coefficient (K_La/H) and the reaction kinetics parameters (μ_{max} and q_{max}) are presented in Figures 8.9-8.11. The mass transfer coefficient determined for this experiment (K_La/H = 5.40 mmol CO/atm•L•h) is lower than most values obtained previously in experiments with basal medium carried out under the same conditions. Similarly, the maximum specific growth (μ_{max}) and CO uptake (q_{max}) rates (0.020 h^{-1} and 21.95 mmol CO/gcell•h, respectively) are significantly lower than those calculated for C. ljungdahlii growing in basal medium. Apparently, nutrient limitation affected both cell growth and the ability to uptake substrate, while slightly improving the product ratio toward ethanol.

9.0 CONTINIUOUS REACTOR STUDIES

9.1 Two-Stage CSTR System

A two-stage CSTR system was used in early studies with basal medium. The first reactor (volume of 350 mL) was used primarily for the growth of *C.*

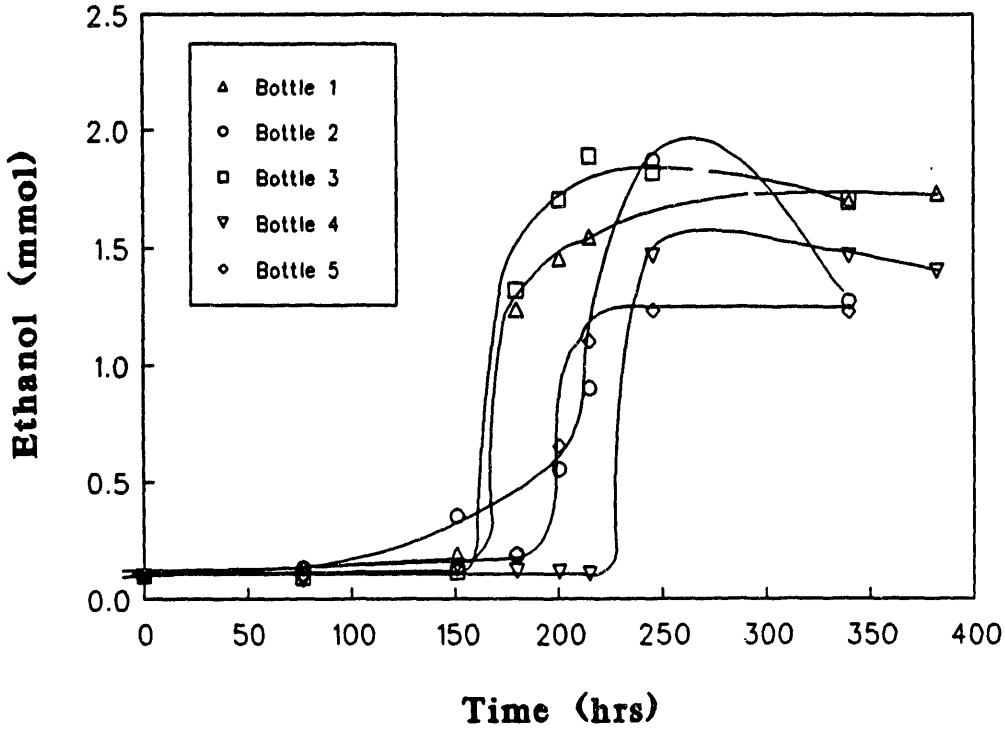

Figure 8.8. Ethanol production profile for *C. ljungdahlii* in batch culture with a defined medium.

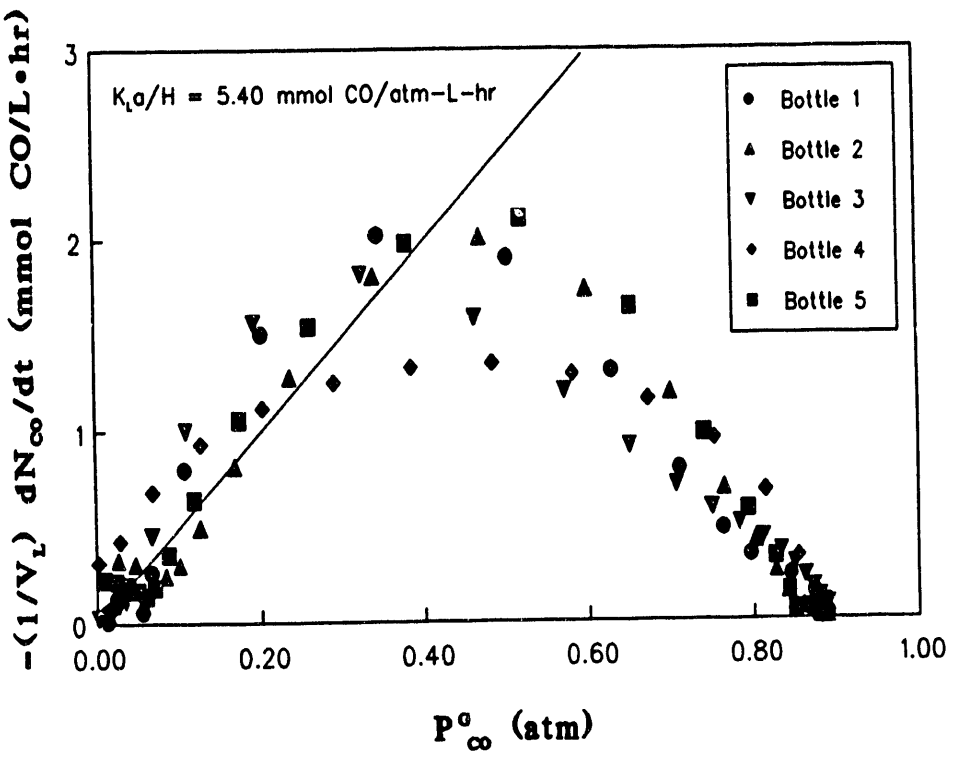

Figure 8.9. Volumetric uptake rate of CO as a function of the gas phase partial pressure in a defined medium.

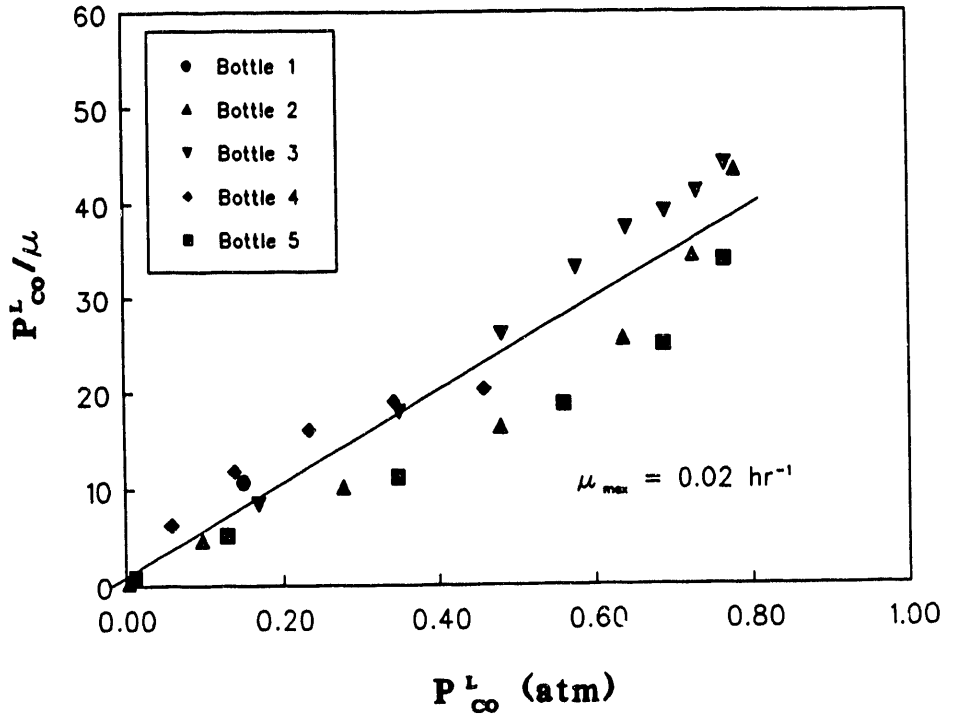

Figure 8.10. Monod model for the rate of cell growth (μ_{max}) in a defined medium.

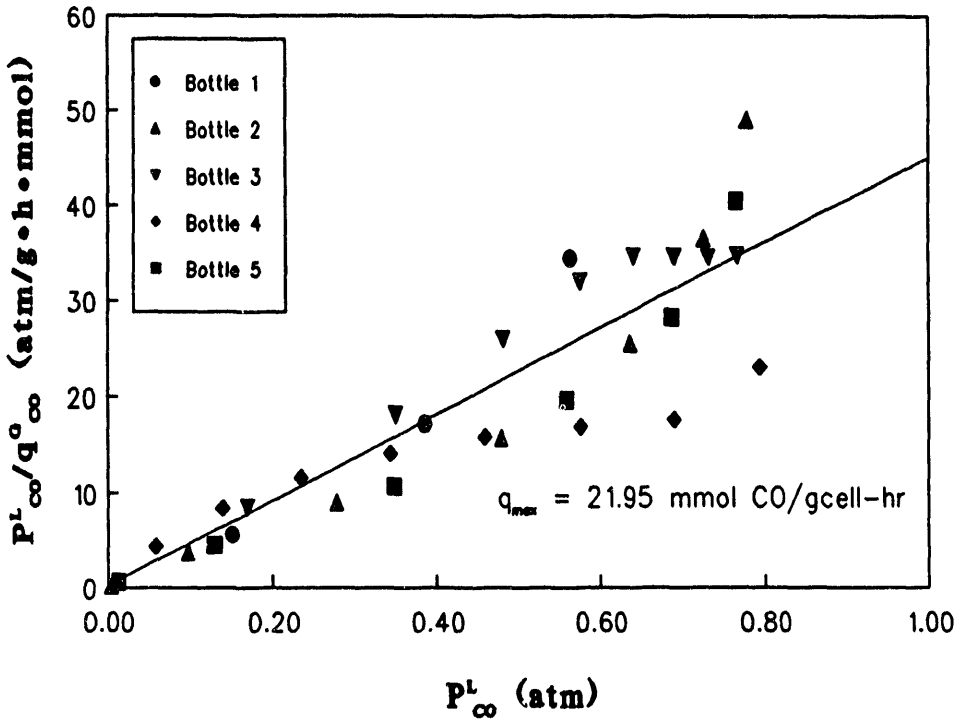

Figure 8.11. Partial pressure of CO (P^L_{CO}) over the specific uptake rate of CO (q^C_{CO}) plotted as a funciton of P^L_{CO} for a defined medium.

ljungdahlii. The liquid feed to this reactor consisted of 0.02 percent yeast extract in basal medium at pH 4.5, with a flow rate of 360 mL/day. In addition, synthesis gas was fed to the reactor to supply carbon and energy sources for growth. Because this reactor was designed primarily for growth, significant acetate production was also expected. The second reactor (volume of 1.44 L) was used primarily for ethanol production by *C. ljungdahlii* cells formed in the first reactor. No additional liquid was fed to the second reactor so that nutrients were limiting. In addition, the pH was adjusted to pH 4.0 and the reducing agent benzyl viologen was added at a concentration of 10-20 ppm. Synthesis gas was bubbled into the second CSTR for conversion to ethanol. it was hoped that only ethanol would be produced from the cells in the second CSTR. However, because the conditions in the second reactor were not conducive for growth, the efficiency of ethanol production in the second CSTR was in doubt. An experiment was thus run with the above system to determine the overall performance of this two-stage system and to determine the suitability of the second stage in efficiently producing ethanol by utilizing the pH shift, nutrient limitation and benzyl viologen addition. The results are summarized below.

9.1.1 Operating Conditions

The reactor volumes and liquid flow rates were held constant at the values shown above throughout the experimental study. In addition, the feed to the first reactor always consisted of 0.02 percent yeast extract in basal medium. The pH varied a bit in each reactor, but was essentially 4.5 in Reactor A (the first reactor in series) and 4.0 in Reactor B.

The gas flow rate to Reactor A varied from 2.34 mL/min during start-up to a high of 3.40 mL/min on day 53. However, during most of the experimental

study the gas flow rate was held constant at 2.76 mL/min. Similarly, the gas flow rate to Reactor B varied from a low of 1.79 mL/min during startup to 2.20 mL/min. Adjustments in these gas flow rate were made periodically in an attempt to improve reactor performance but, as noted, were not significant adjustments.

Benzyl viologen at a concentration of 20 ppm was added to Reactor B on day 13. The higher concentrations utilized in previously batch studies (30-50 ppm) were found to be excessive in continuous culture, resulting in culture death. The concentrations of benzyl viologen was lowered to 10 ppm on day 45. Initially, no benzyl viologen was added to Reactor B.

9.1.2 Results and Discussion

Cell concentration profiles for the two reactors are shown in Figures 9.1 and 9.2. As is noted in Figure 9.1, after a brief start-up period, the cell concentration varied about a cell concentration of approximately 300 mg/L from 270 to 317 mg/L until day 65. A temperature decrease in the constant temperature room is then thought to be responsible for the significant drop in cell concentration seen after day 60. The cell concentration in Reactor B was also seen to gradually increase during start-up until the addition of benzyl viologen on day 13. A cell concentration of 340 mg/L was seen at this point. The reducing agent benzyl viologen, while yielding reduced conditions necessary for ethanol production, also resulted in the death of cells particularly at high concentrations (a high concentration may be as little as 20 ppm, as is noted in Figure 9.2). The cell concentration decreased to only 250 mg/L throughout the addition of 20 ppm benzyl viologen. When 10 ppm benzyl viologen was used instead of 20 ppm, the cell concentration in Reactor B also decreased, but only to a 280 mg/L concentration. Again, the results after day 60 are due to the temperature upset.

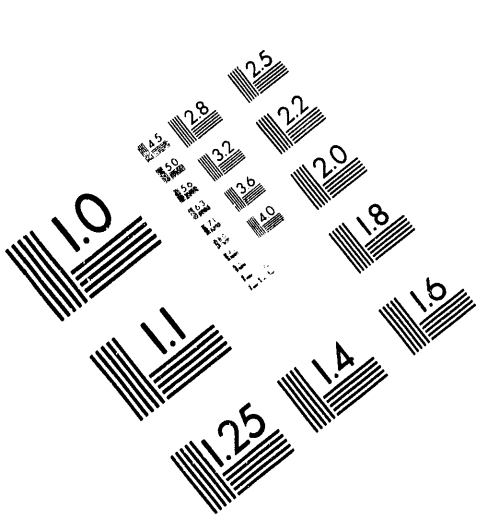

Association for Information and Image Management
1100 Wayne Avenue, Suite 1100
Silver Spring, Maryland 20910
301/587-8202

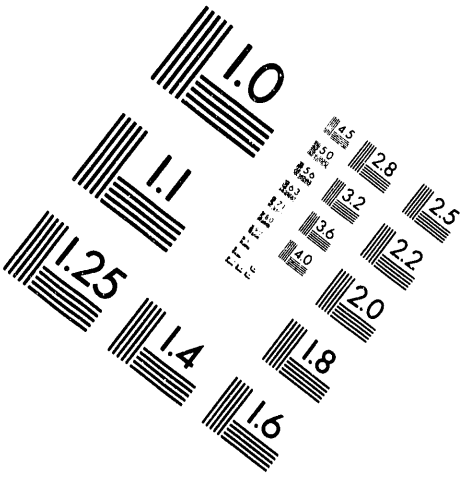

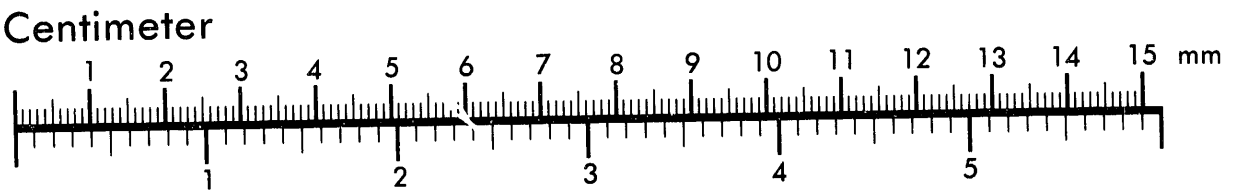

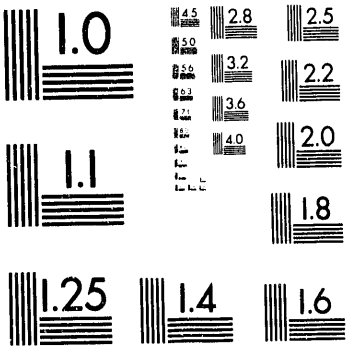

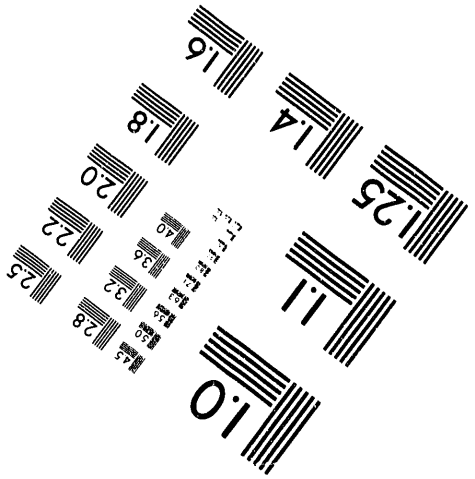

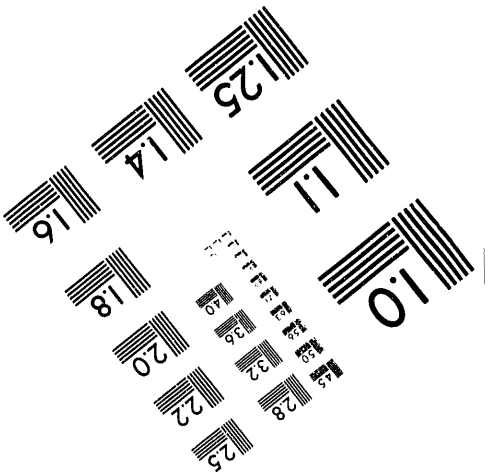

3 of 4

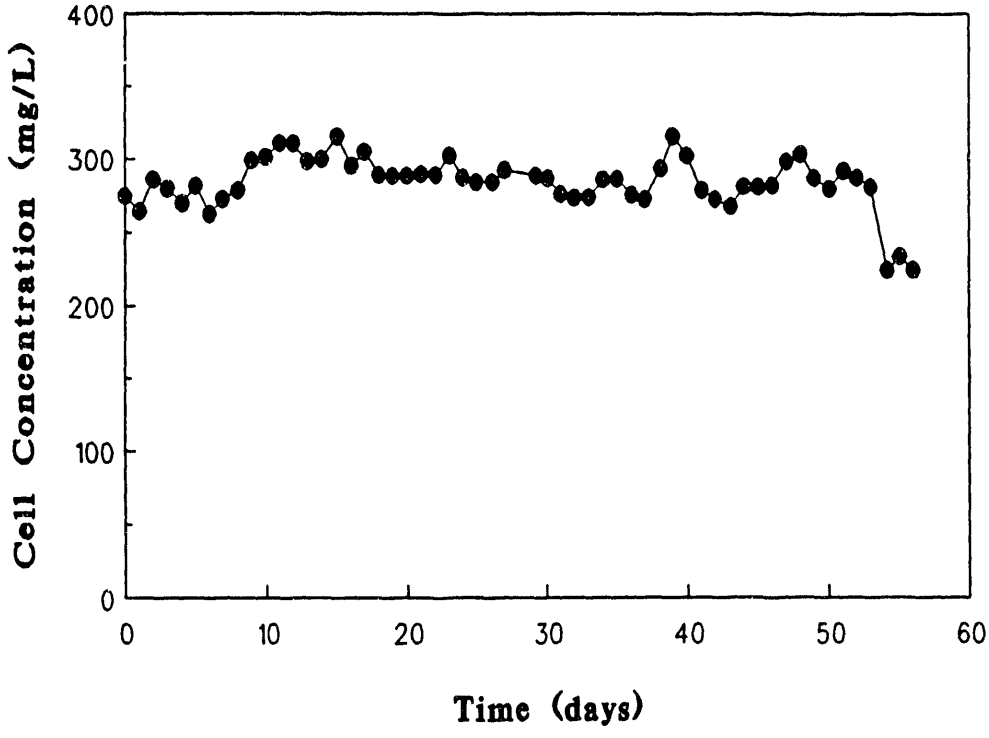

Figure 9.1. Cell concentration profiles in Reactor A in a two-stage CSTR system using *C. ljungdahlii*.

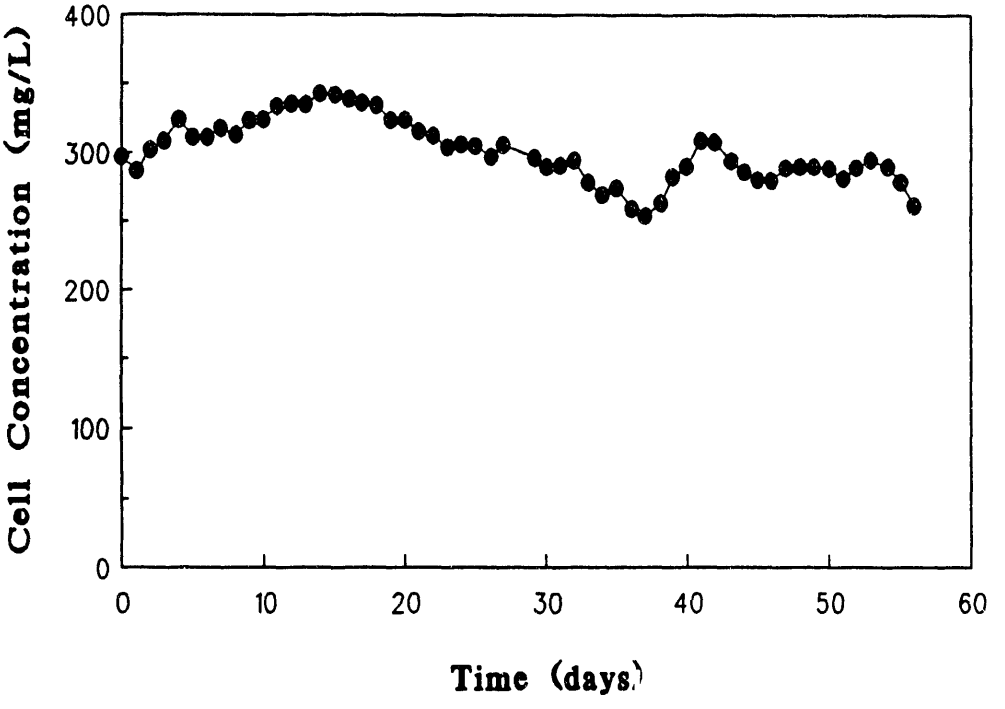

Figure 9.2. Cell concentration profiles in Reactor B in a two-stage CSTR system using *C. ljungdahlii*.

The conversions of CO and H_2 in the synthesis gas feed to Reactors A and B are shown in Figure 9.3 and 9.4. As is noted in Figure 9.3, the conversions of both CO and H_2 remained constant at 90-95 percent throughout the whole experimental study (excluding start-up and the temperature upset). Both the CO and H_2 conversions decreased as a result of benzyl viologen addition in Reactor B (see Figure 9.4) regardless of whether 20 ppm or 10 ppm benzyl viologen was used. This phenomenon has been seen previously in the University of Arkansas laboratories, and may signal that the efficiency of the cells in utilizing substrate or forming product is reduced in the presence of benzyl viologen or other reducing agents.

Product formation in the reactors are shown in Figures 9.5-9.7. As expected, acetate formation was much greater in Reactor A than ethanol formation due to the growth-enhancing conditions employed. Concentrations of approximately 3.5 g/L acetate and 0.5 g/L ethanol were formed except during start-up and after the temperature upset. This translates into a molar ratio of 0.19 moles ethanol per mole acetate, or just over 5 moles acetate produced per mole of ethanol.

Figure 9.6 shows the overall product concentration profile from the two-stage system. As is noted, the concentration of ethanol stayed approximately constant at about 1 g/L, with peak concentrations of about 1.3 g/L. These concentration levels have been exceeded in the past. The concentration of acetate, however, fell with the addition of benzyl viologen, especially when using 20 ppm of the reducing agent. A better idea of what happened upon the addition of benzyl viologen can be seen in Figure 9.7, where the concentrations of ethanol and acetate produced in Reactor A are subtracted from the overall product concentrations. It can be clearly seen that only

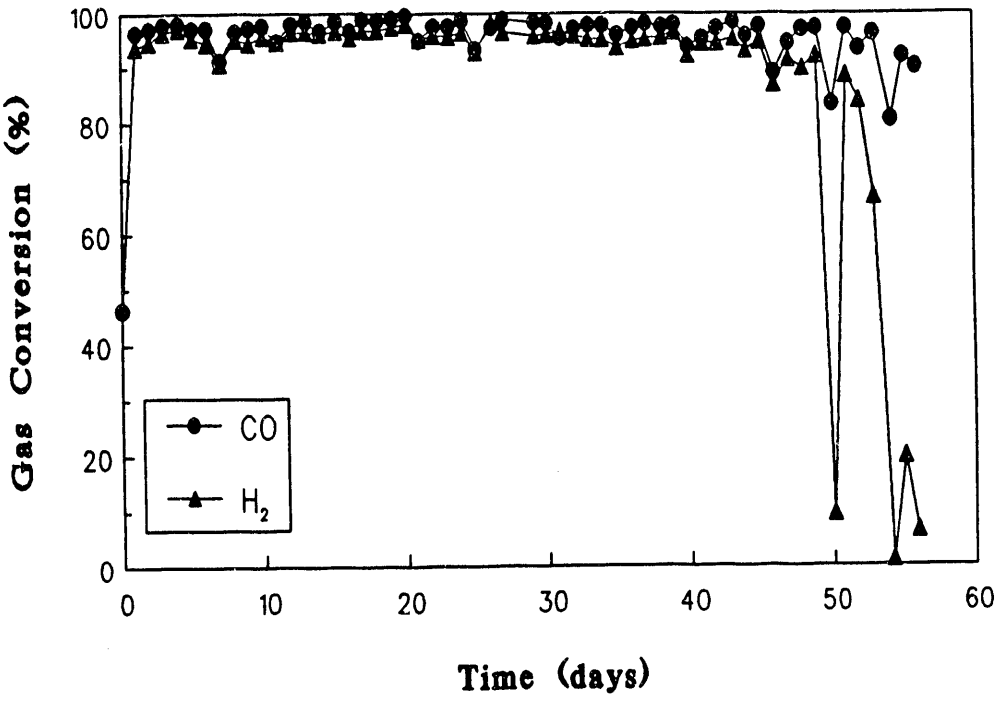

Figure 9.3. CO and H conversion in Reactor A in a two-stage CSTR system using *C. ljungdahlii*.

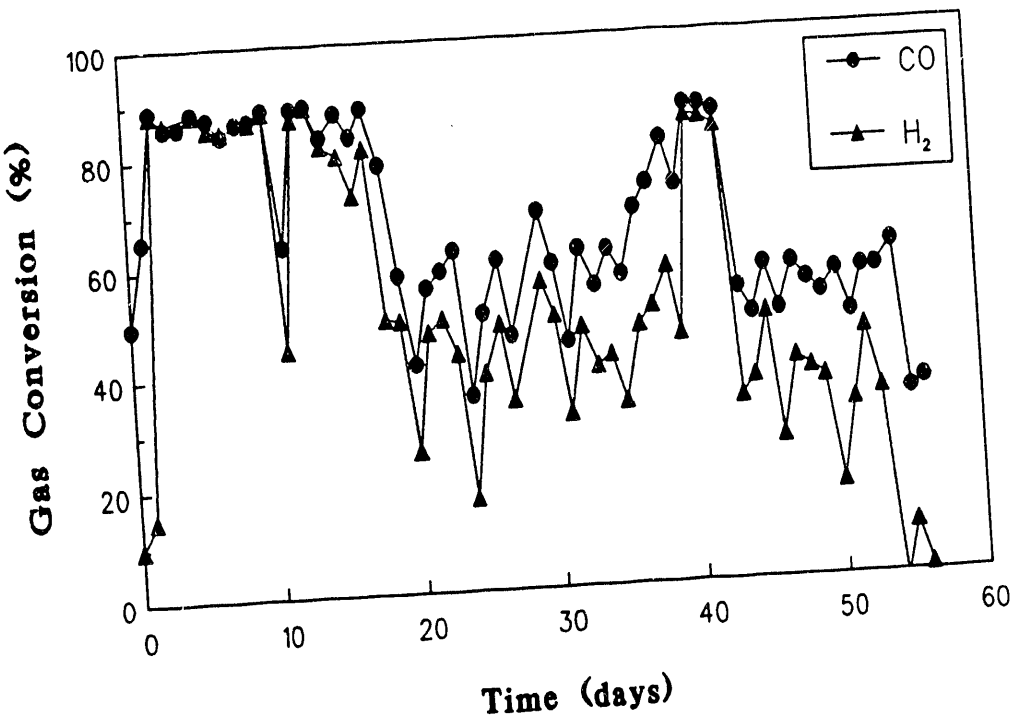

Figure 9.4. CO and H_2 conversion in Reactor B in a two-stage CSTR system using *C. ljungdahlii*.

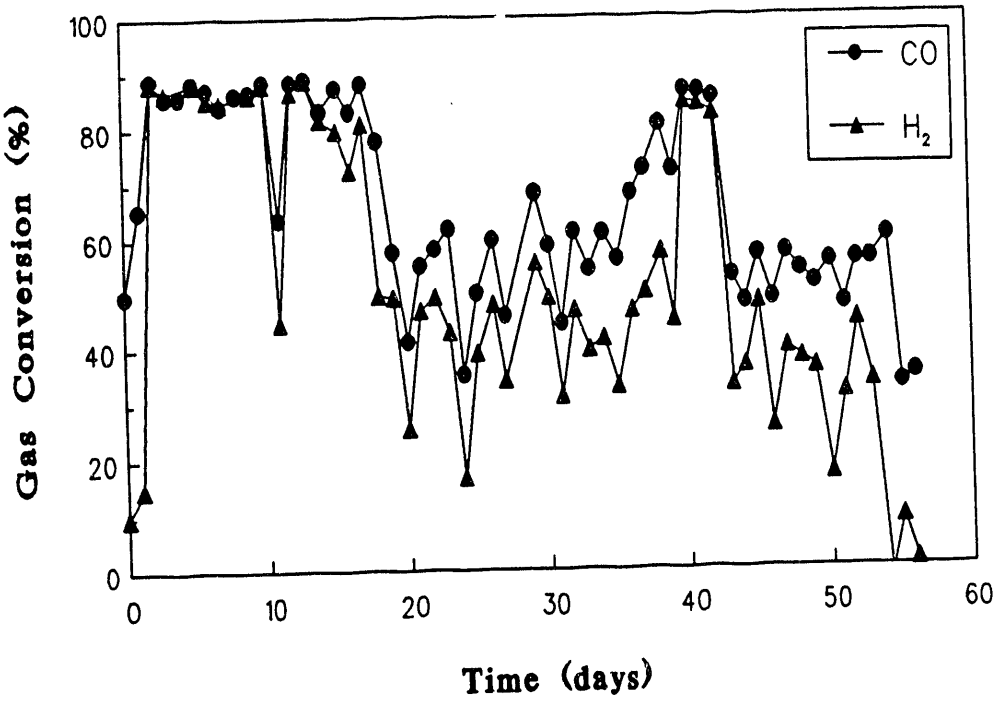

Figure 9.4. CO and H_2 conversion in Reactor B in a two-stage CSTR system using *C. ljungdahlii*.

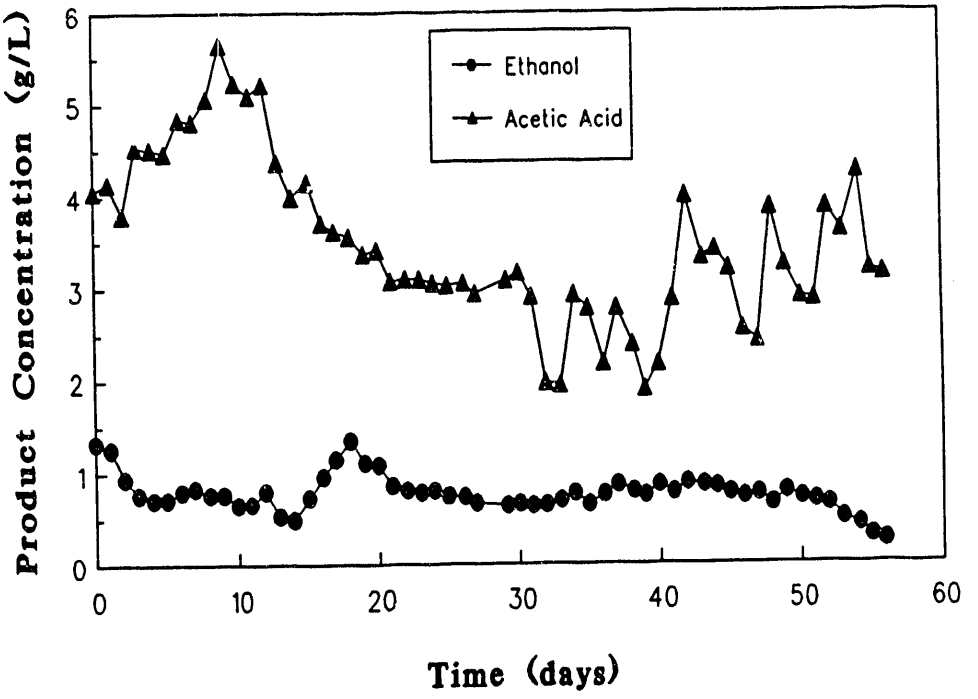

Figure 9.6. Product concentration profiles for the overall two-stage reactor system using *C. ljungdahlii*.

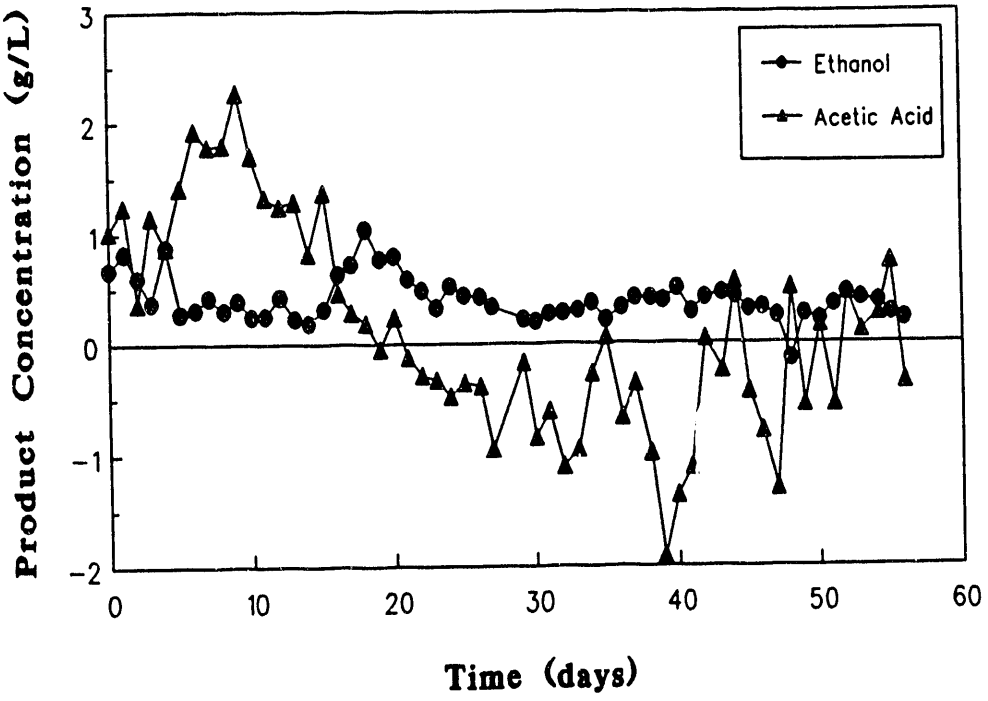

Figure 9.7. Production of ethanol and acetate by *C. ljungdahlii* in Reactor B of a two-stage CSTR system.

ethanol was produced in the second reactor. As a matter of fact, the negative acetate concentrations indicate that acetate was actually being consumed in the second reactor. The only negative aspect of this result is the hope that the ethanol concentrations would have been higher. This probably can be accomplished by varying the benzyl viologen concentration.

9.2 Continuous Stirred-Tank Reactor Studies

A continuous stirred-tank reactor with both continuous liquid and gas feed was prepared in order to demonstrate synthesis gas conversion to ethanol by *C. ljungdahlii* in continuous culture. The principles learned in earlier batch culture studies for maximizing ethanol production (low operating pH, no yeast extract in the medium and limited B-vitamins in the medium) were applied to these CSTR studies. A wide range of important variables are to be studied in the CSTR, including liquid flow rate, agitation rate and gas flow rate. The purpose of these parametric studies is to determine the importance of these variables on the values of cell and product concentrations, yields and productivities.

9.2.1 Liquid Flow Rate Effects

Fermentation profiles of cell concentration, ethanol concentration and acetate concentration as a function of time were obtained in the LCSTR at each liquid flow rate. During these studies the agitation rate was held at 360-400 rpm, the gas flow rate was held at 0.145 mmol/min and the liquid flow rate was varied from 50 to 400 mL/d. The resulting concentration profiles were then used to calculate cell and product yields, specific uptake rates and specific productivities as a function of time. Finally, steady-state values of the concentrations, yields, rates and productivities were plotted as a function of liquid flow rate in order to observe trends in the experimental data as a function of liquid flow rate.

Figures 9.8 and 9.9 show typical cell concentration and product concentration profiles in the CSTR at liquid flow rates of 200 and 100 mL/d. Time plotted on the abscissa ranges from 600 to 1200 h, since these data are part of a longer term study using various liquid flow rates in the CSTR. As is noted in Figure 9.8, a steady-state cell concentration of approximately 300 mg/L was obtained at a liquid flow rate of 200 mL/d, and a steady-state cell concentration of approximately 350 mg/L was obtained at a liquid flow rate of 100 mL/d. Thus, as expected, a decrease in the flow of liquid through the reactor brought about an increase in the steady-state cell concentration. Figure 9.9 presents product (ethanol and acetate) concentration profiles for the same flow rate study. The steady-state ethanol concentrations were approximately 1.8 g/L at 200 rpm and 2.5 g/L at 100 rpm. The corresponding steady-state acetate concentrations were approximately 1.2 and 1.6 g/L at 200 and 100 rpm, respectively.

The cell yield, $Y_{X/S}$, is shown as a function of time for the two liquid flow rates in Figure 9.10. As is noted, the yield remained essentially constant at about 0.6 mg cells/mol substrate. In fact, it was found that the cell yield was unaffected by liquid flow rate over the liquid flow rate range tested in the study. Figure 9.11 presents the product yield from substrate, $Y_{P/S}$, as a function of time for the two flow rates. As with the cell yield, the product yield was found to be essentially independent of liquid flow rate, having a value of approximately 0.3 mol of carbon in the products per mol of carbon in the substrate. It is worth noting that these steady-state values do not correspond well with the values presented earlier in this report during the initial stages of batch growth. The significance of the result needs investigation.

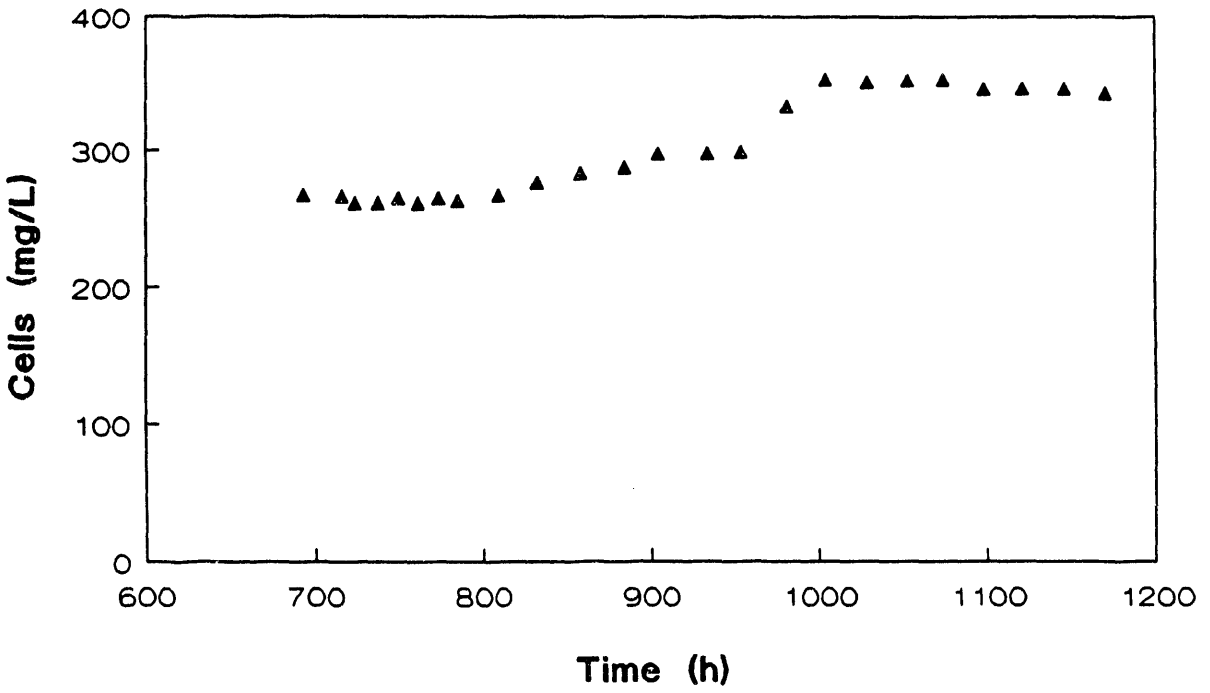

Figure 9.8. Cell Concentration Profile for *C. ljungdahlii* in the CSTR (400 rpm; Gas Flow Rate: 0.145 mmol/min; Liquid Flow Rates: 200, 100 mL/d)

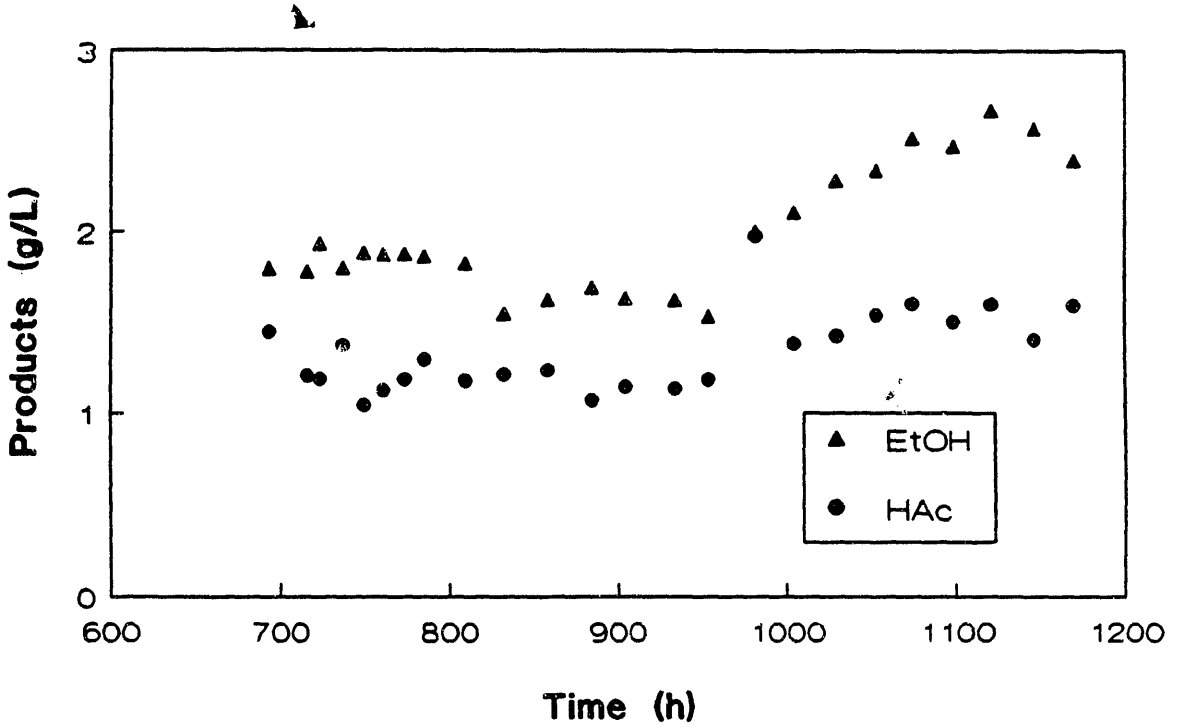

Figure 9.9. Product Concentration Profiles for *C. ljungdahlii* in the CSTR (400 rpm; Gas Flow Rate: 0.145 mmol/min; Liquid Flow Rates: 200, 100 mL/d)

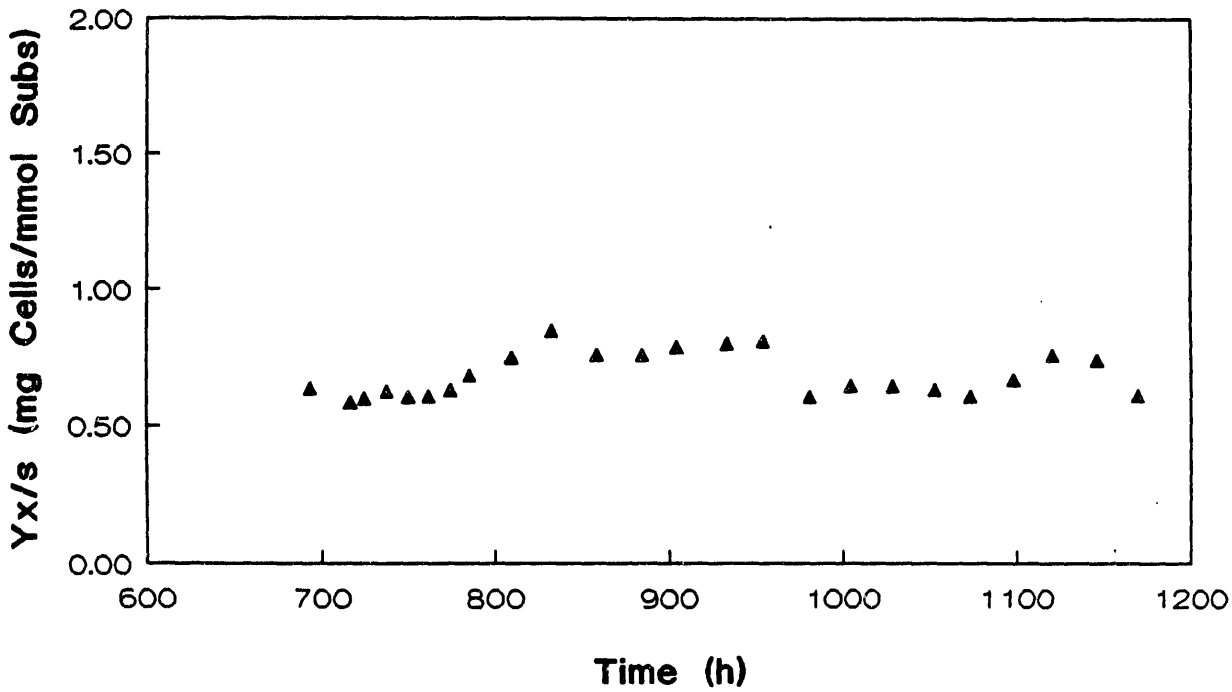

Figure 9.10. Cell Yield from Substrate for *C. ljungdahlii* in the CSTR (400 rpm; Gas Flow Rate: 0.145 mmol/min; Liquid Flow Rates: 200, 100 mL/d)

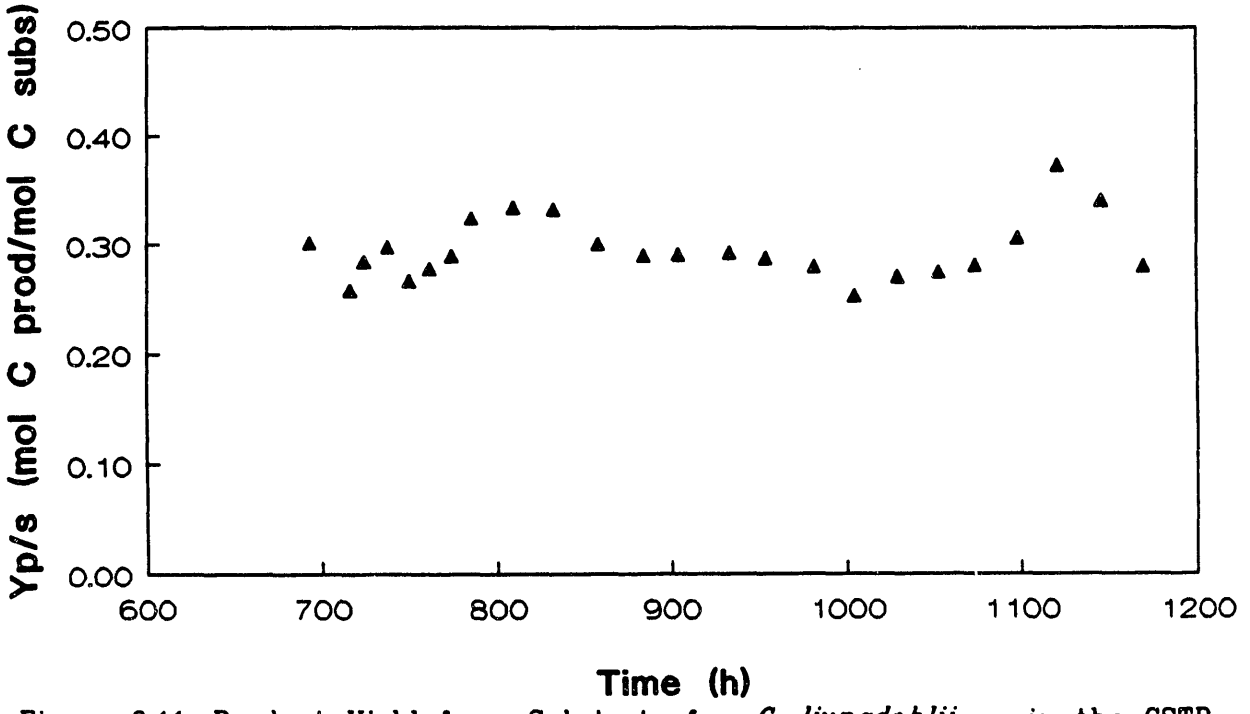

Figure 9.11. Product Yield from Substrate for *C. ljungdahlii* in the CSTR (400 rpm; Gas Flow Rate: 0.145 mmol/min; Liquid Flow Rates: 200, 100 mL/d)

Finally, specific uptake rates in mmol CO/mg cells hr and specific productivities in mmol product/mg cells hr are shown in Figure 9.12 for the two liquid flow rates. The specific uptake rate was found to decrease from 0.04 to 0.02 mmol/mg h for a decrease in liquid flow rate of 200 to 100 mL/d. Similarly, the specific productivity fell from 0.005 to 0.003 for the flow rate decrease. More will be said of these trends later.

A compilation of the CSTR data as a function of liquid flow rate is presented in Figures 9.13-9.17. Studies at two close but very different agitation rates are presented. This small difference in agitation rate is significant because the reaction system changes from gentle to vortex mixing at approximately 400 rpm. With vortex mexing, continuous breaking of the gas-liquid interface surface occurs, thereby significantly affecting gas-liquid mass transfer.

Figure 9.13 shows the effects of liquid flow rate and, to a lesser extent, agitation rate on cell density achieved in the CSTR. As is noted, the cell density decreased along a rather gentle curve, independent of agitation rate. The cell concentration was about 420 mg/L at a liquid flow rate of 50 mL/d, and was about 200 mg/L at a flow rate of 400 mL/d. The results in Figure 9.13 are expected since at lower flow rates, the liquid and cells spend more time in the reactor, thus allowing for the higher cell concentration.

Figure 9.14 shows the effects of liquid flow rate and the two agitation rates on the total products concentration, expressed as mmol of product per liter. As with cell concentration, the total product concentration fell from about 130 mmol/L at a flow rate of 50 mL/d to 30 mmol/L at a flow rate of 400 mL/d. Since it was earlier shown that product formation and cell concentration were directly linked, the results of Figure 9.14 are expected.

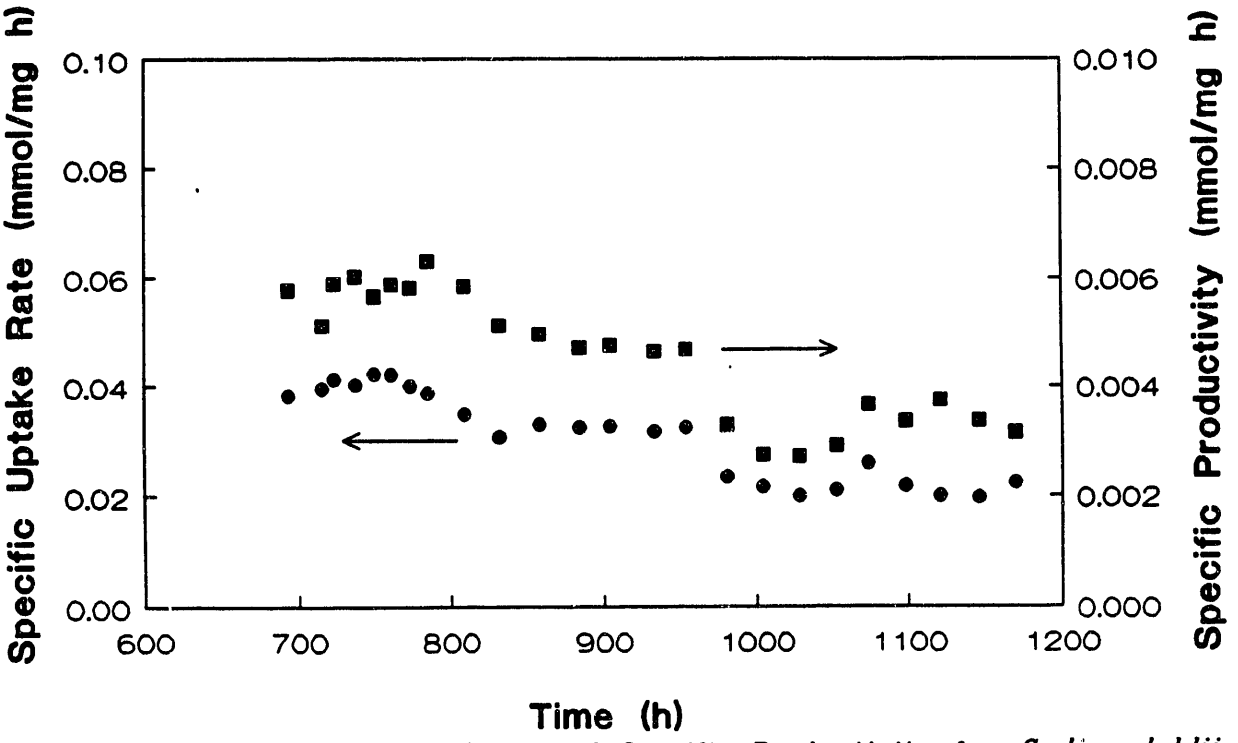

Figure 9.12. Specific Uptake Rate and Specific Productivity for *C. ljungdahlii* in the CSTR (400 rpm; Gas Flow Rate: 0.145 mmol/min; Liquid Flow Rates: 200, 100 mL/d)

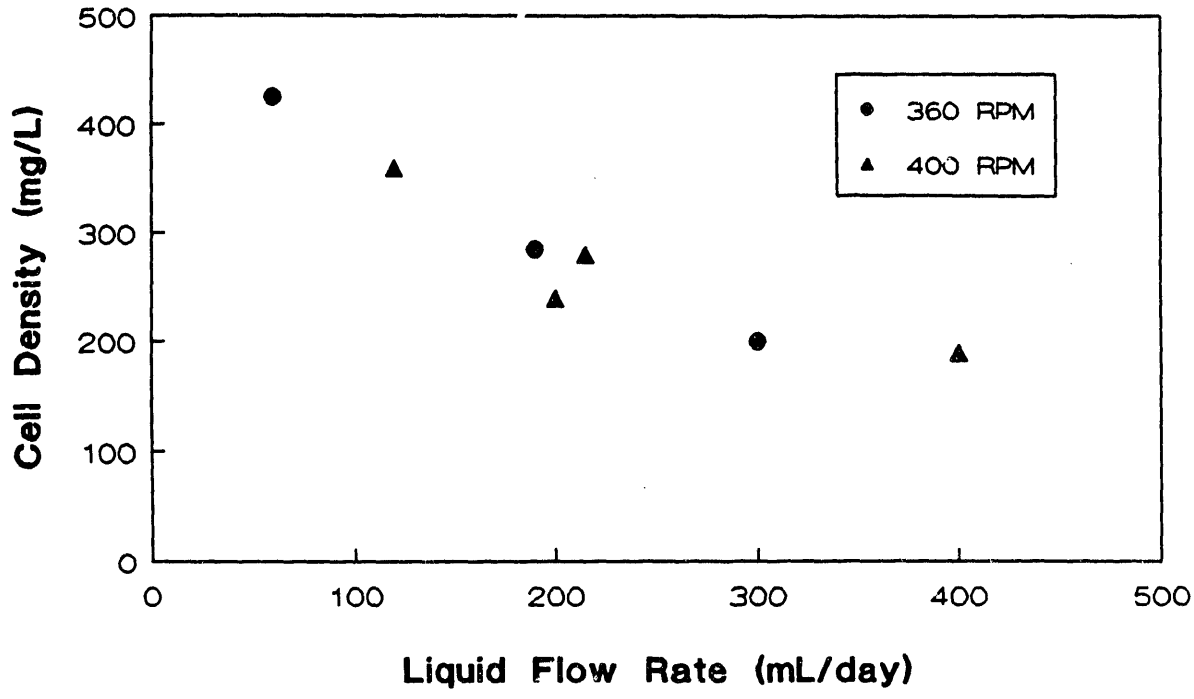

Figure 9.13. The Effects of Liquid Flow Rate On Cell Concentration Using *C. ljungdahlii* in the CSTR.

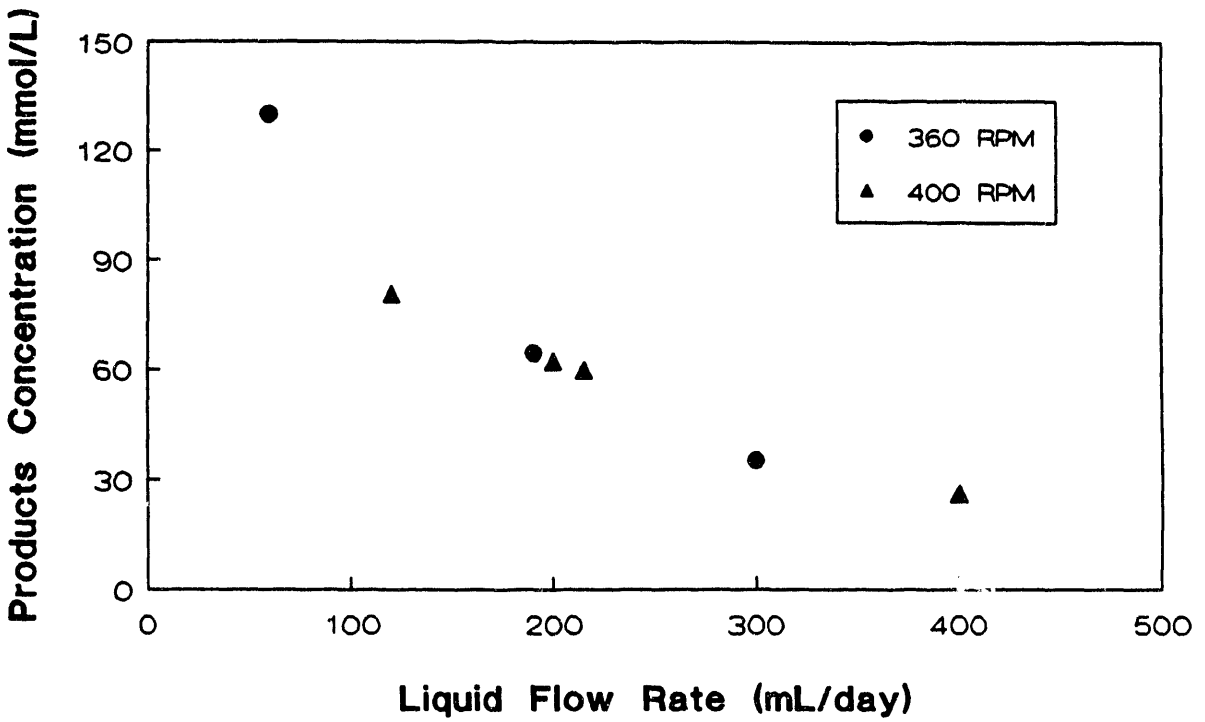

Figure 9.14. The Effects of Liquid Flow Rate on Total Product Concentration Using *C. ljungdahlii* in the CSTR.

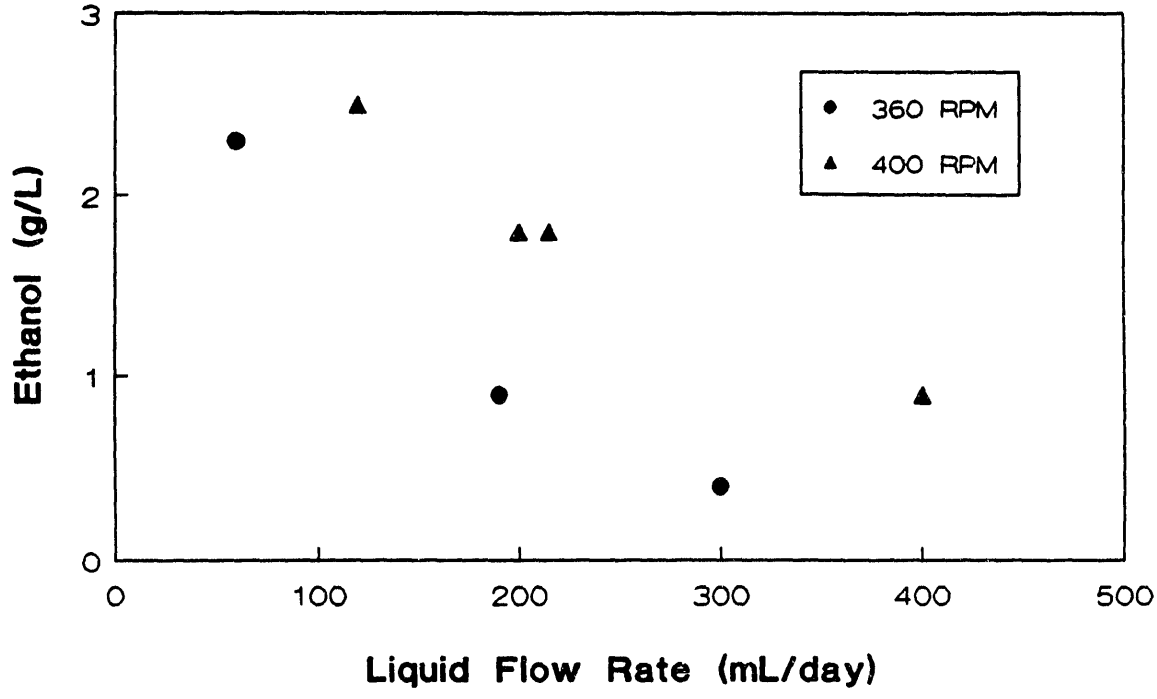

Figure 9.15. The Effects of Liquid Flow Rate on Ethanol Concentration Using *C. ljungdahlii* in the CSTR.

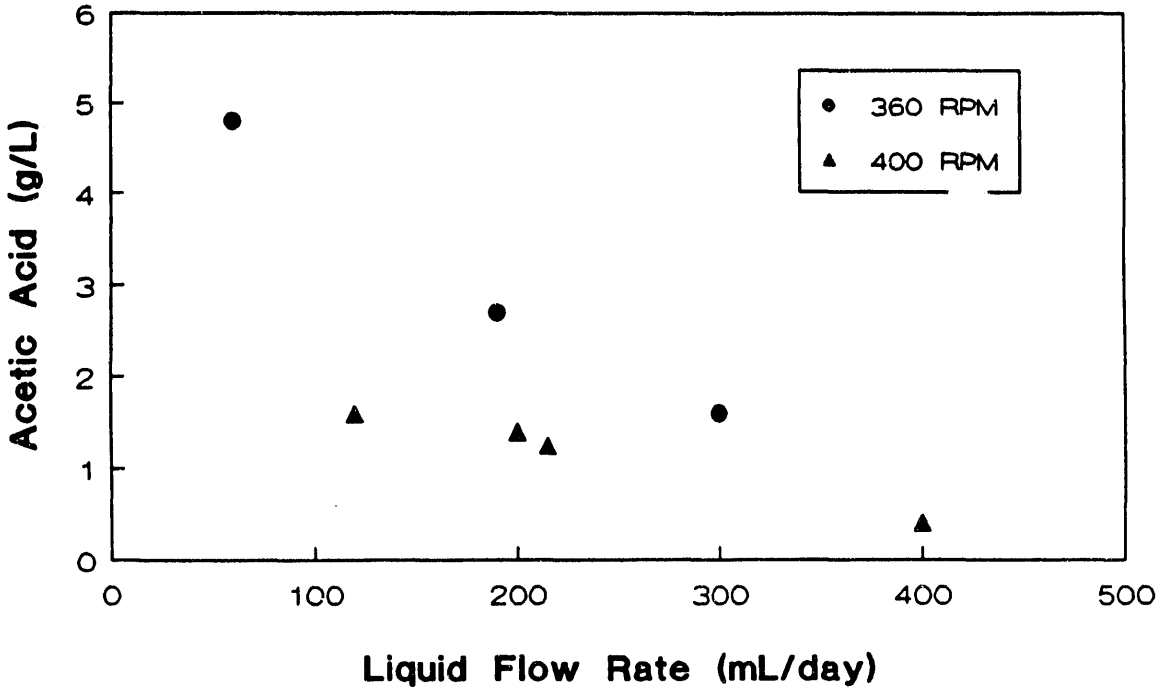

Figure 9.16. The Effects of Liquid Flow Rate on Acetic Acid Concentration Using *C. ljungdahlii* in the CSTR.

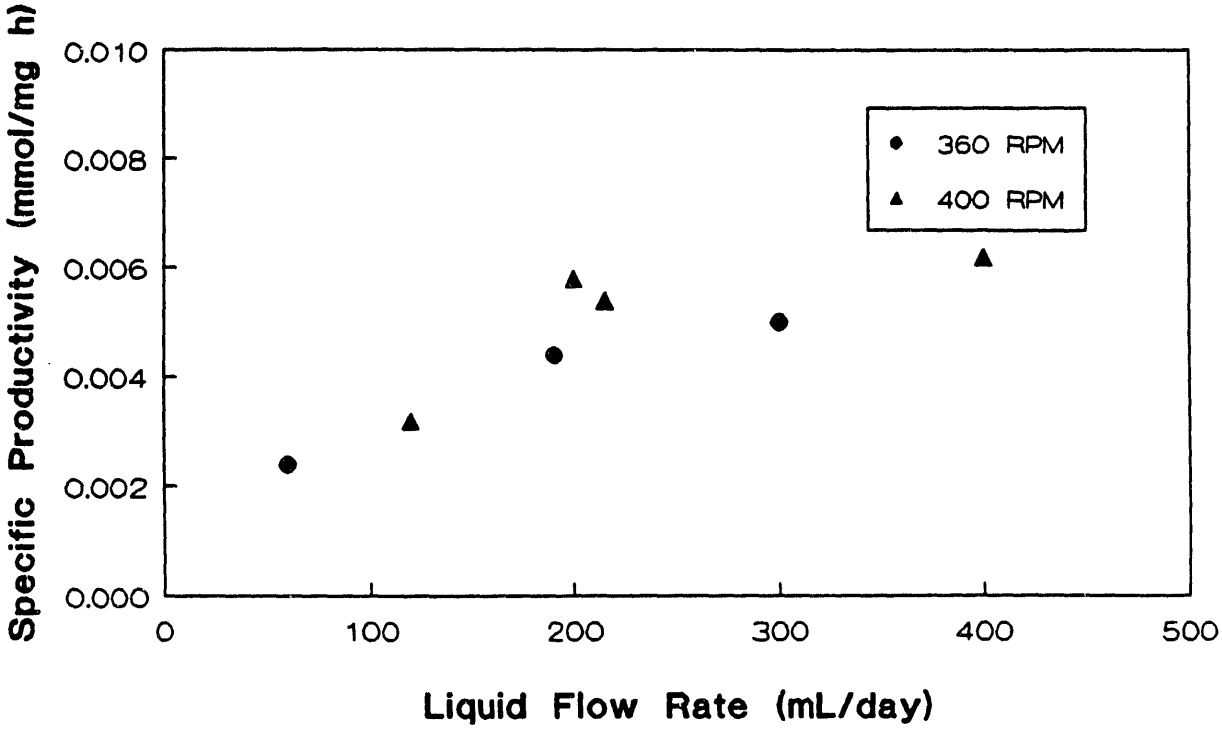

Figure 9.17. The Effects of Liquid Flow Rate on Specific Productivity Using *C. ljungdahlii* in the CSTR.

The effects of liquid flow rate and the two agitation rates on individual product (ethanol and acetate) concentrations are shown in Figure 9.15 and 9.16. In contrast to the total product concentration profile presented in Figure 9.14, the agitation rate was shown to affect both the ethanol and acetate concentrations. Higher ethanol concentrations were obtained at a given flow rate at 400 rpm (see Figure 9.15), and higher acetate concentrations were obtained at a given flow rate at 360 rpm (see Figure 9.16). In projecting continuous curves in the two figures, it is seen that at an agitation rate of 360 rpm and a liquid flow rate of 50 mL/d, the ethanol concentration was about 2.3 g/L and the acetate concentration was about 4,8 g/L. If the agitation rate is changed to 400 rpm at the same liquid flow rate of 50 mL/d, the projected ethanol concentration would be about 3.2 g/L and the acetate concentration would be about 2 g/L. Similar results are obtained at other liquid flow rates. Clearly, from the standpoint of attaining higher ethanol concentrations and higher product ratios, low liquid flow rates and higher agitation rates should be employed. Apparently the higher agitation rates cause more CO to be deposited into the liquid phase which stresses the culture. This stressful or inhibiting situation results in the production of ethanol in favor of acetate. The limits of this theory should be tested in agitation rate studies at a constant liquid flow rate.

The specific productivity (total product) is plotted as a function of liquid flow rate for the two agitation rates in Figure 9.17. A single curve is shown for the two agitation rates which curves gently upward with increasing liquid flow rate. The highest productivity, 0.006 mml product/mg h, is attained at a liquid flow rate of 400 mL/d. It is obvious, as expected, that the more flow through the system, the higher the productivity of the

reactor. The specific uptake rate similarly increases with increasing liquid flow rate (see Figure 9.12).

The key to continuous operation appears to be a high productivity system with high ethanol concentrations and high ethanol to acetate product ratios. Future continuous reactor studies need to concentrate on this important aspect.

9.2.2 Agitation Rate Effects

Fermentation profiles of cell concentration, ethanol concentration and acetate concentration as a function of time were obtained in the CSTR at each agitation rate. During these studies the agitation rate was varied between 300 and 480 rpm, the gas flow rate was held at 0.02-0.15 mmol/min and the liquid flow rate was held constant at 200 mL/d. The resulting concentration profiles were then used to calculate cell and product yields, specific uptake rates and specific productivities as a function of time. Finally, steady state values of the concentrations, yields, rates and productivities were plotted as a function of liquid flow rate in order to observe trends in the experimental data as a function of liquid flow rate.

Figure 9.18 and 9.19 show typical cell concentration and product concentration profiles in the CSTR at increasing agitation rates from 300 to 480 rpm. Time plotted on the abscissa ranged from 500 to 2500 h, since these data are part of a longer term study considering several variables in the CSTR. As may be noted in Figure 9.18, the steady-state cell concentration generally increased with increasing time (agitation rate), showing a concentration of 120 mg/L at 500 h and a value of nearly 500 mg/L at 2000 h. The cell concentration dropped slightly at the end of the study, probably due to the nutrient limitation. Thus, as expected, an increase in agitation rate

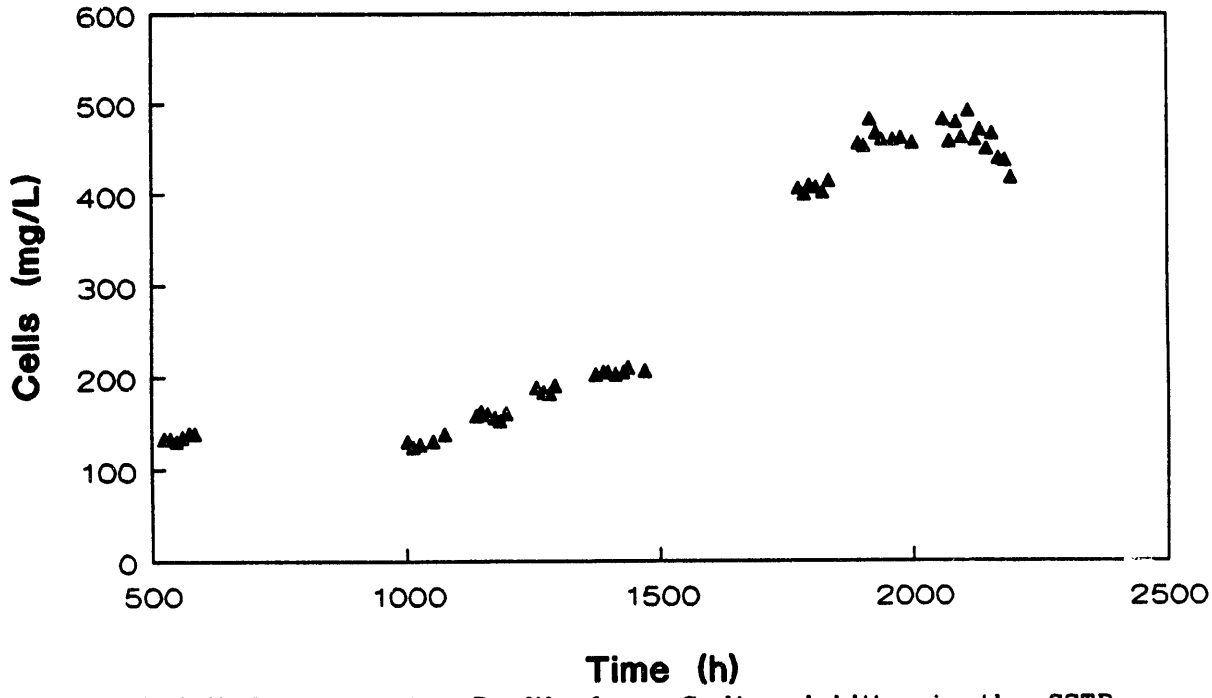

Figure 9.18 Cell Concentration Profile for *C. ljungdahlii* in the CSTR; (Gas Flow Rate: 0.02 - 0.15 mmol/min; Liquid Flow Rate: 200 mL/d; Agitation Rate 300 - 480 rpm)

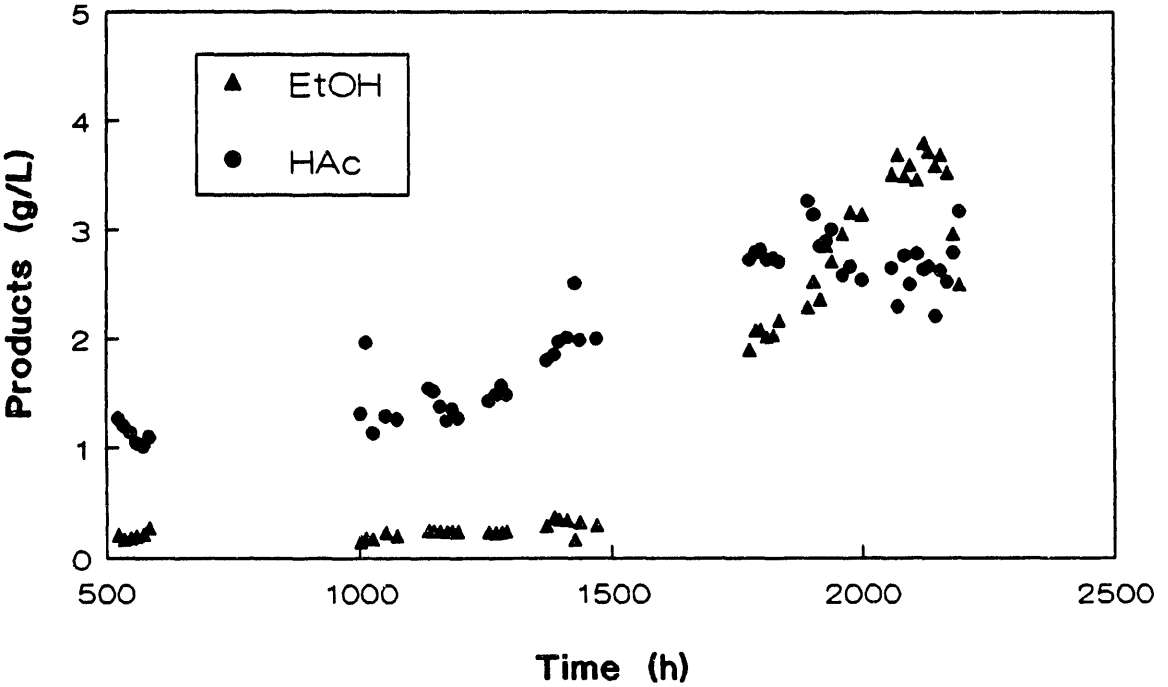

Figure 9.19 Product Concentration Profile for *C. ljungdahlii* in the CSTR; (Gas Flow Rate: 0.02 - 0.15 mmol/min; Liquid Flow Rate: 200 mL/d; Agitation Rate 300 - 480 rpm)

(shown with increasing time) brought about an increase in the steady state cell concentration through increased mass transfer. Figure 9.19 presents product (ethanol and acetate) concentration profiles for the same agitation rate study. The steady state ethanol concentrations were quite low until a time of 1500 h where the ethanol concentration increased dramatically with time. At a time of 2200 h (agitation rate of 460 rpm) the ethanol concentration was 3.6 g/L. The steady-state acetate concentrations increased steadily with time, up to a time of 1800 h. At this point the acetate concentration was nearly constant at 2.8 g/L.

The cell yield, $Y_{X/S}$, is shown as a function of time for the various agitation rates in Figure 9.20. As is noted, the yield remained essentially constant at about 0.2-0.25 mg cells/mol substrate. In fact, it was found that the cell yield was essentially unaffected by agitation rate over the range tested in the study. Figure 9.21 presents the product yield from substrate, $Y_{P/S}$, as a function of time for the agitation rates. As with the cell yield, the product yield was found to be essentially independent of liquid flow rate, having a value of approximately 0.4 mol of carbon in the products per mol of carbon in the substrate.

Finally, specific uptake rates in mmol CO/mg cells hr and specific productivities in mmol product/mg cells hr are shown in Figure 9.22 for the agitation rates. The specific uptake rate was found to vary from 0.01 to 0.03 mmol/mg h during the study. The specific productivity increased from 0.004 to 0.007 mmol/mg•h with increasing agitation rate.

A compilation of the CSTR data as a function of liquid flow rate is presented in Figures 9.23-9.25. Figure 9.23 shows the effects of agitation rate on cell density achieved in the CSTR. As is noted, the cell density

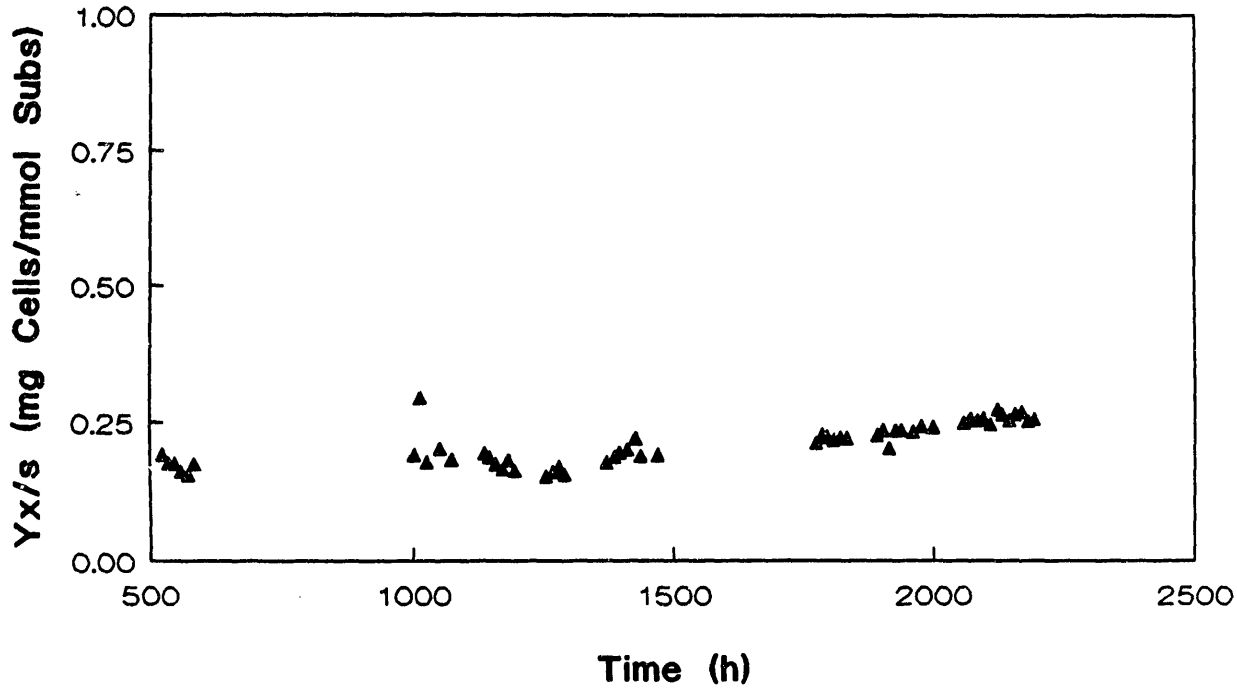

Figure 9.20 Cell Yield from Substrate for *C. ljungdahlii* in the CSTR; (Gas Flow Rate: 0.02 - 0.15 mmol/min; Liquid Flow Rate: 200 mL/d; Agitation Rate 300 - 480 rpm)

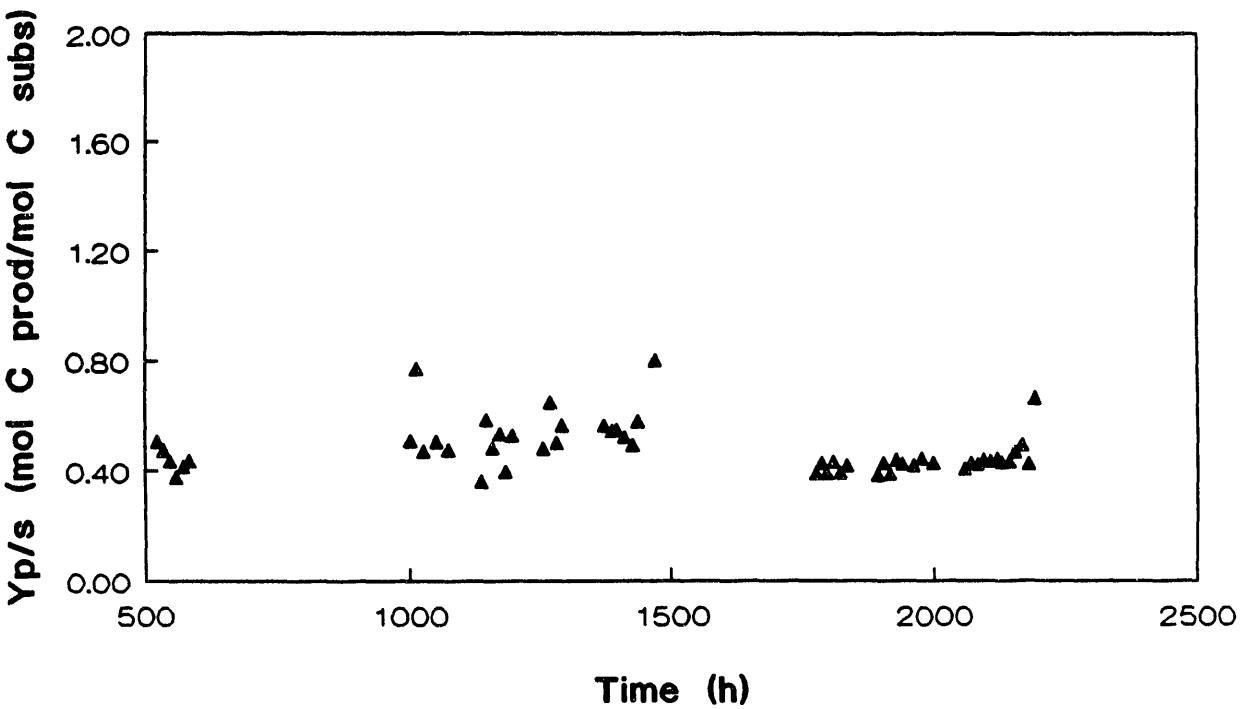

Figure 9.21 Product Yield from Substrate for *C. ljungdahlii* in the CSTR; (Gas Flow Rate: 0.02 - 0.15 mmol/min; Liquid Flow Rate: 200 mL/d; Agitation Rate 300 - 480 rpm)

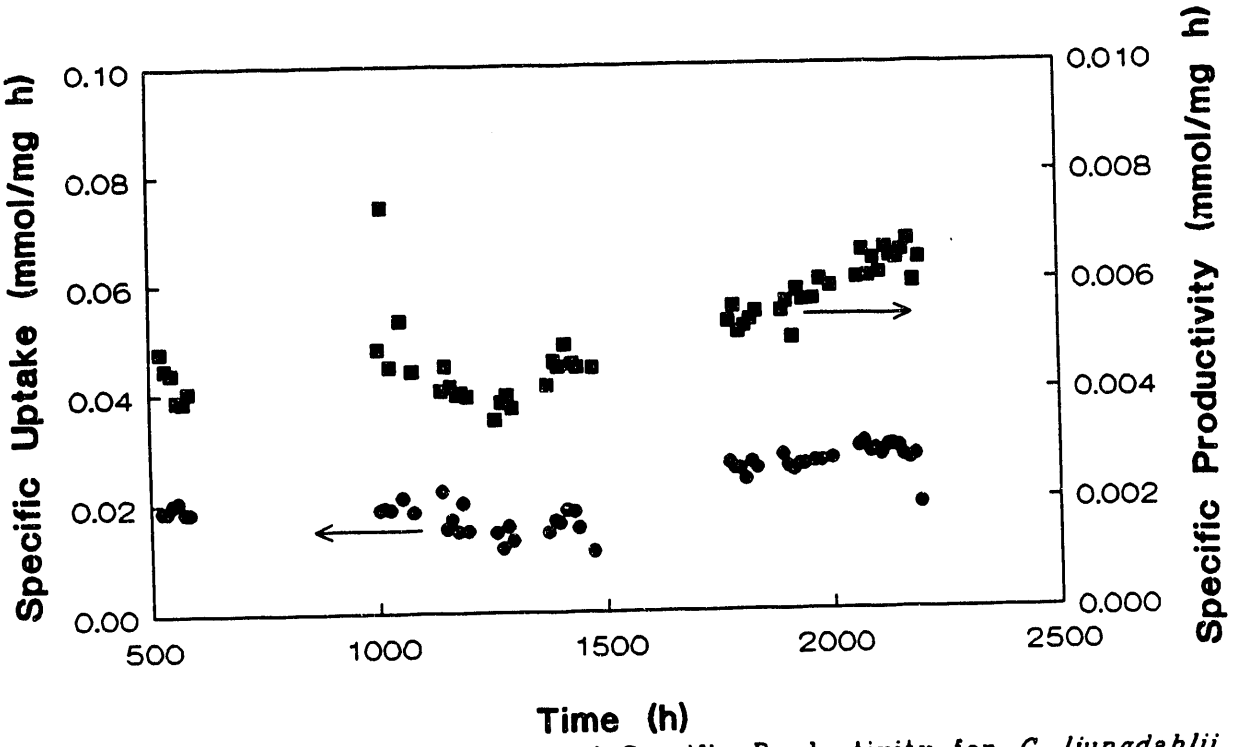

Figure 9.22 Specific Uptake Rate and Specific Productivity for *C. ljungdahlii* in the CSTR; (Gas Flow Rate: 0.02 - 0.15 mmol/min; Liquid Flow Rate: 200 mL/d; Agitation Rate 300 - 480 rpm)

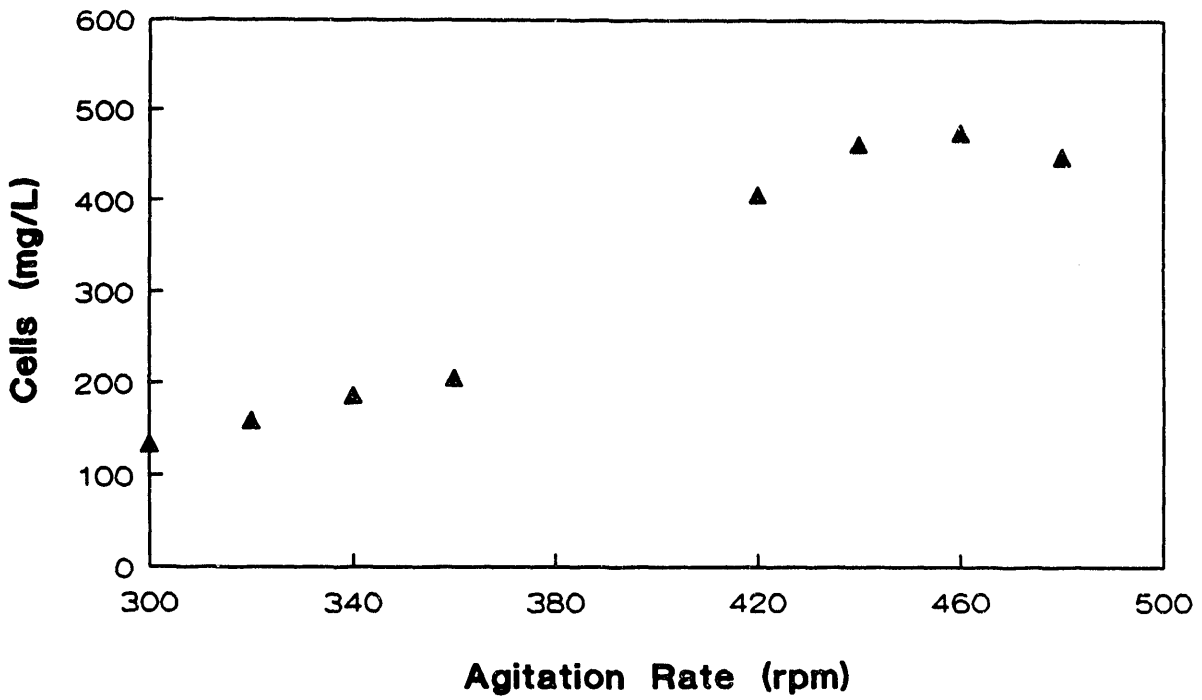

Figure 9.23 The Effects of Agitation Rate on Cell Concentration Using *C. ljungdahlii* in the CSTR.

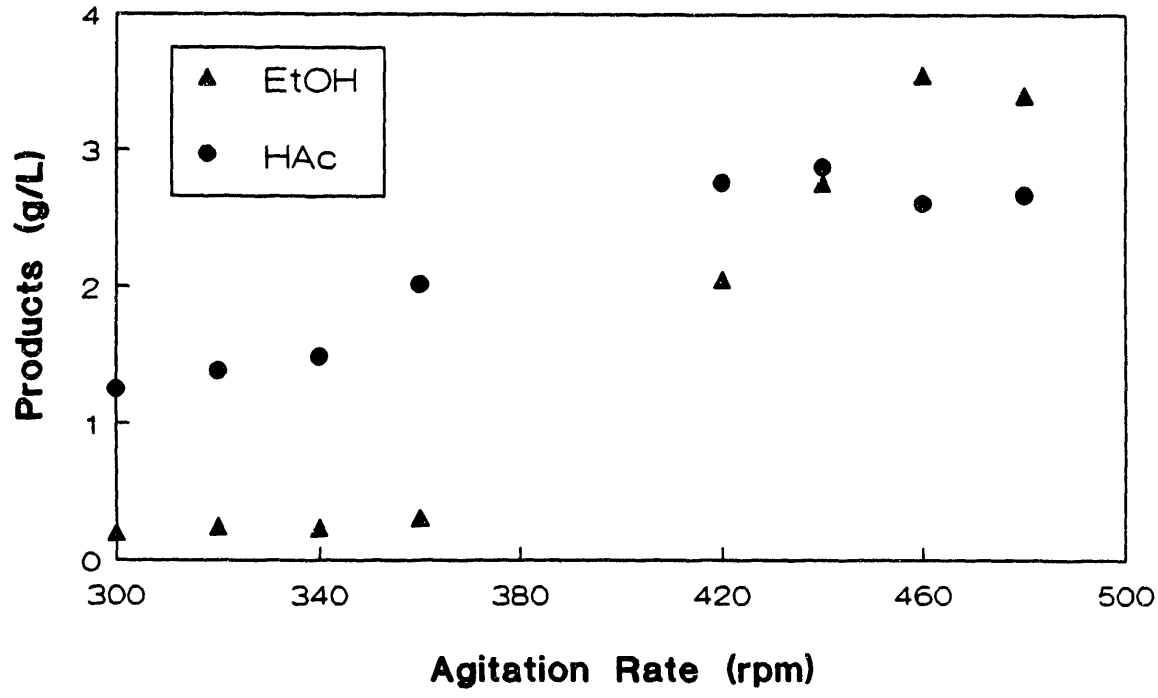

Figure 9.24 The Effects of Agitation Rate on Product Concentrations Using *C. ljungdahlii* in the CSTR.

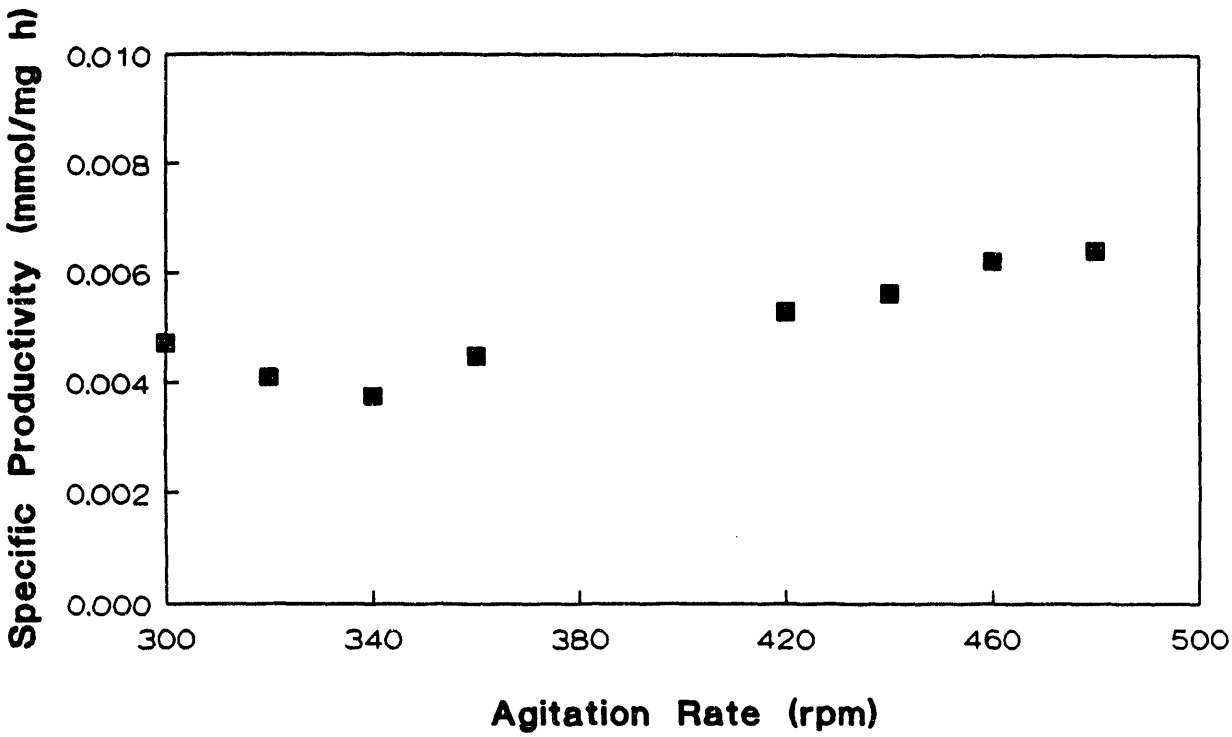

Figure 9.25 The Effects of Agitation Rate on Specific Productivity Using *C. ljungdahlii* in the CSTR.

increased along a rather gentle curve reaching a maximum of about 500 mg/L at agitation rates of 430 and above. The cell density fell slightly at an agitation rate of 480 rpm. This leveling off and decrease in cell density is undoubtedly due to a limitation of nutrients for growth. A richer nutrient mix should result in higher cell concentrations, but could, at the same time, result in acetate production in favor of ethanol.

Figure 9.24 shows the effects of agitation rate on the ethanol and acetate concentrations in g/L. A low agitation rates ($\leq$ 360 rpm), the ethanol concentration remained low at a level of approximately 0.2 g/L. The corresponding acetate concentration was seen to increase over this increasing agitation rate period, reaching a concentration of 2 g/L. It is quite possible that the agitation rate was not high enough to stress the culture with regard to dissolved CO concentration such that acetate production was favored over ethanol production.

At higher agitation rates ($\geq$ 420 rpm), the ethanol concentration increased with agitation rate while the acetate concentration remained nearly constant. At an agitation rate of 460 rpm, the ethanol concentration was nearly 3.5 g/L and the acetate concentration was about 2.5 g/L. When the agitation rate was increased to 480 rpm, the ethanol concentration fell slightly, probably due to nutrient limitation of the culture. As was noted earlier in Figure 9.23 the cell concentration at 480 rpm also decreased slightly from earlier levels.

It should be noted that the higher ethanol concentrations and product ratios occurred when the culture was near nutrient limitation as indicated by the constant cell concentration in Figure 9.23. This follows well with previously reported information stating that culture stress could be at least partially responsible for increased ethanol production.

The specific productivity (total product) is plotted as a function of agitation rate in Figure 9.25. Specific productivity gently increased with agitation rate, reaching a maximum of 0.0065 mmol product/mg•h, attained at an agitation rate of 480 rpm. The more CO available to the cells, the higher the productivity. The key to continuous operation appears to be a high productivity system with high ethanol concentrations and high ethanol to acetate product ratios. Future continuous reactor studies need to concentrate on this important aspect.

It was shown previously that higher agitation rates resulted in higher cell concentrations (up to 480 rpm), higher ethanol concentrations with essentially constant acetate concentrations and higher specific productivities. However, data were not available at agitation rates between 360 and 420 rpm. These data have now been obtained. The effects of agitation rate on cell concentration, products concentration, and specific productivity are shown, respectively, in Figures 9.26-9.28. These data are a compilation of data using procedures presented previously.

Figure 9.26 shows the effects of agitation rate on cell density achieved in the CSTR. As is noted, the cell density increased along a rather gentle curve, reaching a maximum of about 500 mg/L at agitation rates of 430 rpm and above. The cell density fell slightly at an agitation rate of 480 rpm indicating an increase in dissolved CO to inhibitory levels. This leveling off and decrease in cell density is undoubtedly due to a limitation of nutrients for growth. A richer nutrient mix should result in higher cell concentrations, but could, at the same time, result in acetate production in favor of ethanol.

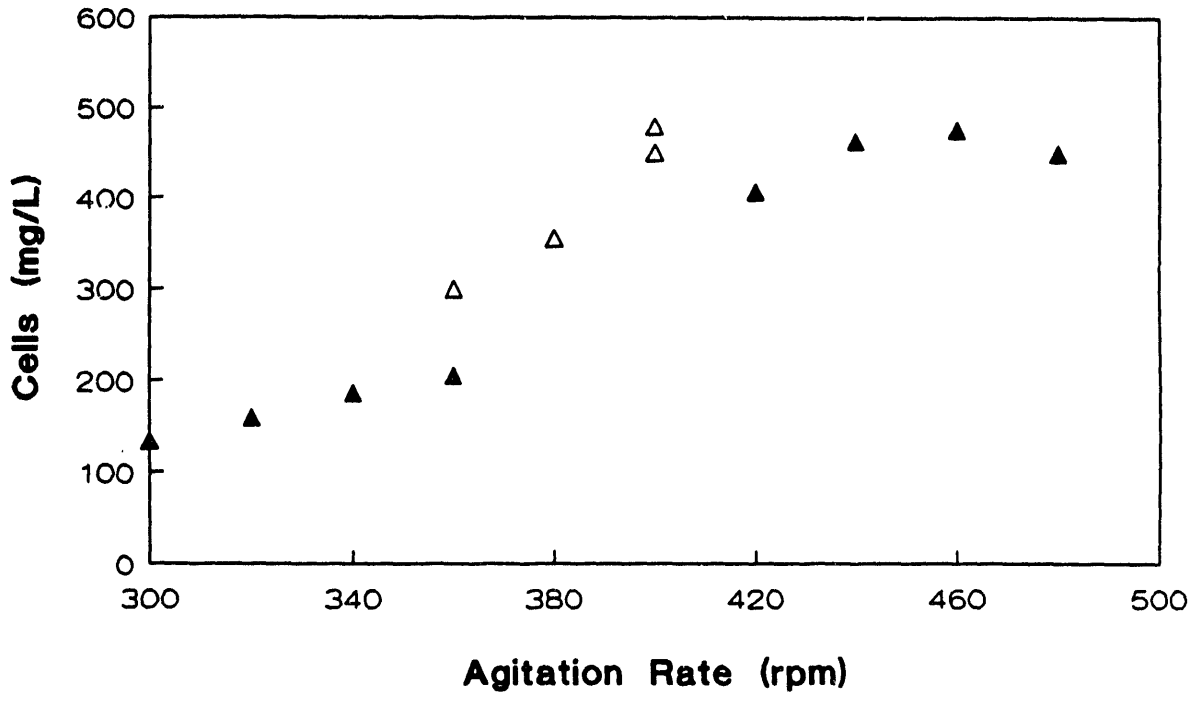

Figure 9.26 The Effects of Agitation Rate on Cell Concentration Using *C. ljungdahlii* in the CSTR.

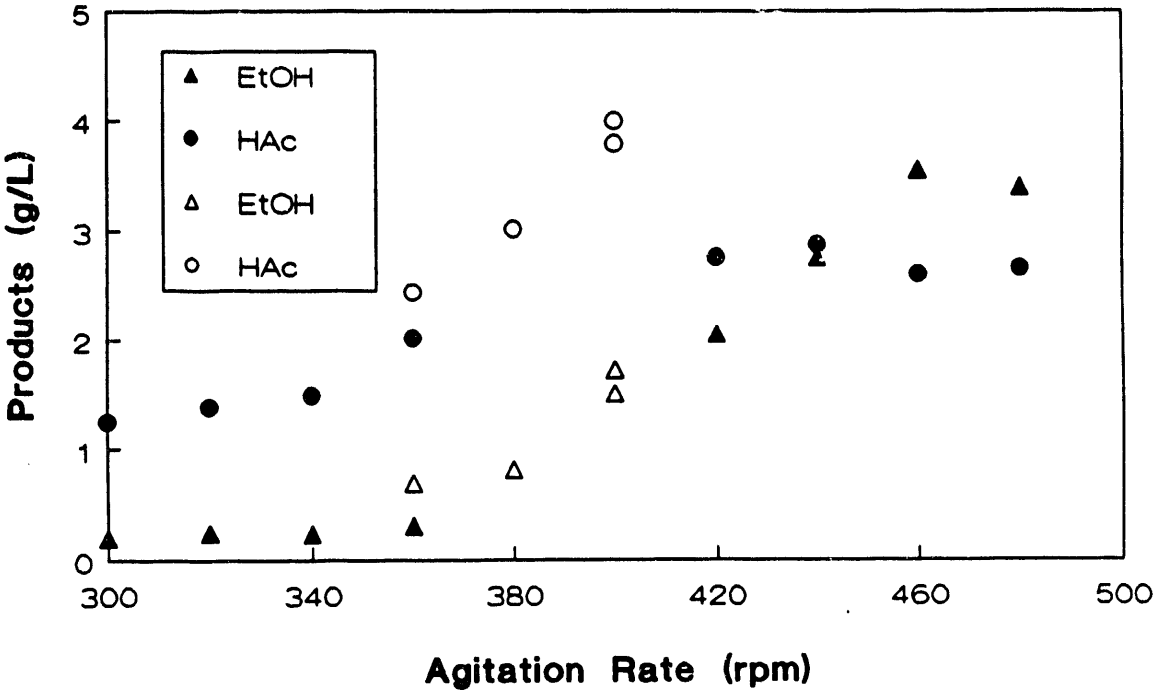

Figure 9.27 The Effects of Agitation Rate on Product Concentrations Using *C. ljungdahlii* in the CSTR.

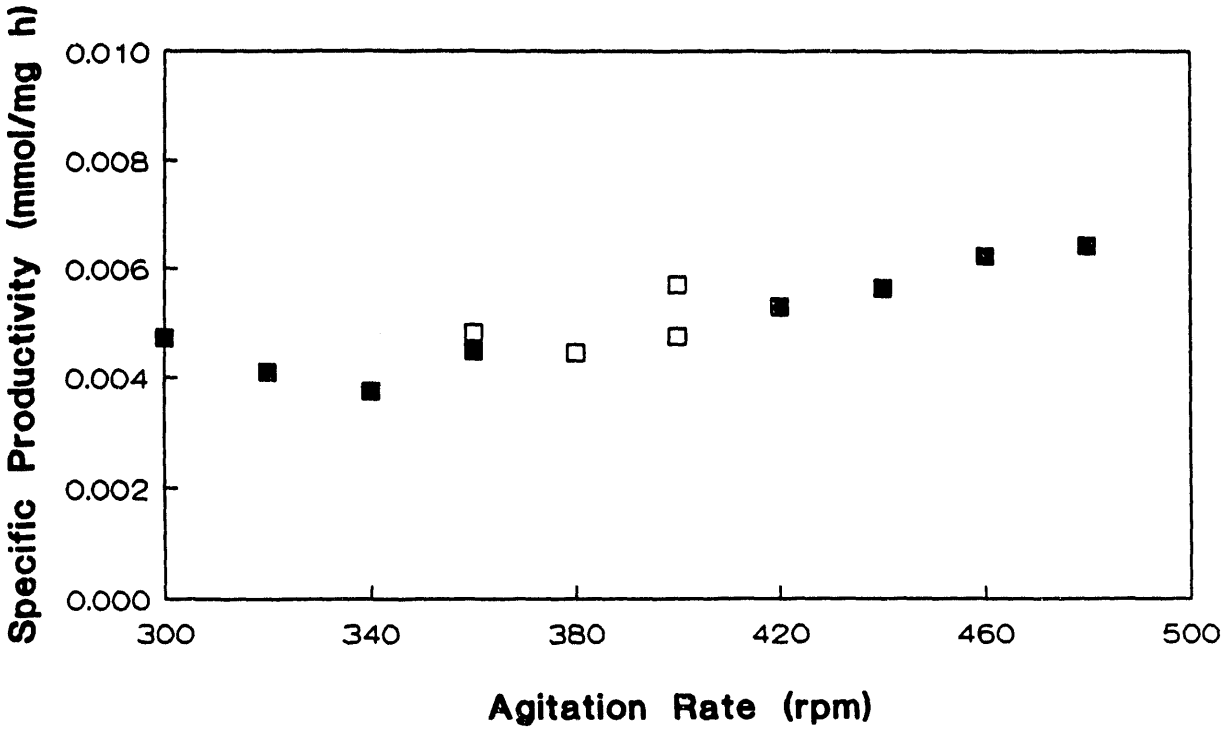

Figure 9.28 The Effects of Agitation Rate on Specific Productivity Using *C. ljungdahlii* in the CSTR.

Figure 9.27 shows the effects of agitation rate on the ethanol and acetate concentrations in g/L. At low agitation rates (≤ 360 rpm), the ethanol concentration remained low at a level of approximately 0.2 g/L. The corresponding acetate concentration was seen to increase over this increasing agitation rate period, reaching a concentration of 2 g/L. It is quite possible that the agitation rate was not high enough to stress the culture with regard to dissolved CO concentration such that acetate production was favored over ethanol production.

A higher agitation rates (≥ 420 rpm), the ethanol concentration increased with agitation rate while the acetate concentration remained nearly constant. At an agitation rate of 460 rpm, the ethanol concentration was nearly 3.5 g/L and the acetate concentration was about 2.5 g/L. When the agitation rate was increased to 480 rpm, the ethanol concentration fell slightly, probably due to nutrient limitation of the culture. As was noted earlier in Figure 9.26, the cell concentration at 480 rpm also decreased slightly from earlier levels.

It should be noted that the higher ethanol concentrations and product ratios occurred when the culture was near nutrient limitation and substrate mass transfer exceeded that required for growth as indicated by the constant cell concentration in Figure 9.26. This follows well with previously reported information stating that culture stress could be at least partially responsible for increased ethanol production.

The specific productivity (total product) is plotted as a function of agitation rate in Figure 9.28. Specific productivity gently increased with agitation rate, reaching a maximum of 0.0065 mmol product/mg•h, attained at an agitation rate of 480 rpm. The more CO available to the cells, the higher the productivity. The key to continuous operation appears to be a high

productivity system with high ethanol concentrations and high ethanol to acetate product ratios. Future continuous reactor studies need to concentrate on this important aspect.

9.2.3 Gas Flow Rate Effects

The effects of inlet gas flow rate on the performance of *C. ljungdahlii* in the CSTR were also studied. In this study, the agitation rate was held constant at 400 rpm, the liquid flow rate was 190 mL/d and the temperature was held constant at 35°C. Figures 9.29-9.31 show the effects of gas flow rate on cell concentration, product (ethanol and acetate) concentrations and the total specific productivity. As is noted in Figure 9.29, the cell concentration increased by almost 30 percent as the flow rate was increased from 0.05 to 0.075 mmol/min. At higher flow rates, the cell concentration leveled off at about 400 mg/L. This latter result is not expected since the cell concentrations should have increased with gas flow rate unless the system was mass transfer limited or the culture was nutrient limited. It is believed that the culture was probably nutrient limited since the conversion of CO was not complete and the nutrient medium employed was poor.

Figure 9.30 shows the effects of gas flow rate on ethanol and acetate concentration. At low flow rates (0.05-0.10 mmol/min), high acetate concentrations and low ethanol concentrations were observed. As the gas flow rate was increased, the acetate concentration nearly leveled off at about 3 g/L while the ethanol concentration increased from 1 to 1.5 g/L. This increase in ethanol concentration was probably due to nutrient limitations coupled with increased gas flow rate. As is noted in Figure 9.31, the specific productivity remained essentially constant at 0.004 mmol/mg h.

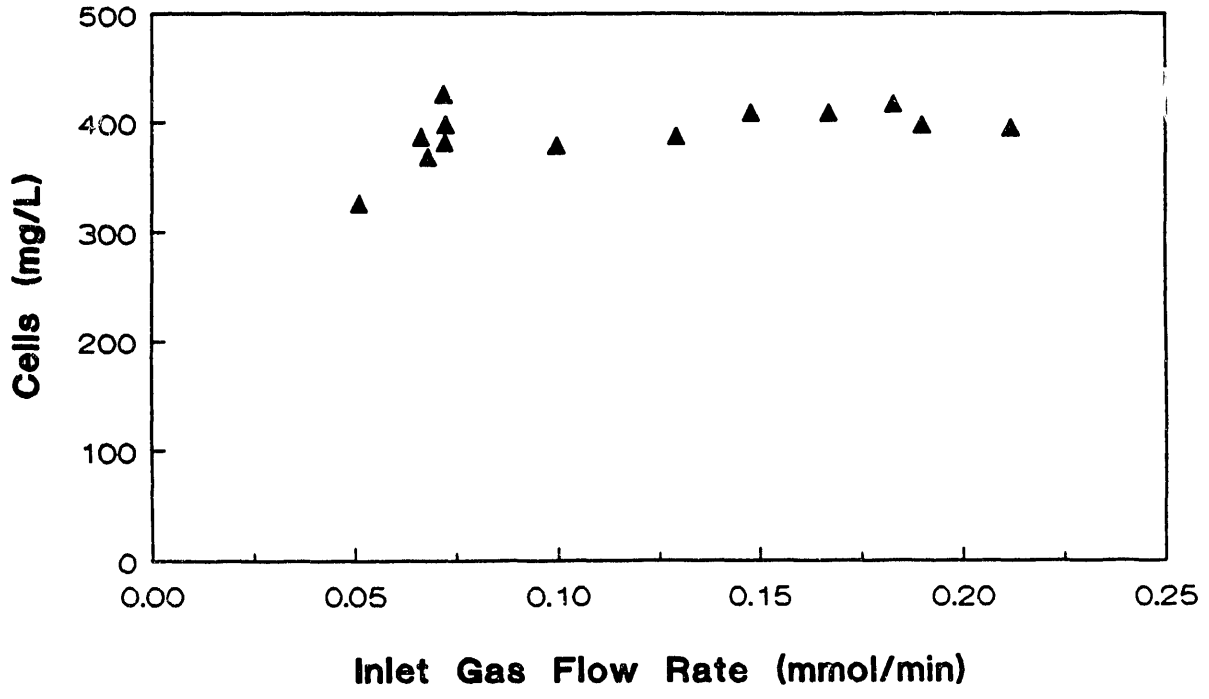

Figure 9.29 The Effects of Gas Flow Rate on Cell Concentration Using *C. ljungdahlii* in the CSTR.

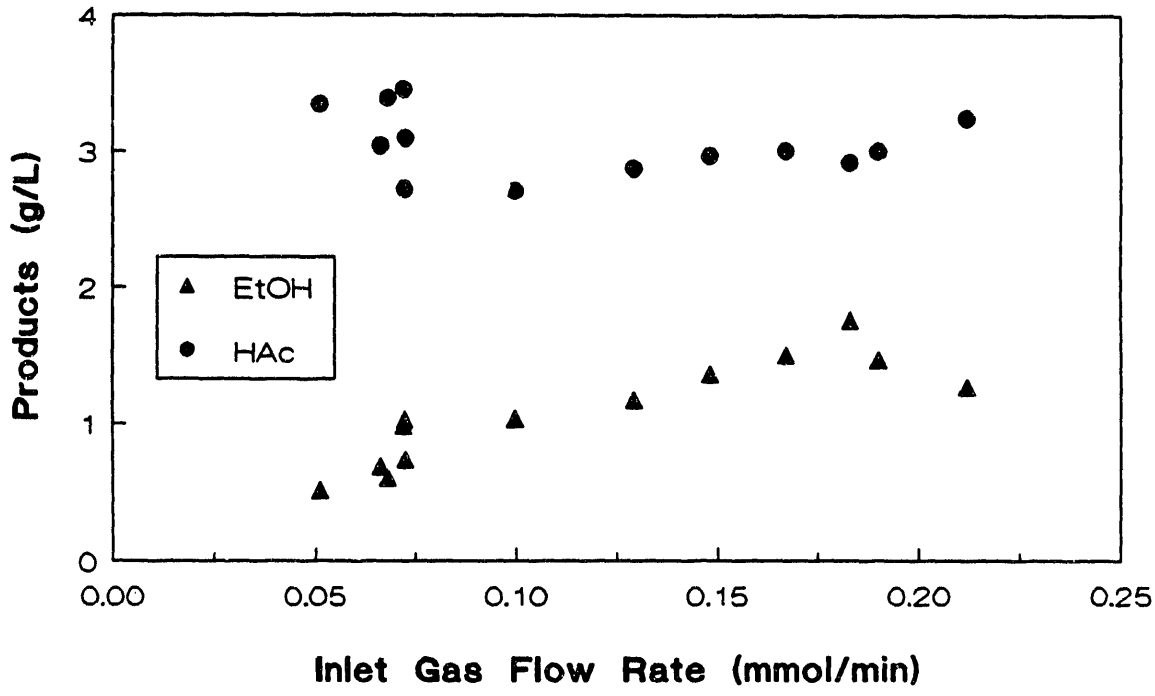

Figure 9.30 The Effects of Gas Flow Rate on Product Concentrations Using *C. ljungdahlii* in the CSTR.

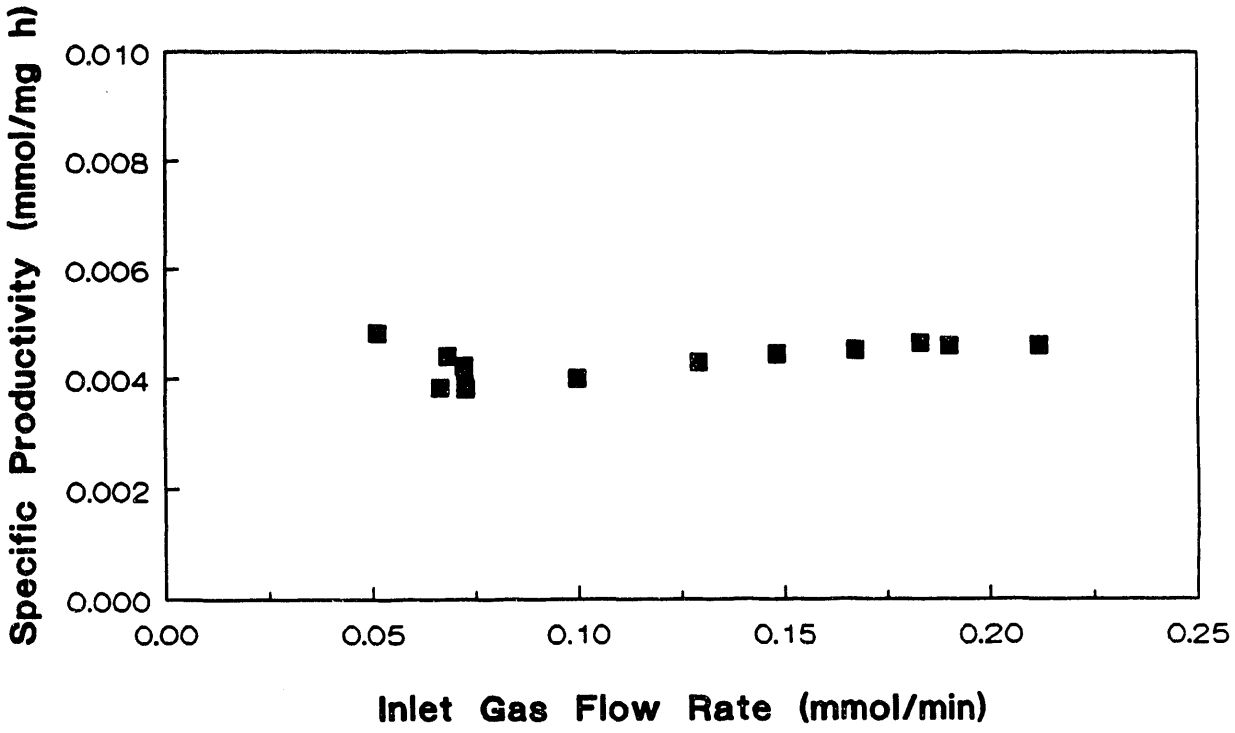

Figure 9.31 The Effects of Gas Flow Rate on Specific Productivity Using *C. ljungdahlii* in the CSTR.

9.2.4 Performance Studies in the CSTR with Designed Medium

Growth, production and the specific production rate in the CSTR are shown for basal medium (Figures 9.32-9.34) and for the designed medium (Figures 9.35-9.37). Growth on the designed medium, while falling well short of the 3.0 grams of cells expected for nitrogen limitation, was 4 to 5 times the level achieved in basal medium (See Figures 9.32 and 9.35). The maximum cell concentration is basal medium was 400 mg/L, and the maximum in the designed medium was 1500 mg/L. The product concentrations in the CSTR (see Figures 9.33 and 9.36) for the designed medium were 5.5 times the concentrations in basal medium on a mass basis and 6.5 times the concentrations on a molar basis. The maximum ethanol concentration in basal medium was about 1.5 g/L and the maximum concentration in the designed medium was about 22 g/L. The product ratio was also dramatically shifted toward ethanol, showing much more ethanol than acetate with the designed medium. The specific production rates calculated for both media were identical (see Figures 9.34 and 9.37). However, if the cell density given for the designed medium is low as suspected, the specific production rate in the designed medium is about 20 percent lower than in basal medium. The dilution rates and thus the specific growth rates in these experiments were 0.024 h^{-1} in basal medium and 0.014 in the designed medium (1.75 and 2.92 days retention time, respectively). The comparison of the media on a gross performance basis is nonetheless valid. Ethanol has been found to be inhibitory at 20 g/L in initial growth experiments with *C. ljungdahlii*. Such inhibition could be manifested as reduced performance in specific growth and production rates in the designed medium.

The design of the medium based on *E. coli* was very successful despite the difference in the model organism in comparison to *C. ljungdahlii*. Culture

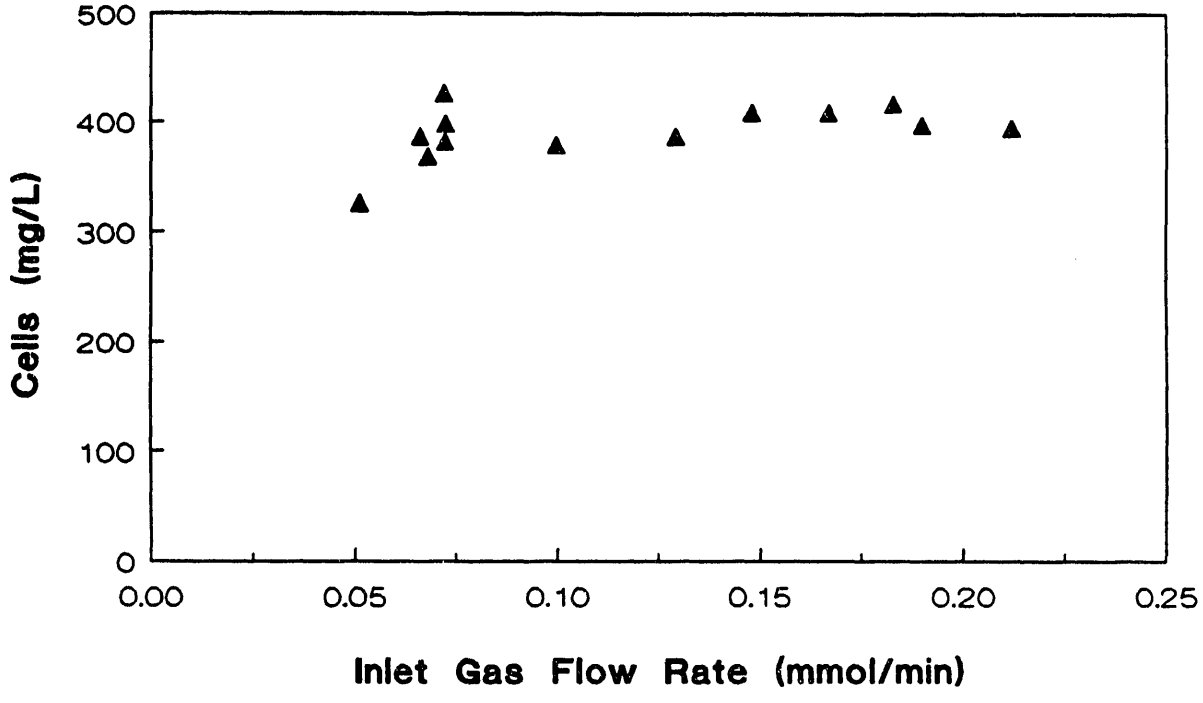

Figure 9.32 Cell Concentration of *C. ljungdahlii* Grown in Basal medium in the CSTR.

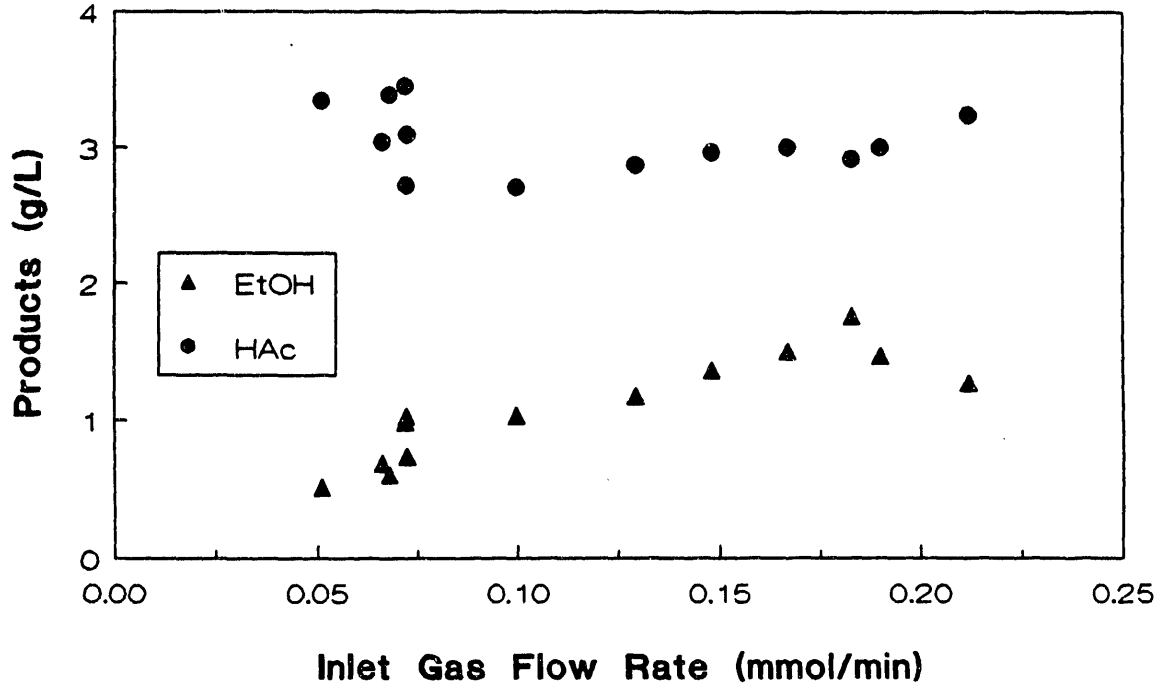

Figure 9.33 Product Concentrations from growth of *C. ljungdahlii* in Basal Medium in the CSTR.

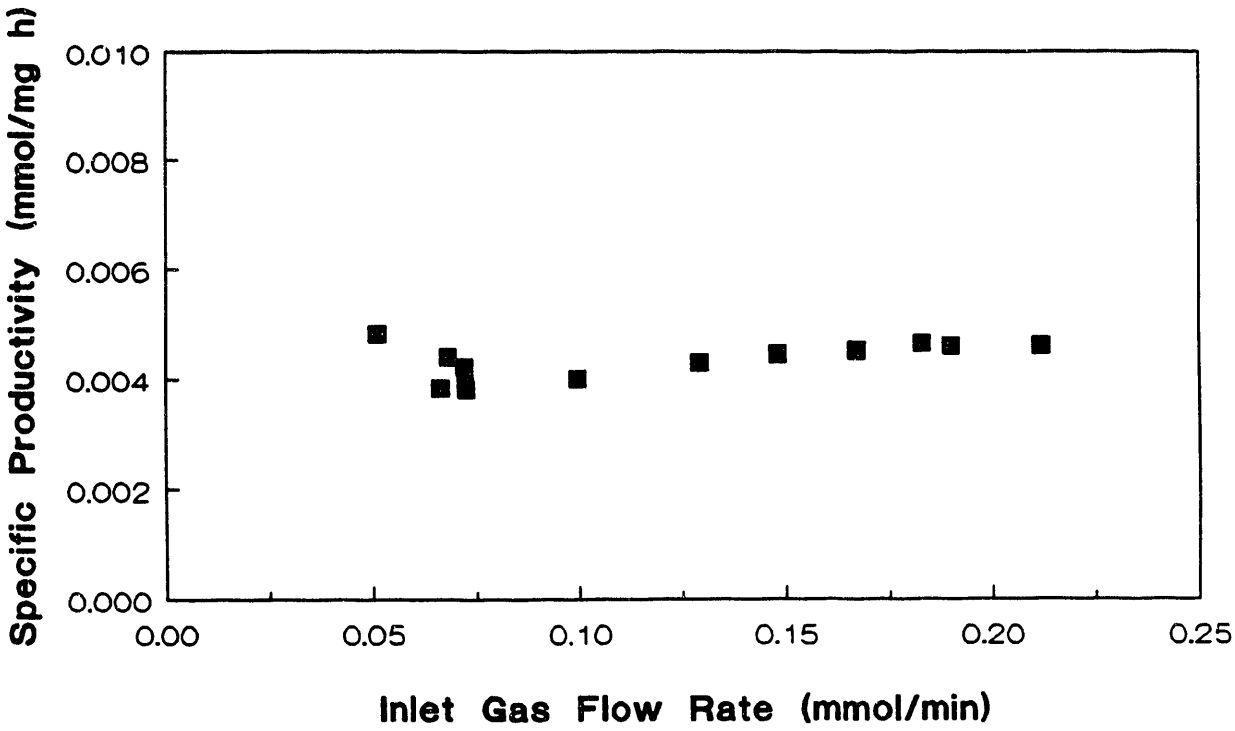

Figure 9.34 Specific Productivity of *C. ljungdahlii* Grown in Basal Medium in the CSTR.

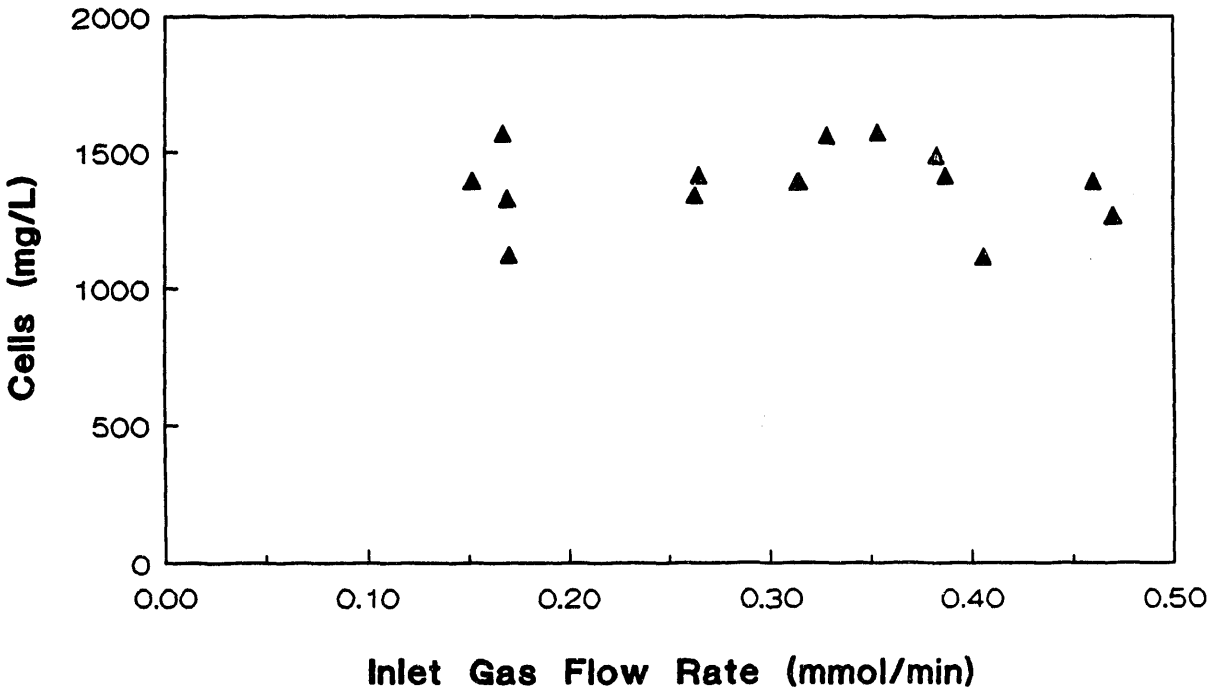

Figure 9.35 Cell Concentration of *C. ljungdahlii* Grown in Designed mediu in the CSTR.

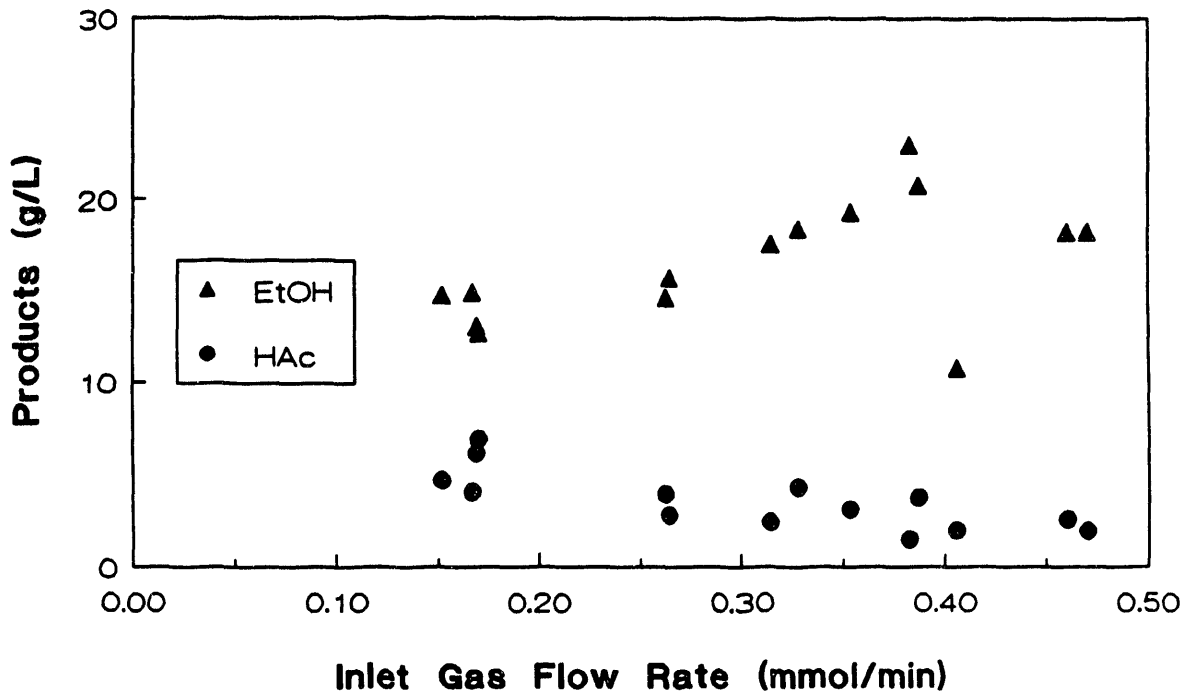

Figure 9.36 Product Concentrations from growth of *C. ljungdahlii* in Designed Medium in the CSTR.

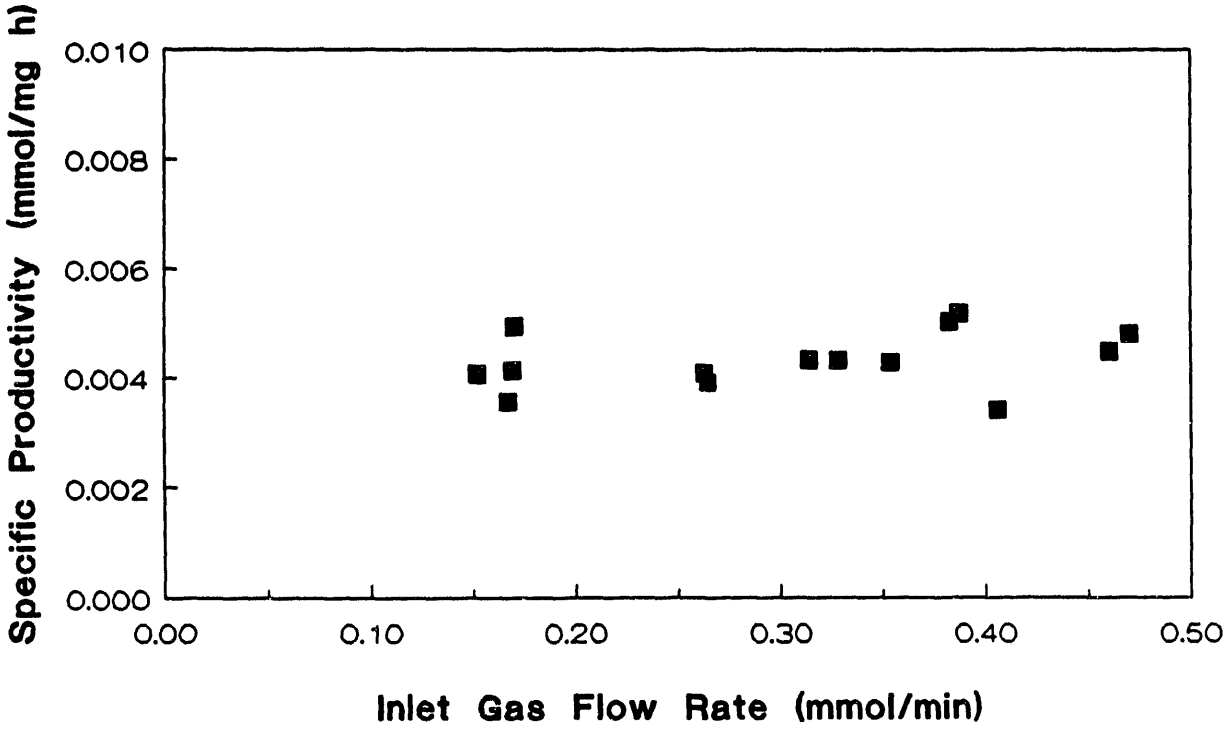

Figure 9.37 Specific Productivity of *C. ljungdahlii* Grown in Designed Medium in the CSTR.

performance should improve further if the medium design can be based on an analysis of *C. ljungdahlii*. Nutrient limitation studies, using an approximation of the basal medium with a specific nutrient concentration reduced, were used to determine minimum requirements of each element in the *E. coli* analysis.

As an example, a summary of the results of the potassium study is shown in Figures 9.38-9.41. Figure 9.38 shows growth limitation from potassium concentration, in basal medium, below 20 mg/L KCl. The maximum production accompanying this growth (Figure 9.39) appears to be relatively insensitive to potassium concentration. The specific growth and production rates (Figures 9.40 and 9.41) increase slightly as the potassium concentration is decreased to 10 mg/L KCl. This study shows a maximum of 71.8 g of cells per g KCl and an optimum concentration of potassium near 10 mg/L KCl. This implies that potassium is about 0.7 percent of the dry weight of *C. ljungdahlii* cells.

A similar study was performed for each of the major elements in the defined basal medium. The results of these studies are summarized in Table 9.1 as an approximate elemental analysis of *C. ljungdahlii*. This analysis will now be used to adjust the production medium for further study.

9.2.5 Arginine Addition to the Medium to Decrease Start-Up Time

Doyle[71] showed that *C. ljungdahlii* utilizes arginine from the peptone/amino acid pool as its primary carbon and energy source. It was thus felt that arginine could possibly stimulate the growth of *C. ljungdahlii*, thereby shortening the time necessary for the start-up of a CSTR fermentation system. The possible negative effects of utilizing aginine such as decreased ability to utilize CO and H_2, increased lag phases upon the addition of CO and H_2, etc. also need to be investigated.

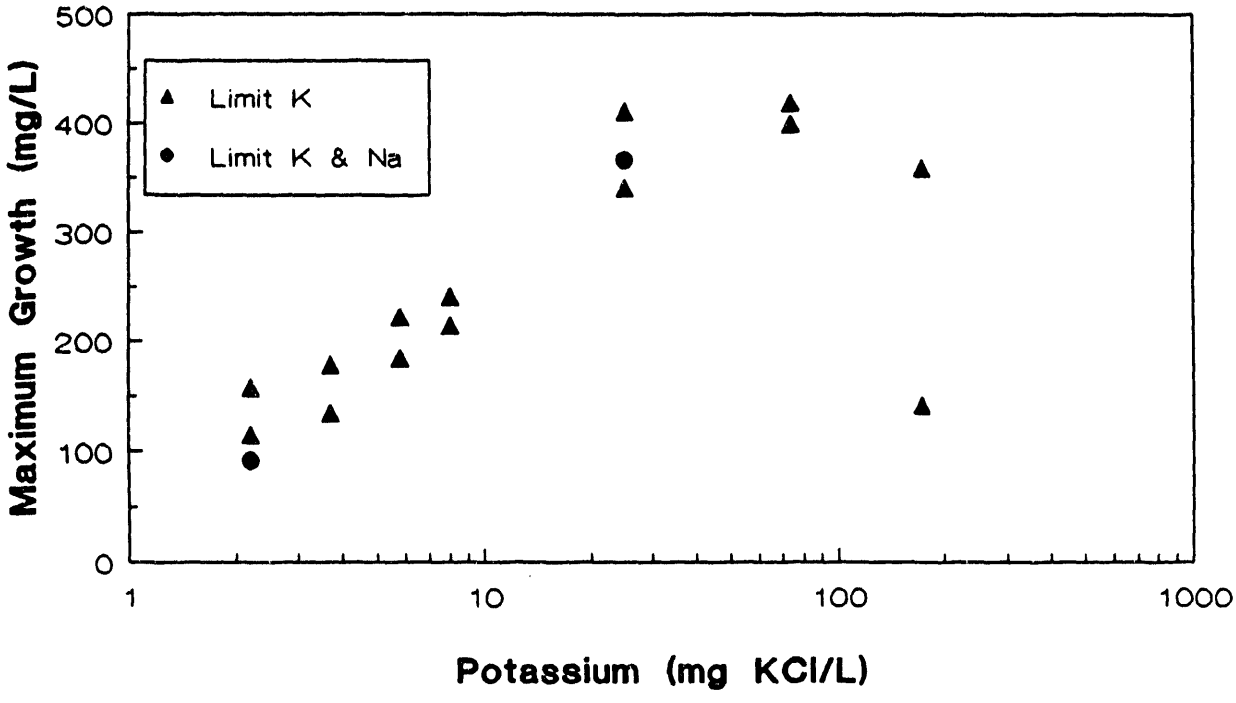

Figure 9.38 Maximum Cell Concentration of *C. ljungdahlii* Grown Under Potassium Limitation in Batch Culture.

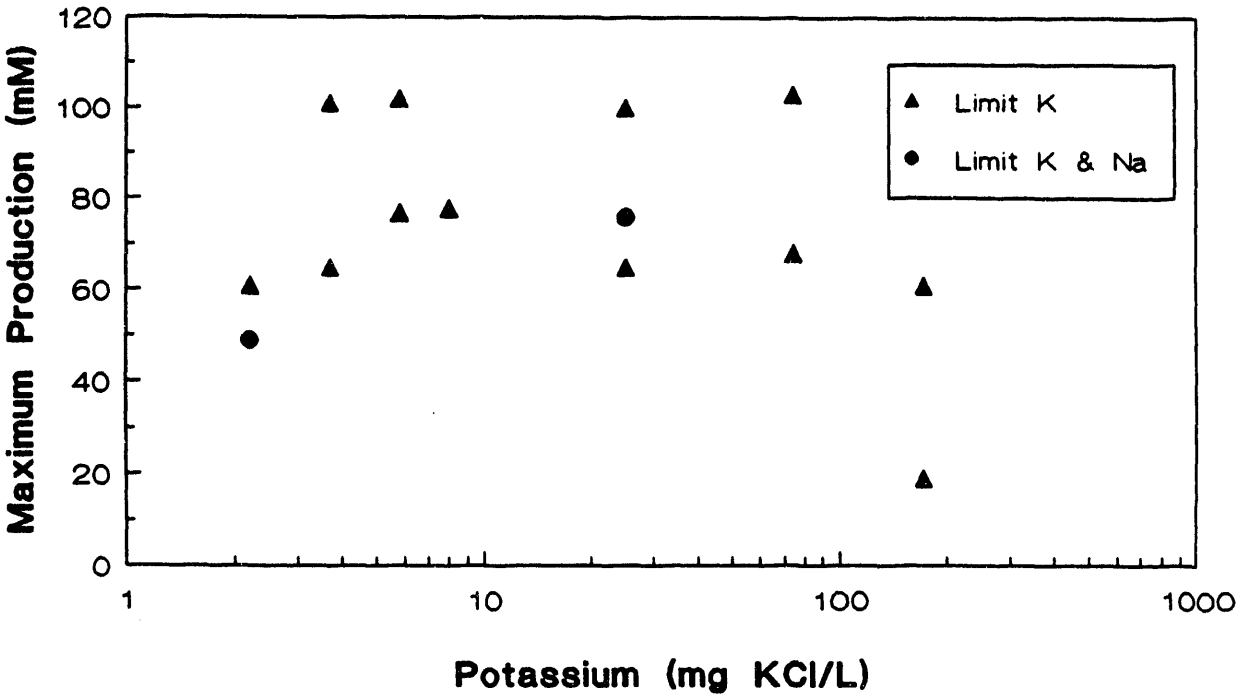

Figure 9.39 Maximum Product Concentration from *C. ljungdahlii* Grown Under Potassium Limitation in Batch Culture.

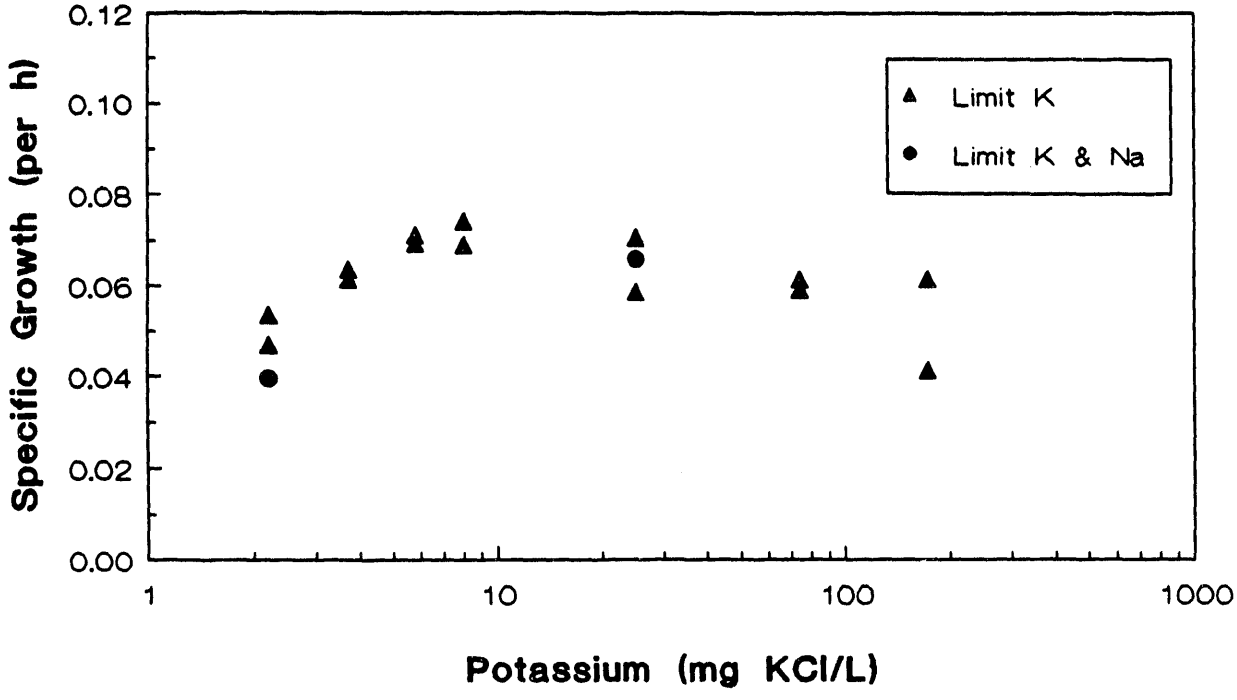

Figure 9.40 Specific Growth Rate of *C. ljungdahlii* Grown Under Potassium Limitation in Batch Culture.

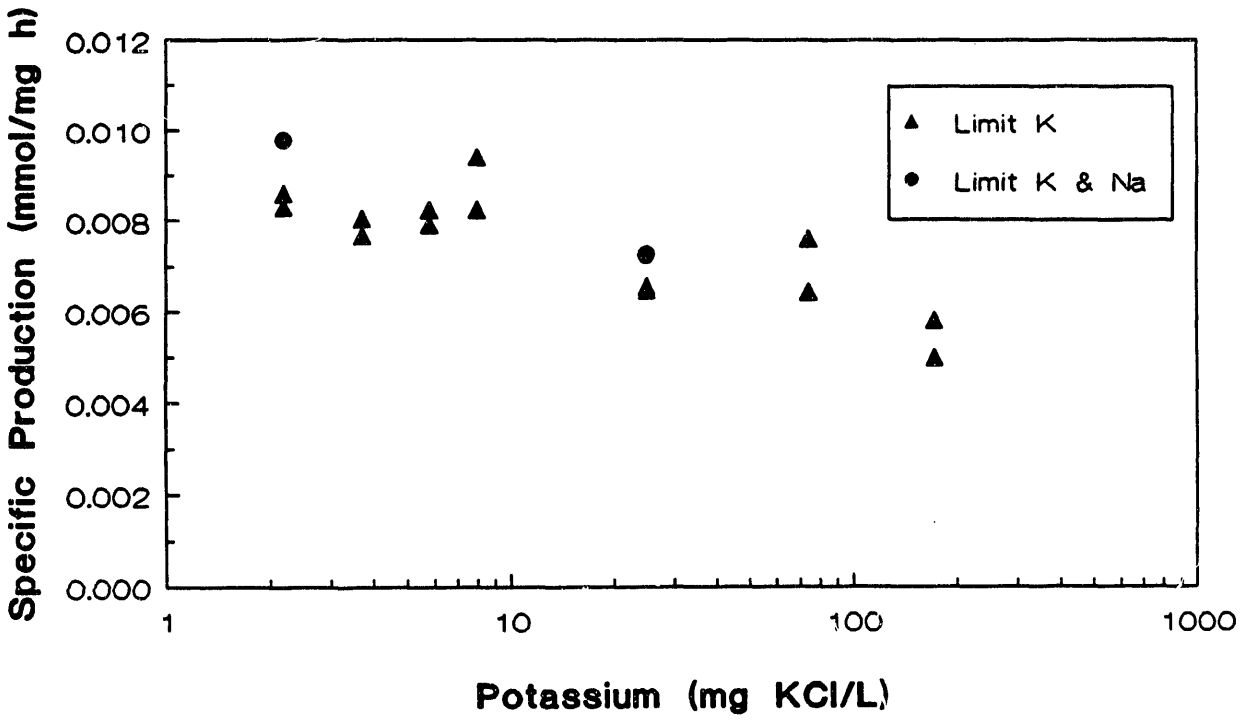

Figure 9.41 Specific Production Rate for *C. ljungdahlii* Grown Under Potassium Limitation in Batch Culture.

Elemental Composition of Bacteria

Percent of Dry Weight

	E. coli	*C. ljungdahlii*
Nitrogen	14.0	14.0
Phosphorus	3.0	1.2
Sulfur	1.0	1.2
Potassium	1.0	0.7
Sodium	1.0	<0.37
Calcium	0.5	<0.03
Magnesium	0.5	<0.086
Chlorine	0.5	*
Iron	0.2	0.097

Analysis of E. coli from J.E. Bailey and D.F. Ollis, "Biochemical Engineering Fundamentals" 2nd ed., McGraw Hill, 1986, Table 2.1 on p.28.

* Chlorine requirements were not determined; Chloride was used to balance ioni

Table 9.1 Bacterial Composition

A small quantity of arginine (10 mg/L) was added to the fermentation medium and fed to a CSTR. The pH of the system was 5.0 and the temperature was 35-37°C. The medium flow rate was held constant at about 180 mL/day, and the gas flow rate was fed at a very low level.

Figures 9.42-9.44 show the results of this experiment as cell concentration measurements, CO and H_2 conversions and product concentration measurements with time. As is noted in Figure 9.42, the cell concentration remained essentially constant at 300 mg/L during arginine addition. The quantity of arginine fed was not enough to support good growth but, as will be shown later, was enough to inhibit CO and H_2 uptake. At a time of 236 hr, the arginine flow was stopped. The cell concentration immediately increased to a concentration exceeding 800 mg/L. The phenomenon shown in Figure 9.42 is the phenomenon of diauxic growth, whereby the preferred substrate (arginine) is utilized entirely prior to secondary substrate (CO and H_2) utilization. One very interesting and important observation related to growth but not shown in Figure 9.42 is the rapid start-up achieved with arginine addition. CSTR start-up with arginine was immediate; start-up with CO, H_2 and basal medium alone often takes up to a week.

Figure 9.43 shows the substrate (CO and H_2) utilization in the CSTR with time. During arginine addition, the CO conversion was about 40 percent and the H_2 conversion was 0-5 percent. After arginine addition, both the CO and H_2 conversions increased to 70-80 percent. Again, this further illustrates the concept of diauxic growth, although a small amount of CO was used during arginine addition.

Figure 9.44 shows the product (ethanol and acetate) concentrations in the CSTR with time. During arginine addition, both product concentrations were

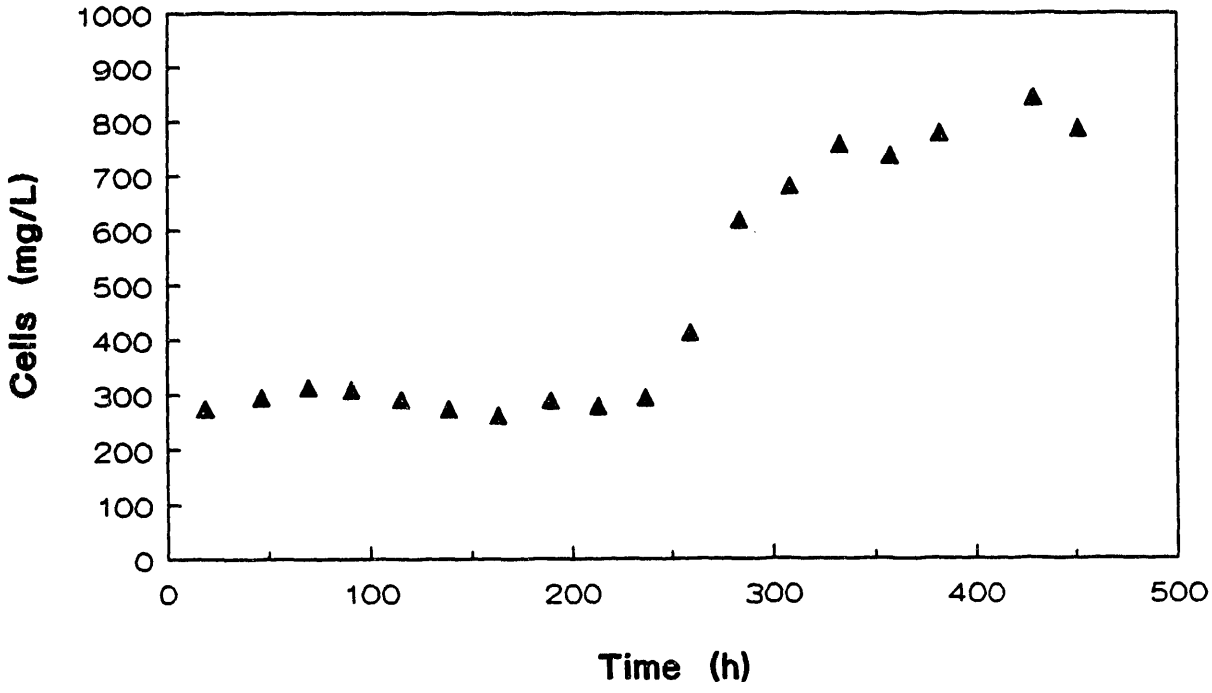

Figure 9.42 Cell Concentration Measurements in the CSTR for *C. ljungdahlii* with Arginine Addition.

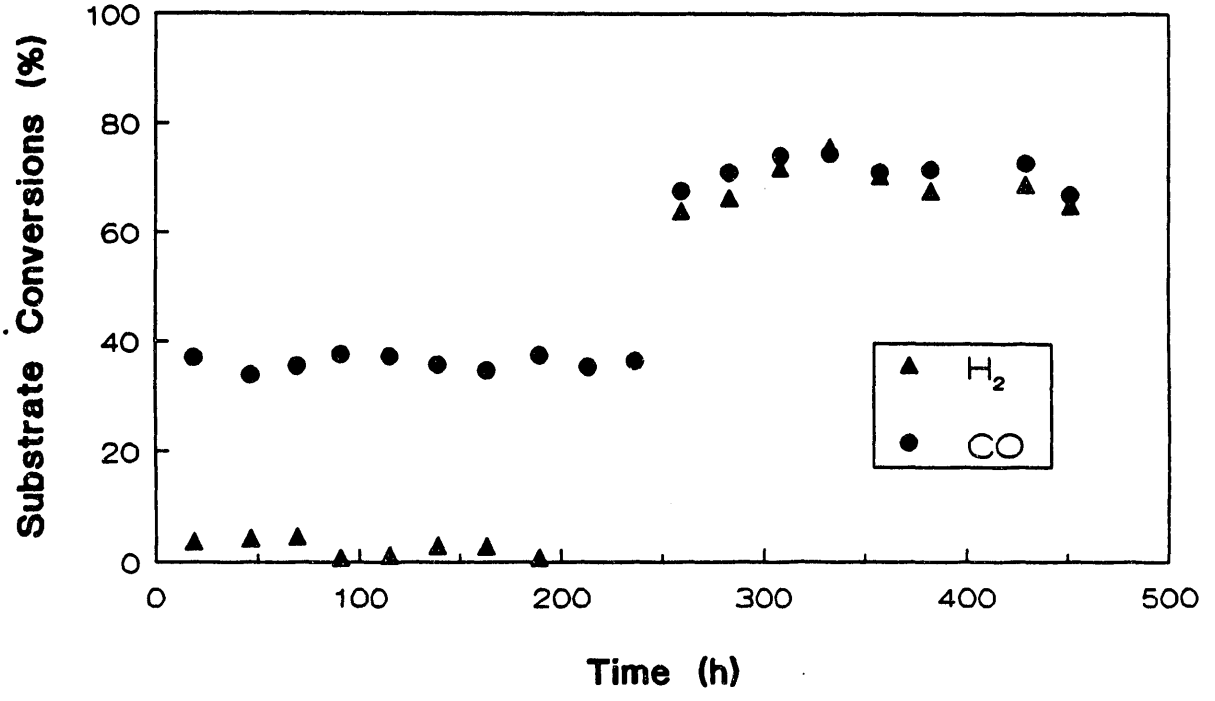

Figure 9.43 Substrate Conversion in the CSTR for *C. ljungdahlii* with Arginine Addition.

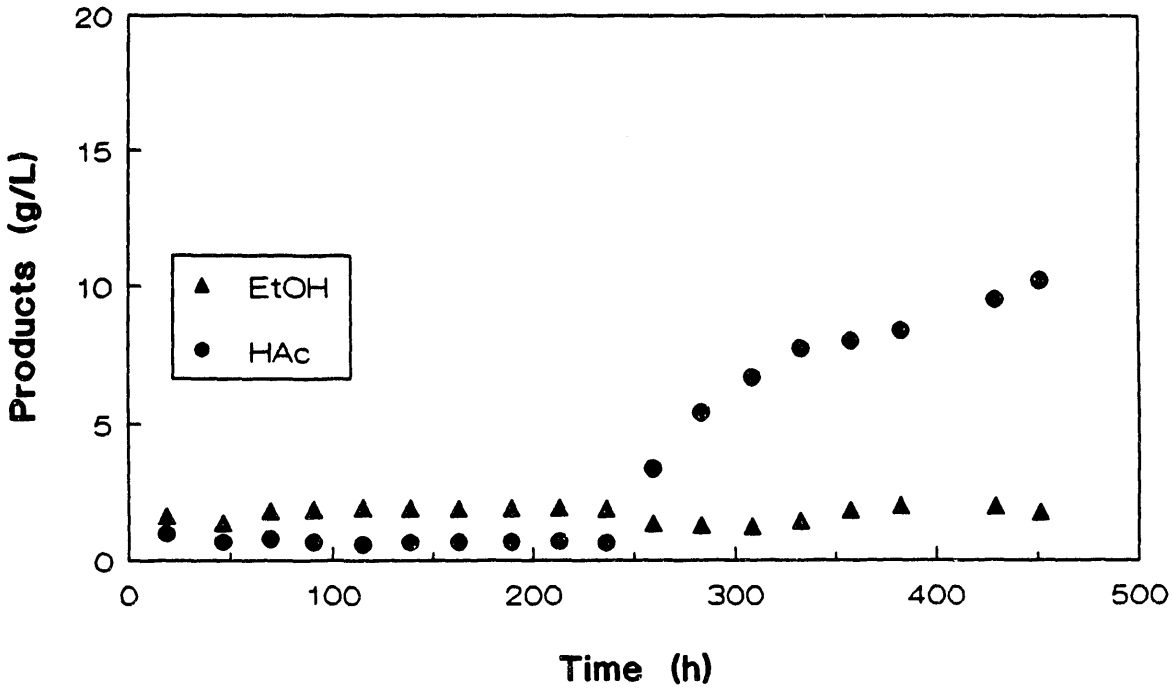

Figure 9.44 Product Concentrations Measurements in the CSTR for *C. ljungdahlii* with Arginine Addition.

very low (1-2 g/L). After arginine addition stopped, acetate production dominated ethanol production, with up to 10 g/L acetate and 2 g/L ethanol. It is expected that increased operation time will reverse the product concentrations trend. However, arginine addition may negatively affect product formation (more acetate than ethanol), which may be its major negative feature.

Figures 9.45 and 9.46 show the product yields and specific productivity of the system, respectively, with time. The yield of product from cells, Yp/x, increased only slightly (and probably not significantly) after arginine addition had stopped. The product yield was essentially constant at 0.20 mmol total product/mg cells, a level obtained in earlier CSTR experiments. The specific productivity was also nearly constant (a slightly increased trend) at 0.004-0.005 mmol/mg h, also a level attained previously. Thus, arginine addition did not affect product yield or specific productivity.

9.2.6 Analysis of the Results of CSTR Studies Employing *C. ljungdahlii*

A large number of CSTR studies have been performed with *C. ljungdahlii* in studying the effects of agitation rate, gas flow rate, liquid rate and other variables on culture performance. Steady-state results from these studies, as well as calculated yields, productivities and rates, are presented in Table 9.2. As is noted in the table, these experiments yielded results which gave both high and low ethanol concentrations, high and low cell densities and high and low ethanol to acetate product ratios (E/A).

CO and H_2 uptake rates in these studies ranged from 0.001 - 0.157 mmol/min. In general, the specific uptake rates for CO were approximately 3 times the values for H_2. The specific production rates ranged from 0.0014 - 0.0081 mol/g hr and the specific uptake rates ranged from 0.0075 - 0.0330 mol/g hr. The ethanol to acetate ratio (E/A) ranged from 0.28-20 mol/mol.

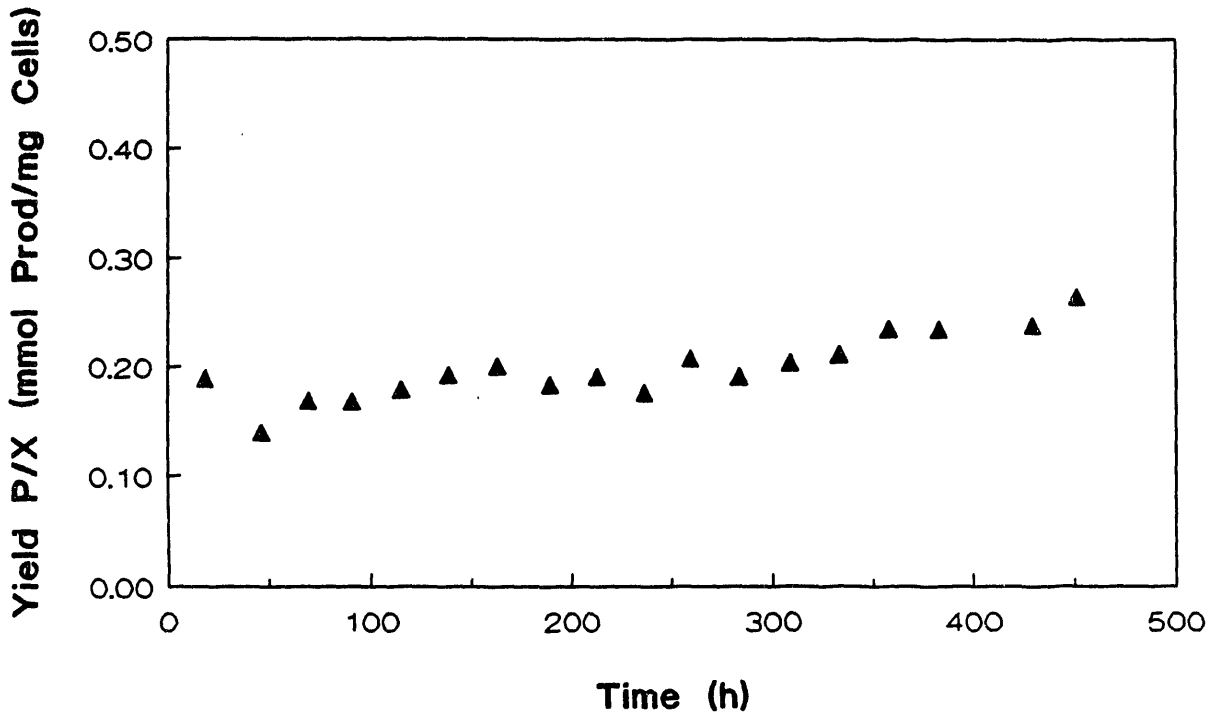

Figure 9.45 Product Yield from Cells for *C. ljungdahlii* in the CSTR with Arginine Addition.

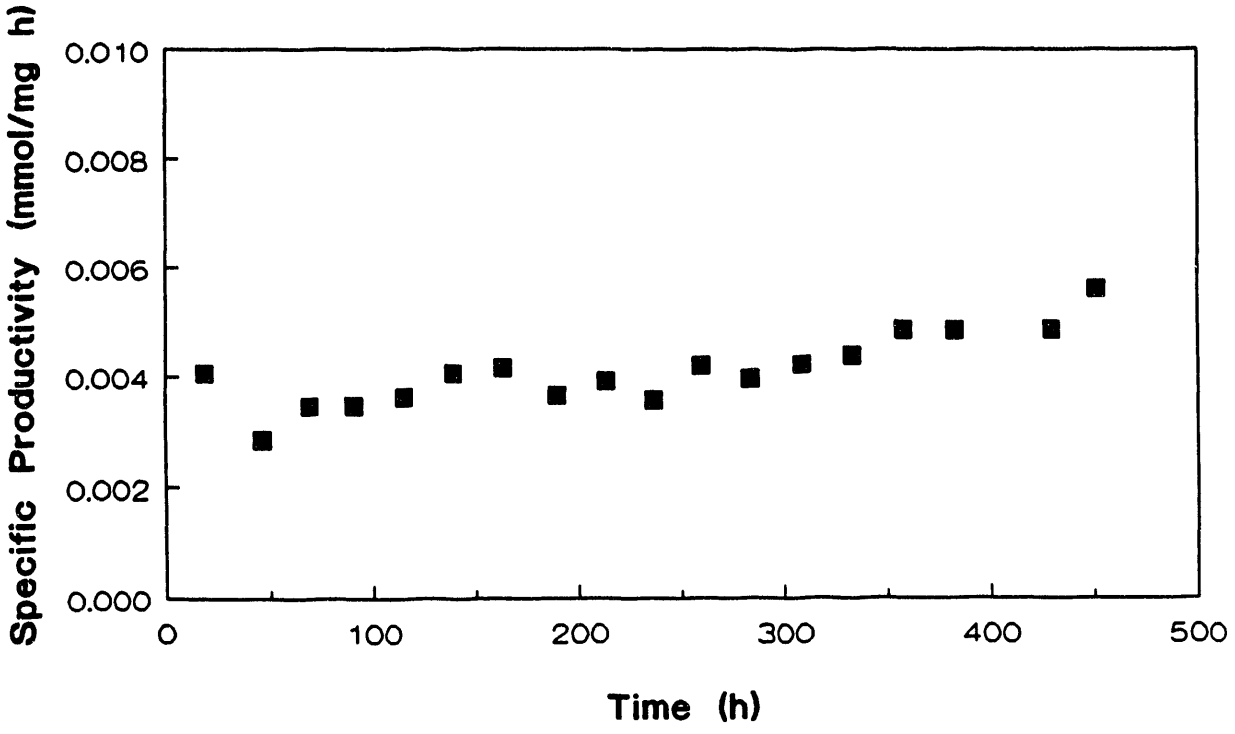

Figure 9.46 Specific Productivity for *C. ljungdahlii* in the CSTR with Arginine Addition.

Table 9.2 Analysis of the Results of CSTR Studies Employing *C. ljungdahlii*.

Expt.	Date	LFR (mL/d)	X (mg/L)	EtOH (g/L)	HAc (g/L)	q CO (mmol/min)	q H2 (mmol/min)	Agitation (rpm)
FO	10/10/91	45	1196	13.460	0.880	0.041	0.011	340
	10/19/91	120	626	6.491	2.648	0.058	0.020	360
	10/28/91	120	849	6.271	6.974	0.076	0.028	380
	11/09/91	120	420	2.503	4.095	0.051	0.007	350
	11/19/91	120	741	3.755	7.249	0.068	0.025	370
	11/27/91	120	912	5.093	7.907	0.074	0.027	370
	12/05/91	120	1017	7.644	6.859	0.084	0.031	380
	12/11/91	120	1191	9.892	7.117	0.081	0.029	380
	12/15/91	120	1329	13.010	5.183	0.082	0.030	380
	12/27/91	120	1135	15.796	3.398	0.090	0.031	390
	01/07/92	120	1341	12.542	5.552	0.078	0.029	400
	01/15/92	120	1502	15.585	3.730	0.096	0.033	400
	01/26/92	120	1406	15.996	3.285	0.119	0.040	400
	02/11/92	121	1575	19.073	3.910	0.155	0.047	420
	02/27/92	120	1386	18.320	2.610	0.152	0.001	420
	03/06/92	120	1157	16.347	2.859	0.141	0.006	450
FR	05/05/92	190	314	1.824	4.335	0.045	0.016	420
	05/12/92	182	451	2.742	6.055	0.062	0.021	420
	06/24/92	196	353	0.037	6.706	0.044	0.002	400
FS	04/25/92	179	240	1.491	0.631	0.030	0.004	350
	05/03/92	178	323	2.631	0.580	0.047	0.004	380
	05/10/92	176	473	2.574	0.612	0.046	0.000	420
	05/27/92	172	280	1.938	0.651	0.030	0.001	400
	06/06/92	174	787	1.909	9.040	0.071	0.026	420
	08/21/92	169	1130	5.459	16.064	0.130	0.043	460
	09/08/92	170	1292	7.703	19.405	0.157	0.047	460

Table 9.2 Continued

D (1/h)	Sp.Prod. (mol/g h)	Sp.Upt. (mol/g h)	E/A (mol/mol)	(6E+4A)/S	Yx/s (g/mol)	Yp/s (mol/mol)	Yp/x (mol/g)	Yp/s (calc'd)
0.0054	0.0014	0.0075	19.96	1.079	0.711	0.183	0.257	0.171
0.0143	0.0042	0.0212	3.20	1.104	0.675	0.200	0.296	0.187
0.0143	0.0043	0.0209	1.17	1.034	0.684	0.204	0.298	0.205
0.0143	0.0042	0.0238	0.80	0.856	0.599	0.175	0.292	0.213
0.0143	0.0039	0.0217	0.68	0.866	0.660	0.180	0.273	0.216
0.0143	0.0038	0.0191	0.84	0.976	0.747	0.199	0.266	0.212
0.0143	0.0039	0.0193	1.45	1.056	0.739	0.204	0.276	0.201
0.0143	0.0040	0.0158	1.81	1.335	0.901	0.252	0.280	0.196
0.0143	0.0040	0.0145	3.27	1.519	0.989	0.275	0.278	0.186
0.0143	0.0050	0.0183	6.06	1.571	0.780	0.275	0.352	0.178
0.0143	0.0039	0.0138	2.95	1.551	1.037	0.282	0.272	0.188
0.0143	0.0038	0.0148	5.45	1.471	0.968	0.258	0.267	0.180
0.0143	0.0041	0.0193	6.35	1.212	0.739	0.212	0.286	0.178
0.0144	0.0044	0.0220	6.36	1.140	0.653	0.199	0.305	0.178
0.0143	0.0046	0.0190	9.16	1.392	0.753	0.240	0.319	0.175
0.0143	0.0050	0.0218	7.46	1.314	0.654	0.228	0.348	0.177
0.0226	0.0081	0.0330	0.55	1.150	0.686	0.244	0.356	0.220
0.0217	0.0077	0.0314	0.59	1.166	0.691	0.246	0.356	0.219
0.0233	0.0074	0.0224	0.01	1.332	1.040	0.332	0.319	0.249
0.0213	0.0038	0.0246	3.08	0.853	0.867	0.155	0.179	0.187
0.0212	0.0044	0.0268	5.91	0.933	0.789	0.163	0.207	0.179
0.0209	0.0029	0.0170	5.49	0.980	1.232	0.172	0.140	0.180
0.0205	0.0039	0.0191	3.88	1.136	1.073	0.203	0.189	0.184
0.0207	0.0050	0.0213	0.28	1.050	0.971	0.237	0.244	0.232
0.0201	0.0069	0.0264	0.44	1.205	0.764	0.261	0.342	0.224
0.0203	0.0077	0.0271	0.52	1.332	0.749	0.285	0.380	0.222

A material balance on Equations (9.1-9.4) indicates that 6 moles of either CO or H_2 are required to produce 1 mole of ethanol and 4 moles of either CO or H_2 are required to produce 1 mole of acetate. Thus, the sum of 6 times the moles of acetate formed, divided by the moles of substrate (CO and H_2) consumed should equal 1. This ratio, shown as (6E + 4A)/S in Table 9.2, actually ranged from 0.85 - 1.5, indicating that a steady-state balance was not always attained. The yield of cells from substate ranged from 0.6-1.2 g/mol and the yield of combined product (ethanol and acetate) from substrate ranged from 0.15 - 0.33, with most of the values in the 0.2 - 0.25 range. The theoretical yield of product from substrate by Equations (9.1-9.4) is 0.17 - 0.25, depending upon whether ethanol or acetate is produced.

9.3 CSTR STudies with Cell Recycle

A cell recycle apparatus was used in conjunction with the standard CSTR as a method to increase the cell concentration inside the reactor. This is particularly important since product formation with *C. ljungdahlii* has been shown to be proportional to the cell concentration inside the reactor.

Fermentations were carried out in a 1.6 L CSTR with cell recycle. The total liquid volume in the reactor was 1.0 L, consisting of basal medium without yeast extract and one-half B-vitamins. The temperature of the reactor was held constant at 37°C and the agitation rate was 400 rpm. The gas flow rate was 16.5 mL/min and the liquid flow rate was 300 mL/d.

Figures 9.47 and 9.48 show cell concentration and product concentration profiles for the CSTR with cell recycle. In these experiments, the CO conversion was rather low at about 20%. As is shown in Figure 9.47 the maximum cell concentration reached was 600 mg/L (ignoring the single data

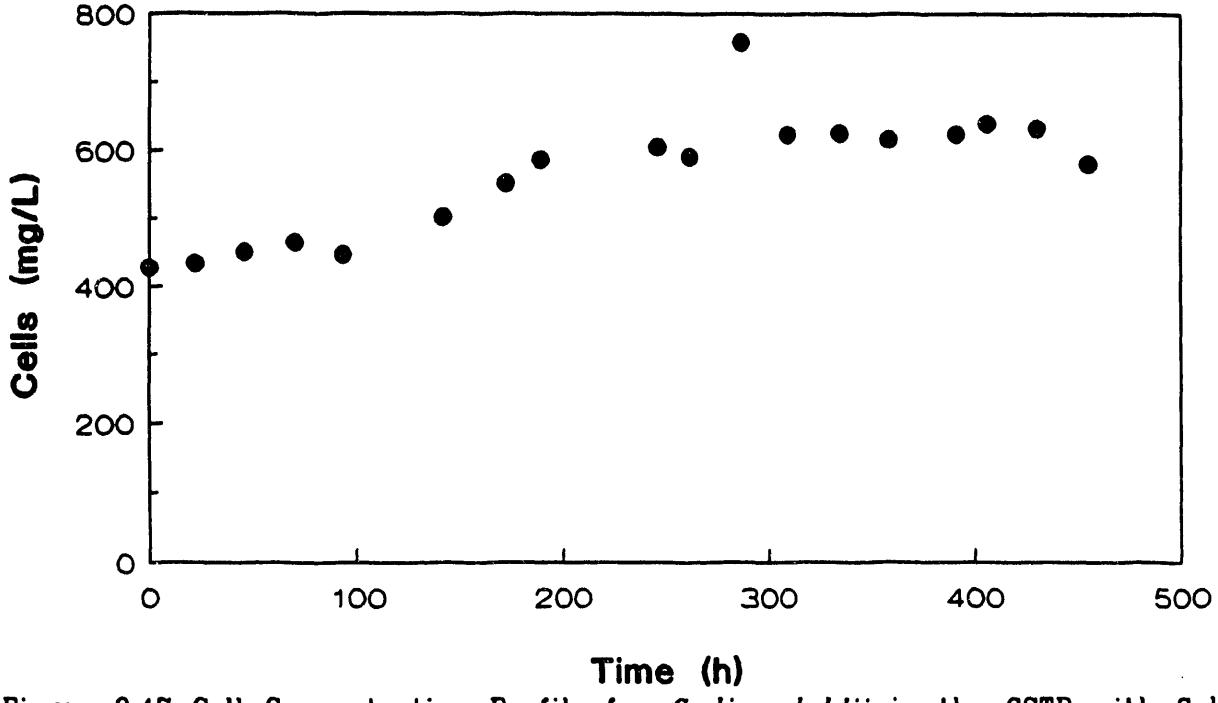

Figure 9.47 Cell Concentration Profile for *C. ljungdahlii* in the CSTR with Cell Recycle. (Basal Medium Contained no Yeast Extract, one half B-vitamins.)

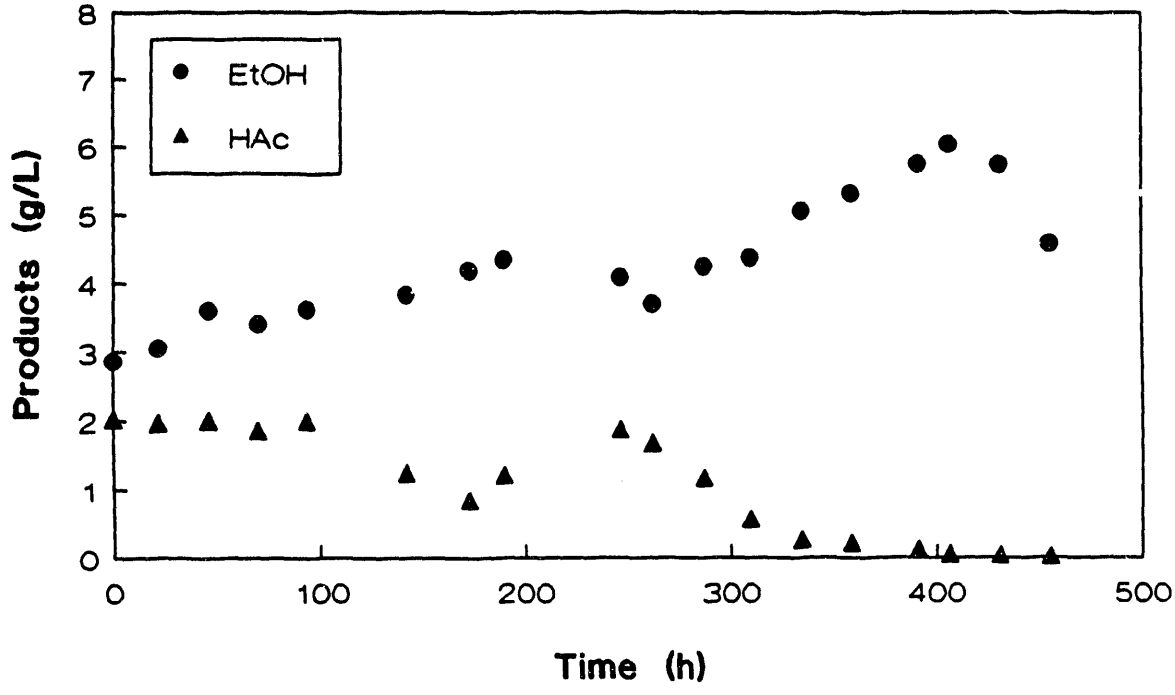

Figure 9.48 Product Profile for *C. ljungdahlii* in the CSTR with Cell Recycle. (Basal Medium Contained no Yeast Extract, one half B-vitamins.)

point of 750 mg/L), a value that was essentially constant for nearly 150 h of fermentation time. The product concentrations, shown in Figure 9.48, behaved somewhat differently. At a time of 250 h (the beginning of the maximum cell concentration), the ethanol concentration was about 4 g/L and the acetate concentration was nearly 2 g/L. At a later fermentation time of 400 h, however, the ethanol concentration reached 6 g/L with a corresponding zero acetate concentration. The product ratio thus increased from 2.0 at 250 h to an infinite value at 400 h. Ethanol production as the only product has thus been shown in a continuous reaction vessel.

It should be noted that, at a time of 450 h, the cell concentration and ethanol concentration fell. It is believed that the fermentation became nutrient limited, so that nutrient addition (perhaps $(NH_4)_3PO_4$ might be beneficial to both growth and product formation.

To help alleviate the problem of nutrient limitation the cell recycle apparatus was operated in a second experimental run using medium supplemented with $(NH_4)_2\ HPO_4$. The ammonium phosphate dibasic was first added daily as spikes in small quantities (0.5 g/L), followed by continuous addition as a component in the medium.

Fermentations were carried out in a 1.6 L CSTR with cell recycle. The total liquid volume in the reactor was 1.0 L., consisting of basal medium without yeast extract and one-half B-vitamins. The temperature of the reactor was held constant at 37°C and the agitation rate was 400 rpm. The gas flow rate was 16.5 mL/min and the liquid flow rate was 300 mL/d.

Figures 9.49 and 9.50 show cell concentration and product concentration profiles for the CSTR with cell recycle. In these experiments, the CO conversion was rather low as had been in previous studies. As is shown in

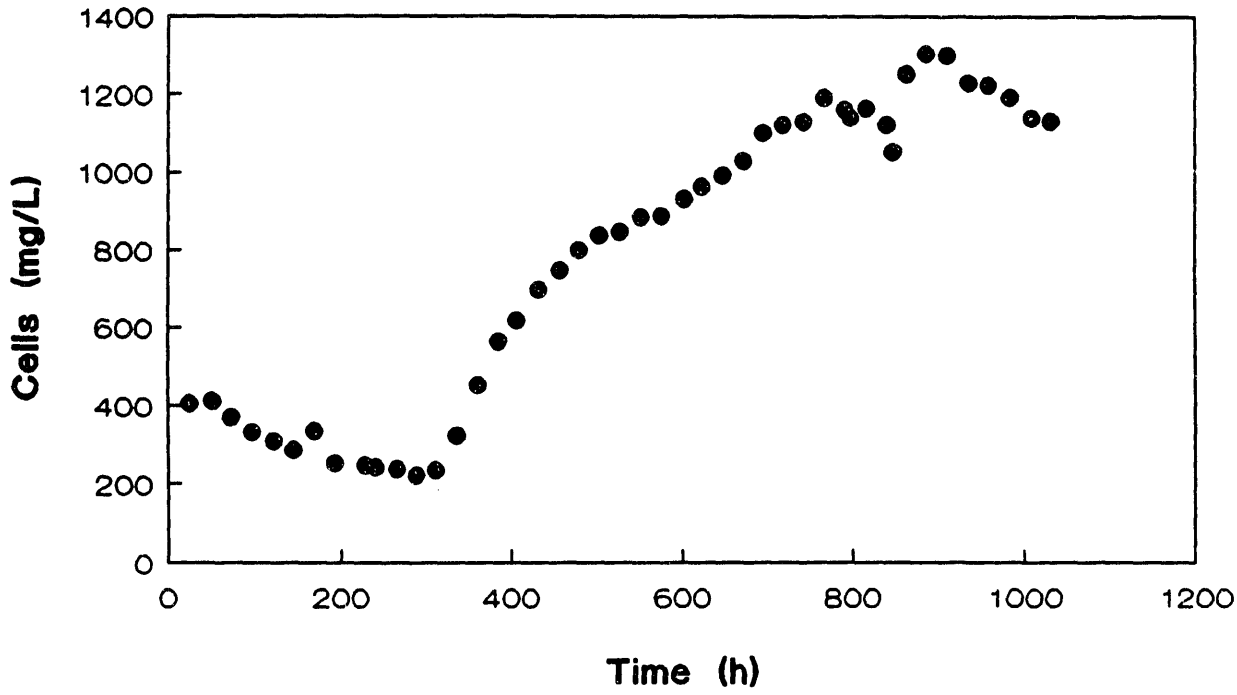

Figure 9.49 Cell Concentration Profile for *C. ljungdahlii* in the CSTR with Cell Recycle (With $(NH_4)_2HPO_4$ Stimulation)

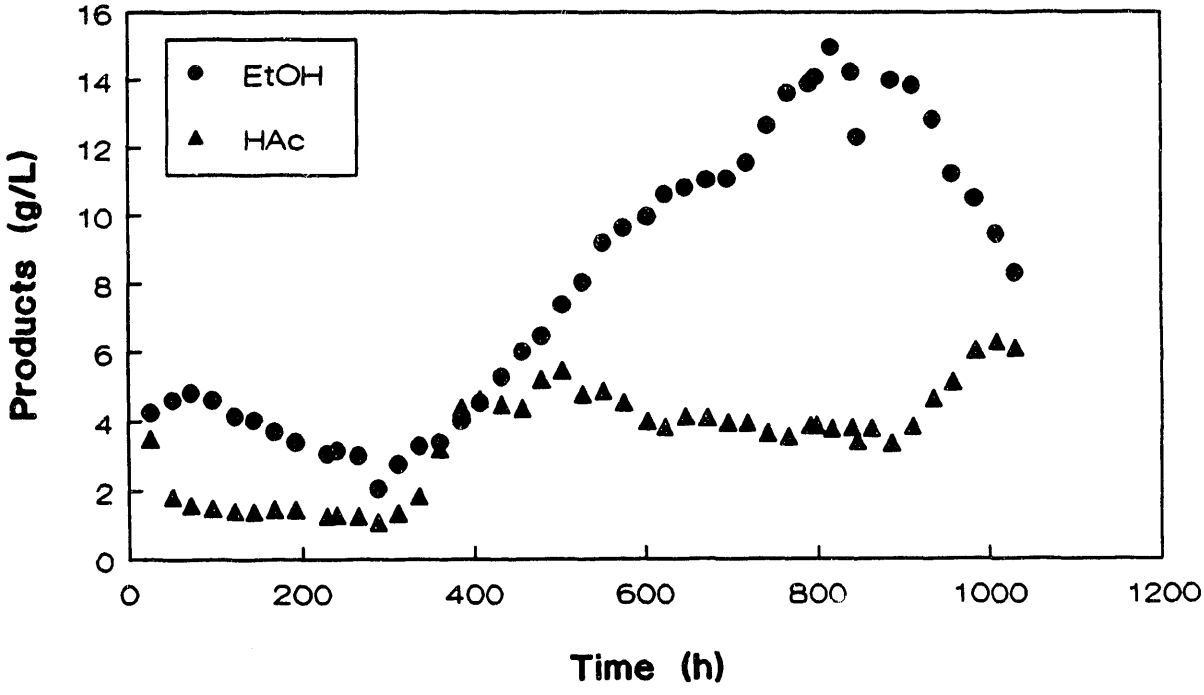

Figure 9.50 Products Concentration Profiles for *C. ljungdahlii* in the CSTR with Cell Recycle (With $(NH_4)_2HPO_4$ Stimulation)

Figure 9.49, the maximum cell concentration reached was over 1300 mg/L, increasing from 200 mg/L with ammonium phosphate addition. This cell concentration was more than double the concentration obtained in the previous studies. The ethanol and acetate product concentrations are shown in Figure 9.50. At a time of about 300 h, the ethanol concentration was about 4 g/L and the acetate concentration was nearly 2 g/L. This corresponds to the data at the same time in the previous work without ammonium phosphate. At a later fermentation time of 800 h, however, the ethanol concentration reached 15 g/L with a corresponding 4 g/L acetate concentration. The product ratio did not become infinite in favor of ethanol as it did in the previous study, yet the ethanol concentration reached levels that were 2.5 times greater. Increasing the all concentration is thus shown to be paramount in obtaining high product (ethanol) concentrations.

Studies were also carried out with *C. ljungdahlii* in the designed medium in a CSTR with cell recycle. In this study, the liquid volume was 1000 mL, the temperature was 35.5°C and the pH was held constant at 4.5. The agitation rate was increased from 300 to 450 rpm and the gas flow rate was increased from 10 to 30 mL/min during the study to accomodate cell growth in the reactor. The liquid flow rate to the cell recycle reactor was 3.5 to 12 mL/h, decreasing with time of operation. Thus, the reactor was effectively a CSTR without cell recycle using a very low liquid flow rate.

Figure 9.51 presents the cell concentration measurements for the CSTR with cell recycle. As is noted, the cell concentration increased (with agitation rate and gas flow rate increases) from approximately 800 mg/L to over 4000 mg/L. The increase is due to an increased mass transfer of CO and H_2 to the liquid phase with the increase in agitation rate and gas flow rate.

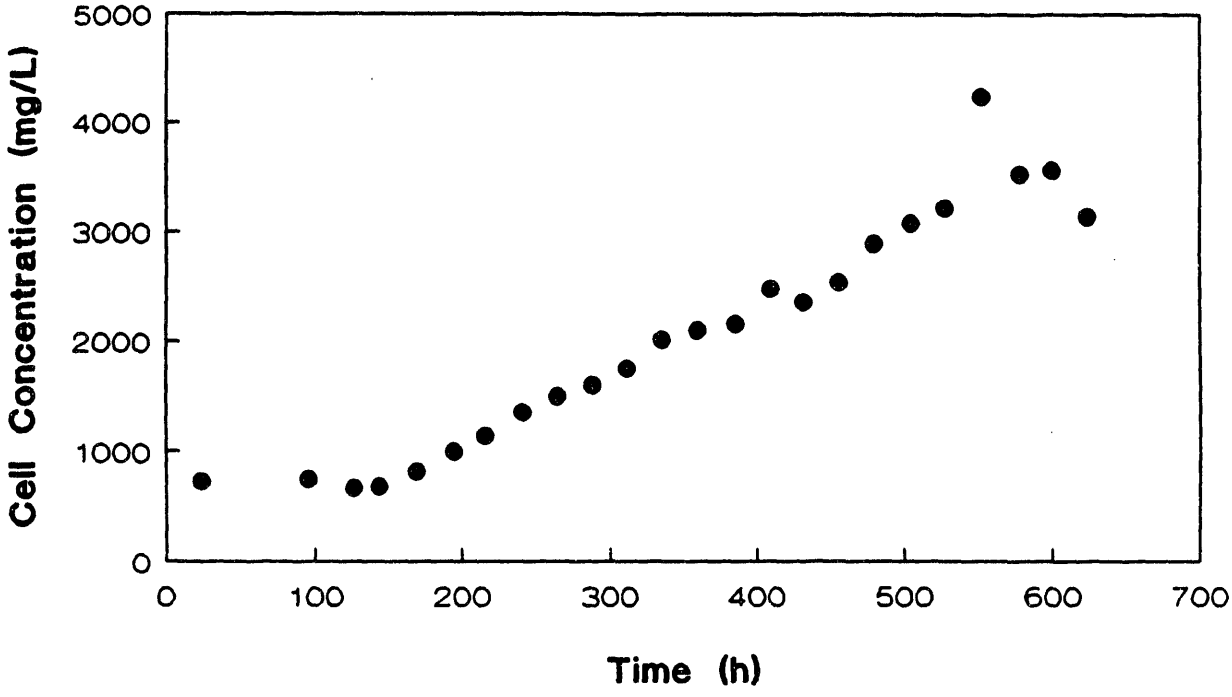

Figure 9.51 Cell Concentration Measurements for *C. ljungdahlii* in the CSTR with Cell Recycle

The maximum in the previous CSTR study without cell recycle was 1500 g/L. The CO conversion, shown in Figure 9.52, hovered around the 90 percent level after 150 h of operation. The corresponding H_2 conversion, on the other hand, averaged 70 percent up to a time of 500 h. At this time, the H_2 conversion fell, probably due to an accumulation of CO in the liquid phase.

Product concentration measurements during the study are shown in Figure 9.53. The ethanol concentration ranged from 6 g/L at the beginning of the study to 48 g/L after 560 h of operation. The corresponding acetate concentrations at these times were 5 g/L and 3 g/L, respectively. The ratio of ethanol to acetate ranged from 1.2 g/g to 16 g/g. Thus, very high ethanol concentrations are possible with favorable product ratios.

9.4 Ethanol Production in a Trickle Bed Reactor

Many contacting schemes may be employed for gas-liquid biological reactors, including mechanically agitated reactors, bubble columns, packed columns, plate columns, spray columns and gas-lift reactors. A packed column or trickle bed reactor is particularly effective for the reactions because of the large mass transfer coefficients obtained in this contacting device without expensive agitation. Although packed beds are normally operated countercurrently; cocurrent operation is possible with irreversible biological reactors since the mean concentration driving force is the same for both modes of operation. Also, the capacity of cocurrent columns is not limited by flooding, and at any given gas and liquid flow rates, the pressure drop in the cocurrent column is less.[72] The principal purpose of this research work is to investigate the feasbility of employing a packed cocurrent column to produce ethanol using *Clostridium ljungdahlii*.

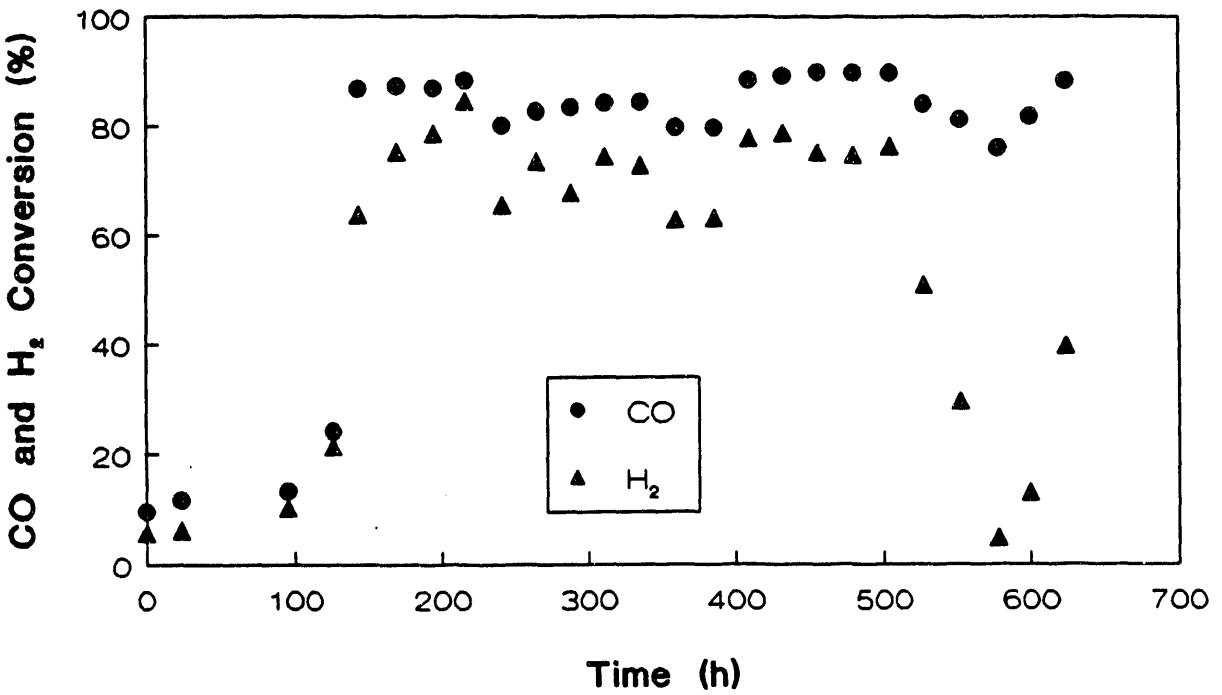

Figure 9.52 CO and H_2 Conversion for *C. ljungdahlii* in the CSTR with Cell Recycle

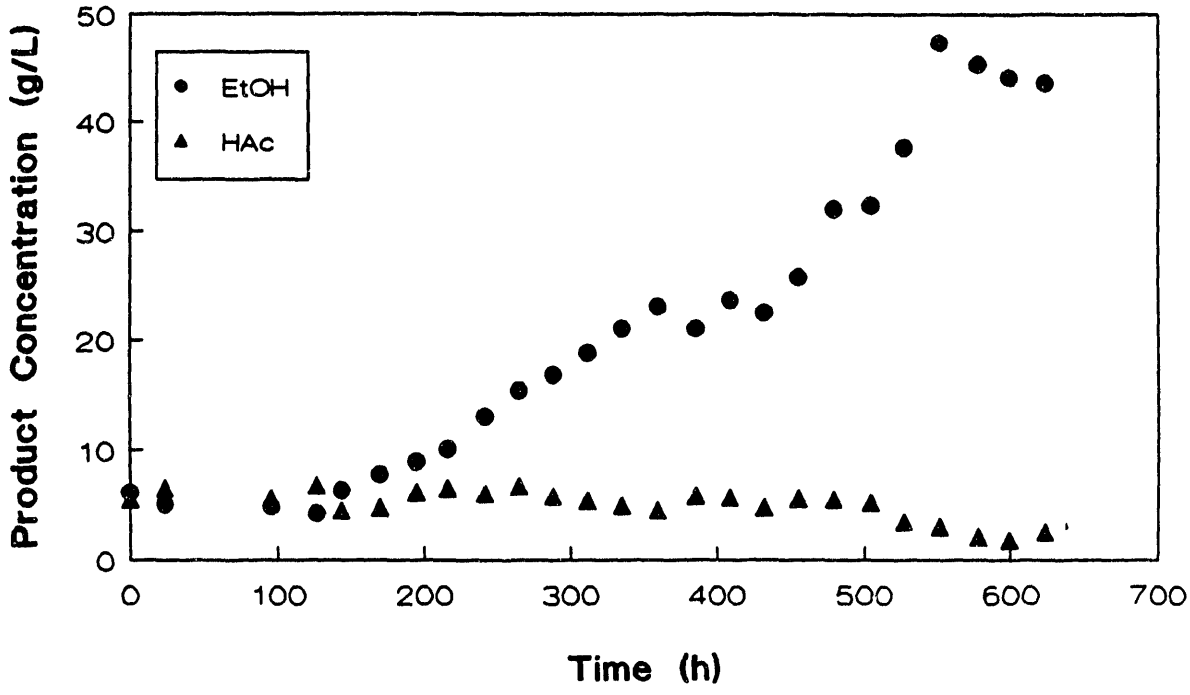

Figure 9.53 Product Concentration Measurements for *C. ljungdahlii* in the CSTR with Cell Recycle

Experiments were carried out in a cocurrent packed column employing a cylindrical ceramic packing (height : 5mm, inner diameter : 2 mm and outer diameter : 5mm). The reactor consisted of a 5.2 cm inside diameter, 54 cm long plexiglass cylinder. The height occupied by the packing was 51.5 cm. The empty reactor volume was 1150 mL and the initial void volume after packing was 650 mL. The bottom of the reactor was provided with a perforated plate between the gas entrance and the packing in an effort to achieve better gas distribution in case the gas is introduced from the bottom with a countercurrent packed column. A sample port was thus installed at the bottom of the reactor to allow for liquid sampling.

The liquid and the gas flowed cocurrently from the top of the column. The liquid level inside the column was maintained with the aid of a level control positioned at the liquid outlet (this control also acted as a gas-liquid separator). The gas (9.9% carbon dioxide, 20.0% hydrogen, 54.9% carbon monoxide and 15.2% argon) flowed from a pressurized tank through a mass flow meter and filter into the reactor. The gas line out of the system was connected to the liquid headspace of the feed and the product reservoirs, as well as the level control device, in order to equilibrate pressures throughout the system while maintaining anaerobic conditions.

The liquid medium was pumped by means of a peristaltic pump from the feed reservoir into the liquid sample port situated at the bottom of the packed cocurrent column, and was kept constant at 42 mL/hr. The liquid from the outlet was recycled by means of a pump to the top of the column, and thereafter, the liquid flow was due to gravitational forces. The liquid recirculation rate in these experiments ranged from 85-415 mL/min. The packed cocurrent column in effect operated as a trickle bed reactor with the

retention of the liquid in the column rather small. The gas flow rates for these experiments varied from 2 mL/min to 14 mL/min. Typically, each gas flow rate was maintained for 3 days during which gas samples were analyzed for CO conversion and liquid samples were analyzed for ethanol and acetate. The medium composition used for these experiments was the designed medium of Table 9.3.

The liquid porosity in the column is shown as a function of the liquid recirculation rate in Figure 9.54. As is noted, the porosity, defined as the ratio of the volume of voids to the total reactor volume, ranged from 0 to 15 percent depending upon the liquid recirculation rate. At recirculation rates of 415 mL/min and above, the liquid porosity was essentially 15 percent.

Figures 9.55-9.58 show CO and H_2 conversion profiles for *C. ljungdahlii* in the trickle bed reactor for liquid recirculation rates of 85, 232, 325 and 415 mL/min, respectively. As is noted in the figures, the conversion profiles at the three higher recirculation rates were quite similar. The profiles at the 85 mL/min recirculation rate were generally higher than at the other rates at a given gas flow rate. At a recirculation rate of 85 mL/min, the CO conversion was 100 percent at a 8 mL/min gas flow rate (1.35 hr gas retention time). The H_2 conversion under these conditions was greater than 90 percent. It is apparent from these results that increased liquid recirculation allowed less cell attachment in the packed column. Fewer attached cells, coupled with mass transfer, permitted better CO and H_2 conversions at the lower recirculation rate.

Product concentration profiles in the trickle bed reactor at the four recirculation rates are shown in Figures 9.59-9.62. These results showed the same trend as the conversion profiles, with a higher total product

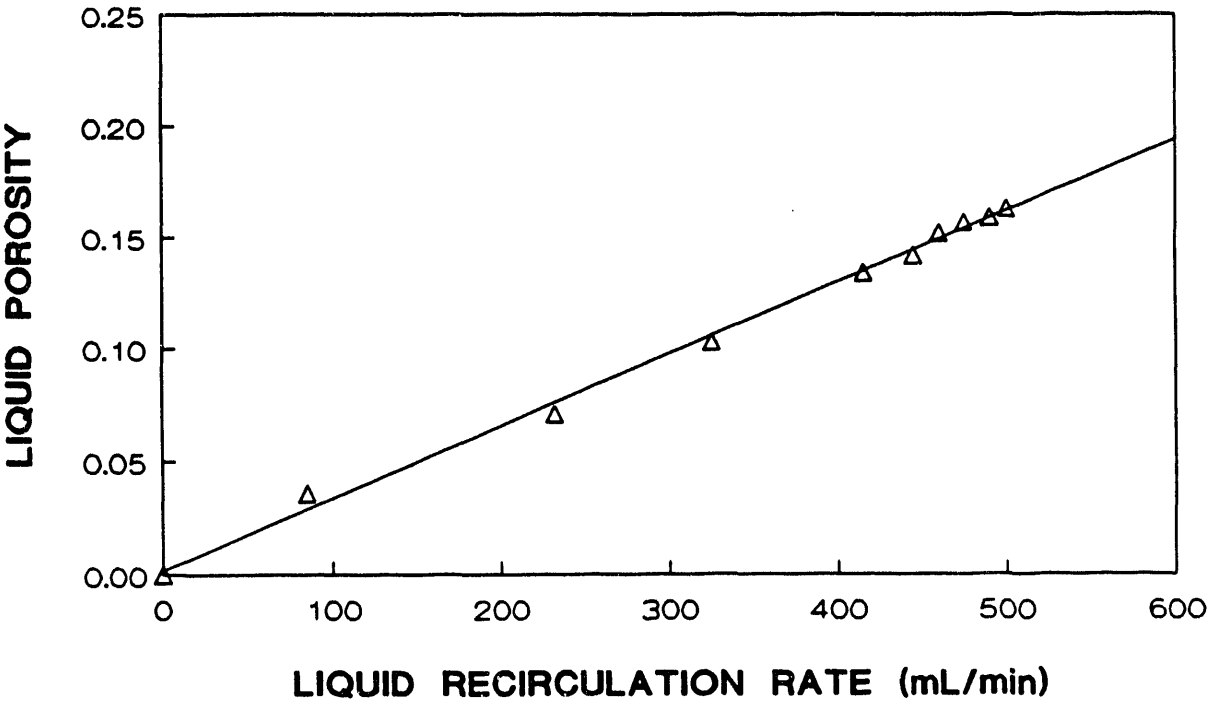

Figure 9.54. Liquid Porosity Measurements in the Packed Column as a Function of Recirculation Rate.

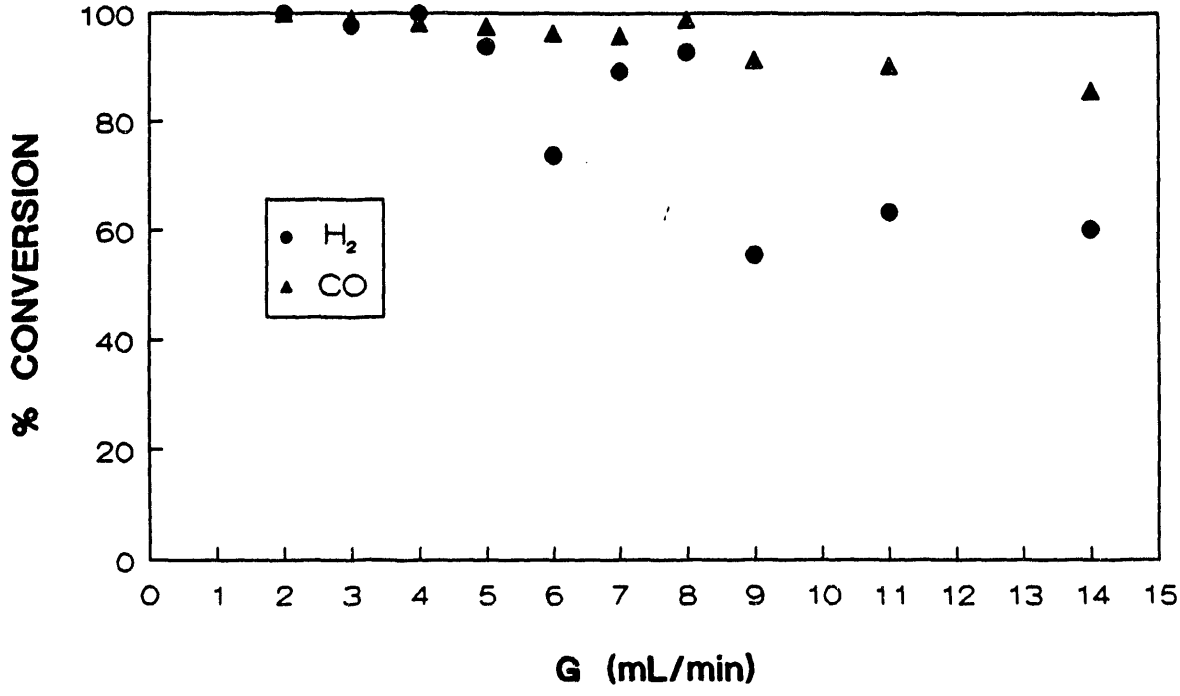

Figure 9.55. CO and H_2 Conversion Profiles in the Packed Bed Reactor (Liquid Recirculation Rate : 85 mL/min).

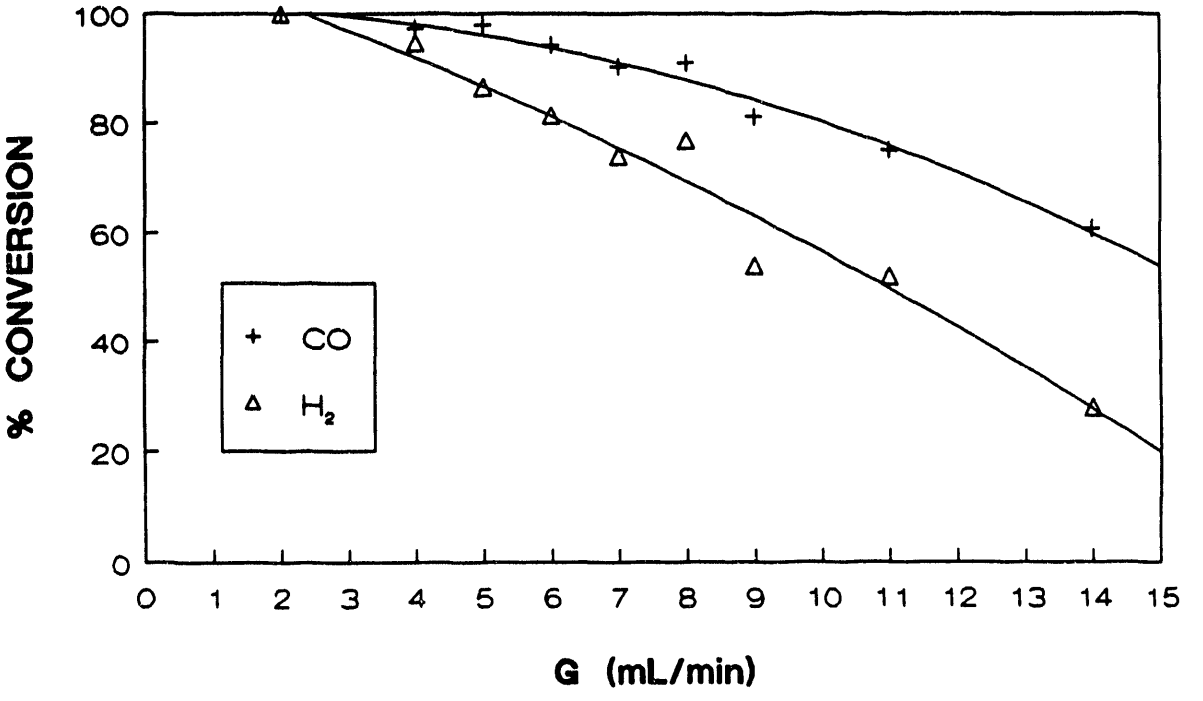

Figure 9.56. CO and H_2 Conversion Profiles in the Packed Bed Reactor (Liquid Recirculation Rate : 232 mL/min).

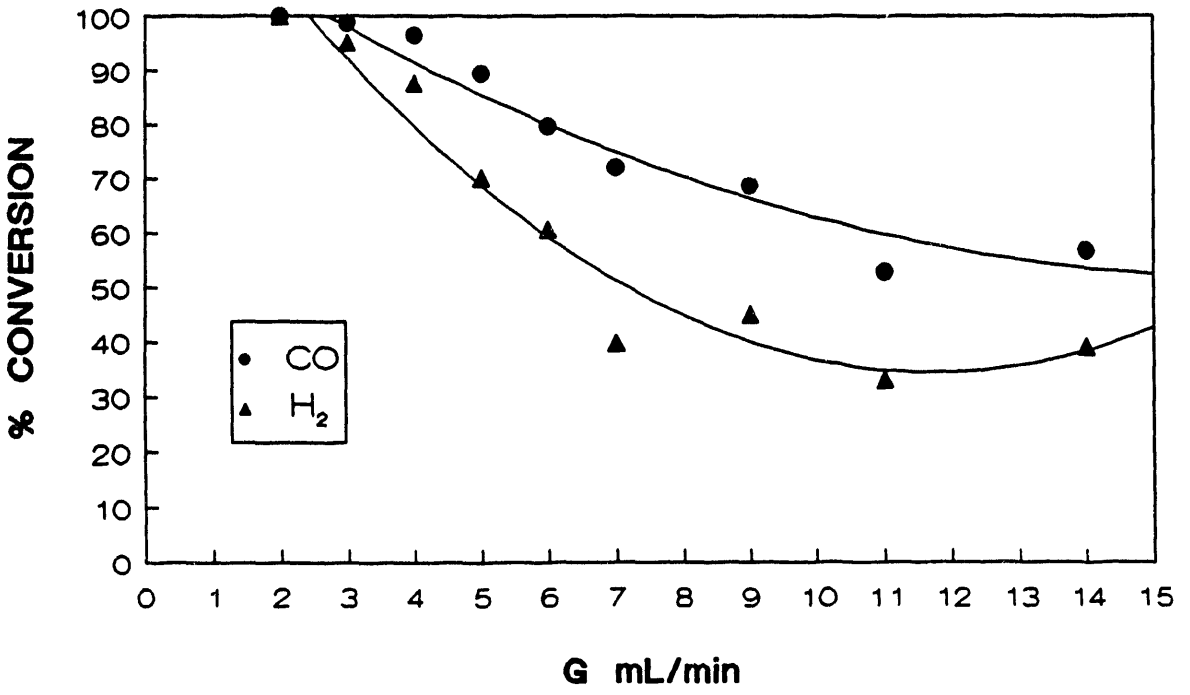

Figure 9.57. CO and H_2 Conversion Profiles in the Packed Bed Reactor (Liquid Recirculation Rate : 325 mL/min).

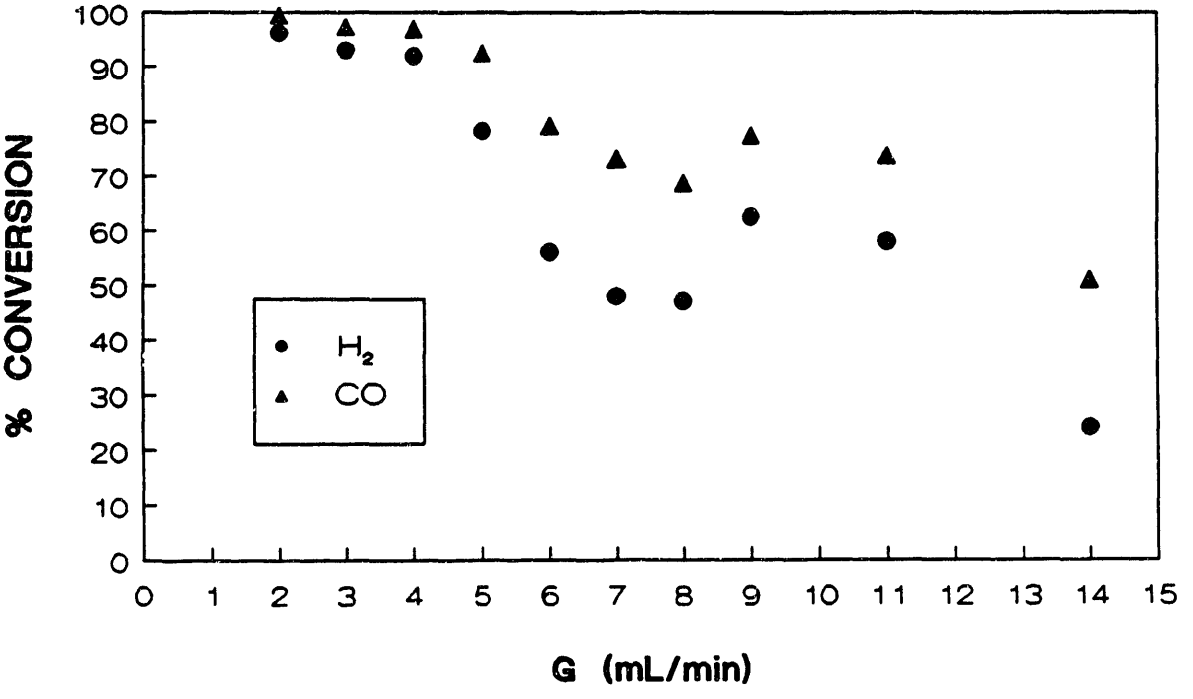

Figure 9.58. CO and H_2 Conversion Profiles in the Packed Bed Reactor (Liquid Recirculation Rate : 415 mL/min).

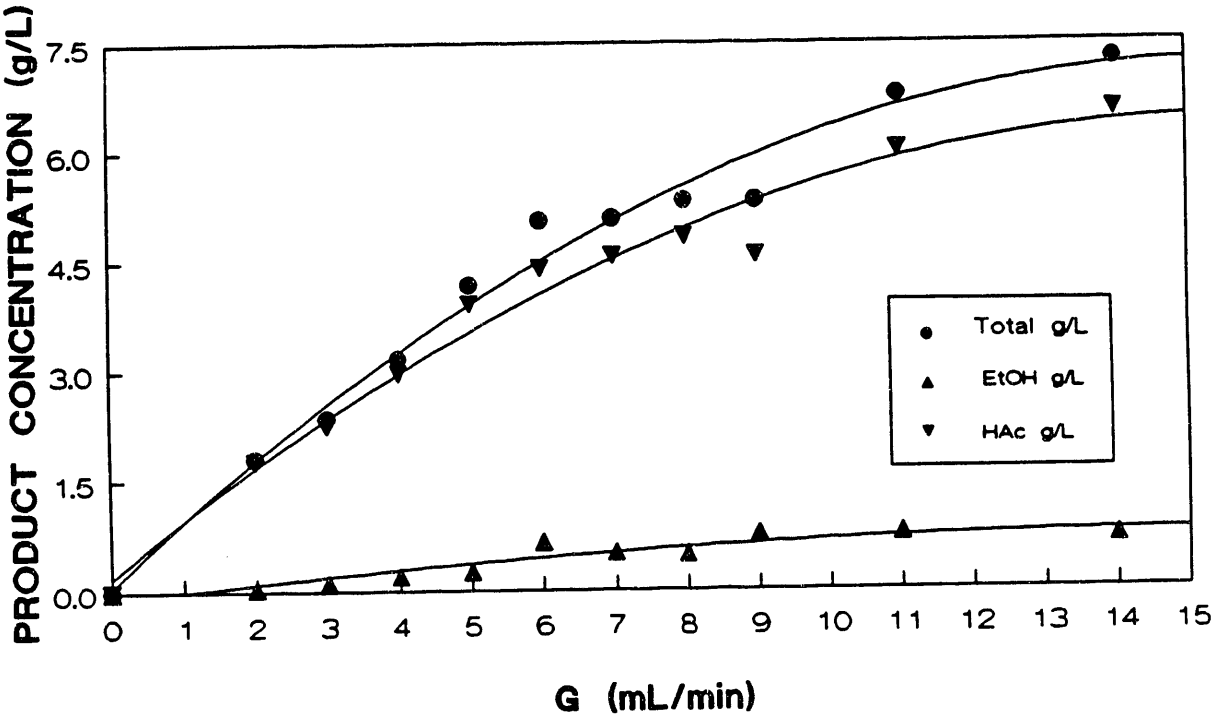

Figure 9.59. Product Concentration Profiles in the Packed Bed Reactor (Liquid Recirculation Rate : 85 mL/min).

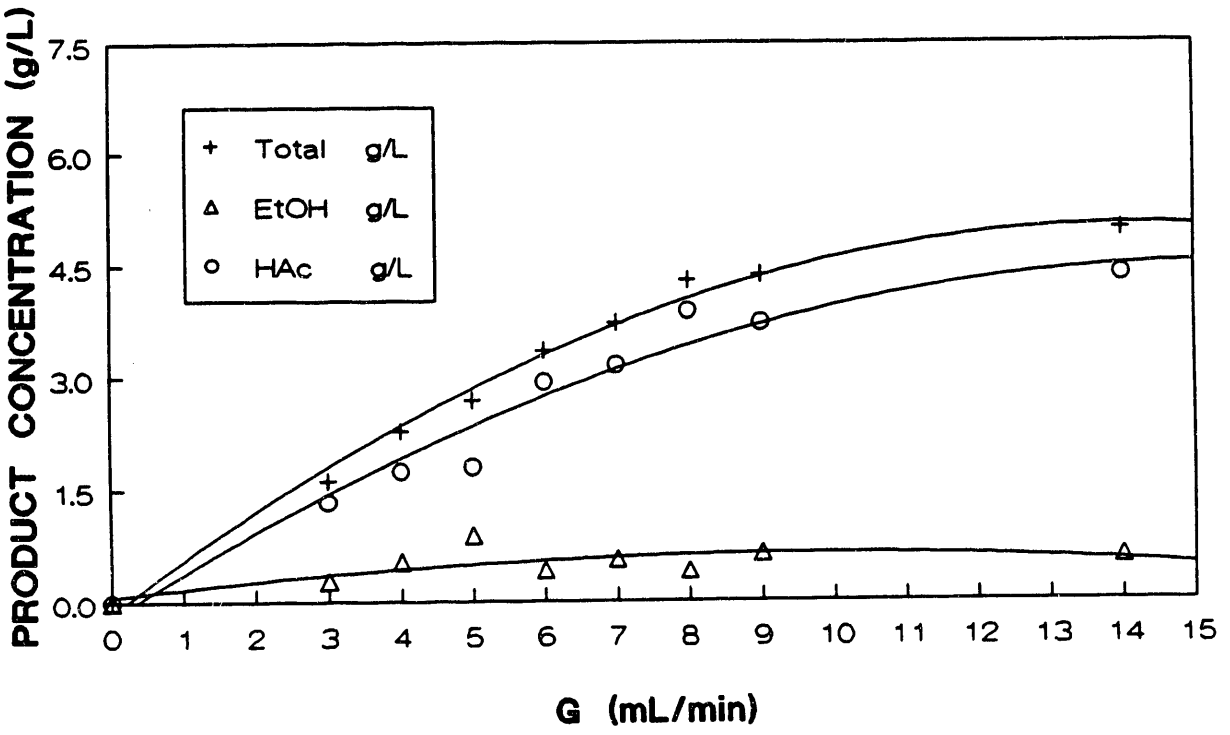

Figure 9.60 : Product Concentration Profiles in the Packed Bed Reactor (Liquid Recirculation Rate : 232 mL/min).

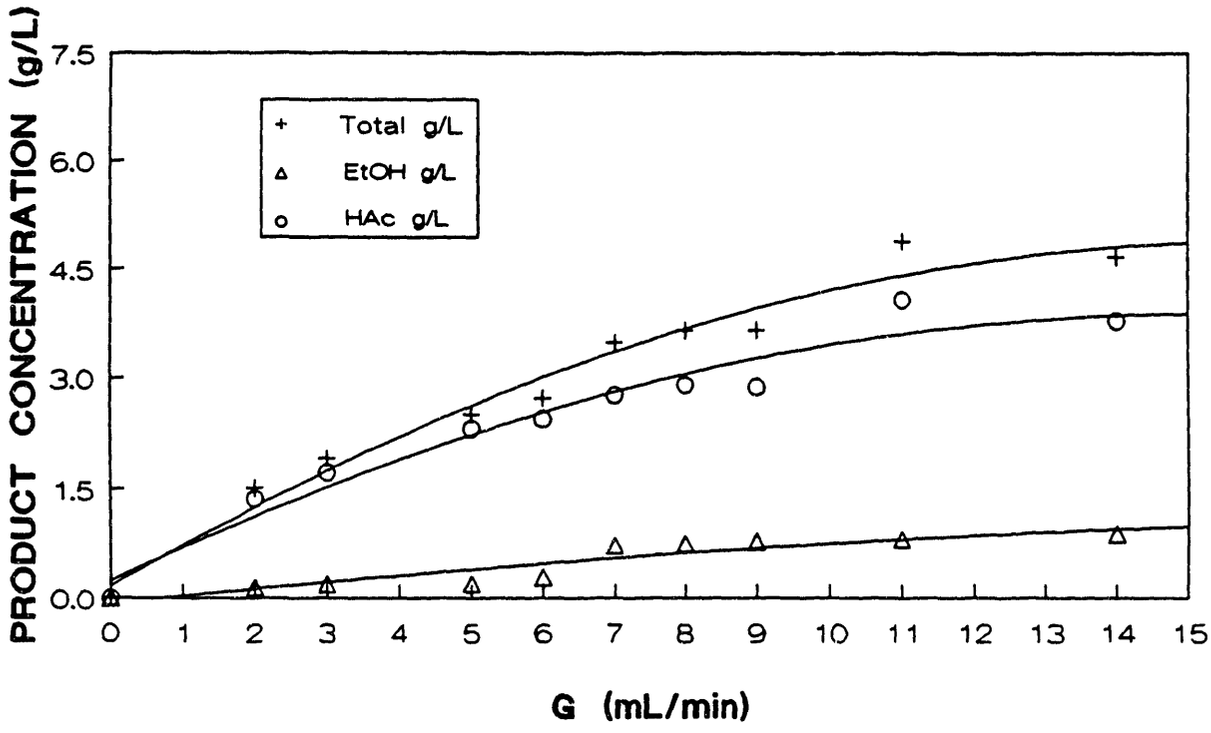

Figure 9.61. Product Concentration Profiles in the Packed Bed Reactor (Liquid Recirculation Rate : 325 mL/min).

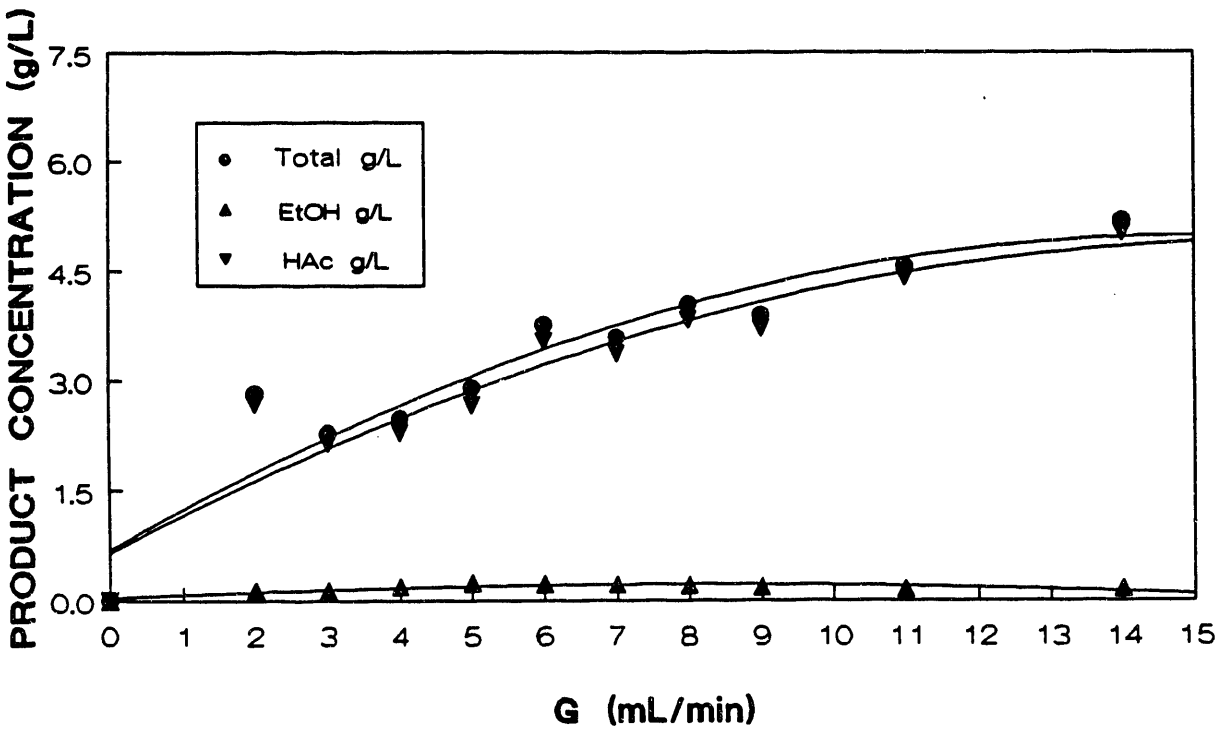

Figure 9.62. Product Concentration Profiles in the Packed Bed Reactor (Liquid Recirculation Rate : 415 mL/min).

concentration at a given gas flow rate with the lowest recirculation rate. A maximum acetate concentration of 6.0 g/L and a maximum ethanol concentration of 0.8 g/L were attained at an 85 mL/min recirculation rate. These results again show the importance of mass transfer and cell attachment. Productivity profiles, shown in Figures 9.63-9.66, showed higher productivities at the lowest recirculation rate. The maximum productivity with an 55 mL/min recirculation rate was 15 mmol/L•hr. The maximum productivity at the other recirculation rates was 10 mmol/L•hr.

The transport of a sparingly water-soluble substrate from the gas phase to the liquid phase may be described by the equation:

$$\text{moles transported} = K_L a/H(P^G - P^L) \qquad (9.1)$$

where P^G is the partial pressure of the substrate in the gas phase. In the same manner, P^L refers to the partial pressure of the substrate in equilibrium with the concentration of the substrate in the bulk liquid phase, $K_L a$ is the overall mass-transfer coefficient and H is the Henry's law constant. In the liquid phase, the substrate is consumed at a maximum rate by the cells according to the equation

$$\text{mole consumed} = q\,X \qquad (9.2)$$

where q is the specific uptake rate and X is the cell concentration. For a system not operating under mass-transfer limitation, the limiting step for substrate consumption is the microbial kinetics described by Equation (9.2). On the other hand, under mass-transfer limitation, the uptake rate is generated by the mass-transfer limitation of the reactor and Equation (9.1). It is important to realize that in both cases the moles of substrate transported from the gas phase to the liquid (Equatior (9.1)) must be equal to the consumption rate by the cells (Equation (9.2)) at steady state.

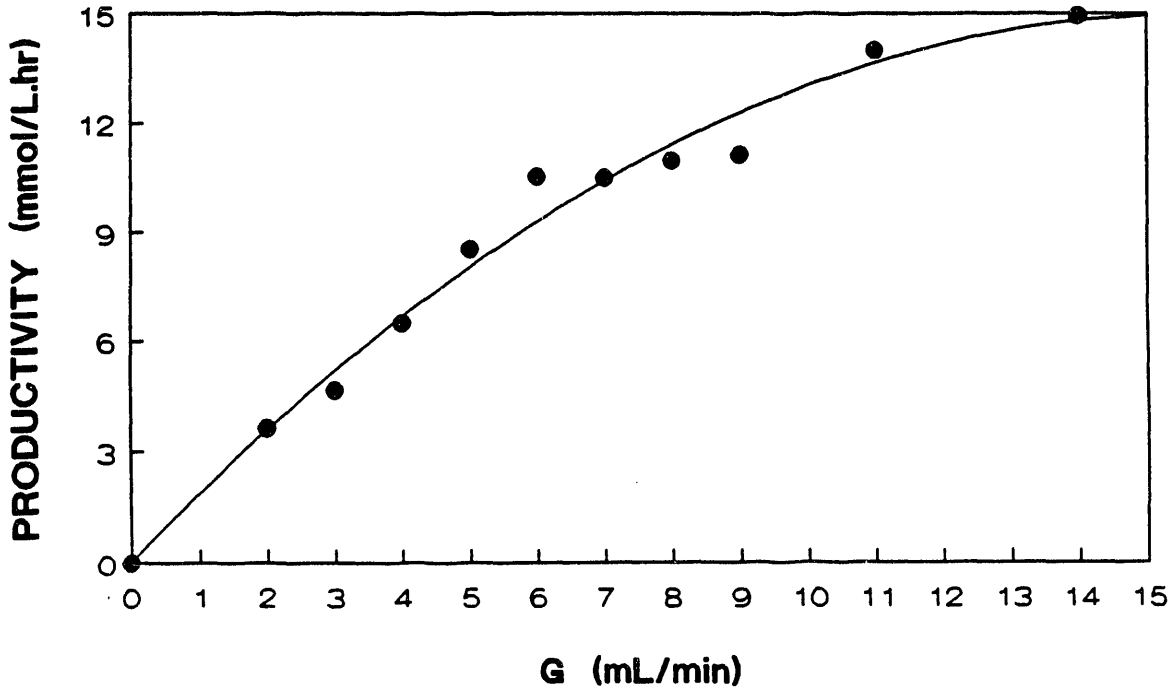

Figure 9.63. Productivity Profiles in the Packed Bed Reactor (Liquid Recirculation Rate : 85 mL/min)

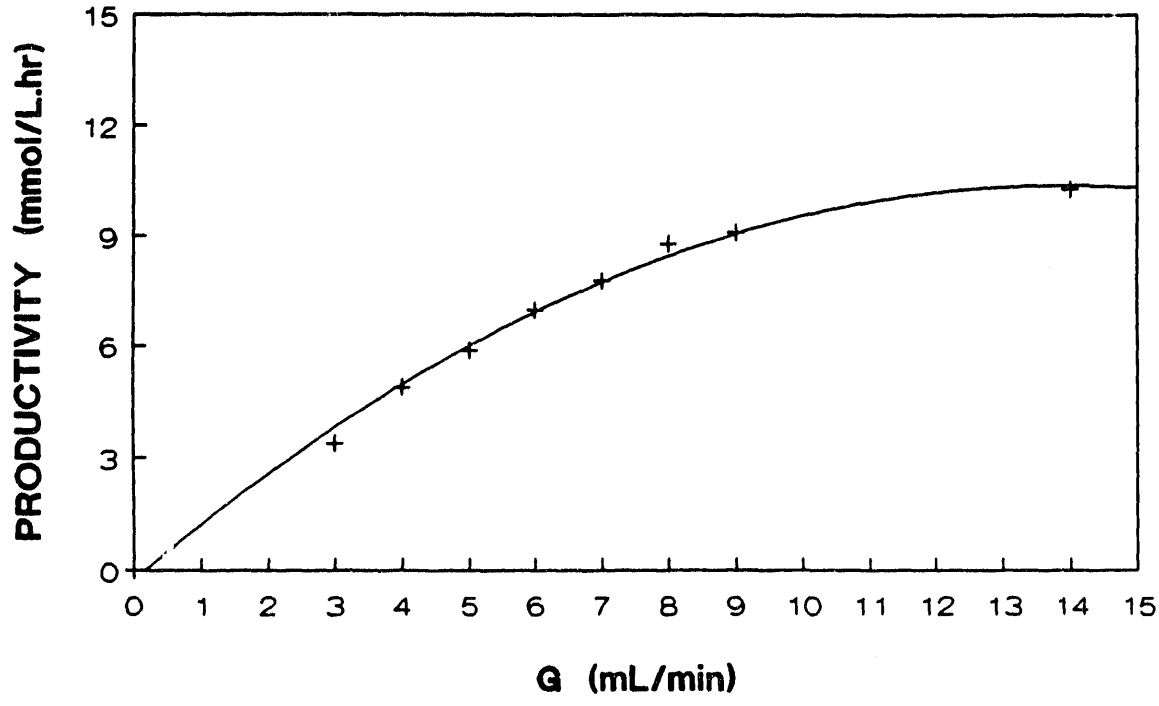

Figure 9.64 : Productivity Profiles in the Packed Bed Reactor (Liquid Recirculation Rate : 232 mL/min).

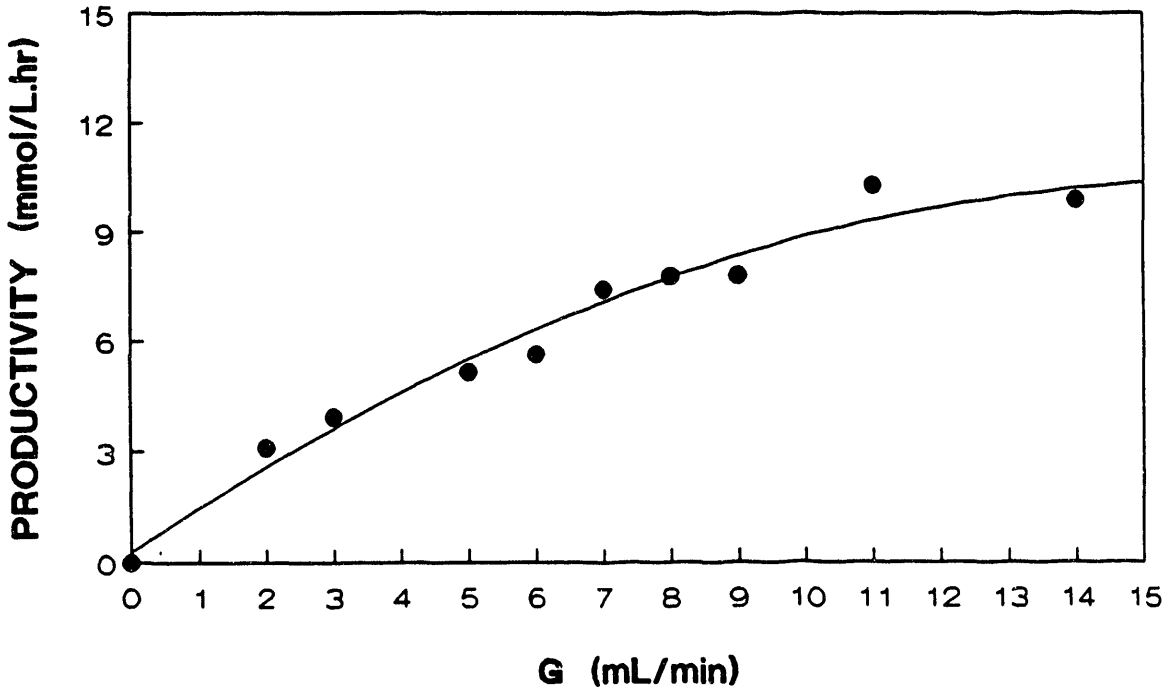

Figure 9.65. Productivity Profiles in the Packed Bed Reactor (Liquid Recirculation Rate : 325 mL/min).

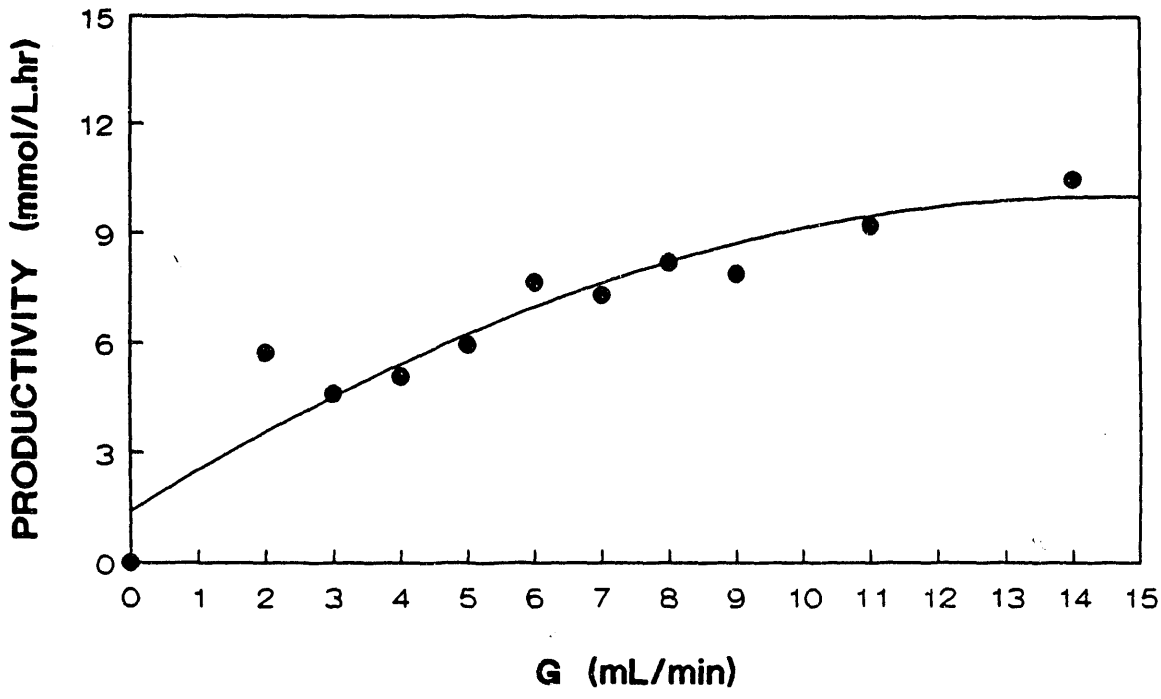

Figure 9.66. Productivity Profiles in the Packed Bed Reactor (Liquid Recirculation Rate : 415 mL/min).

In the column reactor used in this study, the outlet concentration of, for example, CO may be related to the gas flow rate and column parameters through the following equation:[73,74]

$$\ln \left[Y_{CO}^{i}/Y_{CO}^{o}\right] = \left[K_L a/H\right] \epsilon_L \, [ShRT/G] \qquad (9.3)$$

where Y_{CO}^{i} and Y_{CO}^{o} are the molar fraction ratios of CO to an inert gas component (Ar) in the inlet and outlet gases, respectively. Thus, by varying the gas flow rate, G, and measuring the compositions in the inlet and outlet gases, the mass transfer properties of the column reactors may be estimated. The main assumptions made in the derivation of Equation (9.3) are that mass-transfer limiting conditions apply and that the gas flow rate does not change significantly along the length of the column.

The relation of Equation (9.3) for finding the mass transfer coefficient is illustrated in Figure 9.67, where $\ln \left[Y_{CO}^{i}/Y_{CO}^{o}\right]$ is plotted as a function of hRTS/G. As is seen in the figure, the data fell on a straight line through the origin.

The experimental results from the trickle bed showed that acetate was the preferred product of CO, CO_2 and H_2 conversion over ethanol. Results in progress, however, indicate that ethanol is the preferred product over acetate at lower liquid flow rates. At an (inlet) liquid flow rate of 11 mL/hr, the product ratio (ethanol : acetate) was greater than one. Higher rates are possible at even lower liquid flow rate.

10.0 PROCESS DESCRIPTION AND ECONOMIC EVALUATION

10.1 Process Description

A process for the production of ethanol from syngas by fermentation with *C. ljungdahlii* would be quite simple. Syngas is fed continuously to a

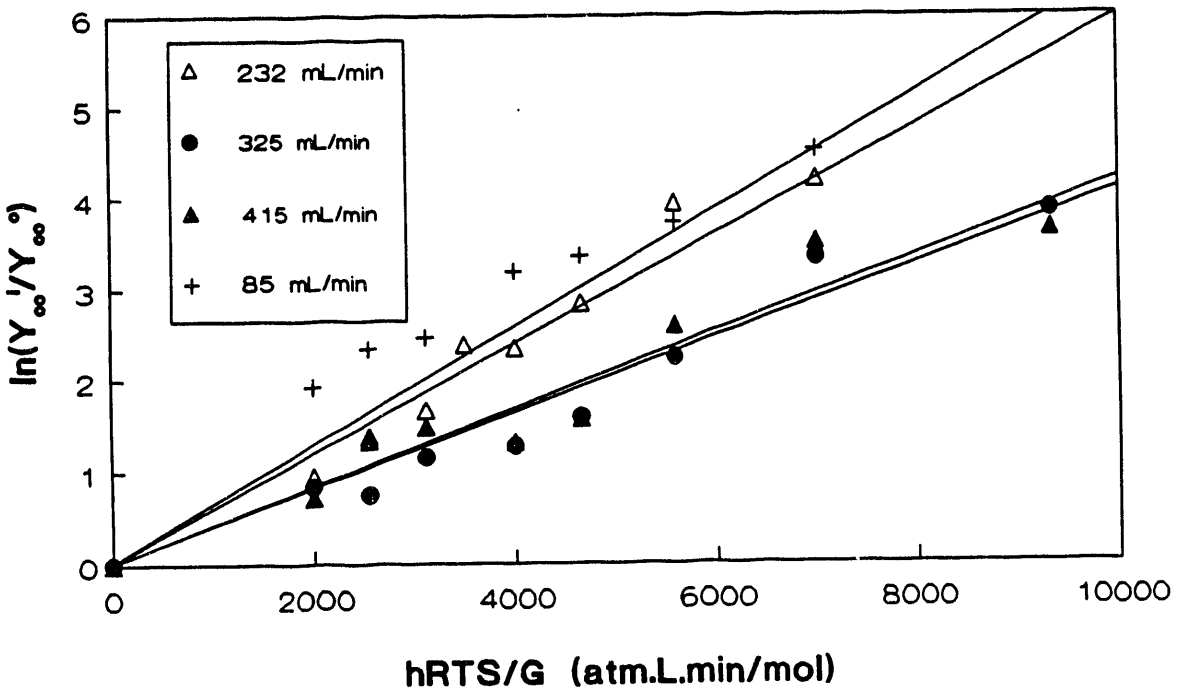

Figure 9.67. Determination of Mass Transfer Coefficient in a Packed Bed Reactor at Different Liquid Recirculation Rates.

continuous stirred tank reactor along with a small liquid medium stream. Ethanol and unused gases (CO_2, CH_4, sulfur gases) exit the reactor in a single stream. The liquid stream flows to a cell recycle apparatus, where the cells are concentrated and returned to the reactor. The gas stream is vented to the atmosphere, although it may first be further treated biologically for sulfur gas removal, if desired.

The liquid permeate exiting the cell recycle apparatus flows to an extraction column where n-hexanol (or other suitable solvent) is used to remove ethanol from the permeate stream. Distillation is then used to separate solvent from ethanol/water, with another distillation unit used to separate ethanol from water to the azeotropic concentration. If desired, the azeotrope may be broken to produce 100 percent ethanol using azeotropic distillation. Water from distillation is recycled back to the reactor.

10.2 Process Assumptions

An economic evaluation has been developed to process 100 million standard ft^3 of syngas per day. This quantity of gas produces 561 million pounds of ethanol per year. It is assumed for this analysis that the syngas contains 65 percent CO and 22 percent H_2.

For the purposes of this evaluation, it is assumed that *C. ljungdahlii* has a cell yield of 0.33 g cells/mole gas. It is further assumed that the culture is not inhibited until an ethanol concentration of 50 g/L is attained. The maximum specific growth rate, q_m, is 0.04 mole gas/g cell•hr. Each of these assumptions has been demonstrated in previous reactor studies.

In this simulation, the operating pressure is 20 atm, the temperature is 37°C, the CO conversion is 90 percent and the cell recycle is 90 percent of the active cells.

10.3 Economic Evaluation

Table 10.1 presents a summary of the equipment necessary to produce ethanol from syngas in the process described above. Eleven 1250 m^3 stirred tank reactors at 20 atm are required for the process. Centrifuges are utilized for cell recycle. The total costs for reaction, extraction and the two distillations are $38.36 million.

Utility requirements are summarized in Table 10.2 As is noted, 8955 hp of electricity is required, 274 million Btu/hr of stream are required and 3 million gal/hr of cooling water are required.

The economic evaluation for the process is summarized in Table 10.3 Ethanol at $1.20/gal yields just over $100 million/yr. Chemicals in the form of medium chemicals, solvent (n-hexanol) and syngas total $17.9 million - $52.8 million depending upon the cost of the raw synthesis gas. Three synthesis gas costs (shown as 1, 2 and 3) are shown:

(1) $0.50/MSCF

(2) $1.00/MSCF

(3) $1.50/MSCF

Thus, all cost analyses shown later in the table are indicated for the three scenarios.

Utilities total $9.2 million, depreciation (at 10 percent of the fixed capital investment (FCI)) totals $3.8 million and maintenance (5% of the FCI) total $1.9 million. Labor is estimated at $0.25 million/yr. The total operating cost is $33.5 - $68.5 million/yr depending upon the syngas cost.

The profit before taxes (38 percent) is $67.5 - $32.5 million/yr and the profit after taxes is $41.8 - $20.1 million/yr. The cash flow is $45.7 - $24.0 million/yr and the payout is 0.8 - 1.6 yr.

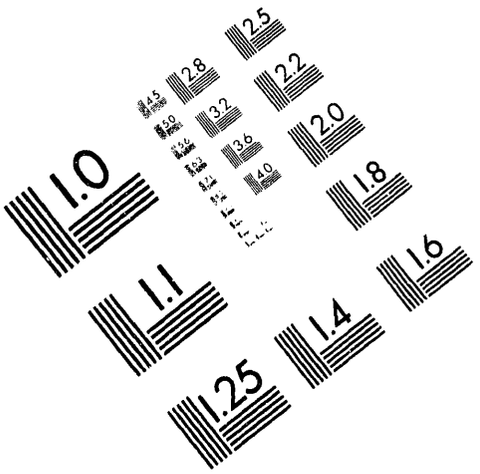

Association for Information and Image Management

1100 Wayne Avenue, Suite 1100
Silver Spring, Maryland 20910

301/587-8202

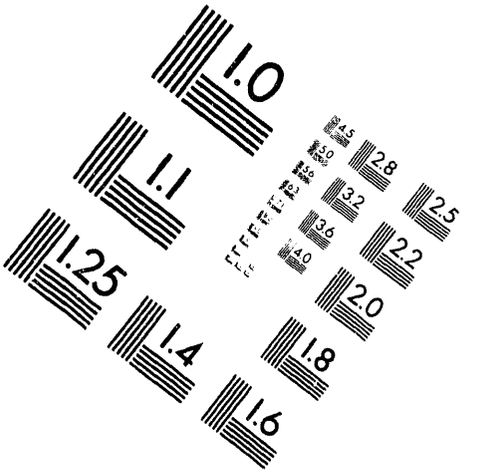

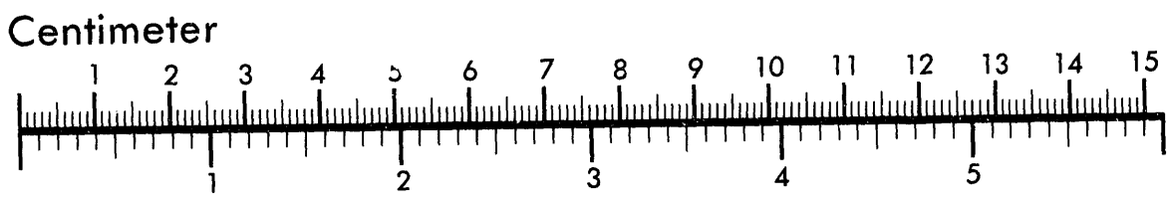

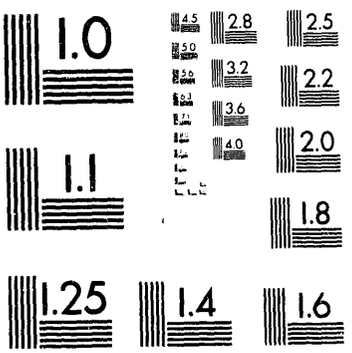

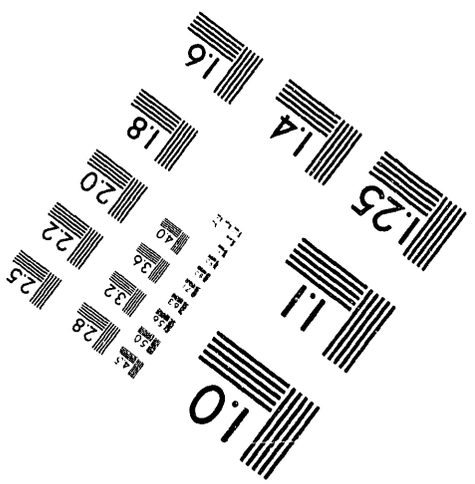

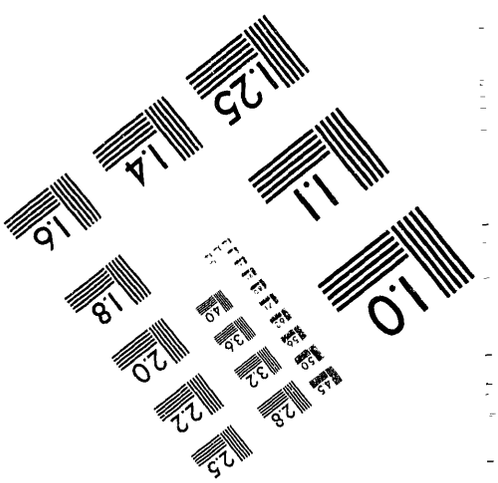

4 of 4

Table 10.1

Equipment Summary

A. Reaction

11 - 1250 m^3 stirred tank reactors
(20 atm)
11 - 675 hp agitators
11 - 30 in. bowl nozzle discharge centrifuge
for cell recycle
(125 hp)

Cost $7.02 million

B. Extraction

3 - 16.4 ft dia x 40 ft high column
(packed with Intalox saddles)

Cost $0.58 million

C. First Distillation

1 - 17.4 ft dia x 40 ft high column with trays
6 - 10,000 ft^2 shell and tubes as condenser
24 - 10000 ft^2 heat exchange units
3 - heat exchange units, 1660 ft^2

Cost $4.53 million

D. Second Distillation

1 - 11.6 ft dia x 40 ft high column with trays
2 - 10,000 ft^2 shell and tubes as condenser
4 - 400 ft^2 plate and frame units as reboiler
1 - 150 ft^2 recycle intercooler

Cost $0.65 million

Total Delivered Equipment Cost = $12.78 million

Fixed Capital Investment = $38.36 million

Table 10.2

Utilities

Section	Electricity	Steam	Cooling Water
Reactor	8800 hp		
Extraction	50 hp		
First Distillation	80 hp	189 $\bar{M}$ Btu/hr	2231 M gal/hr
Second Distillation	25 hp	85 $\bar{M}$ Btu/hr	782 M gal/hr
Total	8955 hp	274 $\bar{M}$ Btu/hr	3013 M gal/hr

Electricity cost: $0.06/kwhr

Steam cost: $2/$\bar{M}$ Btu

Cooling water cost: $0.05/M gal

11.0 CONCLUSIONS

Many variables were investigated to determine their effects on growth, CO and H_2 consumption and ethanol production by *C. ljungdahlii*. The variables having the most effect on the bacterium were found to be pH and liquid medium composition. Reduced pH (4.0-5.0) was found to be necessary for ethanol production, and a designed minimal medium was found to be effective in producing ethanol in high concentrations in favor of acetate. With the designed mediium at pH 4.0-4.5, little to no acetate was produced and ethanol concentrations as high as 47 g/L were obtained depending upon reactor type.

Previous kinetic studies with *C. ljungdahlii* at CO partial pressures of 1.6 atm and below have shown zero order equations for both the specific growth rate, μ, and the specific uptake rate, q, in terms of dissolved CO tension. When an experimental study was carried out over an increased CO partial

Table 10.3

Economic Evaluation

A.	Revenue		
	Ethanol @ $1.20/gal		$101.01 MM/yr
B.	Chemicals Cost		
	Medium $20/hr		$ 0.17 MM/yr
	Solvent $20/hr		$ 0.17 MM/yr
	Syngas		
	(1) $0.50/1000 SCF		$ 17.50 MM/yr
	(2) $1.00/1000 SCF		$ 35.00 MM/yr
	(3) $1.50/1000 SCF		$ 52.50 MM/yr
	Total Chemicals Cost	(1)	$ 17.84 MM/yr
		(2)	$ 35.34 MM/yr
		(3)	$ 52.84 MM/yr
C.	Utilities		
	Electricity		$ 3.34 MM/yr
	Steam		$ 4.59 MM/yr
	Cooling Water		$ 1.27 MM/yr
	Total Utilities		$ 9.20 MM/yr
D.	Depreciation (10% FCI)		$ 3.84 MM/yr
E.	Maintenance (5% FCI)		$ 1.92 MM/yr
F.	Labor		$ 0.50 MM/yr
G.	Supervision (1/2 of Labor)		$ 0.25 MM/yr
H.	Total Operating Costs	(1)	$ 33.54 MM/yr
		(2)	$ 51.04 MM/yr
		(3)	$ 68.54 MM/yr
I.	Profit Before Taxes	(1)	$ 67.47 MM/yr
		(2)	$ 49.97 MM/yr
		(3)	$ 32.47 MM/yr
J.	Taxes (38%)	(1)	$ 25.64 MM/yr
		(2)	$ 18.99 MM/yr
		(3)	$ 12.34 MM/yr

Table 3.3 (continued)

K.	Profit After Taxes	(1)	$ 41.83 MM/yr
		(2)	$ 30.98 MM/yr
		(3)	$ 20.13 MM/yr
L.	Cash Flow	(1)	$ 45.67 MM/yr
		(2)	$ 34.82 MM/yr
		(3)	$ 23.97 MM/yr
M.	Payout	(1)	0.84 Yr
		(2)	1.10 Yr
		(3)	1.60 Yr

pressure range (0-4.27 atm), zero order reactions were again obtained, indicating that the Monod saturation constants, K_p and K_p', were quitae small and that substrate inhibition was not apparent over this CO partial pressure range.

C. ljungdahlii was found to be tolerant of the sulfur gases H_2S and COS at normal concentrations expected in coal-derived synthesis gas. Tolerance to very high sulfur gas concentrations is expected with further acclimation.

The biochemical pathway for the formation of ethanol and acetate from CO, CO_2 and H_2 has been formulated. This pathway was constructed after a careful review of the literature.

The production of ethanol from synthesis gas by the anaerobic bacterium *C. ljungdahlii* has been demonstrated in continuous stirred tank reactors (CSTRs), CSTRs with cell recycle and trickle bed reactors. Various liquid media were utilized in these studies including basal medium, basal media with 1/2 B-vitamins and no yeast extract and a medium specifically designed for the growth of *C. ljungdahlii* in the CSTR. Ethanol production was successful in each of the three reactor types, although trickle bed operation with *C. ljungdahlii* was not as good as with the stirred tank reactors. Operation in the CSTR with cell recycle was particularly promising, producing 47 g/L ethanol with only minor concentrations of the by-product acetate.

A plant processing 100 million SCF of syngas per day and generating 560 million pound of ethanol per year has a payout of 1.6 yr using a syngas price of $1.50/MSCF. If the raw syngas can be obtained for $0.50/MSCF, the payout time reduces to 0.84 yr.

12.0 LITERATURE CITED

1. Clausen, E.C., and J.L. Gaddy, "Advanced Studies of Biological Indirect Liquefaction of Coal: Final Report, "Prepared under DOE contract DE-AC22-88PC79813, Pittsburgh Energy Technology Center, (January 1990).

2. Barik, S., S. Prieto, S.B. Harrison, E C. Clausen and J.L. Gaddy "Biological Production of Alcohols from Coal Through Indirect Liquefaction," presented at the 9th Symposium on Biotechnology for Fuels and Chemicals, Boulder, CO, paper no 28 (May 1987).

3. Ljungdahl, L.G., *Ann. Rev. Microbiol.* 40, 415 (1986).

4. Vega, J.L., S. Prieto, B.B. Elmore, E.C. Clausen and J.L. Gaddy, "The Biological Production of Ethanol from Synthesis Gas," *Applied Biochem. Biotech.* 20/21, 781 (1989).

5. Rogers, P., *Ad. Appl. Microbiol.* 31, 1 (1986).

6. Wood, H.G., H.L. Drake and S.I. Hu, *Proc. Biochem. Symp.*, St. Louis, pp 29-56, Palto Alto, CA, Annual Reviews (1982).

7. Ljungdahl, L.G., In "Organic Chemicals from Biomass" (D. L. Wise, ed.), pp 219-248, Benjamin/Cummings, Menlo Park, California (1983).

8. Bahl, H. and G. Gottschalk, in Sixth Symposium on Biotechnology for Fuels and Chemicals, (D. I. C. Wang and C. D. Scott, eds.), 14, pp. 215-223, Wiley, New YOrk (1984).

9. Bahl, H., W. Andersch and G. Gottschalk, *Eur. J. Appl. Microbiol. Biotechnol.* 15, 201 (1982).

10. Gottschal, J.C. and J.G. Morris, *FEMS Mocrobiol. Lett.* 12, 385-389 (1981).

11. Bailey, J.E. and D.F. Ollis, "Biochemical Engineering Fundamentals, McGraw-Hill, New York (1977).

12. Rao, G. and R. Mutharasan, *Biotech. Letters*, 8, 893 (1986).

13. Rao, G., P.J. Ward and R. Mutharasan, *Ann. NY Acad. Sci.* 506, 76 (1987).

14. Rao, G. and R. Mutharasan, *Biotech. Letters*, 10, 129 (1988).

15. Rao, G. and R. Mutharasan, *Applied and Environ. Micro.* 1232, (June 1987).

16. Kim, T.S. and B.H. Kim, *Biotech. Letters*, 10, 123 (1988).

17. Jones, D.T., A. Van der Westhuizen, S. Long, E.R. Allcock, S.R. Reid and D.R. Woods, *Appl. Environ. Microbiol*, 43, 1434-1439 (1982).

18. Long, S.D., T. Jones and D.R. Woods, *Appl. Environ. Microbiol.* 20, 256-261.

19. Long, S.D., T. Jones and D.R. Woods, *Biotechnol. Lett.* 6, 529-535 (1984b).

20. Gottschal, J.C. and J.G. Morris, *Biotechnol. Lett.* 3, 525-530 (1981).

21. Pheil, C.G. and Z.G. Ordal, *Applied Microbiol.* 15, 893 (1967).

22. Landuyt, S.L., E.J. Hsu and M.Lu, *Ann. N. Y. Acad. Sci.* 413, 474-478 (1983).

23. Hsu, Edward and I. Ordal. *Journal of Bacteriology*, 97, 1511 (1969).

24. McInerney, M.J., M.P. Bryant and N. Pfennig, *Appl. Environ. Microbiol.* 122, 129.

25. Genthner, B.R.S., M.P. Davis and M.P. Bryant, *Appl. Environ. Microbiol.* 42, 12.

26. Savage, M.D. and H.L. Drake, *J. Bacteriol.* 165 (1), 315

27. Hungate, R.E., "Methods in Microbiology, 3B, 117 (1969).

28. Bryant, M.P., *Am. J. Clin. Nutr.* 25, p. 1324-1328 (1972).

29. Balch, W.E. and R.S. Wolfe, *Appl. Environ. Microbiol.* 32, 781 (1976).

30. Luedeking, R., and E.L. Piret, *J. Biochem. Microbiol. Technol. Eng.*, 1, 393-412 (1959).

31. Tyree, R.W., E.C. Clausen and J.L. Gaddy, *Biotechnol. Letters*, 12(1), 51-56 (1990).

32. Stanier, R.Y., M. Doudoroff and E.A. Adelberg, *The Microbiol World*, 3rd ed., Prentice-Hall, Inc., Englewood Cliffs, NJ, p 316 (1970).

33. Smith, K.D., K.T. Klasson, M.D. Ackerson, E.C. Clausen and J.L.Gaddy, "COS Degradation of Selected CO-Utilizing Bacteria," *Appl. Biochem. Biotechnol.*, 28/29, 787 (1991).

34. Clausen, E.C. and J.L. Gaddy, "Advanced Studies of Biological Indirect Liquifaction of Coal," Final Report, prepared under DOE Contract No. DE-AC22-88PC79813, Pittsburgh Energy Technology Center (January 1990).

35. Bailey, J.E. and D.F. Ollis, "Biochemical Engineering Fundamentals," 2nd ed., McGraw-Hill. Table 2.1, p. 28 (1986).

36. Tanner, R.D., L.M. Miller, D. Young, Publication pending (1992).

37. Wood, H.G., S.W. Ragsdale and E. Pezacka, "The Acetyl-CoA Pathway of Autotrophic Growth," *FEMS Microbiol. Rev.*, 39, 345-362, (1986).

38. Baronofsky, J.J., W.J.A. Schreurs and E.R. Kashket, "Uncoupling by Acetic Acid Limits Growth of and Acetogenesis by *Clostridium thermoaceticum*," *Appl. Env. Microbiol.*, 40, n6, 1134-1139, (1984).

39. Shanmugasundoram, T. and H.G. Wood, "Interaction of Ferredoxin with Carbon Monoxide Dehydrogenase from *Clostridium thermoaceticum*," *J. Biol. Chem.*, 267, n2, 897-900, (1992).

40. Hugenholtz, J. and L.G. Ljungdahl, "Metabolism and Energy Generation in Homoacetogenic Clostrida," *FEMS Microbiol. Rev.*, 87, 383-390, (1990).

41. Pezracka, E. and H.G. Wood, "The Autotrophic Pathway of Acetogenic Bacteria: Rate of CO Dehydrogenase Disulfide Reductase," *J. Biol. Chem.*, 261, n4, 1609-1615, (1986).

42. Drake, H.L., S-L. Hu and H.G. Wood, "Purification of Five Components from *Clostridium thermoaceticum* Which Catalyze Synthesis of Acetate from Pyruvate and Methyltetrahydrofolate, Properties of Phosphotransacetylase," *J. Biol. Chem.*, 256, n21, 11137-11144, (1981).

43. Zeikus, J.G., R. Kerby and J.A. Krzycki, "Single-carbon Chemistry of Acetogenic and Methanogenic Bacteria," *Science*, 227, 1167-1173, (1985).

44. Ragsdale, S.W., J.E. Clark, L.G. Ljungdahl, L.L. Lundie, and H.L. Drake, "Properties of Purified Carbon Monoxide Dehydrogenase from *Clostridium thermoaceticum*, a Nickel, Iron-Sulfur Protein," *J. Biol. Chem.*, 258, n4, 2364-2369, (1983).

45. Lindahl, P.A., E. Münck and S.W. Ragsdale, "CO Dehydrogenase from *Clostridium thermoaceticum*: EPR and Electrochemical Studies in CO_2 and Argon Atmopsheres," *J. Biol. Chem.* 265, n7, 3873-3879, (1990).

46. Lindahl, P.A., W.W. Ragsdale, and E. Münck, "Mössbauer Study of CO Dehydrogenase from *Clostridium thermoaceticum*," *J. Biol. Chem.*, 265, n7, 3880-3888, (1990).

47. Ragsdale, S.W., P.A. Lindahl, and E. Münck, "Mössbauer, EPR, and Optical Studies of the Corrinoid/Iron-Sulfur Protein Involved in the Sythesis of Acetyl Coenzyme A by *Clostridium thermoaceticum*," *J. Biol. Chem.*, 262, n 29, 14289-14297. (1987).

48. Hugenholtz, J., D.M. Ivey, and L.G. Ljungdahl, "Carbon Monoxide Driven Electron Transport in *Clostridium thermoautotrophicum* Membranes," *J. Bacteriol.*, 169, n12, 5845-5847, (1987).

49. Dickert, G., "CO_2 Reduction to Acetate in Anaerobic Bacteria," *FEMS Microbiol. Rev.*, 87, 391-396, (1990).

50. Muller, V., M. Blant, R. Heise, C. Winner, and G. Gottschalk, "Sodium Bioenergetics in Methanogens and Acetogens," *FEMS Microbiol. Rev.*, 87, 373-376, (1990).

51. Terracciano, J.S., W.J.A. Schreurs, and E. Kashket, "Membrane H^+ Conductance of *Clostridium thermoaceticum* and *Clostridium acetobutylicum*: Evidence for Electrogenic Na^+/H^+ Antiport in *Clostridium thermoaceticum*," *Appl. Environ. Microbiol.*, 53, n4, 782-786, (1987).

52. Kellum, R. and H.L. Drake, "Effects of Cultivation Gas Phase on Hydrogenase...*Clostridium thermoaceticum*," *J. Bacteriol.* 160, 466-469, (1984).

53. Drake, H.L., "Demonstration of Hydrogenase...from *Clostridium thermoaceticum*," *J. Bacteriol.*, 150, 702-709, (1982).

54. Mayer, F., D.M. Ivey, and L.G. Ljungdahl, "Macromolecular Organization of F_1-ATPase Isolated from *Clostridium thermoaceticum* as Revealed by Electron Microscopy," *J. Bacteriol.*, 166, n3, 1128-1130, (1986).

55. Ivey, D.M., and L.G. Ljungdahl, "Purification and Characterization of the F_1ATPase from *Clostridium thermoaceticum*," *J. Bacteriol.* 165, n1, 252-257, (1986).

56. Yamamoto, I., T. Saniki, S-M. Liu, and L.G. Ljungdahl, "Purification and Properties of NADP-dependent Formate Dehydrogenase from *Clostridium thermoacetium*, a Tungsten-Selenium-Iron Protein," *J. Biol. Chem.*, 258, n3, 11826-1832, (1983).

57. Sun, A.Y., L.G. Ljungdahl, and H.G. Wood, "Total Synthesis of Acetate from CO_2: II. Purification and Properties of Formyltetrahydrofolate Synthetase from *Clostridium thermoaceticum*," *J. Bacteriol.*, 98, 842-844, (1969).

58. Ljungdahl, L.J., W.E. O'Brien, M.R. Moore, and M-T. Liu, "Methylenetetrahydrofolate Dehydrogenese from *Clostridum formicoaceticum* and Methylenetetrahydrofolate Dehydrogenase, Methyltetrahydrofolate Cyclohydrolase (combines) from *Clostridium thermoaceticum*," *Methods Enzymol.*, 66, 509-609, (1980).

59. Clark, J.E. and L.G. Ljungdahl, "Purification and Properties of 5,10-Methylenetetrahydrofolate Reductase, and Iron-Sulfur Flavoprotein from *Clostridium formicoaceticum*," *J. Biol. Chem.*, 259, n17, 10845-10849, (1984).

60. Lu, W.P., S.R. Harder, and S.W. Ragsdale, "Controlled Potential Enzymology of Methyl Transfer Reactions Involved in Acetyl-CoA Synthesis by CO Dehydrogenase and the Corrinoid/Iron-Sulfur Protein from *Clostridium thermoaceticum*," *J. Biol. Chem.*, 265, n6, 3124-3133, (1990).

61. Hu, S-I., E. Pezacka, and H.G. Wood, "Acetate Synthesis from Carbon Monoxide by *Clostridium thermoaceticum* Purification of the Corrinoid Protein," *J. Biol. Chem.*, 259, n14, 8892-8897, (1984).

62. Harder, S.R., W.P. Lu, B.A. Feinberg, and S.W. Ragsdale, "Spectro-electrochemical Studies of the Corrinoid/Iron-Sulfur Protein Involved in Acetyl Coenzyme A Synthesis by *Clostridium thermoaceticum*," *Biochemistry*,, 28, 9080-9087, (1989).

63. Lebertz, H., H. Simon, L.F. Courtney, S.J. Benkovic, L.D. Zydowsky, K. Lee and H.G. Floss, "Stereochemistry of Acetic Acid Formation from 5-Methyltetrahydrofolate by *Clostridium thermoaceticum*," *J. American Chemical Society*, 109, 3173-3174, (1987).

64. Ragsdale, S.W. and H.G. Wood, "Acetate Biosynthesis by Acetogenic Bacteria: Evidence that Carbon Monoxide Dehydrogenase is the Condensing Enzyme that Catalyzes the Final Steps of the Synthesis," *J. Biol. Chem.*, 260, n7, 3970-3977, (1985).

65. Raybuck, S.A., S.E. Ramer, D.R. Abbanat, J.W. Peters, W.H. Orme-Johnson, J.G. Ferry and C.T. Walsh, "Demonstration of Carbon-Carbon Bond Cleavage of Acetyl CoenzymeA by Using Isotopic Exchange Catalyzed by the CO Dehydrogenase Complex from Acetate Grown *Methanosarcina thermophila*," *J. Bact.*, 173, 2, 939-932, (1991).

66. Pezacka, E. and H.G. Wood, "Acetyl-CoA Pathway of Autotrophic Growth: Identification of the Methyl-binding Site of CO dehydrogenase," *J. Biol. Chem.*, 263, n31, 16000-16006, (1988).

67. Ramer, S.E., S.A. Raybuck, W.H. Orme-Johnson, and C.T. Walsh, "Kinetic Characterization of the [3' - ^{32}P] CoenzymeA/Acetyl CoenzymeA Exchange Catalyzed by a Three Subunit Form of the Carbon Monoxide Dehydrogenase/Acetyl-CoA Synthase from *Clostridium thermoaceticum*," *Biochemistry*, 28, 4675-4680, (1989).

68. Raybuck, S.A., U.R. Bastian, L.D. Zydowsky, K. Kobayashi, H.G. Foss, W.H. Orme-Johnson, and L.T. Walsh, "Nickel-Containing CO Dehydrogenase Catalyzes Reversible Decarbonylation of Acetyl CoA with Retention of Stereochemistry at the Methyl Group," *J. American Chemical Society*, , 109, 3171-3173, (1987).

69. White, H., G. Strobl, R. Feicht, and H. Simon, "Carboxylic Acid Reductase: A New Tungsten Enzyme Catalyzes the Reduction of Non-activated Carboxylic Acids to Aldehydes," *Eur. J. Biochem.*, 184, 89-96, (1989).

70. Fraisse, L. and H. Simon, "Observations on the Reduction of Non-activated Carboxylates by *Clostridium formicoaceticum* with Carbon Monoxide or Formate and the Influence of Various Viologens," *Arch. Microbiol.*, 150, 381-386, (1988).

71. Doyle, M, "Preferred Conditions for Growth and Product Formation by *Clostridium ljungdahli* PETC in Complex Media," M.S. Thesis, University of Arkansas, (1992).

72. Charpentier, J.C., "Advances in Chemical Engineering," Vol. II, Academic, New York, (1981).

73. Klasson, K.T., B.B. Elmore, J.L. Vega, M.D. Ackerson, E.C. Clausen, and J.L. Gaddy, "Biological Production of Liquid and Gaseous Fuels from Synthesis Gas," *App. Biochem. Biotechnol.*, 24/25, 857 (1990).

74. Kimmel, D.E., K.T. Klasson, E.C. Clausen, and J.L. Gaddy, "Performance of Trickle-bed Reactors for converting Synthesis Gas to Methane," *Applied Biochem. and Biotech.*,, 28/29, 457-469, (1991).

13.0 APPENDICES

Appendix A
Laboratory Procedures

A.1 Procedures for Media Preparation

1. Using sterilized or disposal pipettes, mix the media constituents.

2. Test the pH of the mixture, it should be a little above what is required, since the usually drops by 0.2 units in the autoclave

   If the pH is too low,; add dropwise sterilized 10% $NaCO_3$ (sodium bicarbonate)

   If the pH is too high, add dropwise 1.0% Acetic Acid.

3. Transfer the media into a 1000 or 500 mL round bottom flask.

4. An 80% N_2, 20% CO_2 gas mixture is bubbled through the media using a 1 ml cotton plugged pipe and attached to the gas hose.

5. Allow the solution to boil for 2 minutes

6. After the solution cools, check the pH
   If the pH is correct, anaerobically transfer the solution into serum bottles and seal with a septa. (This technique will be discussed later)

A.2 Inoculation of Media with Natural Inocula

Fresh natural inocula can be added to jars of media in the anaerobic chamber. Samples must be added to the media as soon as possible after collecting the inocula, trying not to let the sample dry out. After the gas has been added (CO or synthesis gas), put the sample in the incubator. Take gas samples weekly to check the progress of the organisms in the solution. Once gas consumption has begun, transfer a portion of the inoculated media to new media, always keeping the original sample. If the original sample doesn't consume gas after a period of a month to a month and a half, it must be transferred to ensure that the organisms have not depleted the nutrients. Samples have taken from 1 to 6 months to initiate gas consumption. Thus, try not to discard the cultures to soon.

The inoculation procedure must be anaerobic or the organisms may die. The procedures for inoculation are the same as in removing liquid samples:

1. Turn on the gas that is to be used (N_2 or CO or both) and turn the gas heater on.

2. When inoculating a sample, a substance must be added to tie up any dissolved oxygen in the solution. Sodium sulfide can be used. Add 0.2 ml of NaS_2 for every 10 ml of solution. Methane inhibitors should also be added prior to inoculation. BESA or monensin in 0.1 ml quantities for every 10 ml of solution were added.

3. To add something to the solution: Take a sterile or disposable needle and syringe and flush it twice with gas by placing it in the canula. Place methanol on the bottle of NaS_2 (example) and the serum bottle, and then flame the NaS_2 bottle and insert the needle into the septa. Withdraw the exact amount of solution needed. Flame the septa of the serum bottle and put the needle in the septa. After forcing the solution into the bottle, let the plunger come up on its own. This will relieve excess pressure from the serum bottle. Withdraw the needle and dispose of it in the proper container.

4. To remove liquid samples: Flush the needle with gas and put methanol on the top of the septa. Flame the septa and insert the needle into the sample and withdraw the amount needed. Withdraw the needle and place the sample in a sampling tube. Dispose of the needle and syringe. Don't use a syringe twice due to the possibility of cross contamination. Similar procedures are used for the pure culture.

A.3. Gas Addition to Serum Bottles

1. Place methanol on top of the septa. Let it evaporate before addition.

2. Place sterile needles on the gas lines that you will be using, making sure the tubing has been autoclaved.

3. Turn the gas on and turn on the regulator by the hood. Make sure the hood fan is on. Set the regulator for the pressure that is needed. If one atmosphere is required, fill the bottle to two atmospheres, then let the pressure out with a needle. Hold the needles up in the hood and flush the gas through them for a couple of seconds. Then place the needles in the septa. Fill the bottles to pressure, then pull a vacuum. Pressure again and vacuum again. Pressure and vacuum once more. Then fill the bottles with gas once more. Remove the needles and check for leaks in the septa. Turn the gas bottle off and vent any pressure in the lines.

4. If an inert gas is needed, place the gas in a gas bag. Then, using a sterile glass syringe take out the amount that is needed and put in the bottle. Use caution not to over pressure the syringe since they have been known to break.

   NOTE: WHEN ADDING GAS, ESPECIALLY INERTS OR TRACERS, YOU NEED TO RECORD THE BAROMETRIC PRESSURE, VOLUME OF TRACE GAS AND ROOM TEMPERATURE. This enables a mole balance to be done.

A.4 Gas and Liquid Sampling from Serum Bottles

Gas and liquid samples are to be removed using the same procedures as outlined in Appendix A.2. Be sure to shake the bottles to insure

accurate readings. But make sure that liquid is not on the septa, otherwise the gas syringe may become clogged. The amount removed and the computer program used for calculation will depend on the current analysis.

A.5 "Fed Batch" Reactor Start-up

REACTOR: Disconnect the reactor at the quick connect fitting near the inlet gas filter and clamp the tubing between the filter and the reactor to preclude backup of liquid into the filter during autoclaving. Remove the sodium hydroxide injection needle and disconnect the pH probe cable at the back of the pH control module and the gas outlet tubing prior to the check valve. Set the reactor on its stainless steel support plate and clean as needed.

MEDIA: Prepare 400 mL of 0.01 percent basal medium (for one reactor). Rinse the reactor with 20 mL of medium, then charge 350 mL of medium to the reactor. Close the reactor, plugging the gas outlet tubing with a glass wool filter (this will allow the reactor to breathe during autoclaving). Autoclave the assembled reactor, including the reactor, pH probe, thermometer, overflow flask and support plate for 30 min at 120°C.

PURGING: Remove the hot reactor from the autoclave, dry the support plate and install the assembly on the Bioflo. Immediately begin purging the reactor with nitrogen using a sterile cotton filter and needle inserted in the gas sample port. Connect the synthesis gas line to the reactor and open the valves before releasing the clamp on the tubing between the filter and the reactor. Adjust the synthesis gas flow to the maximum flow that registers on the rotameter (about 50 on the rotameter scale). Maintain nitrogen flow for 10 to 15 min; then stop the nitrogen flow and connect the outlet check valve. Maintain the gas purge until the medium has cooled to room temperature and the reactor gas analysis is the same as that for the feed gas. Reduce the gas flow and start gentle agitation (about 200 rpm). Reduce the cooled medium with 7.0 mL of 2.5 percent cysteine hydrochloride solution (1.0 mL per 50 mL of medium). The cooled, reduced medium should be pale yellow at the experimental pH.

INOCULUM: Use 40 mL of the prepared seed culture. Connect the pH controller and pump module using a sterile needle for 3 M sodium hydroxide injection, and adjust pH. Hydrochloric acid solution can be used to lower pH using the basic program, CORRPH, or the pH can be allowed to drop as growth occurs. Agitation rate should remain low with only slight entrainment of the overhead gas until growth is established in the reactor.

A.6 "Fed Batch" Reactor Sampling

GAS COMPOSITION: The gas phase compositions were determined by gas chromatography. Feed gas samples were drawn with a gas syringe, 0.8 mL typical sample size.

LIQUID SAMPLE: Flush a 5.0 mL syringe fitted with a sterile 22 gauge needle several times in the overhead vapor space of the reactor. Draw 3.0 mL of the overhead gas and inject it into the liquid sample dip tube to clear the stagnant liquid. Draw 2.6 mL of the medium for liquid analysis.

OPTICAL DENSITY: Optical density was determined with a Spectronic 21 spectrophotometer at 580 nm versus a water blank. The cell density in mg/L was 473.9 times the OD.

PRODUCT CONCENTRATIONS: Concentrations of ethanol and acetic acid were determined by gas chromatography. A n-propanol internal standard was mixed 1:10 volume parts with the raw sample for injection into the gas chromatograph.

A.7 Inoculum Preparation in the CSTR

The inoculum for the CSTR was prepared from two lines of stock cultures which are maintained in a shaker incubator and transferred weekly. These stock culture lines are designated "BIOB" and "BH2S", respectively. The inoculum was grown as a seed culture in 1.2 L dilution jars adapted for anaerobic transfer and growth of bacteria. The medium was prepared which was very similar to that which was used in the CSTR. The medium was boiled and purged was then filled with 250 mL of the cooled medium, capped and autoclaved. The nitrogen in the sterile bottle was then replaced with synthesis gas and the bottle pressurized to about 7.5 psig. The medium was reduced with 5 mL of a 2.5 percent solution of cysteine HCl (cysteine is not an essential nutrient for *C. ljungdahlii* but enhances growth rates), and inoculated with 10 mL of each line of stock culture. The seed culture was shaken at 37°C and transferred to the reactor during the late exponential growth phase.

A.8 CSTR Start-Up

REACTOR: The quick connect fitting near the inlet gas filter is disconnected and the tubing between the filter and reactor is clamped to preclude the backup of liquid into the filter during autoclaving. The sodium hydroxide injection needle is removed and the pH probe cable at the back of the pH control module is disconnected. The tubing connections and plugged with glass wool filters to maintain sterility following autoclaving. The reactor and its stainless steel support plate is then removed and cleaned as needed. The reactor is filled with about 300 mL of deionized water and one of the screw cap septa is replaced with a glass wool filter. The assembled reactor is autoclaved for 30 min at 120°C.

PURGING: The hot reactor is removed from the autoclave, the support plate is dried and the assembly is installed on the Bioflo. Purging with nitrogen immediately begins using a sterile glass wood filter and needle inserted in the gas sample port. The synthesis gas line is connected to the reactor and the valves are opened before releasing the clamp on the tubing between the filter and the reactor. The flow rate is adjusted to the maximum that registers on the rotameter. Nitrogen flow is maintained for 10 to 15 min; the nitrogen is then shut off and the outlet tubing is connected to the product receiver and liquid feed and equalization tubing to the feed reservoir (allow gas to flow through each line to clear residual air prior to sealing). The pump tubing is replaced with new Masterflex tubing (Tygon 6409-13) and inserted into the pump head. The synthesis gas purge is maintained until the reactor gas analysis matches that for the feed (purge overnight at reduced rates).

INOCULUM: The deionized water is drained from the reactor and, using Facutainer 21G1 blood sampling needle (double ended), the prepared 250 mL seed culture is transferred into the reactor. Agitation begins at low rates (200 rpm), along with fresh medium flow into the reactor. When the liquid covers the pH probe membranes, pH monitoring and control may begin. As the liquid level rises, the agitation rate should be increased to the level appropriate for the experimental work. The use of a seed culture in the exponential growth phase allows immediate initiation of continuous flow, yielding a short start-up time.

A.9 CSTR Sampling

DATA: The data taken include time (date and 24 hour time), pH, temperature, rotameter reading, liquid flow rate, optical density at 580 nm, composition of exiting gas (mole percent hydrogen, argon, carbon monoxide and carbon dioxide), product concentrations (g/L ethanol and acetic acid), gauge pressures at the rotameter and reactor, and atmospheric pressure.

GAS COMPOSITION: The gas phase compositions are determined with a Perkin-Elmer Sigma 300 gas chromatograph with Carbosphere packing. Feed samples (0.8 mL typical sample volume) are drawn from septa in the outlet tubing just after the reactor and in the feed line just after the rotameter.

LIQUID SAMPLE: A 5 mL syringe fitted with a sterile 22 gauge needle is flushed several times in the overhead vapor space of the reactor. 3 mL of the overhead gas is withdrawn injected into the liquid sample dip tube to clear the stagnant liquid. 2.6 mL of the fermentation broth is obtained for liquid analysis.

OPTICAL DENSITY: Optical density is determined with a Spectronic 21 spectrophotometer at 580 nm using a water blank. The cell density in mg/L is obtained by use of a calibration curve.

PRODUCT CONCENTRATIONS: Concentrations of ethanol and acetate as acetic acid are determined using a Varian 3400 gas chromatograph with Porapak QS packing. n-Propanol in HCl (the internal standard) is mixed 1:10 volume parts with the raw sample for injection into the gas chromatograph.

Appendix B
Gas Consumption Under Quantitative Conditions

Preparation of the media was carried out anaerobically in an atmosphere of 80 percent nitrogen (N_2), 20 percent CO_2 as described by Hungate and Ljungdahl and Wiegel. The medium was then transferred to serum bottles, 157.5 mL in volume. The bottles are sealed with butyl rubber stoppers and aluminum seals. The bottles were then autoclaved at 121°C for 21 minutes. A seed culture was started from a stock culture in a bottle similar to those described above about 48 hours before the experiment was to begin. This seed culture was grown in a shaker incubator kept at 37°C and 100 rpm. Once the seed culture was ready, sodium sulfide was added to the bottle and left in the shaker incubator for about 15 minutes to allow for complete oxygen removal and temperature acclimation. Then, 10 mL of seed culture were aseptically added to each bottle. The bottles were then flushed with the gas to be employed and pressurized to the desired level (up to 3 atm maximum) with the use of adjustable check valves. A measured amount of an inert gas was then introduced with a Leur-lock syringe. In these experiments 20 cc of methane will be as inert gas. The inert gas allows determination with high accuracy the changes in total pressure inside the bottle and thus the total amount of carbon monoxide present in the gas phase.

The bottles were left in the shaker incubator (100 rpm) at 37°C during the experiment. Sampling for gas composition, optical density, pH, acids and alcohols were carried out at adequate intervals. An outline of the experimental procedure is shown in Figure A.1.

The cell concentration (dry weight) may then be determined from an appropriate calibration curve of optical density as a function of dry cell weight. Acetate and ethanol concentration may be determined from a gas chromatograph calibration curve. Finally, the moles of carbon monoxide at any time may be found using the ideal gas law the gas chromatographic analysis, and the inert gas composition. The procedure is illustrated in Figure A.2.

Yields may then be determined by plotting cells or product produced as a function as the CO consumed. The yields are then found from the slopes of these plots.

Figure A.1

BATCH EXPERIMENTAL PROCEDURE FOR DETERMINING REACTION STOICHIOMETRY

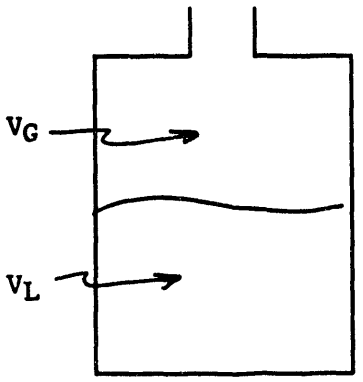

V_T = 157.5 mL (total volume)

V_L° = 86.5 mL (initial liquid volume)

V_G° = 71.0 mL (initial gas volume)

Start-up

1. Anaerobically, fill the bottle with 75 mL of liquid medium.
2. Vent the gas phase with the desired gas mixture.
3. Sterilize the bottles in the autoclave.
4. Add 1.5 mL of Sodium Sulfide ($Na_2S.9H_2O$)(2.5%).
5. Shake for 20 minutes at 37°C.
6. Add 10 mL of seed culture.
7. Vent the gas phase with the desired gas mixture. Use variable cracking pressure check valves in the gas outlet.
8. Add 20 mL of CH_4 (inert gas) at room temperature and pressure.
9. Measure initial optical density and gas composition.
10. Place in the shaker incubator at 37°C.

Sampling

11. Sample the gas phase for gas composition (0.4 mL).
12. Sample the liquid phase for optical density, pH, ethanol and acetate (3 mL).

Figure A.2

DETERMINATION OF QUANTITATIVE INFORMATION DURING A GAS FERMENTATION

1. Cell concentration (dry weight) from OD (optical density) calibration curve.

2. Moles of carbon monoxide present in the gas phase from gas percent analysis:

   - At start-up:

$$N_{CH_4} = \frac{P_{room}\, V_G^o}{R \cdot T_{room}} \Rightarrow N_T^o = \frac{100}{(\%\ CH_4)}\, N_{CH_4}^o$$

$$N_{CO}^o = \frac{(\%CO)}{100}\, N_T^o$$

   - At each sampling time:

$$N_{CH_4}^i = N_{CH_4}^o - \sum_{j=1}^{i-1} \frac{V_{gas\ sample}}{V_G}\, N_{CH_4}^j$$

$$N_t^i = \frac{100}{(\%CH_4)}\, N_{CH_4} \Rightarrow N_{CO}^i = \frac{(\%CO)}{100}\, N_T^i$$

Thus, the moles of methane depend upon the initial amount of methane and the number of samples.

(3) Ethanol and acetate concentration from G.C. calibration curve.

Appendix C
Analytical Procedures

C.1 Bacterial Growth

A standard curve of absorbance as a function of cell density for the pure isolated culture has been developed. For this purpose, several different volumes of a ten-day old culture growing on synthesis gas were filtered through a 0.45 μm filter paper and dried in the oven until a constant weight was obtained. The dry cell weight density of the solution was found to be 0.167 g/L as from the slope of the line in Figure A3. The culture diluted to several levels and the absorbance at 580 nm measured to obtain the calibration curve shown in Figure A4. The result in Figure A4 can be expressed by the equation:

$$X \text{ (mg/L)} = 473.9 \ (OD)_{580}$$

where X = cell concentration (mg/L), and

$(OD)_{580}$ = optical density measurement at 580 nm.

C.2 Gas Analysis

The composition of the gas phase was determined by gas-solid chromatography in a Varian 3400 gas chromatograph. Samples (0.15 mL) were injected using a Pressure-Lok syringe into a 6 ft x 1/8 in. column packed with Carbosphere, 60/80 mesh, to allow the determination of H_2, N_2, Ar, CO, CH_4 and CO_2. A temperature program was required for the adequate separation of hydrogen and air components. The optimal program conditions were determined to be 30°C for 4 minutes, an increase in temperature to 125°C at 30°C/min for 5 minutes, and a final period at 200°C for 8 minutes, required to condition the column prior to analysis of the next sample and to remove any traces of water in the column. The detector and injector temperatures were both 175°C and the carrier gas used was helium at a flow rate of 40 mL/min. The total time for the analysis was approximately 20 minutes.

C.3 Liquid Analysis

Liquid analyses were also carried out by gas chromatography in the Varian 3400 gas chromatograph. Separate procedures for the analysis of alcohols and acids were required to avoid peak interference.

Alcohol analysis was performed using a 2 ft x 1/8 in column packed with Poropak QS, pretreated with NaOH. In a typical run, a 250 μl sample was mixed with 40 μl of NaOH to avoid acid peaks. The injection volume into the chromatograph was 1 μl. The oven temperature was 150°C. Both the detector and injector temperatures were 220°C and the carrier gas was helium at a flow rate of 40 μl/min. To separate methanol, ethanol, propanol and butanol, approximately 15 minutes were required.

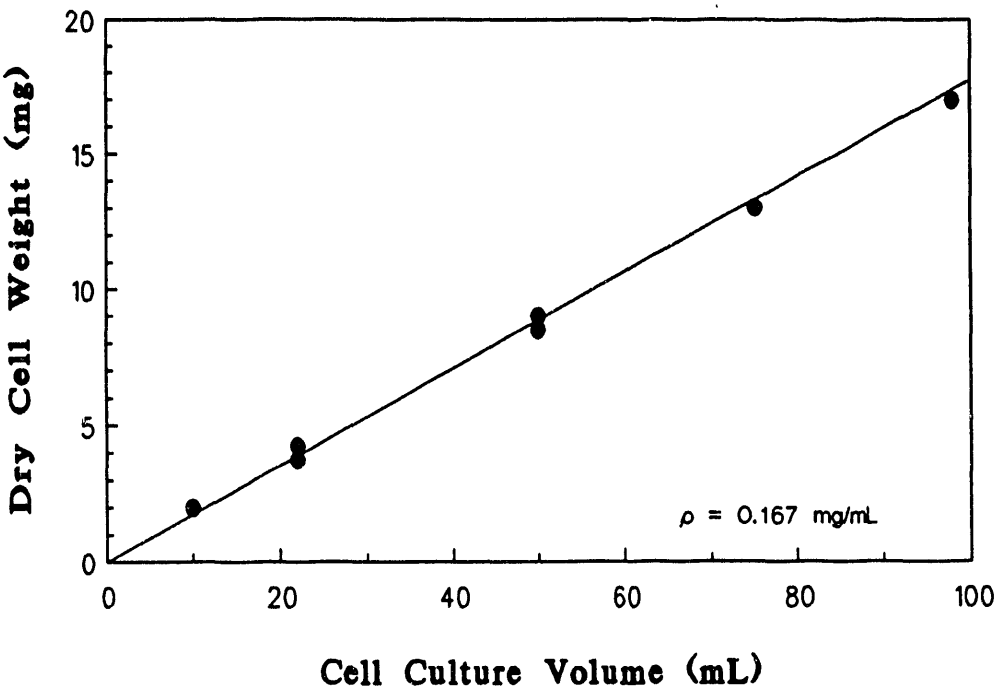

Figure. A3. Determination of culture density.

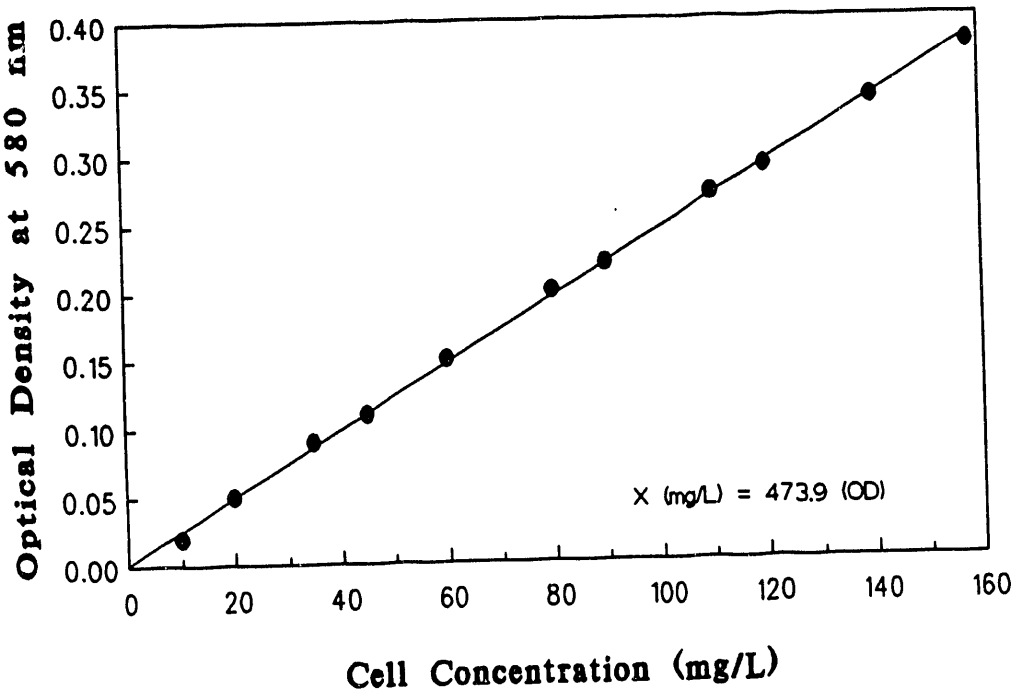

Figure A4. Optical density vs. cell dry weight concentration.

Acid analysis was performed using a 2 ft x 1/8 in column packed with Poropak QS, previously conditioned with H_3PO_4. A 250 μl sample was mixed with 40 μl of 50% H_3PO_4. A 1 μl sample of this mixture was injected into the chromatograph for analysis. The oven temperature was 170°C. The detector and injector were both maintained at 220°C and the carrier gas was helium at a flow rate of 40 μl/min. Approximately 15-20 minutes were necessary to separate acetic, propionic and butyric acid.

To switch from alcohol to acid analysis it was necessary to change the columns, followed by conditioning at 200°C overnight.

DATE
FILMED
8/3/93
END